UNIVERSITE DE LIEGE
FACULTE DE MEDECINE VETERINAIRE
DEPARTEMENT DES MALADIES INFECTIEUSES ET PARASITAIRES
LABORATOIRE D'IMMUNOLOGIE ET DE VACCINOLOGIE

Aperçus de l'impact des helminthes sur le système immunitaire : des macrophages aux lymphocytes T CD8$^+$ mémoires virtuels

Insight into how helminths shape the immune system : from macrophages to bystander memory CD8$^+$ T lymphocytes

ROLOT Marion

THESE PRESENTEE EN VUE DE L'OBTENTION DU GRADE DE
Docteur en Sciences Vétérinaires

ANNEE ACADEMIQUE 2018-2019

Remerciements

Personne[1] ! Je ne remercie personne[2] !

Ce travail est le mien[3] et rien qu'à moi[4] !

Depuis le 1[er] jour[5] et jusqu'à cet instant[6], j'ai œuvré seule !

Les peines[7], les joies[8]

Les soirées interminables au FACS[9],

J'ai tout affronté seule[10] !

[1] *Bon, quand même, j'ai eu la chance d'être accueillie au sein du laboratoire d'Immunologie-Vaccinologie par un promoteur présent et impliqué. Des tous débuts, lorsqu'il a fallu patiemment m'expliquer comment utiliser une pipette sans arracher la moitié du tapis cellulaire jusqu'à tes tentatives (infructueuses mais persévérantes) de relativiser le stress de l'écriture de cette thèse, merci Benjamin d'avoir été si disponible. Merci d'avoir été un si bon professeur, d'avoir pris le temps de m'expliquer, le temps de réfléchir avec moi, de m'écouter. Je plaide totalement coupable de m'être laissée embarquer pour en faire toujours plus, la recherche est une passion et tu m'as assez efficacement transmis ce virus. Merci de m'avoir guidée au travers des aléas de la science pour mener à bien cette thèse. Je te remercie également de m'avoir mise suffisamment à l'aise que pour laisser déborder mon trop plein d'honnêteté et oser t'avouer les (plus ou moins grosses) bétises que je faisais dans le labo, ce qui nous a parfois permis de rattrapper le coup.*

[2] *Au cours de cette thèse, j'ai également pu profiter du précieux soutien de mon co-promoteur Alain Vanderplasschen ainsi que de celui de Laurent Gillet. Merci Alain de si bien partager ton amour de la science et de me rappeler à chacune de tes présentations pourquoi j'ai choisi l'immunologie. Merci Laurent d'être aussi sérieux et critique dans la science que tu es moqueur et boute-en-train en dehors (ou est-ce l'inverse ?). Merci à tous les deux pour vos encouragements et vos conseils avisés.*

[3] *Mouais, en fait j'ai été « un peu » aidée. Annette, je tiens à te remercier chaleureusement de m'avoir initiée à ce monde étrange qu'est la parasitologie. Merci d'avoir été toujours si positive et de m'avoir poussée à l'être aussi. Merci pour tout ton travail qui a servi de base solide au projet « VM » et encore plus à venir ! Merci Loïc pour ton implication au cours de ton stage.*
I would also like to thank William Horsnell and Alisha Chetty with whom we collaborated on coinfection projects (and more). Thank you for the pleasant and productive exchanges during the past four years. It was a pleasure to visit you in South Africa.

[4] *Cela va sans dire que Justine a également toute ma gratitude pour tout ce qu'elle m'a aidé à accomplir durant cette thèse ! Désolée de t'avoir demandé de te lever à l'aube pour couper des foies (si peu !) et merci ! Merci de l'avoir fait avec le sourire et d'avoir résisté à mon stress. Plus encore, je te remercie d'être une si bonne amie.*

Je suis également profondémment reconnaissante à notre team de choc, Chris et Lo ! Merci Christina de toujours tout faire pour nous aider à résoudre nos soucis et incompréhensions administratifs mais surtout merci d'être présente et à l'écoute. Merci Lorène pour ton aide technique, merci d'endosser le role ingrat mais ô combien important de travailleur de l'ombre. Votre travail est très précieux à la bonne marche du labo et nous permet à tous de travailler dans des conditions optimales. De plus, et ce n'est pas négligeable, une petite pause au sécrétériat est toujours revigorante, surtout lors de longues journées.

Merci à Emeline (D), Aurélie, Glawdys et Cédric pour leur gestion quotidienne des animaleries et pour les soins apportés aux animaux. Je tiens à m'excuser auprès d'Emeline et d'Aurélie : désolée de toujours vous accueillir avec l'appréhension d'une mauvaise nouvelle à propos des animaux alors que vous voulez juste me dire bonjour, je travaille sur cette angoisse !

[5] Avant de devenir la vieille de quelqu'un je tiens à remercier mes vieux à moi, ceux qui ont fait que je me suis sentie à l'aise dés mes premiers jours au labo, ceux vers qui je pouvais (et peux toujours !) me tourner quand j'étais perdue. Il y a bien longtemps, dans une galaxie lointaine … Non, pardon, je m'égare ! Une immense merci à Françoise, Béné et Max, les indélogeables, les personnes qui te permettent de croire que tout ne part pas totalement en vrille. Merci d'être des sources d'informations inépuisables et de participer à la bonne ambiance du labo. Les moments partagés avec vous au labo et surtout en dehors sont toujours des moments très agréables ! Merci Françoise pour ta bienveillance, merci pour tes conseils et tes encouragements. Merci Béné pour ton expertise, merci pour ta disponibilité et ta générosité. Merci Max de toujours savoir me faire rire, merci pour ton implication dans le labo. Merci à Emeline (G) d'avoir partagé les stress et les joies du FRIA. Merci pour ton ouverture d'esprit, merci pour toutes ces conversations (totalement non professionnelles) qu'on a eues. Merci à Catherine, Caro et Léa pour tous les moments partagés au labo et en dehors, pour les pics-nics, les glaces, les restos et les soirées ! Merci à Océane, Céline (L.), Maygane, Anusyah, Mickael, William, Ludovic, Bilal ou encore Kris. Les gens s'en vont petit à petit et à chaque départ on pense que ce ne sera plus pareil.

[6] Quand les nouveaux arrivent, en effet ce n'est plus pareil, la dynamique change mais finalement chacun trouve sa place et l'ambiance reste. Merci à Amira, Haiyan, Ravo, Milena, Virginie, Lucie, Annalisa, Mickael, Yuan, Yunlong, Xiang, Mamadou et Owen de contribuer à cette ambiance.

[7] Heureusement pour moi, dans ces moments là des personnes bienveillantes ont tout fait pour me réconforter, merci à elles.

[8] Mais comme la joie a plus de saveur quand elle est partagée, il est important de bien s'entourer. Merci à Louisa, Justine, Natacha, Pauline et Céline (M.) d'être toujours partante pour une soirée, partager une pizza après une in vivo ou se réunir autour d'un repas. Merci pour les discussions absurdes mais tellement rafraichissantes. Merci pour les coups de gueule et les fous rires. Merci pour les déboires partagés.

[9] Nop, là pour le coup j'ai beau chercher, je crois bien il n'y avait vraiment personne …

[10] N'importe quoi ! J'aurais probablement implosé si j'avais du affronter ça toute seule. Je tiens à remercier du fond de mon cœur ma famille, au soutien indéfectible, qu'elle soit à 100, 600 ou 6000km. Merci à mes parents et mes grands-parents pour les valeurs qu'ils m'ont transmises, merci d'avoir fait de moi quelqu'un de curieux. Merci à tous ces amis que je ne vois pas assez souvent mais qui ont

quand même réussi à m'offrir d'appréciables moments de décompression durant cette thèse. Particulièrement, merci à Emilie d'avoir été au bon endroit au bon moment le jour de l'accueil en 1er bac, merci à ta famille de m'avoir toujours accueillie à bras ouverts, merci de m'avoir confié Lukas durant ces 4 années de thèse, il m'aura permis plus d'une fois de m'évader après une journée pénible.

Finalement, la réalisation de cette thèse est loin d'avoir été un travail triste et solitaire. C'est dans les moments de stress et de doutes que l'on se rend compte à quel point il est important d'être entouré de gens de qualité. De l'aide technique indispensable à l'organisation de moments de détente et de décompression en passant par le précieux partage d'expertises variées, cela a été un réel plaisir de travailler au sein du laboratoire d'Immunlogie-Vaccinologie. Cet endroit possède une telle concentration de personnes altruistes et dévouées que cela devrait probablement faire l'objet d'une étude sociologique …

Last but not least, les travaux présentés dans cette thèse ont nécessité la réalisation d'études « in vivo ». En espérant avoir apporté mon petit caillou à l'édifice de la science, je suis reconnaissante envers les centaines de souris (et quelques rats) qui ont contribué à ces études.

Par contre, je ne remercierai pas

- *l'informatique ! Tu ne m'aimes pas, je ne t'aime pas non plus mais crasher le document de ma thèse 3 jours avant l'impression et me faire perdre 2 jours de travail, vraiment, je pensais qu'on avait dépassé ça !*
- *les foies fibrotiques. Je ne vous remercie pas pour les crampes aux mains ! Et il en reste … 23 à couper …*
- *les bugs du FACS après 4h d'analyses alors qu'il reste 3 tubes à passer*
- *les B6 de 3 semaines qui bondissent hors de leur cage*
- *les bugs de l'IVIS avant la dernière cage de souris*
- *l'informatique ! Tu ne m'aimes pas, je ne t'aime pas non plus mais attendre que je baisse ma garde, que j'oublie d'enregistrer mon analyse FlowJo pour crasher le programme après 3h d'analyses, vraiment, je pensais qu'on avait dépassé ça !*
- *les pompes à perfusion qui t'explosent à la figure*
- *les poignées de porte de -80°C qui te restent dans la main (le w-e … toujours le w-e …)*
- *(liste non exhaustive)*

Abbreviations

aaMφ	Alternatively activated macrophages
Ag	Antigen
Arg1	Arginase 1
BAL(F)	Broncho-alveolar lavage (fluid)
BCL	B-cell lymphoma
Blimp-1	B-lymphocyte-induced maturation protein-1
BM	Bone marrow
caMφ	Classically activated macrophages
CCR	CC chemokine receptor
CD	Cluster of differentiation
CLR	C-type lectin receptor
Cre	Cre recombinase
CSP	Circumsporozoite protein from *Plasmodium yoelii*
CXCR	CXC chemokine receptor
DAMP	Danger associated molecular pattern
DC	Dendritic cells
DC-SIGN	DC-specific ICAM-3-grabbing non integrin
DE	Differentially expressed
DT(R)	Diphteria toxin (receptor)
EdU	5-Ethynyl-2-deoxyuridine
EEC	Early effector cells
Eomes	Eomesodermin
ES	Excretory-secretory
FACS	Fluorescence-activated cell sorting
FDR	False-discovery rate
FOXO	Forkhead box O
FTY720	Fingolimod
GATA-3	GATA-binding protein 3
GzmB	Granzyme B
H-2D/K	Classical MHC class I antigens subclasses
H&E	Hematoxilin eosin
HIV	Human immunodeficiency virus
IBD	Inflammatory bowel disease
ID	Inhibitor of DNA binding
IFN	Interferon
IL	Interleukin
IL-4c	IL-4-antibody complexes
IL-4Rα	IL-4 receptor α chain
ILC	Innate lymphoid cells
iNOS	Inducible NO synthase
i.n.	Intranasal
i.p.	Intraperitoneal
i.v.	Intravenous
KC	Kupffer cell
KLF	Kruppel-like factor
KLRG1	Killer-cell lectin receptor G1

L3	Stade 3 larvae
LN	Lymph node
Luc	Luciferase
Lyz2	Lysozyme 2
MAIT cells	Mucosal-associated invariant T cells
MFI	Median fluorescence intensity
MGL	Macrophage galactose-type lectin
MHC	Major histocompatibility complex
MPEC	Memory precursor effector cells
MR	Mannose receptor
MuHV-4	Murid herpesvirus 4
Ndfip1	Nedd4-family interacting protein 1
NES	Normalized enrichment score
NK	Natural killer
ns	Not significant
NTD	Neglected tropical diseases
ORF	Open reading frame
OVA	Ovalbumin
PAMP	Pathogen associated molecular pattern
PBS	Phosphate-buffered saline
PCA	Principal-component analysis
PFU	Plaque-forming unit
pi	Post-infection
PMA	Phorbol 12-myristate 13-acetate
PRR	Pattern recognition receptor
PLZF	Promyelocytic leukemia zinc finger
pvi	Post-viral infection
RAG	Recombinant-activating gene
Relm	Resistin-like molecule
RNA	Ribonucleic acid
s.c.	Subcutaneous
SEA	Soluble egg antigens
SEM	Standard error of the mean
SLEC	Short-lived effector cells
Sm	*Schistosoma mansoni*
SP	Surfactant protein
SPF	Specific pathogen free
STAT	Signal transducer and activator of transcription
STH	Soil-transmitted helminthiasis
Tbet	T-box expressed in T cells
T_{CM}	Central memory T cells
TCR	T-cell receptor
(td)RFP	(tandem dimer) red fluorescent protein
T_{EM}	Effector memory T cells
TGF-β	Transforming growth factor-β
TLR	Toll-like receptors
TNF	Tumor necrosis factor
Treg	Regulatory T cells
T_{RM}	Tissue-resident memory T cells

TSLP	Thymic stromal lymphopoietin
T_{VM}	Virtual memory $CD8^+$ T cells
WHO	World Health Organization
WT	Wild type
Ym1	Chitinase 3-like 3
γc	Common gamma chain
ω-1	Omega-1 (secreted protein from *S. mansoni* eggs)

Abstract

Abstract

Helminth infections are widely distributed around the world but the highest prevalence is found in developing countries where they constitute a major public health threat. Helminthiasis are mostly associated with chronic insidious pathologies profoundly impacting population health status and constitute a major concern for socio-economic development.

Immune response elicited during helminth infection is a complex balance between effector type 2 immunity mediating helminth expulsion, repair functions preserving integrity of tissues during parasite migration and regulatory elements allowing tolerance of chronic infection that cannot be cleared. Dysregulation of this equilibrium can generate extensive pathologies. Furthermore, as helminths profoundly impact their host's immune system, they also alter immune response during bystander inflammatory/infectious processes.

Two studies are presented in this thesis, both independently addressing questions on the impact of helminth infections on the immune response.

The first study presented here examined the role of alternatively activated macrophages (aaMφ) as actors of anti-helminth response balance, more precisely during *Schistosoma mansoni* infection. During schistosomiasis, an important type 2 granulomatous inflammation is elicited by the eggs trapped in the tissue (liver or intestine). Type 2 immunity is essential for survival during the acute phase of schistosomiasis but the role of aaMφ, an important component of granulomas, remains unclear. Using $Il4ra^{-/lox}Lyz2^{Cre}$ and $Il4ra^{-/-}$ mice, we characterized the dynamics of monocytes/macrophage responses in the liver of *S. mansoni* infected mice and found that IL-4Rα signalling is dispensable for monocyte infiltration and differentiation. Accumulation of monocyte-derived macrophages was associated with progressive disappearance of resident macrophages. While resident macrophages did not seem to play a role in the regulation of egg-induced pathology, alternative activation of monocyte-derived macrophages was shown to modulate hepatic granulomatous inflammation. However, infiltrating monocytes likely display alternative activation in $Il4ra^{-/lox}Lyz2^{Cre}$ mice thus other functions of aaMφ in this pathology cannot be excluded. Thus, this work provided a better understanding of the role of aaMφ in schistosomiasis.

The second study focused on the impact of helminth exposure on subsequent bystander immune responses and more particularly on anti-viral $CD8^+$ T cell response. IL-4 is a canonical cytokine from type 2 immune response associated with helminth infection. Previous reports showed that IL-4 can condition $CD8^+$ T cells by inducing expansion of antigen-inexperienced memory-like $CD8^+$ T cell called virtual memory T cells (T_{VM}). These cells have the particularity to display heightened effector functions,

similar to conventional memory cells. Our work showed that IL-4 can also induce expansion of T_{VM} in the context of helminth infection, depending on direct IL-4 signalling on $CD8^+$ T cells. Strikingly, helminth infection was also associated with IL-4-dependent enhanced protection against subsequent infection with the γ-herpesvirus MuHV-4 resulting from increased virus-specific $CD8^+$ T cells effector response. We provide here a new mechanism by which helminth can modulate the immune response against bystander infections.

Preamble

Preamble

The work presented in this thesis focused on two independent but important aspects of immunity to helminths in the mouse model: (*i*) the role of IL-4Rα-dependent alternative macrophage activation during schistosomiasis, and (*ii*) how helminth induced IL-4 can condition bystander memory $CD8^+$ T cell responses.

In a first study, we investigated the dynamics and the roles of the macrophage responses in the liver after *Schistosoma mansoni* infection. Macrophages are highly plastic cells. During type 2 immune responses like anti-helminth response, they adopt an anti-inflammatory and repair phenotype, called alternatively activated macrophages (aaMφ). Type 2 immune response mediates several crucial functions for the protection against helminth infection like parasite expulsion, impairment of parasite fitness or wound healing. Although aaMφ have been implicated in these functions, there exact role or whether they are essential for host protection remained unclear.

In a second study, we have investigated the influence of helminth infection on subsequent bystander immunity by studying its impact on anti-viral $CD8^+$ T cell responses through alteration of virtual memory $CD8^+$ T cells (T_{VM}). TCR-unrestricted and antigen-inexperienced memory-like $CD8^+$ T cells (among which T_{VM}) have been described in naive, pathogen-free or germ-free mice. These cells are believed to arise either in the thymus, instructed by IL-4 or high self-antigen reactivity, or in the periphery through lymphopenia-induced homeostatic proliferation. In the periphery, IL-4 and IL-15 can further expand the population in a mouse strain-specific manner. Helminth-induced immune response is dominated by IL-4 production and could therefore impact T_{VM} reponses and the subsequent ability of $CD8^+$ T cells to mount antigen-specific effector responses after a viral infection.

The following introduction aims at presenting the different theoretical concepts and recent findings that could help the understanding of our work. With that objective in mind, chapter 1 describes important helminthiasis of humans, their epidemiology and examples of mouse models as well as the main features of anti-helminth immune response. Chapter 2 focuses on the origin, activation and roles of macrophages during helminthiasis, emphasizing their role in schistosomiasis. To understand the wide diversity of helminths effect on bystander immune processes, chapter 3 presents their influence on both immunopathologies and coinfections, in particular on viral coinfections. Finally, chapter 4 includes a description of the important characteristics of the $CD8^+$ T cell response dynamic, from activation to memory formation and presents antigen-inexperienced memory $CD8^+$ T cells, including innate, bystander and virtual memory $CD8^+$ T cells.

Introduction

1 Helminth infections

1.1 Taxonomy

The term “helminth” is not associated with any particular phylogenetic classification. Helminths are described as complex multicellular eukaryotic invertebrates with tube-like or flattened bodies exhibiting bilateral symmetry mainly belonging to the unrelated Nematoda, Platyhelminths or Acanthocephala phyla (Cox, 2009). Species from the Nematoda and Platyhelminth phyla are either free-living or parasitic worms (including parasites of plants or vertebrates). The term “helminth” is sometimes used as a synonym of “worm” but, although there is no clear consensus, it is usually restricted to parasitic worms. Their common particularity as pathogens is that their life cycle is not usually completed in a single individual. Indeed, with some limited exceptions, they do not proliferate within their final host as opposed to other pathogens such as protozoans, bacterias or viruses that have a strong potential of *in situ* exponential population growth. Eggs or larvae are rather externalized to complete the life cycle and infect a new host.

Nematoda are commonly called “roundworms” referring to their long tubular body. Along with arthropods, they belong to the Ecdysozoa clade which share the common characteristic of moulting during growth. Indeed, larvae will go through several maturation steps during their life cycle. Parasitic nematodes count a wide diversity of important pathogens of humans or other vertebrates such as *Ascaris* spp. , *Anisakis* spp., whipworms (e.g. *Trichuris* spp.), pinworms (e.g. *Enterobius* spp.), hookworms (e.g. *Ancylostoma* spp. and *Necator* spp.), filarial worms (e.g. *Onchocerca* spp.), *Trichinella* spp. or *Strongyloides stercoralis*. Infections with hookworms, whipworms, *Ascaris* spp. or *Strongyloides stercoralis* are refered to as “soil-transmitted helminthiasis” (STH) (Jourdan et al., 2017) because transmission occurs through contact with faecally contaminated water, soil or food: adult worms live in their host’s intestine and eggs excreted in the feces contaminate soil. To reach an infective stage, eggs need to mature in the environment, however these helminths do not need an intermediate host. Infection by *Ascaris lumbricoides* or whipworms occurs by faeco-oral transmission, while hookworm larvae can actively penetrates intact skin (Jourdan et al., 2017). On the contrary, filarial worms, *Anisakis* spp. and *Trichinella* spp. are not transmitted *via* the soil but are arthropod- or food-borne parasites. Adults filarial worms living in lymphatic vessels (*Wurchereria bancrofti*), serous cavities or subcutaneous tissue (*Onchocerca volvulus*) release larvae (microfilariae) which have to be taken up by an arthropod vector during a blood meal to be transmitted to another host. *Trichinella* spp. adult worms deliver larvae in intestinal mucosa. After migration through lymphatic and blood vessels, these larvae encyst in muscles and will infect a new host upon ingestion (Gottstein et al., 2009). *Anisakis* spp. have an indirect cycle which depends on predation involving fish and marine mammals and are therefore transmitted *via* seafood.

Because of their flattened shape, **Platyhelminths** are also called flatworms. Two main groups of parasitic worms of vertebrates are found in this Phylum: **Cestoda** and **Trematoda**.

Cestodes (*Taenia* spp., *Echinococcus* spp.) are hermaphrodite segmented worms. These helminths are characterised by an indirect life cycle with production of encysted larvae (metacestode) in muscles or other tissues of the intermediate host and transmission to the final host *via* feeding on these tissues.

Within **Trematoda**, the order Digenea contains the most important parasitic species. Digenea have indirect development with an asexual reproduction phase in their intermediate host, usually an invertebrate such as a gastropod. Infectious larvae (cercariae) are released from intermediate host and can encyst on aquatic weeds or in the tissues of a second intermediate host (e.g. a fish) (Fürst et al., 2012a). In these cases, infections may be acquired by consumption of aquatic products (foodborne trematodiases). Concerning the members of the genus *Schistosoma*, cercariae are released in the water from a freshwater gastropod and actively penetrate the skin of their final host. The majority of members of the order Digenea are hermaphrodites, however schistosomes have separated genders with a clear dimorphism.

Finally, **Acanthocephala** (thorny- or spiny-headed worms) are all parasites with complex life cycles including an encysted stage in an arthropod intermediate host. Transmission depends on predation and adult worms are hooked to the intestinal wall of their final host.

1.2 Epidemiology

Human helminths are widely distributed around the world but the highest prevalence is found in sub-Saharan Africa, the Middle East, Asia, South and Central America and the Caribbean (Herricks et al., 2017). Given their high prevalence in developing countries, the majority of helminthiases are considered as Neglected Tropical Diseases (NTDs) prioritised by the World Health Organization (WHO). Above all, helminthiasis account for the vast majority of NTDs cases (Herricks et al., 2017). As such, these infections are subjected to specific strategies aiming at their prevention, control or eradication (World Health Organization, 2018a). Efforts to control helminthiasis have been implemented by the WHO and include water safety, sanitation and hygiene improvement as well as mass drug administration and vector control (Albonico et al., 2006).

Helminths may induce specific, significant morbidities: intestinal obstruction, volvulus and intussuception for *Ascaris lumbricoides* (Jourdan et al., 2017), lymphedema/elephantiasis or blindness with filarial worms (Nutman, 2013), hypertension, ascites and digestive tract varices caused by

schistosome egg-induced granuloma and fibrosis (Colley et al., 2014), biliary obstruction and cholangitis in foodborne trematodiases (Keiser and Utzinger, 2009) or neurological symptoms due to development of cestode cysts in the brain (Coyle et al., 2012). Certain helminth infections are also associated with development of cancers (e.g. *Schistosoma haematobium*, *Clonorchis sinensis*, *Opisthorchis viverrini*) (Bouvard et al., 2009; Gryseels et al., 2006; Keiser and Utzinger, 2009). In addition, more insidious effects associated with low burden chronic infections cannot be overlooked (Hotez et al., 2008). These aspecific disabling morbidities are usually the consequences of an altered nutritional status linked to gut inflammation, diarrhea, intestinal bleeding and parasites feeding on tissues (World Health Organization, 2018c) leading to weakness and impaired development. Helminth infections thus have a profound impact on population health status based upon both their high prevalence and debilitating consequences. The "Disability-Adjusted Life Year" (DALY) parameter helps summarize and quantify this impact by integrating both mortality and morbidity. Calculated as the sum of years of life lost due to premature mortality and years of healthy life lost due to disability, DALY expresses the impact of a disease or injury on health status when compared to an ideal health status (Lopez et al., 2006; World Health Organization, 2014). For helminthiases, grade of disability depends on infection intensity and associated symptoms or sequelae (Pullan et al., 2014).

The most prevalent helminth species belong to the STH group with *A. lumbricoides* infecting around 800 million people and inducing 1.27 million DALYs followed by *T. trichiura* and hookworms with approximatively 480 and 470 million of cases and 0.58 and 2.18 million DALYs, respectively (Herricks et al., 2017) (Figure 1). The majority of cases occurs in Asia, mostly India and China, with a prevalence that can reach up to 50% or more in some Asian countries (Malaysia or the Philippines) or certain islands of Oceania. Sub-Saharan Africa and Latin America also have high absolute numbers of cases and/or high prevalences (Herricks et al., 2017; Pullan et al., 2014).

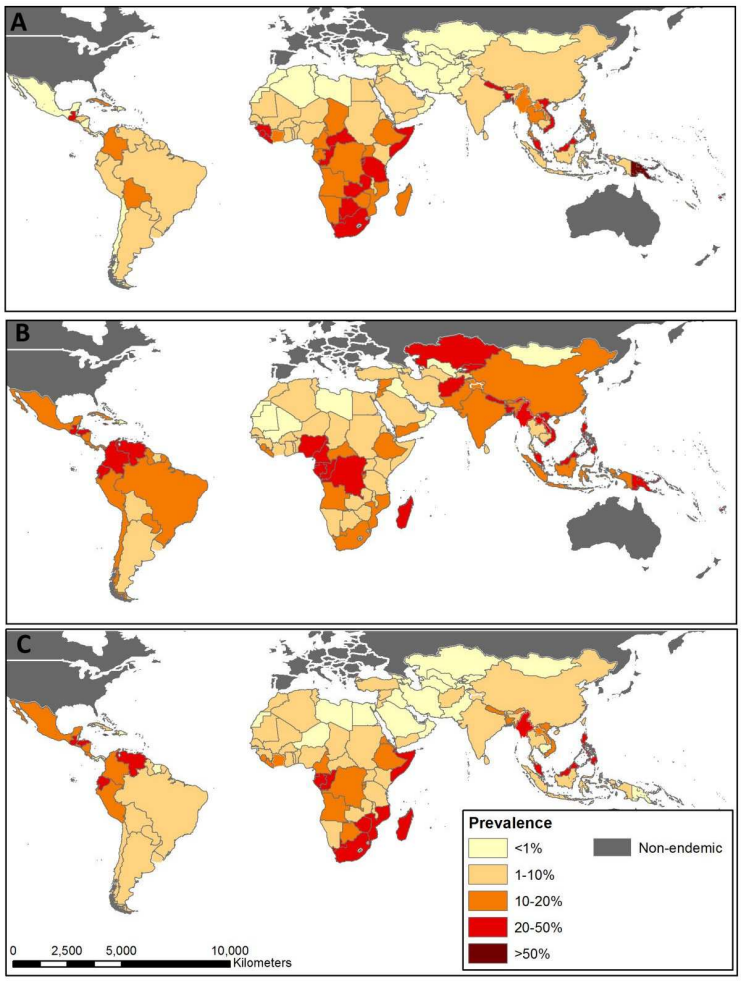

Figure 1. Distribution of soil-transmitted helminth infection prevalence in 2010 by species. (A) hookworm, (B) *Ascaris lumbricoides* and (C) *Trichuris trichiura*; based on geostatistical models for sub-Saharan Africa and available empirical information for all other regions. From (Pullan et al., 2014).

Schistosomiasis is also a higly prevalent disease with 290 million cases reported around the world and 3.06 million DALYs (Herricks et al., 2017). The main species of schitsosomes infecting humans are *S. mansoni*, *S. japonicum*, *S. mekongi*, *S. intercalatum* (intestinal and hepatic schistosomiasis) and *S. haematobium* (uro-genital schistosomiasis) (Gryseels et al., 2006) (Figure 2). Ninety percent of schistosome infections occur in sub-Saharan Africa, but schistosomiasis is also present in the Arabian Peninsula, South-east Asia and South America (World Health Organization, 2018b). Schistosome species have an important specificity for their intermediate host, therefore their distribution correlates with that of the freshwater snail species that sustain their asexual replication (Gryseels et al., 2006).

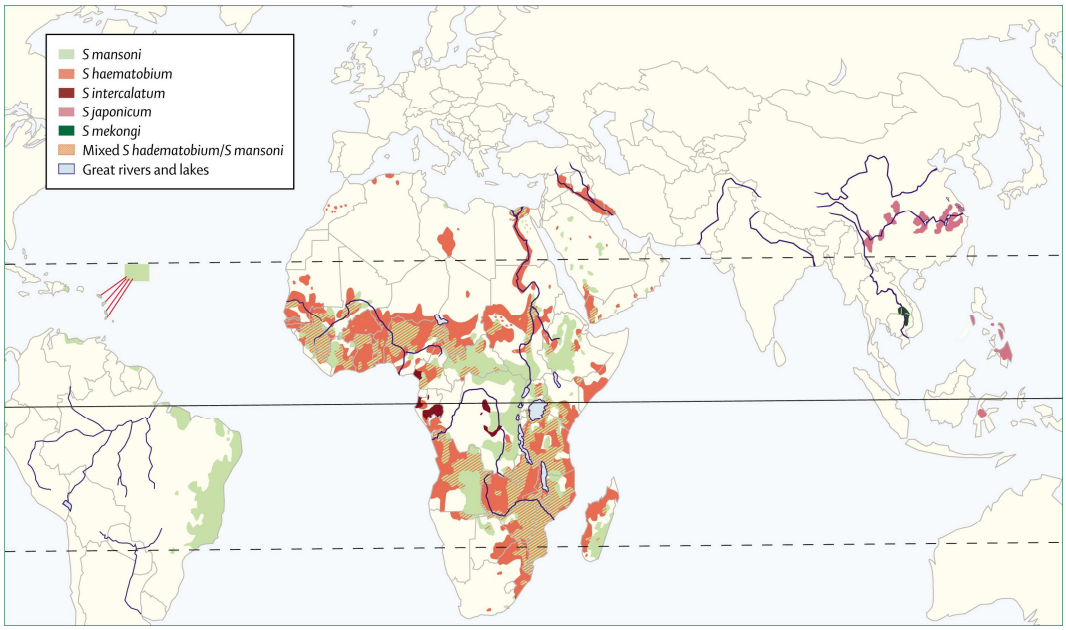

Figure 2. Global distribution of schistosomiasis. Main foci: *S mansoni* -much of sub-Saharan Africa, northeast Brazil, Surinam, Venezuela, the Caribbean, lower and middle Egypt, the Arabic peninsula; *S haematobium* - much of sub-Saharan Africa, Nile valley in Egypt and Sudan, the Maghreb, the Arabian peninsula; *S japonicum* - along the central lakes and River Yangtze in China; Mindanao, Leyte, and some other islands in the Philippines; and small pockets in Indonesia; *S mekongi* - central Mekong Basin in Laos and Cambodia; *S. intercalatum* - pockets in west and central Africa. From (Gryseels et al., 2006).

Foodborne trematodiases comprise infections with liver flukes (*C. sinensis*, *Fasciola hepatica*, *F. gigantica*, *O. felineus*, *O. viverrini*), lung flukes (*Paragonimus* spp.) and intestinal flukes (*Echinostoma* spp., *Fasciolopsis buski*, *Heterophyes* spp., *Metagonimus* spp.) (Fürst et al., 2012b), concern 80 million people and induce 3.63 million DALYs (Herricks et al., 2017). The geographical distribution of these infections, which are mostly found in Asia and South America, can be linked to eating habits such as consumption of raw fish products (Fürst et al., 2012a), however *Fasciola* spp. and *Paragonimus* spp. are more broadly distributed with cases reported in North America, Europe and Africa (Fürst et al., 2012a; Keiser and Utzinger, 2009).

Lymphatic filariasis is a mosquito-borne disease that affects 44 million people and induces 2.02 million DALYs, mostly in sub-Saharan Africa and South and South-east Asia (Herricks et al., 2017). The majority of cases are caused by infection with *W. bancrofti* but two other filarial nematodes (*Brugia malayi* and *B. timori*) may also be the source of the infection (Taylor et al., 2010). Another species of filarial nematodes, *O. volvulus*, is responsible for onchocerciasis affecting 17 million people with 1.18 million DALYs, mostly in sub-Saharan Africa (Herricks et al., 2017).

Infections with cestodes are much less frequent but can have severe consequences. Indeed, while infection with adult worms is not associated with major complications, development of cystic larval stages in host tissues may have substantial health impacts. *T. solium* cysticercosis and cystic

echnicoccosis concern one and 0.8 million people and induce 0.34 and 0.18 million DALYs, respectively (Herricks et al., 2017). *T. solium*, *E. granulosus* and *E. multilocularis* were ranked as the top three food-borne parasites based on multiple criteria including incidence, disease severity or trade relevance (Boireau, 2014) and therefore pose both human and veterinary medical challenges. *T. solium* is mostly found in sub-saharan Africa, Asia and Latin America (Devleesschauwer et al., 2017; World Health Organization, 2016), *E. multilocularis* distribution is limited to the Northern Hemisphere while *E. granulosus* is more widely distributed (Deplazes et al., 2017). Unlike infections with other helminths, cestode infections remain a public health concern in developed countries (Devleesschauwer et al., 2017; Gottstein et al., 2015), probably due to the important health risks and difficulties of treatment. Furthermore, data indicate that the presence of *E. multilocularis* in red foxes is spreading through Europe with a prevalence that can reach more than 10% in the most affected European countries such as Estonia, Latvia, Lithuania, France, Switzerland or Germany (Gottstein et al., 2015; Oksanen et al., 2016).

Trichinella spp. is present all over the world, Antartica being the only continent where this parasite is not observed (Pozio and Darwin Murrell, 2006). However, the vast majority of human cases occur in Europe (mostly central and eastern countries) (Murrell and Pozio, 2011). Trichinellosis has a much lower global burden than other foodborne helminthiasis, with 500 DALYs (Devleesschauwer et al., 2015).

1.3 Investigating anti-helminth immune response: experimental mouse models

As presented in section 1.1, the term “helminth” encompasses a number of different families and genera from different Phylae and, correspondingly include a wide diversity of life cycles, from direct transmission between hosts to complex life cycles with intermediate hosts, including species with free-living stage. This diversity is also reflected in the variety of organs impacted by helminth infections. Therefore, helminth models involve diverse interactions with the host that allow broad study of type 2 immune responses in many different contexts. An adverse consequence of this feature is that, as opposed to viruses or bacteria, tools for *in vitro* study of helminths are very limited (White and Artavanis-Tsakonas, 2012), although important advances are being made in uncovering full parasite genomes and should open new avenues for genome manipulation in the future (www.wormbase.org).

An important majority of helminths target the gastro-intestinal tract and infect their host orally (soil-transmitted or food-borne helminthiasis), however infection can also occur by direct penetration of the skin or even *via* mosquito bites. The most commonly used helminth models in research will be presented in the following sections.

1.3.1 Nematodes

Three nematode models are frequently used to study the immune response against helminths in mice: hookworm-related *Nippostrongylus brasiliensis* and *Heligmosomoides polygyrus* and filarial worms (*Litomosoides sigmodontis*). Besides, other nematodes infecting humans are also patent in mice (*Trichinella spiralis* or *T. pseudospiralis*, *B. malayi*, *A. suum* or *A. lumbricoides*) or have mouse equivalent (*Trichuris muris*, *Strongyloides venezuelensis*) and are also used in experimental models.

N. brasiliensis is a gastro-intestinal parasite of rodents (naturally infecting rats), similar to the human hookworms *A. duodenale* or *N. americanus*, with an extensive migratory phase. *N. brasiliensis* eggs are excreted in the faeces and release a free-living larva that needs a period of maturation in the environment before becoming infective: following hatching, the L1 larvae molt twice to produce the highly motile and infective L3 stage. Infection occurs through skin penetration, larvae reach blood vessels rapidly (from 11h post-infection) and are transported to the lung where a third molt produces L4 larvae. Larvae then cross the alveolo-capillary barrier, causing lung hemorrghages and chronic lesions leading to emphysema. They migrate up the respiratory tract, are coughed and swallowed to ultimately reach the intestine. After a fourth moult, adult worms mate and the females release eggs begining from day 6 post-infection (Camberis et al., 2003) (Figure 3). Experimental infection of mice is usually performed *via* subcutaneous (sc) injection of L3 larvae. As opposed to rats, infected mice naturally clear *N. brasiliensis* infection by day 9-11 post-infection, with the exception of parasite strains adapted to the mouse. Nevertheless, full migration is completed and a strong systemic type 2 immune response is induced.

H. polygyrus is a mouse gastro-intestinal helminth used to model hookworm infections. Its lifecycle differs from that of *N. brasiliensis* by being exclusively gastro-intestinal. Experimental infections are performed by gavage of infective L3 larvae. Importantly, as a mouse parasite, it can establish chronic infection in susceptible mice, even though a great variation in susceptibility exists between mouse strains (Reynolds et al., 2012). Eggs are excreted for months in the faeces and hatch in the environment. Similarly to *N. brasiliensis*, larvae moult twice before becoming infective L3. After faceo-oral transmission, L3 encyst in the duodenal serosa by day 1 or 2 post-infection and moult twice. Adults return to the intestinal lumen at day 10 to mate, and egg laying begins around day 14 (Camberis et al., 2003; Johnston et al., 2015). The immune response during *H. polygyrus* infection is first dominated by a type 2 immune response before development of a regulatory response (Finney et al., 2007).

As opposed to filarial nematode species such as *Onchocerca* spp. and *Brugia* spp. that do not complete their lifecycle in mice, the filarial nematode *L. sigmodontis* is a natural parasite of the cotton rat *Sigmodon hispidus* and succesfully completes its cycle in BALB/c mice. *L. sigmodontis* L3 larvae

are transmitted by mite bites but subcutaneous injection can also be used for infection. Larvae then migrate via lymphatic system and reach serous cavities (pleural cavity) in 3 to 6 days. There, they mature, molt and become adults by day 25-30 post-infection. Filarial worms are ovoviviparus, adults *L. sigmodontis* releasing microfilariae (the first larval stage) that will invade the blood circulation, whereupon they can be ingested by their intermediate host in which they then mature in L1 larvae and further develop to reach the infective L3 stage (Hoffmann et al., 2000). *L. sigmodontis* induces a type 2 immune response, however, certain naturally infection-resistant strains develop a mixed type 1 – type 2 response (Babayan et al., 2003). The presence of a regulatory response in BALB/c mice drive their susceptibility (Taylor et al., 2005).

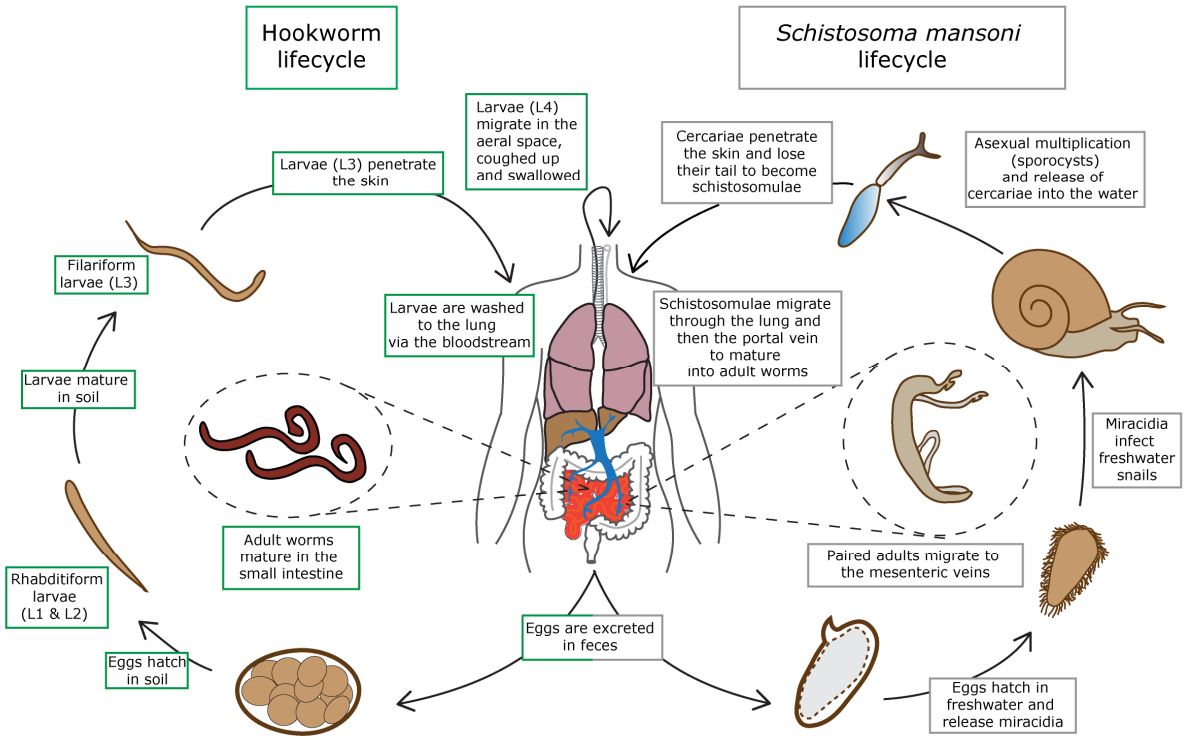

Figure 3. Graphical representation of the life cycles of hookworms (human: *Necator americanus* or *Ancylostoma duodenale*; mouse: *Nippostrongylus brasiliensis*) and *Schistosoma mansoni*. From (Rolot and Dewals, 2018).

1.3.2 Trematodes

Studies of immune responses against trematodes have mostly focused on *Schistosoma* spp. parasites. *S. mansoni* is the species most studied within the genus *Schistosoma*. As a trematode, it has an indirect life cycle with a freshwater snail as its intermediate host. Eggs are excreted in the faeces of the final host and hatch in contact with water. The ciliated larvae, called miracidia, thus released reach and penetrate the intermediate host. The larvae then develop into sporocysts and begin to reproduce asexually. Four to 5 weeks after infection, the snail begin to release large numbers of cercariae, the larval infective stage for vertebrates. Cercariae penetrate the final host's skin, transform into a schistosomula and reach the

circulation within 48 hours. They then migrate first through the lung and then within the systemic circulation to reach the portal system and the mesenteric vessels. There, adults live for up to 30 years as a a mating pair, the long and thin female lying within the gynaecophoric canal of the shorter but larger male. Egg laying begins 4 to 6 weeks after infection. Eggs are laid in the mesenteric vein and burrow their way through the intestinal wall to reach the lumen and be excreted in the faeces. However, a significant proportion of eggs are swept away by the blood flow and get trapped in the liver where they elicit a strong type 2 granulomatous inflammation (Allen and Wynn, 2011; Gryseels et al., 2006; Walker, 2011) (Figure 3). Inflammation as well as tissue damage and remodeling elicited in reaction to the worms' eggs are responsible for the main clinical signs including diarrhoea, hematochezia, hepatomegaly, splenomegaly, ascites or hematuria (Colley et al., 2014). In the first weeks of infection, the immune response is dominated by a type 1 response however with onset of egg laying, it is surpassed by the emergence of a strong type 2 immune response. Indeed, the eggs are strong inducers of type 2 immune responses (Grzych et al., 1991; Pearce et al., 1991; Pearce and MacDonald, 2002; Vella and Pearce, 1992). More precisely, the secreted glycoprotein omega-1 (ω-1) from *S. mansoni* eggs and also found in solube egg antigens (SEA) mixture, is one of the main driver of type 2 immunity (Everts et al., 2009; Steinfelder et al., 2009). After a peak at around 8 weeks post-infection, the type 2 immune response is then downmodulated.

S. mansoni cercariae successfully infect mice percutaneously and complete the entire life cycle. *S. mansoni* infection of laboratory mouse is well-described and has previously been used as a model for human pathology (Fallon, 2000). To study the immune response restricted to *S. mansoni* eggs, eggs collected from infected livers can also be used for direct immunization. A first sensitization by intraperitoneal (ip) injection of eggs, followed by an intravenous injection 14 days later leads to a robust formation of granulomas in the lung (Joyce et al., 2012). Injections of SEA or ω-1 can also be used to induce strong type-2 immune responses in mice (Everts et al., 2009).

1.3.3 Cestodes

Cestodes have a strict indirect life cycle. Eggs eliminated in the faeces of the final host are ingested by the intermediate host (arthropod or vertebrate, depending on the species) and larvae (oncospheres) develop into metacestodes after tissue migration. Ingested metascestodes lead to the formation of adult worms in the intestine of the final host. Alternatively, when humans ingest eggs of *T. solium* or *Ecchinococcus* spp. they develop metacestodes in various tissues.

The human parasites *Hymenolepis diminuta* and *H. nana* also productively infect mice. Both the intestinal adult and metacestode stages are studied. The intestinal adult stage is achieved by oral gavage

of metacestodes and metacestodes can be studied either following ingestion of eggs or by direct injection of metacestodes (Ito et al., 1988; McKay et al., 1990).

Taenia solium is responsible for human cysticercosis, and mouse models include the intraperitoneal or intracranial injection of *Mesocestoides corti* or *T. crassiceps* metacestodes (Alvarez et al., 2010; Cardona et al., 1999; Terrazas, 2008). The particularity to reproduce asexually in the metacestode stage is used in biological models: *T. crassiceps* larvae injected in peritoneal cavity cause long-lasting infection and reproduce by asexual budding. An early type 1 immune response at the infection site is shifted to a mixed type 1/type 2 response with production of both IFN-γ and IL-4 (Toenjes and Kuhn, 2003; Toenjes et al., 1999).

Intraperitoneal injection of proscoleces extracted from *E. multilocularis* or *E. granulosus* hydatid cysts leads to formation of cysts and is used to study cystic echinococcosis (Ma et al., 2016; Wang et al., 2016). *E. granulosus* induce an initial type 2 immune response which changes to a more mixed type 1/2 later on (Dematteis et al., 1999).

1.4 Immune response to helminths

1.4.1 Orientation of the immune response

For several reasons, helminth infections may represent a challenge for the host immune system. First, the helminth size amply surpasses that of immune cells, making direct phagocytosis impossible. Instead, killing of helminth larvae has been shown to be achieved *in vitro* by accumulation of eosinophils around their target (Buys et al., 1981; Patnode et al., 2014). Secondly, the host immune system must be able to deal with the different life cycle stages of the parasite (eggs, larvae or adult worms) against which the development of different responses may be needed. In addition, as helminths often establish chronic infections in which elimination of the parasite is not possible, tolerance mechanisms often develop to dampen unsuccessful excessive inflammation and collateral damages. Furthermore, numerous helminths are characterized by a multi-organ migration phase which is often associated with tissue damage. Immune responses aimed at containing parasites and/or maintaining tissue integrity are therefore needed. For these reasons, immunity to helminth infections is a fine equilibrium between parasite containment and/or elimination (control) and minimization of collateral damages associated with inflammation (tolerance).

The immune system is composed of numerous elements, either cells or molecules. These elements can be enrolled in an important variety of mechanisms. Thanks to this variety, the immune system response can be precisely shaped to face specific threats. As illustrated in figure 4, the orientations of

immune responses are classified based on $CD4^+$ T lymphocyte polarizations, each orientation being characterized by typical cytokines and transcription factors and associated with particular pathological processes.

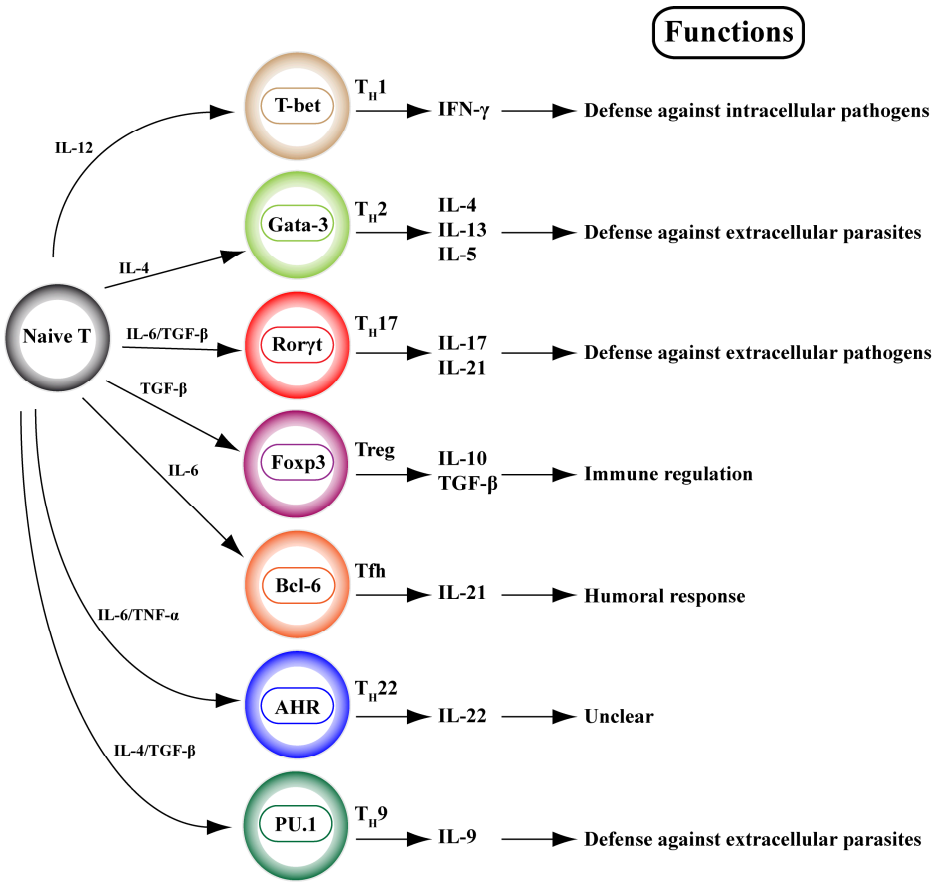

Figure 4 : Polarization of T helper cell responses. Summary of the different orientations that $CD4^+$ T cell can adopt during activation by their cognate antigens, in response to cytokine environment. Each subtype of $CD4^+$ T cells expresses a specific transcription factor, produces a particular set of cytokines and displays specific effector functions. Adapted from (Bonelli et al., 2014)

As rapidly replicating intracellular pathogens, viruses typically induce type 1 immunity that is based mostly on pro-inflammatory and cytotoxic factors. Such response appears unsuitable to deal with macroparasites for the reasons listed above. Instead and despite their wide diversity, helminth infections are consistently associated with type 2 immunity which major characteristics are anti-inflammatory and wound-healing properties. As discussed in the next section, the type 2 immune response is mostly associated with protection against helminth infection. A protective role for type 2 immune responses was also found against venoms (Marichal et al., 2013; Palm et al., 2013). However, similar responses may also be deleterious when they develop against normally harmless substances and mediate allergic pathologies (Holgate, 2012).

In type 2 immunity, $CD4^+$ T helper lymphocytes are commited towards a Th2 activation state characterized by the expression of transcription factor GATA-binding protein 3 (GATA-3) and signal

transducer and activator of trancription(STAT)-5 and -6 and by the production of type 2 cytokines interleukin(IL)-4, IL-13, IL-5 and IL-9. The type 2 immune response also involves secretion of immunoglobin(Ig)E and IgG1 by B lymphocytes and recruitment and activation of innate immune cells such as eosinophils, alternatively activated macrophages (aaMφ), basophils, mast cells or group 2 innate lymphoid cells (ILC). These elements will also produce type 2 cytokines, participate in initiation and maintenance of type 2 immune responses and, through their effector functions, induce typical pathological changes associated with type 2 immunity (e.g. smooth muscle contractility, mucus hyperseretion, tissue remodeling).

1.4.2 Initiation of helminth-induced type 2 immunity

An immune response against a pathogen is induced upon recognition of typical molecular patterns by pattern recognition receptors (PRR), amongst which membrane-bound toll-like receptors (TLR) or C-type lectin receptors (CLR). PRRs, harbored by innate immune cells, recognize various sets of foreign or anormal molecular patterns associated with infection with different classes of microorganisms. Recognition of these pathogen- or danger-associated molecule patterns (PAMPs or DAMPs) by innate immune cells will lead to production of signals that will tailor the immune response. These molecular features, their signalling pathways and the characteristics of the response they induce are well described for type 1/type 17 responses against viral, bacterial or fungal infections but much less is known about induction of type 2 immune responses, especially during helminth infections (Iwasaki and Medzhitov, 2015). Nevertheless, several PRRs have been implicated in the recognition of helminth products and molecular patterns from both parasite surfaces and excretory-secretory (ES) products are susceptible to be recognised by PRRs (White and Artavanis-Tsakonas, 2012). Products from various helminth species such as *S. mansoni*, *T. spiralis*, *N. brasiliensis* or *L. sigmodontis* may notably signal through TLR2, TLR3 or TLR4 (Aksoy et al., 2005; Pellefigues et al., 2017; Rodrigo et al., 2016; van der Kleij et al., 2002; Zhang et al., 2018). Shared motives in helminth glycans are not commonly found in vertebrates. They constitute targets for the host immune system and have been identified to drive type 2 immune responses (Okano et al., 1999; Prasanphanich et al., 2013; White and Artavanis-Tsakonas, 2012). Thus C-type lectin receptors (CLRs) have been suggested to represent major PRRs in the case of helminth infections (Vázquez-Mendoza et al., 2013). In accordance with this, numerous molecular patterns from helminth carbohydrates are recognized and internalized by CLRs, notably dendritic cell (DC)-specific intercellular molecule-3-grabbing non-integrin, macrophage galactose-type lectin or mannose receptor and trigger immune signals (deSchoolmeester et al., 2009; Everts et al., 2012; Hussaarts et al., 2014; van Die et al., 2003; van Liempt et al., 2007; van Vliet et al., 2005).

Antigen-presenting cells, amongst which DCs are the principal representant, are the link between the innate and the adaptive immune responses. Their role in presentation of captured foreign antigens to adaptive cells, along with production of costimulatiory signals, leads to activation and importantly polarization of lymphocytes that specifically recognize the pathogen against which the response is being mounted. Thus, DCs not only play a role in activation of the adaptive immune response, they also shape this response depending on the signals they receive and are thereby a key factor in its adequacy to the risks presented by a particular pathogen. To be able to induce a T cell response, DCs recognize, process and present foreign antigens sampled from their environment and undergo maturation events such as upregulation of class II major histocompatibility complexes (MHC), costimulatory molecules (CD40, 80 and 86) and production of pro-inflammatory cytokines, which help drive T helper lymphocytes polarization. DCs clearly participate in the polarization of T lymphocytes during helminth infections, since it has been shown that the Th2 response against several helminth infections is impaired in mice devoid of $CD11c^+$ cells (Phythian-Adams et al., 2010; Smith et al., 2012; Smith et al., 2011). Moreover, DCs stimulated with helminth products induce Th2 differentiation in vitro or in vivo, indicating that DCs are sufficient to drive Th2 polarization (Balic et al., 2004; MacDonald et al., 2001; Smith et al., 2012; Whelan et al., 2000). On the contrary, the type 2 innate immune response is not affected by $CD11c^+$ cells depletion (Smith et al., 2012). Surprisingly, helminth products mostly fail to induce classical signs of DCs maturation such as upregulation of CD40, 80 or 86 (MacDonald et al., 2001; Whelan et al., 2000). Helminth products rather appear to have a role in rendering DCs refractory to conventional type 1 stimulation. For example, they have a striking inhibitory effect on type-1 polarizing capacities of DCs, countering LPS-induced proinflammatory activation (Kane et al., 2004; Rodríguez et al., 2015; van Liempt et al., 2007) and suppressing IL-12 production from DCs (Balic et al., 2004; Cervi et al., 2004; Kane et al., 2004). It is thought that in absence of Th1 priming signals, DCs spontaneously induce Th2 differentiation. Consistent with an inhibitory role of helminth products on DCs, CLR detection of ω-1 from *S. mansoni* SEA is not sufficient to polarize towards a type 2 immune response but needs its RNase activity. After internalization, depending on its glycosylation, ω-1 impairs protein synthesis in DC in a RNase-dependent manner (Everts et al., 2012). However, the DC response to helminths is not limited to a « deactivation » state. Polarization of Th2 cells by DCs is associated with activation of several pathways. It was notably shown that NF-κB1 pathway, STAT-5, IRF4, upregulation of Notch ligand Jagged-2 or OX40L are involved in the ability of DCs to polarize Th2 differentiation (Artis et al., 2005; Gao et al., 2013; Ito et al., 2005).

Helminths have an important damaging action on the host tissue. Injured barrier sites such as epithelial cells release cytokines named **alarmins** that act as potent inducers of type 2 immune responses. Moreover, induction of type 2 immune responses is typically observed in tissue or cellular damaging circumstances: physical wounds, exposition to allergens or venoms enzymes (Kheradmand et

al., 2002; Palm et al., 2013), inert particles (Mishra et al., 2011b) or adjuvants (alum) (Gause et al., 2013; Kool et al., 2011). Early events in the induction of anti-helminth responses include the secretion of the epithelial cytokines thymic stromal lymphopoietin (TSLP), IL-33 and IL-25 which are involved in initiating type 2 immunity including stimulation of ILC2 and Th2 $CD4^+$ lymphocytes to produce type 2 cytokines (Fort et al., 2001; Ito et al., 2005; Schmitz et al., 2005). The relative importance of these cytokines in type 2 immune responses depends on the helminth species involved and on the localization of the response (Harris and Loke, 2017), in addition evidence indicates that they may have redundant or synergistic roles (Vannella et al., 2016).

IL-33 is released during cellular necrosis, and is therefore relevant in helminth-induced tissue damage, but can also be secreted by living cells such as macrophages (Mirchandani et al., 2012; Ohno et al., 2009). Signalization *via* its receptor IL-33R/T1/ST2 has been shown to play a role in inducing an optimal type 2 immune response (Humphreys et al., 2008; Schmitz et al., 2005; Townsend et al., 2000). IL-33 is an actor in the protection against several helminth infections (Ajendra et al., 2014; Hung et al., 2013; Scalfone et al., 2013) but could also be involved in exacerbation of type 2 pathologies associated with helminth infections (Du et al., 2013; Yu et al., 2015). Many cell types from both the innate and adaptive immune system express IL-33R and respond to IL-33 stimulation (Lott et al., 2015). Moreover, conditionning of DCs by IL-33 has been shown to induce Th2-like and Treg polarization in $CD4^+$ T cells (Matta et al., 2014; Rank et al., 2009). Nonetheless, typical consequences of IL-33 *in vivo* injection, such as eosinophil infiltration, goblet cell hyperplasia and airway hyperreactivity, also occur in recombinant-activating gene(Rag)-deficient mice (Kondo et al., 2008), and are thus T cell/B cell independent. In line with these observations, the protective role of IL-33 in helminth infection has been shown to be mediated by ILC2 that express high levels of IL-33R (Bouchery et al., 2015; Neill et al., 2010) and macrophages (Yang et al., 2013).

IL-25 (or IL-17E) is involved in early production of type 2 cytokines (Fort et al., 2001) and is essential for protection against several nematode (Fallon et al., 2006; Owyang et al., 2006; Pei et al., 2016; Price et al., 2010; Zaiss et al., 2013) or trematode infections (Muñoz-Antoli et al., 2016) independently of the presence of lymphocytes (Fallon et al., 2006). Initially, IL-25 was shown to be expressed by Th2 cells (Fort et al., 2001) but recent data comprehensively identified tuft cells, an intestinal epithelial cell subset as the main source of IL-25 in naive mice (Gerbe et al., 2016; Howitt et al., 2016; von Moltke et al., 2016). Tuft cells have been shown to constitutively produce IL-25 but not IL-33 or TSLP. Furthermore, during *N. brasiliensis* infection, tuft cells appear to be the main source of IL-25 in the intestine. At steady state, IL-25 secreted by intestinal tuft cell induces the production of IL-13 by ILC2, which in turn maintains intestinal tuft cells numbers. This homeostatic mechanism is amplified by helminth infections, leading to increased production of IL-13 by ILC2 and intestinal tuft

cell accumulation. It has been shown that through production of IL-25, tuft cells are the central actor of the induction of type 2 immune response and the protection against intestinal nematodes (Gerbe et al., 2016; von Moltke et al., 2016). Thus, it has been proposed that similarly to PRR-dependent activation of innate immune cells, tuft cells could be triggered by detection of parasite presence *via* their taste receptors (Howitt et al., 2016). Although the short chain fatty acid succinate produced during infection with the protozoan *Tritrichomonas* spp. is sufficient to induce tuft cell expansion, it however remains unknown how helminths do trigger tuft cells activation (Nadjsombati et al., 2018; Schneider et al., 2018)

TSLP secretion by epithelial cells is induced by mechanical injuries or protease detection (Kouzaki et al., 2009; Oyoshi et al., 2010). Mast cells and basophils are also a potential source of TSLP during type 2 immune responses (Sokol et al., 2008; Soumelis et al., 2002). It is a central factor in induction of type 2 immune responses during allergic airway inflammation (Zhou et al., 2005) but its requirement for induction of type 2 immune responses during helminth infections is highly variable, from essential during *T. muris* infection (Taylor et al., 2009a) to dispensable against *H. polygyrus* (Massacand et al., 2009). The main target of this cytokine are DCs (Liu et al., 2007). Signalling of TSLP on DCs involves the transcription factor STAT-5 (Bell et al., 2013), induces OX40L and prevents expression of type-1 polarizing cytokines interferon(IFN)-γ and IL-12p40. OX40L expression by DCs trigger Th2 cells differentiation only if IL-12 is not present.Thus through increased OX40L expression and decreased IL-12 production, TSLP-activated DCs allow commitment of T cells towards Th2 activation (Ito et al., 2005). TSLP has been shown to be dispensable during *H. polygyrus* and *N. brasiliensis* infections, since they both secrete products with equivalent effects (Massacand et al., 2009). There is also evidence for a direct action of TSLP on $CD4^+$ T cells for induction of Th2 cells (Omori and Ziegler, 2007).

Other molecules such as uric acid or extracellular ATP are associated with tissue damages and are potent inducers of type 2 immune responses (Kool et al., 2011; Kouzaki et al., 2011).

ILC2s can be activated by alarmins to secret large amounts of type 2 cytokines IL-5 and IL-13. The expansion of ILC2s is a hallmark of helminth infections (Nausch and Mutapi, 2018). Interestingly, rIL-25 treatment of *N. brasiliensis*-infected Rag-deficient mice renders this susceptible strain resistant through an action on ILC2s (Fallon et al., 2006; Price et al., 2010). However, expulsion of *N. brasiliensis* requires the presence of both lymphocytes and IL-25 signalling on ILC2s in the absence of treatment with rIL-25 (Neill et al., 2010). Furthermore, IL-25 and IL-33 expression during *H. polygyrus* infection helps worms expulsion in wild-type (WT) but not Rag-deficient mice (Zaiss et al., 2013). Interestingly, while induction of IL-4 production by IL-25 required the presence of lymphocytes, IL-25 or IL-33 treatment of Rag-deficient mice still induces significant IL-5 and IL-13 production as well as histological changes (Fort et al., 2001; Moro et al., 2010). These data indicate that ILC2s play a central

role in the induction of the type 2 immunity against helminths but may not be sufficient to mediate critical effector functions leading to worm expulsion.

A role in the induction of the type 2 immune response was also proposed for other immune and non-immune cell types. In response to *N. brasiliensis* infection, neurons from the submucosal plexus secrete neuromedin U which is a strong and fast inducer of type 2 cytokines production by ILC2s and has been shown to play a role in efficient parasite expulsion (Cardoso et al., 2017; Klose et al., 2017). Mast cells are essential for induction of type 2 immune responses after *H. polygyrus* or *T. muris* infection, with the ability to respond to extracellular ATP and a link to production of IL-25 and IL-33 stimulating IL-13 production from ILC2s (Hepworth et al., 2012; Shimokawa et al., 2017). Basophils may also represent an early source of IL-4 (Gessner et al., 2005). Indeed, besides the classical IgE-dependent activation, they also respond to IL-33, TSLP, proteases or IL-18 stimulation (Kondo et al., 2008; Phillips et al., 2003; Siracusa et al., 2011; Yoshimoto et al., 1999). Similar to IL-33, IL-18 precursor is present in epithelial cells and can be released from dying cells. IL-18 is also expressed by macrophages and dendritic cells (Dinarello et al., 2013). Furthermore, eosinophils, basophils and mast cells might act as antigen presenting cells (Kambayashi and Laufer, 2014).

The initiation of type 2 immunity involves an intricate network of interactions that is summarized in figure 5. The multiple paths leading to type 2 immunity induction reflect the variety of stimuli resulting in the initation of such response. Identifying the key factors involved in the initiation of type 2 immune responses during helminth infection is a complex task, mainly due to the redudancy within the immune system (Allen and Maizels, 2011). As an example, *S. mansoni* ω-1 has been identified as the main driver the Th2 response against *S. mansoni* eggs. However, despite an impaired capacity to condition DCs to induce Th2 differentiation *in vitro*, ω-1-depleted SEA was still able to induce type 2 immune responses *in vivo*, highlighting the existence of more complex mechanisms *in vivo* (Everts et al., 2009). Furthermore, induction mechanisms are likely to vary depending on helminth species and tissues involved.

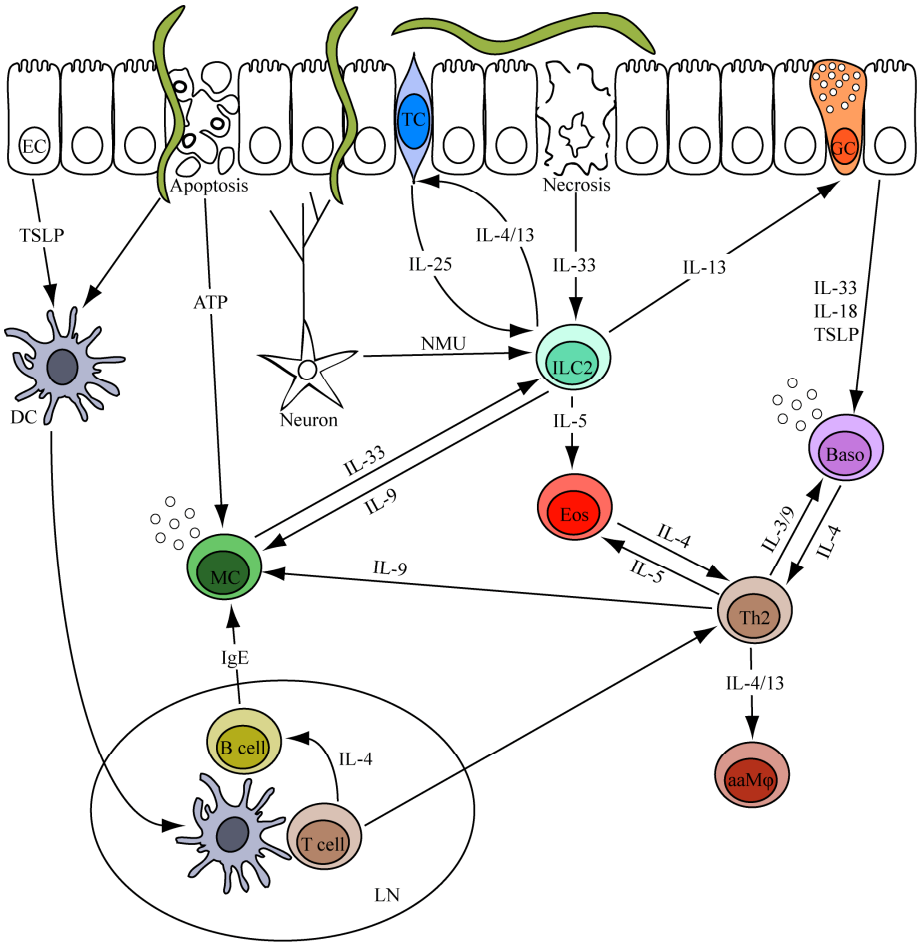

Figure 5 : Induction of type 2 immunity against helminths. Helminth infections can trigger several pathways leading to initiation of type 2 immunity. DCs play a central role in the initiation as they can directly detect helminth molecules, migrate to draining lymph nodes and instruct $CD4^+$ T cells to adopt a Th2 phenotype. DCs capacity to stimulate Th2 differentiation is also influenced by alarmins such as TSLP. Th2 cells secrete large amounts of type 2 cytokines IL-4, IL-13 and IL-5 and sustain B cells isotype switch towards production of IgE and IgG1. Alarmins induce activation of other type 2 immune mechanisms. ILC2, which produce IL-5, 13 and 4, are stimulated by IL-33 released by damaged epithelia, IL-25 released by tuft cells or neuromedin U secreted by neurons, the latter two being able to sense helminth products. Other cell types such as mast cells or basophils also respond to alarmins (extracellular ATP, TSLP or IL-33) and are an early source of IL-4. ATP, also released during tissue damage, stimulates mast cells to produce IL-33, further activating ILC2. Mast cells degranulation is also stimulated by IgE binding or IL-9 secreted by both ILC2 and Th2 cells. IL-5 from ILC2 and Th2 cells attract and expand eosinophils that in turn (like basophils) secrete IL-4 to sustain Th2 responses. IL-4 and 13 promote differentiation of macrophages in alternatively activated macrophages (aaMφ). Cytokine and immune mediators secreted by all these cells promote parasite expulsion and wound healing.
EC = epithelial cell; TC = tuft cell; GC = goblet cell; DC = dendritic cell; ILC2 = type 2 innate lymphoid cell; Baso = basophil; MC = mast cell; Eos = eosinophil; aaMφ = alternatively activated macrophage; TSLP = thymic stromal lymphoietin; NMU = neuromedin U; IL = interleukin; LN = lymph node.
Based on (Gause et al., 2013; Hammad and Lambrecht, 2015; Harris and Loke, 2017)

1.4.3 Effector functions of type 2 immune responses

Anti-helminth immune responses are aimed at eliminating helminths (either by killing or expelling them) to reach sterile immunity whenever possible or, more frequently, to keep the parasite burden to a minimum and to mediate tolerance. Besides, anti-helminth immune responses must deal with tissue

damage. Canonical type 2 cytokines IL-4 and -13 are central players of maintenance and amplification of type 2 immune responses as well as mediation of effector functions. Signalling of both IL-4 and IL-13 is dependent on expression of IL-4Rα (CD124), either in combination with common γ chain (γc, IL-2Rγ or CD132) to form type I IL-4 receptor or with IL-13Rα1 to form type II IL-4 receptor, and is transduced via phosphorylation of STAT-6 (Figure 6). The common γ chain and therefore type I IL-4 receptor is mainly expressed on hematopoietic cells and specifically binds IL-4. Non-hematopoietic cells express high levels of IL-13Rα1 and only low levels of γc, therefore mostly expressing the type II IL-4 receptor which can bind both IL-4 and IL-13. Myeloid cells express both types of IL-4 receptor (Junttila, 2018). IL-13 also bind IL-13Rα2 with high affinity. IL-13Rα2 can act as a secreted decoy receptor to neutralize IL-13 but also has a role as a cell surface receptor. Signaling of IL-13 on IL-13Rα2 induces activation of *TGFB1* promoter and promotes fibrosis (Fichtner-Feigl et al., 2006). Thus, while these cytokines have overlapping functions, they also mediate specific functions. As proven in different settings using IL-4-antibody complexes (IL-4c) treatment or mice deficient for IL-4, IL-13, STAT-6, and/or IL-4Rα, protection against helminth infections requires the correct development of type 2 immune responses with a central role for IL-4 and IL-13 (Bancroft et al., 1998; Brunet et al., 1997; Finkelman et al., 2004; Herbert et al., 2004; McKenzie et al., 1999; Urban et al., 1995; Urban et al., 1998).

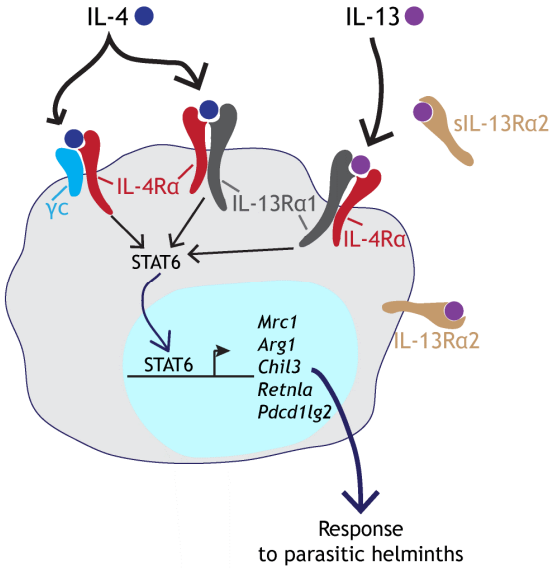

Figure 6. IL-4Rα-dependent alternative macrophage activation during helminth infection. Type 2 innate and adaptive immune cells produce the cytokines IL-4 and IL-13 after exposure to parasitic helminths. In the laboratory mouse, these cytokines induce aaMφ which are characterized by the upregulation of signature genes. IL-4Rα, IL-4 receptor alpha chain; γc, common gamma chain; IL-13Rα1, IL-13 receptor alpha 1 chain, IL-13Rα2, IL-13 receptor alpha 2 chain (sIL-13Rα2, secreted form); STAT-6, signal transducer and activator of transcription 6; *Mrc1*, mannose receptor (CD206); *Arg1*, arginase 1; *Chil3*, chitinase-like 3 (Ym1); *Retnla*, resistin-like molecule alpha (Relm-α), *Pdcd1lg2*, programmed cell death 1 ligand 2 (PD-L2). From (Rolot and Dewals, 2018).

Cells from both innate and adaptive immune systems cooperate in a complexe network to sustain induction, maintenance and effector function of the type 2 immune response (Figure 5). Each contributing cell type produces cytokines and inflammatory mediators to activate or enhance other immune cell functions or to instruct non-haematopoietic cells such as epithelial or smooth muscle cells to mediate effector functions. While Th2 cells are seen as the central actor of type 2 immune response, innate immune cells do not only initiate Th2 differentiation, but they also directly participate in

protective effector functions, some of which can be mediated even in the absence of lymphocytes (Gause et al., 2013; Kondo et al., 2008).

Different strategies are developed by the type 2 immune response to defeat helminth infection, including the so-called “weep and sweep” response, impairment of parasite fitness, wound repair (and parasite encapsulation) and regulation of excessive inflammation.

In the digestive tract, parasite clearance is facilitated by the **“weep and sweep”** response, which includes increase of epithelium permeability, mucus production, epithelium turn over and smooth muscle contractility to sweep out the worms present in the lumen. The responsiveness of intestinal epithelial cellto type 2 cytokines IL-4 and -13 is crucial in this response (Gerbe et al., 2016; Herbert et al., 2009; Urban et al., 2001). IL-13 particularly has an important impact on worm expulsion, it stimulates goblet cell hyperplasia and drives overproduction of mucus (McKenzie et al., 1998). Increase of permeability of intestinal epithelium, induced by type 2 cytokines, also contributes to the “weep and sweep” response (Finkelman et al., 2004; Madden et al., 2004). Through secretion of immune mediators containing proteases, mast cells mediate the degradation of tight junctions and modify epithelium permeability (McDermott et al., 2003). Mast cells are critically involved in the expulsion of certain helminth species (Knight et al., 2000; Sasaki et al., 2005). IL-13-driven increase in intestinal epithelial cells proliferation and migration along crypts during *T. muris* infection is associated with increased resistance to the parasite. This process is especially relevant for a parasite such as *T. muris* which lives partially buried in the intestinal epithelium (Cliffe et al., 2005). IL-4 and IL-13 increase the contractile capacity of smooth muscle cells favoring intestinal helminth expulsion (Horsnell et al., 2007; Zhao et al., 2003). Interestingly, during helminth infection smooth muscle cells interact with other component of type 2 immunity and impact on goblet cell hyperplasia and type 2 cytokines production (Horsnell et al., 2007).

Type 2 cytokines stimulate the intestinal epithelium to produced effector molecules that **impair parasite fitness**. While Muc2 is physiologically produced in the intestine, Muc5ac is only produced during inflammation. When Muc5ac is produced, the porosity of the mucus network is decreased and affects worm viability in *T. muris* infection (Hasnain et al., 2011). Modification in the composition of mucus can increase the barrier between luminal worms and the intestinal epithelium, impairing the capacity of worms to feed on epithelial cells (Bansemir and Sukhdeo, 2001). However, Muc5ac appears to directly act on the parasite to alter its viability (Hasnain et al., 2011). Resistin-like molecule(Relm)-β is expressed by goblet cells in response to IL-4 and IL-13 and interferes with a worm’s chemosensory organs hampering its nutrition, fecundity and viability (Artis et al., 2004; Herbert et al., 2009). Impairment of worm fitness is also mediated by arginase(Arg)-1, secreted by aaMφ. Arg-1 metabolizes

L-arginine and produces L-ornithine which helps in trapping *H. polygyrus* larvae by directly impacting their motility (Anthony et al., 2006; Esser-von Bieren et al., 2013).

Eosinophils, neutrophils and macrophages are able to mediate an **antibody-dependent cellular cytotoxic reaction**. Antibody-coated worms are recognized by the Fc receptor of these cells and mediates release of toxic molecules which directly kill larvae by secretion (O'Connell et al., 2011; Venturiello et al., 1993, 1995). Release of extracellular traps by these cells has also been proposed to help with the killing process by trapping larvae (Bonne-Année et al., 2014). The role of eosinophils in protection is not straigthfoward, some evidence indicates a role for protection (Huang et al., 2015; Shin et al., 1997; Vallance et al., 2000), however eosinophils may not be an absolute requirement and, on the contrary, may sometimes protect larvae (Gebreselassie et al., 2012).

The type 2 immune response is associated with **wound healing** (Gause et al., 2013; Seno et al., 2009) which is essential to maintain tissue integrity during helminth infection. Type 2 immune response-mediated tissue healing is especially important against damaging migrating larvae (Chen et al., 2012a) or to avoid bacterial contamination from the intestine (Herbert et al., 2004). In addition, production of toxic enzymes may need to be contained by the formation of granulomas to protect the healthy surrounding tissue (Herbert et al., 2004). Wound healing critically depends on IL-13 through induction of fibrosis (Fallon et al., 2000; Fichtner-Feigl et al., 2006). Macrophages respond to IL-13 and secrete various effector molecules involved in fibrosis. During metabolization of L-arginine, Arg1 secreted by aaMφ produce proline, a component of collagen (Wynn, 2004). Matrix metalloproteinases regulate matrix degradation. Other aaMφ-derived products, such as TGF-β and Relm-α act directly on fibroblasts to stimulate collagen formation (Gieseck et al., 2018). It is noteworthy that direct IL-4Rα signalling on fibroblasts may be critical for fibrosis (Gieseck et al., 2016). Insulin-like growth factor 1 expressed by aaMφ has also been implicated in restoration of tissue integrity (Chen et al., 2012a).

Amphiregulin has been shown to be important for epithelium integrity (Monticelli et al., 2011). This epidermal growth factor-like molecule can be secreted by various cell types (basophils, mast cells, neutrophils, ILC2, $CD4^+$ T cells) in a context of type 2 immune responses and is a factor of *T. muris* resistance (Zaiss et al., 2006; Zaiss et al., 2015a) and *H. polygyrus* expulsion (Minutti et al., 2017b).

Thus, the type 2 immunity is mostly associated with increased protection against helminth infection. However, some helminth-associated pathologies are linked to a deleterious aspect of the type 2 immune responses. Unlike in nematode infections, protection against *S. mansoni* infection is not dependent on parasite expulsion. *S. mansoni* adult worms persist for years within their host (Pearce and MacDonald, 2002) and mice with higher survival rates can harbour a number of worms similar to more susceptible

strains but show decreased egg-induced inflammation (Herbert et al., 2008; Pesce et al., 2009a; Vannella et al., 2014). Thus, protection against schistosomiasis rather depends on the control of egg-induced inflammation. The type 2 immune response, notably *via* signalization through IL-4Rα, is essential for survival during schistosomiasis through its capacity of down-regulating the tissue-damaging type 1 inflammatory immune response, supporting the suitable formation of granulomas around eggs that sequester toxins and promoting wound healing to ensure tissue integrity (Brunet et al., 1997; Herbert et al., 2004; Herbert et al., 2008; Jankovic et al., 1999). During chronicity however, type 2 immune responses and in particular IL-13 also lead to hepatic fibrosis which is an important complication in schistosomiasis and is responsible for major symptoms (Chiaramonte et al., 1999; Ramalingam et al., 2008). When IL-13, but not IL-4, signalling is impaired, an important reduction of hepatic fibrosis is associated with increased long-term survival (Fallon et al., 2000; Ramalingam et al., 2008). However, given the counter-regulatory role of type 1 and type 2 immune response on each other, blocking of part of the type 2 immune response lead to deleterious increased in type 1 immune response. Blocking both IL-13 and IFN-γ avoids this problem. (Ramalingam et al., 2016).

In some cases, a type 1 rather than a type 2 immune response is beneficial for the host. The immune response is skewed towards a type 1 immune response during the first weeks of *S. mansoni* infection and a strongly polarized type 1 immune response is associated with increased resistance to reinfection by *S. mansoni* cercariae (Wynn et al., 1996). The type 1 immune response also mediates protection against larval stages of *T. crassiceps* infection (Rodríguez-Sosa et al., 2004).

1.4.4 Helminth induced immune modulation

Numerous helminths establish chronic infection without inducing any overt pathology or killing their host. This coexistence is possible because helminths have developed immune-regulatory elements to bias immune responses and prevent elimination and immunopathologies. Indeed, asymptomatic but chronicaly infected patients harbor a strong regulatory response that is not present in patients that develop overt pathologies. Furthermore, development of pathology is associated with a strong and more effective type 2 immune response leading to a lower worm burden (McSorley and Maizels, 2012). In other words, regulatory immune responses may be beneficial for both the parasite and its host. Elimination of helminths by chemotherapy often rescued immune responsiveness, thus proving evidence for an active role of helminth in the suppression of immune responses (Grogan et al., 1996; Passeri et al., 2014; Sartono et al., 1995).

With the need for controlling potential excessive amplification of type 2 immune response, leading to immunopathologies, helminths actually often elicit a “modified” type 2 immune response. This response combines type 2 with regulatory immune elements and is associated with chronic infections.

Helminths can, for example, induce expression of IL-10 and transforming growth factor-β (TGF-β), playing an important role in the control of inflammation and in the downregulation of type 2 (as well as type 1) immune responses, impairing helminth elimination (Worthington et al., 2013; Wynn et al., 1997). TGF-β has been shown to promote expansion of $Foxp3^+$ regulatory T cells (Tregs) during helminth infection, Tregs being in turn a source of anti-inflammatory functions and their expansion is correlated with long-term persistence of helminth infections and control of immunopathologies (D'Elia et al., 2009; Taylor et al., 2009c; Turner et al., 2011). Strikingly, some helminths produce their own TGF-β homologues (Johnston et al., 2017). DCs are involved in the induction of Tregs, some helminth signalling pathways on DCs can lead to their ability to promote Tregs while some DC subpopulations appear to specifically induce Tregs (Rodríguez et al., 2017b; Smith et al., 2011; van der Kleij et al., 2002). Induction of co-inhibitory molecules CTLA-4 or PD-1 on T cells is also associated with dampening Th2 cell responses and reduced helminth control (McCoy et al., 1997; van der Werf et al., 2013). Development of an anergic phenotype in $CD4^+$ T cells can also be mediated by repeated stimulation of these cells indicating a physiological response of immune cells to chronic antigen stimulation rather than any specific effect of the pathogen (Taylor et al., 2009b).

Likewise, regulatory elements can be triggered by helminths at the level of innate immunity as well. *H. polygyrus* elicits production of IL-1β, which decreases IL-25 and -33 production early during infection, impairing parasite expulsion (Zaiss et al., 2013).

Besides induction of regulatory elements of the immune response, helminth products actively obstruct the immune response that they elicit: induction of immune cell apoptosis (Guasconi et al., 2012; Serradell et al., 2007), degradation of immunoglobulins (Berasain et al., 2000), alteration of antigen presentation competence of macrophages (Robinson et al., 2012), blocking of cytokine release and activation pathways, including small RNA delivery (Buck et al., 2014; Osbourn et al., 2017) or inhibition of mast cell degranulation (Melendez et al., 2007).

2 Macrophage activation and functions during helminth infection

2.1 Origin of macrophages

Macrophages are innate immune cells, which were initially described mainly by their phagocytic properties, although the function of these cells goes beyond a mere role of engulfing invading micro-organisms and clearing dead cells and debris. Macrophages are highly plastic. They respond to their environment to adapt and ensure tissue homeostasis (both at steady state and during inflammatory processes), and sustain suitable immune responses. Typically, macrophages have been thought for decades to originate from circulating monocytes, themselves arising from bone marrow precursors (van Furth et al., 1972). However, it is now clear that not all macrophages populations comply with this general assumption. The existence of an alternative to bone marrow in the origin of macrophages was evidenced in two circumstances: the first one concerns tissue resident macrophages at steady state and the second one the origin of inflammatory macrophages during the type 2 immune responses.

Fate mapping experiments in the mouse model have provided evidence that **resident macrophages** are established in the different tissues, including serous cavities, by embryonic hematopoiesis from yolk sac and fetal liver precursors during organogenesis and shortly after birth (Perdiguero et al., 2015; Schulz et al., 2012; Yona et al., 2013). They are characterized by their ability to self-renew by homeostatic proliferation that allows them to be maintained in their tissue niche independent of the input or circulating monocytes, as shown in several studies (Ajami et al., 2007; Hashimoto et al., 2013; Merad et al., 2002). However, the capacity of resident macrophages to be maintained in the long term without contribution of blood monocytes appears to be highly tissue-dependent. Evidence indicates their progressive replacement by bone-marrow derived monocytes in specific tissues such as heart, pancreas, peritoneal and pleural cavities, skin or the intestines (Bain et al., 2014; Bain et al., 2016; Calderon et al., 2015; Molawi et al., 2014; Tamoutounour et al., 2013), while strain (Campbell et al., 2018) or sex (Bain et al., 2016) might be important confounding factors. The tissue-dependent variability of the kinetics and amplitude of yolk sac, fetal liver or bone marrow contributions to resident macrophage populations is illustrated in figure 7. In tissues like liver or lung, resident macrophages of embryonic origin are long-lived and can be maintained long term with only limited contribution from infiltrating bone marrow-derived monocytes. Experiments showed that bone-marrow derived monocytes can integrate the pool of resident macrophages in the liver during the first weeks of life, while their contribution was much more limited for alveolar macrophages in the lung. However, in adult mice, no evidence of integration of bone marrow-derived monocytes into an intact pool of resident macrophages in liver or lung was found over several weeks (Jakubzick et al., 2013; Scott et al., 2016). Nonetheless, as bone marrow-derived monocytes progressively replace embryonically-derived resident macrophages in several tissue

with various kinetics, it remains possible that this replacement in liver or lung is so slow that it could only be observed on a longer term or in older subjects.

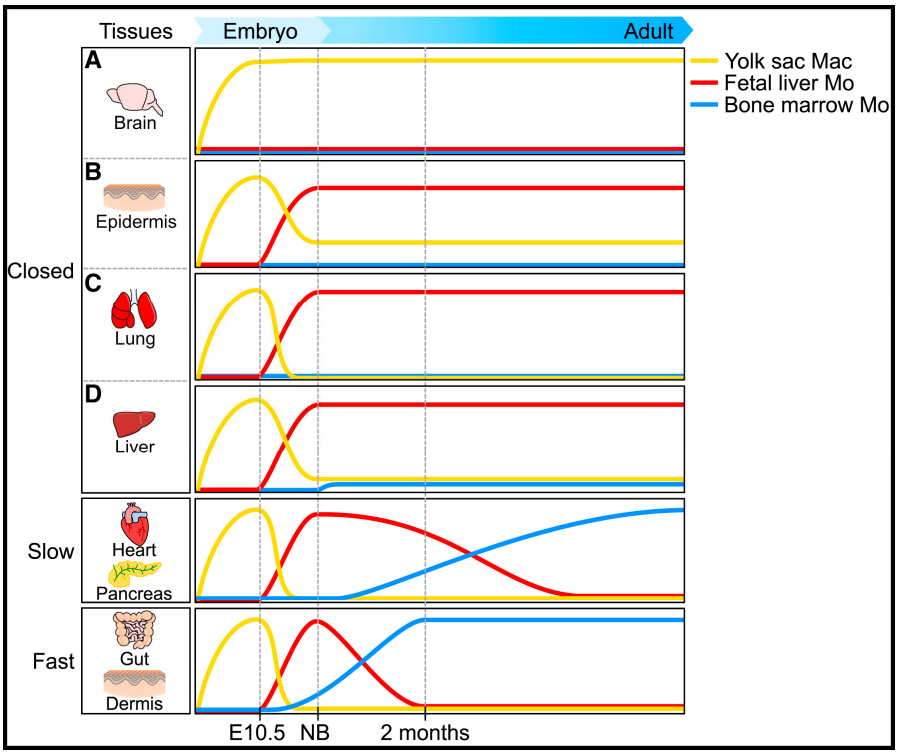

Figure 7 : Tissue-dependent origin of tissue-resident macrophages at steady state. First, macrophages observed in embryonic tissues arise from the yolk sac. With the exception of the brain, a second wave of macrophages of fetal liver origin partially or completely replace yolk sac macrophages. After birth, organs are considered either as closed since monocytes do not contribute to the tissue-resident macrophage population, or open with a slow or fast replacement of macrophages of embryonic origin by monocyte recruitment and differentiation into macrophages. Low-level engraftment of circulating monocytes can still bu observed in some organs considered as “closed” like the liver.
From (Ginhoux and Guilliams, 2016)

Current theory propose that limited space in tissue is available for each population of resident macrophages (the niche) and bone marrow-derived monocytes do not dislodge macrophages that are already estabiched in these niche to differentiate in macrophages. The increasing contribution of monocytes to the resident macrophage pool overtime in some organs might translate a impaired hability of resident macrophages to self-maintained in these organs (Guilliams and Scott, 2017). Inflammatory process or injury can render the niche available by inducing the disappearance of all or part of the resident macrophages that occupy it. In these cases, macrophages of bone-marrow origin can take over the niche and differentiate into resident macrophages, as observed in diphteria toxin (DT)-treated Clec4f-DTR mice, Kupffer cell (KC) necroptosis caused by *L. monocytogenes* infection or MuHV-4-mediated depletion of lung alveolar macrophages (Bleriot et al., 2015; Machiels et al., 2017; Scott et al., 2016). Critically, the tissue niche is highly important in defining the phenotypic and functional behaviour of resident macrophages as attested by transcriptomics data (Gautier et al., 2012; T'Jonck et al., 2018). Resident macrophages sustain the tissue functions in numerous different tissues and this

imply functionnal specialization to the tissue they reside in. Interestingly, monocytes-derived resident macrophages have been shown to be able to adopt a phenotypical and transcriptional profile very close to that of embryonic resident macrophages, including the ability to self-renew through proliferation (Scott et al., 2016).

Macrophage populations present in a given tissue can dramatically expand during inflammation. Here again, circulating monocytes were thought to be the main source of additional macrophages. However several studies have pointed out that tissue-resident macrophages could expand beyond homeostatic levels through local proliferation in response to inflammatory conditions (Ajami et al., 2011; Chorro et al., 2009; Jenkins et al., 2011). The type 2 immune responses, and IL-4 in particular, has been described as driving important local proliferation of tissue-resident macrophages which accumulate independently of circulating monocytes in the pleural cavity of mice infected with filarial nematode *L. sigmodontis* (Jenkins et al., 2011). Thioglycollate is a typical trigger for classical inflammation associated with monocyte infiltration. A mixed stimulation of thioglycollate and IL-4c administered together led to an accumulation of macrophages with characteristics of monocyte origin (low expression of F4/80), similar to the elicited population after thioglycollate injection alone. However, IL-4c/thioglycollate-elicited cells were able to proliferate whereas proliferation could hardly be detected with thioglycolatte only. Thus, both processes are likely to coexist in response to helminth infection which are likely to also induce classical inflammation, for example from invading bacteria due to compromise intestinal barrier. Indeed, monocyte infiltration has been observed in other helminth models. During schistosomiasis, macrophages are an important component of the granulomas that form around eggs. Despite significantly increased proliferation of tissue-resident macrophages during *S. mansoni* infection, expansion of macrophage populations was dominated by infiltration of monocytes which later differentiated into macrophages (Girgis et al., 2014; Nascimento et al., 2014), and, CCR2-dependent-monocytes infiltration was shown to be critical for host protection in murine schistosomiasis (Nascimento et al., 2014). Thus, the origin of macrophages during helminth infection appears to be highly dependent on the helminth species and, more strikingly on the mouse strain studied, C57BL/6 mice being much more prone to local proliferation of pleural resident macrophages than BALB/c mice during *L. sigmodontis* infection (Campbell et al., 2018).

2.2 Alternative macrophage activation

As mentioned in the previous section, macrophages are highly plastic. In response to canonical type 2 cytokine IL-4, macrophages adopt a phenotype called “alternative activation”, **aaMφ** or M2 or M[IL-4]. The work of Siamon Gordon first identified alternative activation of macrophages by opposition to classical activation (caMφ or M1) and reflects the type 2/type 1 immunity in macrophages as they are

induced by IL-4/IL-13 or IFN-γ/LPS, respectively (Stein et al., 1992; Taub and Cox, 1995). CaMφ macrophages have pro-inflammatory properties, secrete inflammatory cytokines and inducible NO synthase (iNOS). AaMφ however have anti-inflammatory properties, secrete IL-4 and IL-13 and express specific markers such as arginase 1 (Arg1), mannose receptor (MR or CD206), Relm-α or chitinase 3-like 3 (Ym1) (Edwards et al., 2006; Stein et al., 1992) (Figure 6). However, besides these very clear and antagonistic polarizing conditions, macrophages can respond to a vast diversity of environmental cues and can adopt a spectrum of activation states defined by distinct patterns of gene and protein expression and therefore of effector functions (Murray et al., 2014). This highlights the need to use a combination of markers to clearly defines the population of macrophages in question.

***In vivo* characterization of macrophages** may be complicated by the variety of potential activating mediators. Macrophages present at helminth infection sites share numerous properties with and are therefore assimilated to aaMφ (Jenkins and Allen, 2010). Indeed, their phenotype is driven by type 2 cytokines IL-4 and -13 (Hesse et al., 2001; Linehan et al., 2003; Loke et al., 2002) and they harbor a phenotype associated with alternative activation with expression of Relm-α, Ym1 and Arg1. AaMφ can be consistently found in numerous helminth infections (Reyes and Terrazas, 2007). While aaMφ are generally activated through IL-4 and IL-13 signalling *via* type I or type II IL-4 receptors (Figure 6), similar phenotype can also by induced independently of IL-4Rα signalling. Helminth products can directly signal on macrophages and induce upregulation of aaMφ markers by an IL-4Rα-independent pathway (Du et al., 2014). Besides, during antibody-mediated adherence to *H. polygyrus* larvae, macrophages harbor certain features of alternative activation such as IL-4Rα-independent expression of Arg1 (Esser-von Bieren et al., 2013; Esser-von Bieren et al., 2015). *In vivo*, IL-4/13-dependent alternative macrophage activation has also been shown to be assisted and/or amplified by several additional local signals (Minutti et al., 2017b). IL-4-driven alternative macrophage activation could be enhanced in a tissue-specific way by IL-4-dependent expression of surfactant protein (SP)-A (in the lung) and the complement factor C1q (in the liver) and upregulation of their receptor, myosin 18A. During *N. brasiliensis* infection in absence of SP-A, lung aaMφ showed reduced levels of aaMφ markers and failed to proliferate, resulting in impaired control of worm burden. Consistent with a direct role of SP-A on macrophages to boost IL-4-mediated macrophage activation, *in vitro* treatment with SP-A and IL-4 increased proliferation and upregulation of aaMφ markers in wildtype but not *Il4ra*$^{-/-}$ alveolar macrophages, compared to IL-4c treatment alone (Minutti et al., 2017b). Similarly, SP-D was also shown to interact with alveolar macrophages after *N. brasiliensis* infection and to increased aaMφ markers expression induced *ex vivo* by IL-4/IL-13 treatment (Thawer et al., 2016). IL-21 signalling was associated with increased expression of IL-4Rα and IL-13Rα1 on macrophages, resulting in amplification of alternative activation (Pesce et al., 2006). As already discussed, the type 2 immunity is strongly associated with tissue damage. Interestingly, sensing of dying cells has been involved in

alternative macrophage activation. Here, detection of apoptotic cells by bone marrow-derived macrophages potentiated the ability of IL-4 stimulation to upregulate the expression of genes associated with wound healing. Moreover, blocking phosphatidyl-serine receptor (involved in the detection of apoptotic cells) was also shown to downregulate some aaMφ markers in response to IL-4 stimulation or *N. brasiliensis* infection. Lung damage during *N. brasiliensis* infection was aggravated in the absence of detection of apoptotic cells (Bosurgi et al., 2017). Necroptosis in the liver after *Listeria monocytogenes* infection was associated with release of the alarmin IL-33 and this appeared to be involved in the anti-inflammatory roles of macrophages (Blériot et al., 2015). Furthermore, IL-33 signalling has been shown to be required for alternative macrophage activation after *L. sigmodontis* infection (Jackson-Jones et al., 2016). Rather than acting directly on macrophages, IL-33 likely stimulates other IL-4-secreting innate immune cells such as basophils or ILC2s although a direct role for IL-33 and IL-25 in stimulating production of type 2 cytokines from macrophages has also been described (Yang et al., 2013).

The **origin of aaMφ** could also have important consequences in their phenotype and functions. AaMφ derived from infiltrating monocytes or from proliferation of tissue-resident macrophages displayed distinct phenotypes, with monocyte-derived aaMφ being associated with immune regulation or suppresion properties (Campbell et al., 2018; Gundra et al., 2014). Macrophage origin can therefore influence how they contribute to a given pathology, as shown in bleomycin-induced lung fibrosis (Misharin et al., 2017) or protection against pathogens (Campbell et al., 2018). Interestingly, monocyte-derived aaMφ can differentiate into tissue-resident macrophages. This process is dependent on vitamin A and is crucial for proper granuloma formation and survival during *S. mansoni* infection (Gundra et al., 2017).

Alternative macrophage activation is characterized by the expression of several **specific markers**. Although several molecules identifying caMφ and aaMφ in mice do not have equivalents in humans, recent efforts have been made to provide characterization of a similar dichotomy in human macrophages (Beyer et al., 2012; Jaguin et al., 2013; Tarique et al., 2015; Xue et al., 2014). Molecules used as markers also mediate numerous effector function of aaMφ.

Chitinase 3-like 3 (*Chi3l3* or Ym1) belongs to family 18 of chitinases but has no chitinolytic activity. Enzymatically inactive, chitinase-like molecules have arisen from recent gene duplication events and are highly diverse despite being widely present in mammalian species (Bussink et al., 2007). They are mostly expressed by macrophages but also by lung epithelial cells (Homer et al., 2006) and antigen presenting cells (Nair et al., 2005). Ym1 was shown to contribute to the wound healing properties of aaMφ through binding to extracellular matrix components (Chang et al., 2001). Various roles in

modulation of the immune responses have also been attributed to Ym1. Evidence indicates that Ym1 can promotes type 2 immune responses as it enhanced type 2 cytokine production by Th2 cells (Cai et al., 2009). A recent study found a role for Ym1 during *N. brasiliensis* infection in stimulating accumulation of neutrophilsthrough expansion of an IL-17-secreting population of γδ T cells (Sutherland et al., 2014), a mechanism described as a tradeoff between nematode killing and tissue damage. In addition, Ym1 is a potent chemoattractant of eosinophils (Owhashi et al., 2000). Finally, Ym1 was also found to directly impair anti-viral effector $CD8^+$ T cell responses (Osborne et al., 2014).

Resistin-like molecule α (Relmα) is another molecule associated with aaMφ but is also expressed by eosinophils (especially during *S. mansoni* infection) (Pesce et al., 2009b), epithelial cells (Nair et al., 2009) and antigen presenting cells (Nair et al., 2005). Its main contribution seems to be in the modulation of immune responses. Relm-α notably inhibits type 2 immune responses by directly binding to Th2 cells and it impairs protection against *N. brasiliensis*, while reducing pathologies linked to excessive immune responses (Nair et al., 2009; Pesce et al., 2009b). In addition, Relm-α enhances Th17 and regulatory responses (Chen et al., 2014b; Cook et al., 2012). Suprisingly, while Relm-α could control fibrosis through modulation of Th2 responses in *S. mansoni* egg-induced inflammation, Relm-α also stimulated collagen production and differentiation of myofibroblasts during bleomycine-induced lung fibrosis (Liu et al., 2004). Indeed, Relm-α appeared to be a mediator of the tissue repair activity of aaMφ as absence of aaMφ-derived Relm-α in skin wounds of $Il4ra^{-/lox}Lyz2^{cre}$ mice was recently associated with impaired healing response (Knipper et al., 2015). Besides its action on the immune system, Relm-α also regulates metabolism (Lee et al., 2014; Munitz et al., 2009) and has angiogenic properties (Teng et al., 2003).

As opposed to the two previous molecules, **arginase 1** (Arg1) expression is mainly restricted to macrophages during helminth infection (Reese et al., 2007). IL-13, which is dispensable for induction of several features of IL-4-induced aaMφ, was required for Arg1 expression in the liver following *S. mansoni* infection (Ramalingam et al., 2008). Arg1 competes with caMφ enzyme iNOS for the metabolization of L-arginine. Metabolization of L-arginine by Arg1 results in production of ornithine and urea and can have several consequences. First, ornithine can be metabolized to proline, required for collagen deposition (proline and polyamine both playing roles in tissue repair and fibrosis) (Witte and Barbul, 2003). Second, by competing for its substrate, Arg1 inhibits the production of NO by iNOS (Munder et al., 1998). Third, L-ornithine and polyamines and their metabolites have deleterious effects on larvae fitness, impacting their motility (Esser-von Bieren et al., 2013). Fourth, L-arginine depletion from the surrounding environment leads to inhibition of T cell proliferation by amino acid starvation (Bronte et al., 2003). Inhibition of T cell proliferation by competition for L-arginine appears to be an important mechanism during chronic *S. mansoni* infection for aaMφ-mediated inhibition of Th2-induced fibrosis (Pesce et al., 2009a). During *S. mansoni* infection, Arg1 has also been shown to regulate

deleterious type 1 immune responses. Arg1 downregulated production of IL-12/IL-23p40 and maintained Treg/Th17 balance (Herbert et al., 2010). Thus, Arg1 acts both on the immune response and on parasite fitness.

C-type lectins could represent an important PRR in the induction of immune response to helminth infection. The mannose receptor (MR or CD206) is upregulated on macrophages upon treatment with IL-4, IL-13, and IL-10 (Martinez-Pomares et al., 2003; Stein et al., 1992) as well as prostaglandins PGE1 and PGE2 (van Die and Cummings, 2017). *S. mansoni* egg secreted glycoprotein ω-1 is the main antigen responsible for the induction of type 2 immune responses (Everts et al., 2009; Steinfelder et al., 2009) and is mainly recognized by CD206-expressing dendritic cells. Upon recognition, ω-1 is internalized and thereby impairs protein synthesis through its RNAse activity (Everts et al., 2012). In addition to *S. mansoni*, CD206 has been shown to bind other helminth species such as *T. spiralis* muscle larvae (Gruden-Movsesijan and Milosavljevic Lj, 2006), *T. muris* excretory/secretory products (deSchoolmeester et al., 2009) or *F. hepatica* tegumental proteins (Aldridge and O'Neill, 2016). Nonetheless, the role of aaMφ-specific CD206 expression remains elusive during helminth infection, although CD206 seems to be relevant surface marker for monocyte-derived aaMφ (Gundra et al., 2017). The macrophage galactose-type C-type lectin 2 (MGL2 or CD301b) is another C-type lectin upregulated in aaMφ in response to IL-4 and IL-13 or helminth triggers (Raes et al., 2005). While $CD301b^+$ dendritic cells have been shown to be essential for the induction of optimal type 2 immune responses during ovalbumin (OVA) immunization or helminth infection (Kumamoto et al., 2013; Rodríguez et al., 2017a), CD301b-expressing macrophages appeared to play an important role in wound healing (Shook et al., 2016).

Programme death ligand 2 (PD-L2) is up-regulated in monocyte-derived aaMφ, whereas it is poorly expressed on IL-4-treated resident macrophages (Loke and Allison, 2003). PD-L2, a ligand of PD-1, a potent inhibitory receptor expressed on effector T cells and macrophages, has been shown to potently inhibit T cell proliferation (Huber et al., 2010). PD-L2 expression was upregulated in lung macrophages after *N. brasiliensis* infection whereas STAT-6 deficient mice displayed low levels of macrophage PD-L2 (Huber et al., 2010). In addition, *in vivo* blockade of PD-L2 during *N. brasiliensis* infection increased type 2 cell-mediated cytokine responses in the lung, further indicating that aaMφ inhibit Th2 cells by expression of PD-L2. PD-L2 is used as a relevant surface marker to distinguish between resident and monocyte-derived macrophages following antigenic stimulation or *S. mansoni* infection (Gundra et al., 2017; Gundra et al., 2014). Thus, differences in the dynamics of macrophage responses between strains could explain difference in susceptibility. Recent work by Campbell and colleagues (2018) showed that macrophage responses against *L. sigmodontis* infection in susceptible BALB/c mice was dominated by

infiltration of monocytes with immunosuppressive PD-L2^{+} phenotype, as opposed to resistant C57BL/6 mice in which expansion of resident cells was the main source of macrophages (Campbell et al., 2018).

2.3 Effector functions of macrophages in helminth infections

2.3.1 General functions

Helminth-induced aaMφ are involved in effector functions of type 2 immunity against helminth infections described in section 1.4.3. They are therefore important effectors in controlling helminth infection. However, the involved mechanisms depend on the helminth species. The following section will therefore give a more detailed overview of the effector functions of aaMφ during helminth infection.

Tools available to study aaMφ functions specifically may fail to provide clear information on their specific role after helminth infection mainly due to the difficulty to directly target aaMφ without affecting other cell populations. Indeed, commonly used tools involve depletion of macrophages by administration of clodronate liposomes, hindrance of CCR2-dependent monocyte trafficking, total knockout for genes associated with alternative macrophage activation, or conditional cre/lox mouse strains targeting macrophage populations. *Lyz2*^{cre} mice are commonly used as targeting myeloid cells. *Lyz2* (encoding lysozyme M) is expressed in neutrophils and macrophages but, although it is used to impair alternative macrophage activation in *Il4ra*$^{-/lox}$*Lyz2*^{cre} mice, studies have highlighted the presence of macrophages with features of alternative activation in these mice (Dewals et al., 2010; Vannella et al., 2014). Nevertheless, these various tools can help elucidate how aaMφ contribute to the protection against helminth infections.

The “weep and sweep” response is an important element of the protection against intestinal nematodes. During primary *N. brasiliensis* infection, absence of macrophages has been shown to increase the number of worms recovered from the intestine, this being interpreted as a delayed expulsion. This observation was linked to an Arg1-dependent increase in smooth muscle contractility mediated by macrophages, although Arg1 blockade did not delay expulsion to the same extent as macrophages depletion (Zhao et al., 2008). However, using *Il4ra*$^{-/lox}$*Lyz2*^{cre} mice, Herbert and colleagues showed that IL-4Rα signalling on macrophages was not required for expulsion of *N. brasiliensis* parasites (Herbert et al., 2004). During secondary infection with migrating nematodes such as *N. brasiliensis* and *H. polygyrus*, increased protection could be associated with enhanced trapping of migrating larvae in the skin or lung (for *N. brasiliensis*) or intestinal mucosae (for *H. polygyrus*). Macrophages accumulate around larvae in the tissue and impair their viability, preventing migration to the intestine lumen (Anthony et al., 2006; Chen et al., 2014a). These studies highlighted a role for Arg1. As already discussed, products of Arg1 activity have direct deleterious effect on larvae motility. This has

particularly been shown against *H. polygyrus* larvae (Esser-von Bieren et al., 2013). Furthermore, although the role of macrophages was initially demonstrated in the context of clodronate liposome mediated depletion, *in vitro* and adoptive cell transfer experiments have shown a crucial role of alternative activation, at least against *N. brasiliensis* infection (Bouchery et al., 2015; Chen et al., 2014a). Important damages are elicited by *N. brasiliensis* during its migration through the lung. Tissue damage has been associated with IL-17-dependent recruitment of neutrophils and resolved 7 days after *N. brasiliensis* inoculation. Lung macrophages express high levels of genes associated with wound healing such as *Arg1*, *Igf1* and *Mmp13* during *N. brasiliensis* infection and participate to the control of hemorrhages and inflammation (Chen et al., 2012a).

Macrophages elicited in response to helminth infection have also been shown to take part in immunoregulation. They may notably directly inhibit proliferation of T cells *in vitro* (Loke et al., 2000) through several mechanisms involving PD-1/PD-L1 (Smith et al., 2004; Terrazas et al., 2005), TGF-β (Taylor et al., 2006) or nutriment depletion (Pesce et al., 2009a). Although regulation of excessive immune responses is beneficial to avoid immunopathologies, immunosuppressive PD-L2^{+} monocyte-derived macrophage populations elicited during *L. sigmodontis* infection in BALB/c mice drive the susceptibility of this strain to *L. sigmodontis* infection (Campbell et al., 2018).

Control of infection with the cestode *T. crassiceps* is strikingly different from that of other nematodes or trematodes, with initial type 1 immune response described as critical for parasite resistance by controlling larval growth (Rodríguez-Sosa et al., 2004; Terrazas et al., 1998; Terrazas et al., 1999). Through NO production, caMφ are suggested to be key effectors in the control of *T crassiceps* infection. Indeed, blocking the enzyme NO synthase in susceptible wild-type BALB/c or even resistant *Stat6*$^{-/-}$ mice resulted in increased parasite loads (Alonso-Trujillo et al., 2007). Further supporting a role for caMφ in the control of *T. crassiceps* infection, mice lacking migration inhibitory factor (MIF) were shown to be highly susceptible despite similar IFN-γ levels. Their peritoneal macrophages failed to respond to *ex vivo* restimulation with LPS and IFN-γ and produced low levels of caMφ-associated molecules such as IL-12, TNF-α or NO upon *ex vivo* restimulation (Rodríguez-Sosa et al., 2003). Presence of aaMφ in these different cestode infections was mostly associated with an immunoregulatory role (Reyes and Terrazas, 2007; Terrazas et al., 2017; Terrazas et al., 2005). Regulation of immune responses might be essential to avoid deleterious inflammation of the healthy tissue surrounding the metacestode (Terrazas, 2008), however aaMφ presence and overexpression of aaMφ-associated molecules like PD-L1 and PD-L2 has also been associated with increased susceptibility to infection with *T. crassiceps* (Reyes et al., 2010; Togno-Peirce et al., 2013). This immunoregulatory role appears to have a more proemint role during *M. corti* infection as *Il4*$^{-/-}$ or *Stat6*$^{-/-}$ mice are highly susceptible and die from infection (Mishra et al., 2011a; O'Connell et al., 2009).

2.3.2 Schistosomiasis

The outcome of *S. mansoni* infection critically depends on the establishment of an equilibrium between efficient granulomas formation around the parasite eggs to avoid tissue damage and regulatory mechanisms to avoid excessive fibrosis. Macrophages (along with $CD4^+$ T cells and eosinophils) are the main cellular component of granulomas and important efforts have been made to dissect their role in the protection against *S. mansoni* (Hams et al., 2013).

The main pathological outcomes of schistosomiasis develop in the chronic phase of schistosomiasis as consequences of excessive fibrosis. As previously reported, Arg1 has been associated with promotion of fibrosis through metabolization of L-arginine. However, it appears that liver fibrosis developing during *S. mansoni* infection is not dependent on Arg1 expression. *S. mansoni* infected *Il13ra1*$^{-/-}$ mice displayed less hepatic fibrosis than wildtype mice in response to *S. mansoni* infection in spite of normal levels of aaMφ markers being expressed in the liver *(Ramalingam et al., 2008)*, while neutralization of IL-13 by injection of a decoy receptor (sIL-13Rα2) attenuated *S. mansoni* induced hepatic fibrosis to a greater extent than suppression of IL-4 (Chiaramonte et al., 1999). These data indicated that IL-13 and not aaMφ is responsible for increased fibrosis. Furthermore, Arg1 deficient mice, specifically those deficient in macrophages and neutrophils (*Arg1*$^{-/lox}$*Lyz2*^{cre} mice) or in all hematopoietic cells (*Arg1*$^{-/lox}$*Tie2*^{cre} mice) have been shown to have enhanced fibrosis levels, larger granulomas and lower survival rates than wildtype controls (Pesce et al., 2009a). Arg1 could therefore reduce rather than increase fibrosis. In line with this role, data published by Pesce and colleagues suggested that through expression of Arg1, aaMφ competed with T cells for the use of L-arginine and leading to suppressive activity on T cell proliferation (Pesce et al., 2009a). Adding to these observations, Relm-α-deficient mice also developed increased granulomatous inflammation, fibrosis and type 2 immune response during schistosomiasis (Nair et al., 2009; Pesce et al., 2009b). Relm-α was shown to directly bind to $CD4^+$ T cells and inhibit type 2 cytokines production, with no effect on activation or proliferation (Nair et al., 2009). During *S. mansoni* eggs-induced inflammation, Relm-α is also expressed by epithelial cells and eosinophils, but co-culture experiments have shown that Relm-α-dependent type 2 immune response inhibition can be supported by macrophages (Nair et al., 2009). However, in the liver of *S. mansoni* infected mice, eosinophils appear to be the main, if not the exclusive, source of Relm-α (Pesce et al., 2009b).

These data indicate a deleterious role for excessive type 2 responses and fibrosis in schistosomiasis. However, several deficiency models convincingly showed that the type 2 immunity, particularly through IL-4Rα signalling, is essential for survival during the acute phase of schistosomiasis by controlling severe intestinal and liver pathologies (Brunet et al., 1997; Herbert et al., 2004; Herbert et al., 2008;

Jankovic et al., 1999). AaMφ were initially described as the main contributors of this type 2 dependent protection against the acute schistosomiasis (Herbert et al., 2004). Herbert and colleagues studied *S. mansoni* infection in *Il4ra*$^{-/lox}$*Lyz2*^{cre} mice which lack IL-4Rα specifically on macrophages and neutrophils. They observed that *Il4ra*$^{-/lox}$*Lyz2*^{cre} did not have IL-4/13-dependent aaMφ while developing a normal type 2 immune response, but developed an acute wasting and lethal disease similar to *Il4ra*$^{-/-}$ mice, with evidence of hepatotoxicity and endotoxemia. But the role of aaMφ in schistosomiasis might not be so clear. In contradiction with results from the former studies, Vannella and colleagues (2014) did not observe increased mortality, nor hepatotoxicity in *S. mansoni* infected *Il4ra*$^{-/lox}$*Lyz2*^{cre} mice compared to *Il4ra*$^{-/lox}$ controls. Instead, size of granulomas from *S. mansoni* infected *Il4ra*$^{-/lox}$*Lyz2*^{cre} mice was increased compared control mice (Vannella et al., 2014). These results rather suggested a role for IL-4/13-dependent aaMφ in the control of granulomatous inflammation but less crucial role for survival. Interestingly, Vannella and colleagues highlighted an incomplete deletion of IL-4Rα among the heterogeneous macrophage population of *S. mansoni* infected *Il4ra*$^{-/lox}$*Lyz2*^{cre} mice. They observed an insufficient expression of *Lyz2*, thereby of cre-recombinase, in newly-recruited, immature F4/80^{hi}CD11b^{hi} macrophages which retained features of alternative activation. Interestingly, these data further provide an alternate explanation to the presence of IL-10-dependent Ym1- and CD206-expressing macrophages in the granulomas of *Il4ra*$^{-/lox}$*Lyz2*^{cre} mice (Dewals et al., 2010). Moreover, two recent studies demonstrated that aaMφ in the liver after *S. mansoni* infection resulted from the maturation of recruited Ly6C^{hi} monocytes (Girgis et al., 2014; Nascimento et al., 2014). Thus, aaMφ protective roles during acute schistosomiasis and control of intestinal permeability remain unclear, and further urges for the development of new tools to investigate the functions of aaMφ during schistosomiasis. What is also less clear is the involvement of macrophage IL-4/IL-13 responsiveness in the dynamics of liver macrophage responses after *S. mansoni* infection, and whether Lyz2-expressing aaMφ in the liver (absent in *Il4ra*$^{-/lox}$*Lyz2*^{cre} mice) could have a role in the control of excessive granulomatous inflammation . Taken together, these data about the role of aaMφ during *S. mansoni* infection revealed that distinct subsets of aaMφ could mediate distinct protective or pathologic functions. Further investigation could therefore be needed to reveal which specific macrophage population and mechanisms are involved.

3 Bystander effects of helminthiasis

3.1 Immunomodulation and consequences on immunopathologies

Tolerance of chronic helminth infection means the existence of immunoregulatory mechanisms. Helminths have evolved several mechanisms discussed in section 1.4.4 that downregulate immune response allowing their persistence but also avoiding deleterious consequence of excessive and prolonged type 2 immune responses on the host. These mechanisms drew a lot of attention as they can also influence bystander effects notably by enhancing the control of excessive and harmful inflammation. Figure 8 illustrates the diversity of effect helminth infection may have on bystander immunity, either beneficial or deleterious.

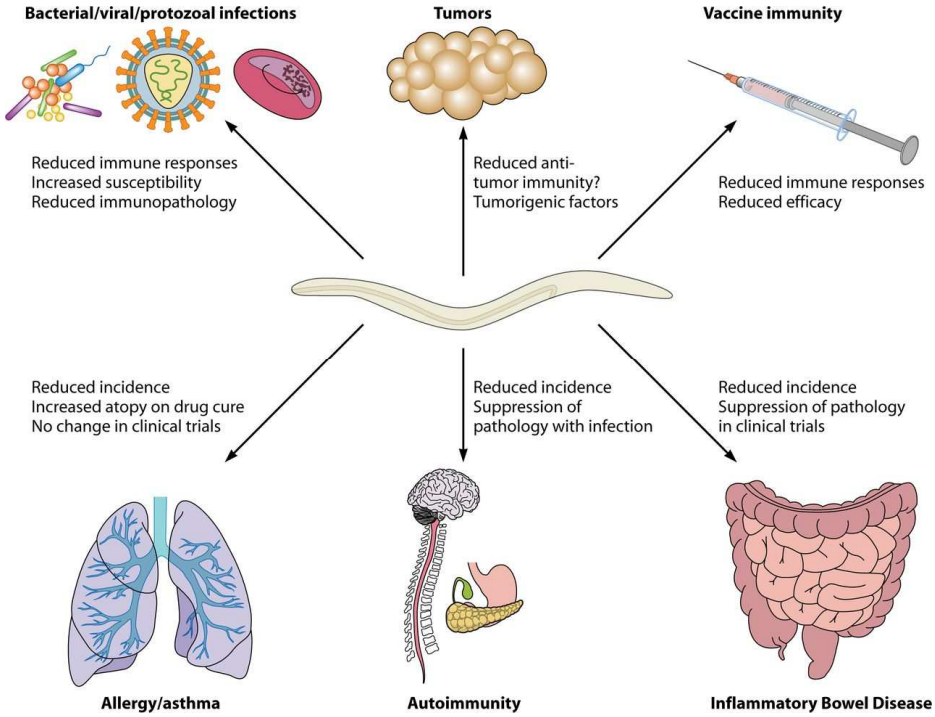

Figure 8. Immunoregulatory effects of helminths on bystander responses. Helminths can suppress a wide range of bystander immune responses, including those of both immunopathogenic and protective natures. Coinfection with helminths suppresses antibacterial, antiviral, and antiprotozoal immunity, leading to increased susceptibility and attenuated immunopathology or, in some cases, exacerbated pathology due to higher infection burdens. Antitumor immunity may be suppressed by helminth infections, which may also release directly carcinogenic factors, potentially leading to increased numbers of malignancies in infected individuals. Vaccine efficacy is compromised by helminth infections due to suppressed immune responses. Immunopathologies such as asthma, autoimmune diseases, and inflammatory bowel diseases are all reduced in prevalence in areas where helminth disease is endemic, and direct effects of helminth infections on the suppression of disease have been shown in clinical trials for inflammatory bowel diseases. From (McSorley and Maizels, 2012)

Helminth infections have been shown to have beneficial effects on various immunopathologies. Increased prevalence of immune dysregulation observed in developed countries, correlating with improved sanitary situation, led to the formulation thirthy years ago of the “hygiene” or “old friends” hypotheses. These concepts suggest that exposure to microorganisms and parasites play a crucial role in

the proper development and balance of the immune system and that reduction in microbial exposure is one of the parameters explaining the increased prevalence of immunopathologies such as allergy or auto-immune disorders in developed countries (Stiemsma et al., 2015; Strachan, 1989). In line with these hypotheses, prevalence of allergy has risen in urbanized area where helminth infections have declined, which supported the idea that helminth-host interactions are valuable for immune system equilibrium (Flohr et al., 2009). Experimental data in animal models confirmed the relationship between helminth infection status and immunopathologies and uncovered mechanisms involved. Studies have implicated various helminth species in the protection against different immunopathologies including allergiy, inflammatory bowel disease(IDB)-like colitis, type 1 diabetes or experimental autoimmune encephalomyelitis (modeling multiple sclerosis) (McSorley and Maizels, 2012). Protection is often correlated with worm burden (Smits et al., 2007) and is sometimes associated with a specific life cycle stage (He et al., 2010; Mangan et al., 2006; Smith et al., 2007). Immune mediators involved in the protection depend on the context and include IL-10 and TGF-β signalling (Ince et al., 2009; Kitagaki et al., 2006), Treg (Yang et al., 2007), B cells (indeed some B cells can also secrete IL-10) (Mangan et al., 2006), DCs (Matisz et al., 2017), macrophages (including aaMφ) (Espinoza-Jiménez et al., 2017) or ILC2 (McSorley et al., 2014). Interestingly, numerous helminth products, either excretory/secretory products or recombinant molecules, successfully recapitulate protection induced by infection and could therefore be used as safer traitements for immunopathologies (Du et al., 2011; McSorley et al., 2012; Schnoeller et al., 2008). Furthermore, adoptive transfer of immune cells like macrophages (Ziegler et al., 2015), T cells (Grainger et al., 2010) or dendritic cells (Matisz et al., 2017), treated with helminth-derived products has proven efficient in recapitulating the protection they induce. Effect of helminth on inflammatory disorders could also be mediated by an alteration of microbiota. In recent years, studies unraveled the important role of microbiota in the correct development and regulation of immune system. Modification of its composition dysregulates the crosstalk with the host and impact homeostasis of several system, including immune system favoring the development of chronic inflammatory diseases (Belkaid and Hand, 2014). Alteration of the composition of gut microbiota and prevention of the expansion of deleterous and pro-inflammatory bacteria species by helminth infections reduce immunopathologies like allergic asthma or IBD (Ramanan et al., 2016; Zaiss et al., 2015b).

However, despite the substantial amount of convincing data from animal models, observation of a clear protective effect of helminth infections or helminths products on immunopathologies in human is less straightforward. Epidemiological data do not always confirm an inverse correlation between infection and immunopathology status. Atopy, as studied by skin test reactivity to allergens, is the parameter which is the most consistently negatively correlated with helminth infections (Flohr et al., 2009). But the trend is less clear when considering allergy. Some studies found a negative correlation between helminth infections and development of allergy, while other did not (Briggs et al., 2016; Feary

et al., 2011; Wammes et al., 2014). Yet, effects of helminth infections appear highly variable depending on the species involved, some of them, in particular *A. lumbricoides*, were even associated with increased risk of developing asthma (Leonardi-Bee et al., 2006). Still, several data support the idea of a beneficial role for helminth infection on immunopathologies. For example, patient suffering from multiple sclerosis who naturally acquire helminth infections show lower relapse rate (Correale and Farez, 2007). Studies of population in endemic area for helminths indicate that deworming might be associated with an increased inclination to develop immunopathology, as indicated by increased skin test reactivity to allergen or increased level of autoantibody (Flohr et al., 2010; Mutapi et al., 2011; van den Biggelaar et al., 2004). However effect on clinical allergies was either null or contradictory (Almeida et al., 2012; Flohr et al., 2010; Lynch et al., 1997).

Besides, the role of helminths in inducing inflammatory diseases can not be overlooked. Migration of *A. lumbricoides* larvae in the lung affect tissue integrity and multiple exposures can be responsible of an asthma phenotype (Nogueira et al., 2016). Similarly, chronic trichuriasis in mice is associated with colitis that shares several features with Crohn's disease (Briggs et al., 2016). Thus helminths might represent a cause of inflammatory disease as well as a protective agent. Futhermore, some helminth infections are also linked to carcinogenesis (Pastille et al., 2017) so extreme precautions must by taken when considering the use of helminth as a therapy.

Nevertheless, treatment of inflammatory disorder with helminth products in mice yielded promising results and led to the investigation of the therapeutic use of helminth live infections or helminth products in humans. Again, this has brought conflicting results. Some studies showing an improvement in clinical signs or lesions, particularly the use of *T. suis* ova had positive outcomes in IBD or multiple sclerosis (Fleming et al., 2011; Summers et al., 2005a; Summers et al., 2005b). But again, other studies fail to assign a protective role to helminths (Bager et al., 2010; Daveson et al., 2011; Feary et al., 2010; Voldsgaard et al., 2015). Better understanding of how helminth manipulate the host immune response and identification of specific helminth molecules with potential for regulation of immunopathologies is required for future use of helminth products as a therapy.

3.2 Coinfections

3.2.1 Effect of helminthiasis on coinfections

Immune responses required to handle extracellular helminths or intracellular micro-organisms are strikingly different and are characterized by mutual inhibition. Helminth infections elicit strong type 2 and regulatory immune response, typically associated with a suppression of type 1 immune response and could therefore negatively impact protection against microbial pathogens. As distribution of

helminths often overlap that of major microbial threats, identifying the role of helminth infection in resistance to micro-organisms is crucial (Salgame et al., 2013).

Although sometimes contradictory and dependent on helminth species considered, epidemiological data indicate association between helminth infection and microbial infection like *Mycobacterium tuberculosis*, human immunodeficiency virus-1 (HIV) or malaria (Salgame et al., 2013). Some studies associated helminth infection with development of active tuberculosis (Elias et al., 2006) while other did not (Chatterjee et al., 2014). However, helminth infections impair immune response against *M. tuberculosis* that could be restored by deworming (Babu et al., 2009; Babu and Nutman, 2016; Resende Co et al., 2007). Similarly, association of helminth infection and *Plasmodium* infection is inconsistent in the literature. *S. mansoni* and hookworm infection were often linked to increased prevalence and malaria clinical signs (Degarege and Erko, 2016). *A. lumbricoides* and *T. trichiura* however have been shown to decrease the risk of development of cerebral malaria (Abbate et al., 2018). Schistosomiasis has been shown to increase the probability of being infected by HIV and was associated with increased viral loads (Downs et al., 2017). Although a slower development of adverse HIV outcomes was also described in people coinfected with schistosomes (Colombe et al., 2018). Yet, erradication of ongoing helminth infections in HIV-positive people might have a little but beneficial impact on viral load and $CD4^+$ T cell count (Means et al., 2016).

Again, variability of data obtained from **human epidemiological studies**, besides reflecting differences in methodologies, might be explained by the complexity of the interactions between helminths, micro-organisms and their host. Helminth infections can affect host resistance to micro-organisms in different ways. On one hand, inhibition of protective type 1 immunity can lead to decrease control of pathogen propagation (Helmby et al., 1998). Lesions induced by helminths can also promote host colonization by other pathogens. For example, urogenital schistosmiasis is associated with increased prevalence of HIV infection (Downs et al., 2011). On the other hand, regulatory responses elicited by helminths can be beneficial to lessen pathologies induced by inflammatory responses against micro-organisms (Furze et al., 2006). Type 2 immune response may also be beneficial to return to tissue homeostasis after microbial infection (Blériot et al., 2015). Effects of helminth infection on subsequent microbial infection is also dependent on the timing of coinfection (Salazar-Castañón et al., 2018). For example, a beneficial role of helminth infection for protection against infection by mycobacteria was observed when coinfection occured early after *N. brasiliensis* (5 days post-infection) and resulted in increased immune response and clearance of bacteria infection (du Plessis et al., 2013). Likewise, type 2 immunity potentially impairs early stage of HIV infection, including viral entry and replication (Bailer et al., 2000; Creery et al., 2006; Denis and Ghadirian, 1994). Another confounding factor is the co-existence of multiple parasite infections. Abbate and colleagues (2018) showed that presence of *T.*

trichiura in patients with hyperparasitemic malaria was associated with a reduced risk to develop cerebral malaria. However, when patients were coinfected with hookworms and *T. trichiura*, the protection conferred by the later was reduced, although infection with hookworms alone had no effect on cerebral malaria occurence (Abbate et al., 2018). Mouse models also showed variability in the effect of helminth infections on the outcome of microbial infections and highlighted that this variability is potentially dependent on mouse genetic background, timing of coinfection, identity of helminth and micro-organism involved (including difference between species of the same micro-organism genus) and inoculation route (Babu and Nutman, 2016; Salazar-Castañon et al., 2014). Helminth identity, and therefore its life cycle particularities, could influence the outcome of coinfections. First they may migrate through different organs and consequence of coinfection could be different if both players share the same niche or not (Moriyasu et al., 2018). Then, they are all characterized by a particular immune response dynamic, potentially including early type 1 immune response (which can limit micro-organism proliferation but can also be associated with increased inflammatory pathology) followed by type 2 and regulatory immune responses of variable strength (Babu and Nutman, 2016; Salazar-Castañon et al., 2014). Thus, uncovering specific mechanisms that link helminth infections to modifications of the immune response against concurrent or subsequent micro-organisms is needed to better understand how coinfection could be beneficial or detrimental for the host.

Furthermore, interaction of helminths with the host immune system might have prominent effects on efficacy of **vaccination**. Indeed, history of infection was shown to greatly impact vaccine response. Reese and colleagues (2016) developed a model of sequential infection of laboratory mice, including herpesviruses, influenza virus and helminths mimicking common infection history that humans could undergo. They showed that the response to a yellow fever virus vaccine was altered by this previous sequential exposition to pathogens (Reese et al., 2016). Adding to these observations, helminth infections have been associated with impairing vaccine efficacy. Unless dewormed before immunization, *H. polygyrus* or *S. mansoni* infected mice failed to develop protection against *Plasmodium* infection after immunization with plasmodium antigen or infection followed by treatment (Laranjeiras et al., 2008; Su et al., 2006). Interestingly, *H. polygyrus* similarly impact efficiency of DNA-based vaccine but did not impair protection conferred by irradiated sporozoïtes (Noland et al., 2010). *S. mansoni*, but not *H. polygyrus*, infection impaired the protection induced by BCG vaccination against *M. tuberculosis* infection (Elias et al., 2005; Rafi et al., 2015). Hepatitis B vaccination was also impaired in *S. japonicum* infected mice (Chen et al., 2012b). However, results from Guan and colleagues indicated that different life cycle stade of the same parasite could have distinct influence on vaccine response (Guan et al., 2013). Furthermore, some helminth products were also used as vaccine adjuvant and increased type 1 immune response (Jiang et al., 2014). Still, these results might have important repercussion on vaccine efficacy in helminth-endemic regions and might explain lower efficacy

observed in developing countries (Cherian et al., 2012). Consistant with that, human studies show that deworming before vaccination ameliorates response to vaccination against tuberculosis (BCG) (Elias et al., 2008), tetanus (Nookala et al., 2004) or cholera (Cooper et al., 2001).

3.2.2 Influence of helminth infections on anti-viral responses

The present section will focus on the influence of helminth infection on anti-viral immunity. Viruses are typical inducers of type 1 immunity that is crucial for their control, including cytotoxic $CD8^+$ T cell effector responses. This immune response can be considered as the integration of different components which can all be modified by bystander infections like helminthiasis as illustrated in figure 9 (Stelekati and Wherry, 2012).

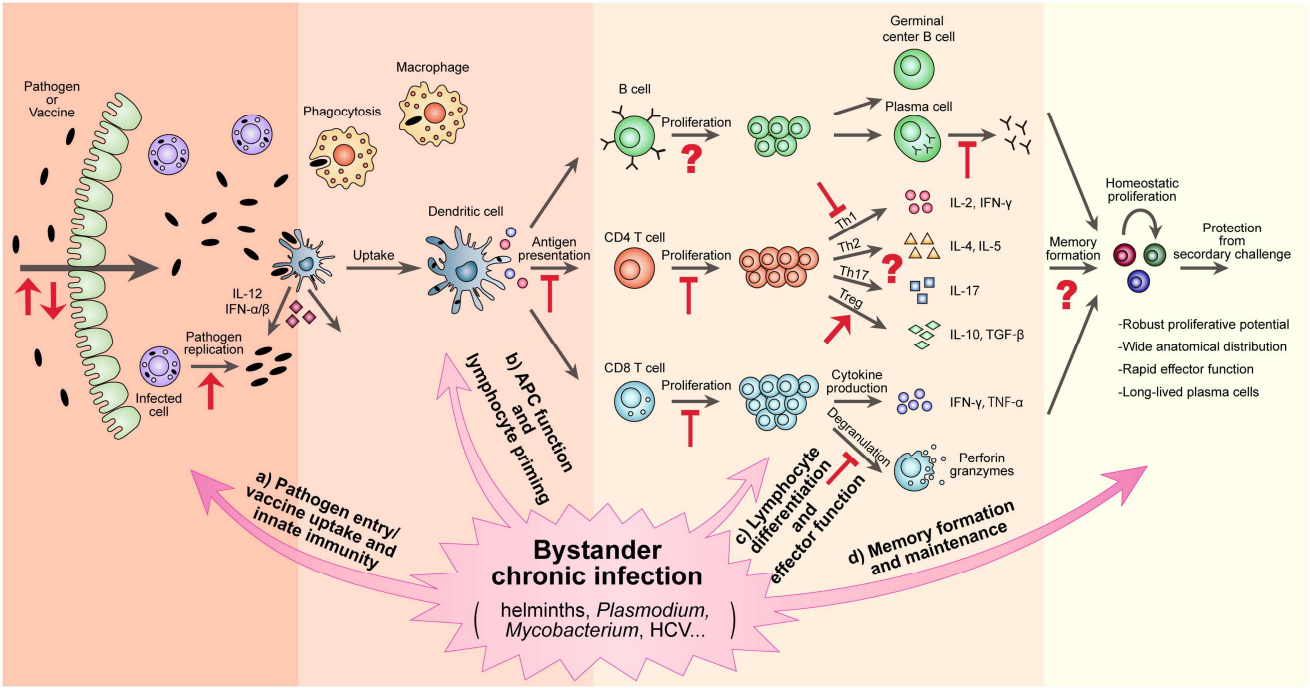

Figure 9 : Modification of immune response to unrelated antigen by bystander infection.
This figure illustrates crucial steps of effective immune response against invading pathogens and how bystander infection like helminth infections may impact its different components. First, pathogen access to the organism may be modified due to changes at physical barriers (for example through altered epithelium integrity or mucus production), at target cells (by modifying their availability or susceptibility to viral entry or replication) or at early antimicrobial mediators. Availability, effector capacities or cytokine production of innate immune cells like macrophages, neutrophils, ILC or NK cells (not depicted here) may be impacted. Then, capacity of antigen presenting cells to prime suitable adaptive immune response may be altered, including expression of costimulatory molecules, cytokine production, presentation of antigen or support from other innate immune cells. Proliferative and cytokines production capacities of activated lymphocytes may be modifed together with differentiation of T helper cells, cytotoxic function of $CD8^+$ T cells and humoral response from B cells, as a result of impairing priming by antigen presenting cells or intrinsic modification in lymphocytes. Finally, development, maintenance and recall responses from memory cells may be perturbated either by direct effect of helminth infection or as a consequence of altered effector responses.
From (Stelekati and Wherry, 2012)

Recent studies in mice highlighted that both innate and adaptive components of the anti-viral immune response can be impacted by helminth infections. Using *H. polygyrus* infection and *S. mansoni* egg

exposure, the first study revealed that helminth-induced type 2 immune response elicited reactivation of latent γ-herpesvirus through binding of STAT-6 to a viral gene controlling the switch between lytic and latent state. In this process, both IL-4 production and inhibition of IFN-γ were required. Furthermore, aaMφ were shown to be more permissive to γ-herpesvirus (Reese et al., 2014) and murine norovirus (Osborne et al., 2014) replication. Besides, intestinal tuft cells were recently described as the main cellular target of murine norovirus and IL-4 and IL-13 have been shown to stimulate proliferation of tuft cells (Gerbe et al., 2016). Thus type 2 cytokines production induced during helminth infections could enhance susceptibility to murine norovirus infection through expansion of tuft cells (Wilen et al., 2018). $CD8^+$ T cells are a hallmark of adaptive immune response against viruses. Osborne and colleagues (2014) showed that type 2 immune response induced by *T. spiralis* or *H. polygyrus* infection impaired $CD8^+$ T cell response against a subsequent viral infection with a murine norovirus, both in term of cell number and polyfunctional effector functions. Interestingly, anti-viral response was not only impaired locally (in the intestine) but also in distant organs such as the lung, as response against influenza infection was also reduced (Osborne et al., 2014). This modulation of adaptive anti-viral immune response involved Ym1 that is highly expressed by aaMφ during helminth infection. These mechanisms are summarized in figure 10.

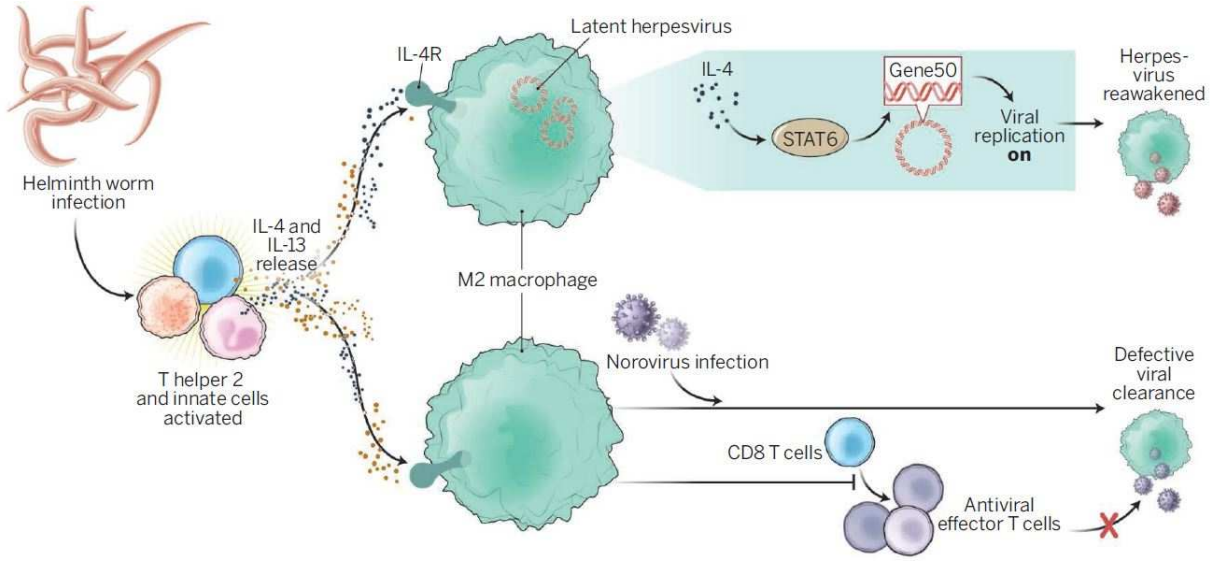

Figure 10 : Helminth-induced type 2 immune response alter anti-viral immune response. Top: Activated of STAT-6 transcription factor by IL-4 signalling pathway binds to γ-herpesvirus reactivation transactivator ORF50 and stimulate reactivation of latent infection (Reese et al., 2014). **Bottom**: Alternatively-activated macrophages express high levels of the chitinase-like molecule Ym1 which directly inhibits $CD8^+$ T cell proliferation during viral infection (Osborne et al., 2014). From (Maizels and Gause, 2014).

Although numerous data indicate that helminth infections are detrimental for anti-viral protection, several studies highlighted a protective role. Notably, *S. mansoni* chronic infection was associated with increased protection against pulmonary virus influenza A and pneumovirus of mice (Scheer et al., 2014).

H. polygyrus infection protected against respiratory syncytial virus (RSV) infection of mice, coinfected mice showing lower viral load and reduced lung inflammation. In this case, signalization through IL-4Rα was not required for protection, neither was adaptive immune response but it was dependent on the presence of intestinal microbiota and type I IFN. The authors proposed that invading microbiota through *H. polygyrus* induced gut wall lesions induced a systemic anti-viral type I IFN response to control RSV infection (McFarlane et al., 2017). In another study, the protection induced by *T. spiralis* against influenza infection was strikingly different. Indeed, this protection was observed late during viral infection as an enhanced recovery rate in coinfected group. Here, no difference in lung viral load was observed between groups, instead protection was likely linked to decrease inflammation, independently of IL-10 production (Furze et al., 2006). Other data on the effect of filarial cystatin on RSV infection confirmed that helminth products are potent regulator of virus-induced excessive inflammation without impacting infection itself. In this study, modulation was mediated by macrophages (Schuijs et al., 2016). These results indicate that excessive inflammation during viral infection might be deleterious for the host without any beneficial counterpart in the control of the virus. Helminth infection could act independently in both control of viral load and inflammation.

These data illustrate how helminth infections can act in various steps of both innate and adaptive mechanisms of anti-viral immune responses, even in distant organs, with either beneficial or detrimental effects for the host. Of course, numerous other mechanisms already discussed in previous sections could influence the outcome of viral infection in helminth-infected host. For example, helminth products could increased viral replication *in vitro* as it is the case for SEA on cell culture of hepatitis C virus (Bahgat et al., 2010). Helminth products can also condition DCs that become “refractory” to induction of type 1 immune response (Everts et al., 2009; Metenou et al., 2012). Proliferation of effector T cells might also be compromised by helminth-induced expression inhibitory costimulation molecules like expression of PD-L2 on aaMφ (Huber et al., 2010). Finally, modification of the host’s microbiota by the presence of helminth could impact several parameters including immune system balance (Belkaid and Hand, 2014), epithelium composition (Wilen et al., 2018) or, by its interaction with incoming virus, alter establishment of viral infections (Pfeiffer and Virgin, 2016).

4 Antigen-inexperienced memory CD8$^+$ T lymphocytes

4.1 Effector and memory CD8$^+$ T lymphocytes

4.1.1 Dynamics of CD8$^+$ T lymphocyte responses

The ability to "remember" a pathogen (or an antigen) against which an immune response has been mounted and to better react to a second encounter with this same pathogen is called "**immunological memory**". Immunological memory represents one of the hallmarks of the adaptive immune system and differentiates it from innate immunity. Immunological memory is supported by the persistence, after resolution of infection, of memory T and B cells. As part of the adaptive immune system, CD8$^+$ T lymphocytes are activated upon specific recognition of epitopes from foreign (non-self) molecular patterns (antigens). In secondary lymphoid organs, specific interactions between the unique T-cell receptor (TCR) from a CD8$^+$ T lymphocyte and the MHC Class I-peptide complex presented by an antigen-presenting cell (signal 1), along with costimulatory signals (signal 2) associated with an inflammatory context (signal 3), induce the activation of a naive CD8$^+$ T cell into an effector CD8$^+$ T cell. The broad diversity of TCR receptors in the naive population of CD8$^+$ T cells allow them to specifically recognize and react to an exceptionally wide variety of antigens. Antigens from intracellular pathogens such as viruses are processed in antigenic peptides to be bound to a MHC Class I molecule and exported to the surface of the infected cell, allowing the presentation of the MHC Class I-peptide complex to specific effector CD8$^+$ T cells. Although MHC Class I are dedicated to the presentation of endogenous antigens, cross-presentation can occur in DCs to allow presentation of exogenous antigens in a context of MHC Class I (Joffre et al., 2012). Antigen-specific activation of CD8$^+$ T cells results in the production of a greatly enlarged population of effector cells with the same antigenic specificity towards the pathogen, thanks to two mechanisms: clonal expansion and acquisition of functional and phenotypic effector features (Blattman et al., 2002). A mouse possesses about 25 million naive CD8$^+$ T cells, among which about 100 to 1000 cells are specific to a given antigenic peptide (Jenkins and Allen, 2010). Upon Ag recognition and activation, specific cells undergo clonal expansion and can produce up to 10 million effector CD8$^+$ T cells in a week (expansion phase, Figure 11), which function to eradicate invading pathogens (Smith et al., 2018). Effector CD8$^+$ T cells are also called cytotoxic T cells as their principal function is to recognize and kill infected cells. Beside their cell-killing role (i.e. through secretion of cytotoxic molecules such as granzymes and perforin or apoptosis-induction through Fas-ligand), effector CD8$^+$ T cells also secrete inflammatory cytokines such as IFN-γ and tumor necrosis factor (TNF)-α. Following elimination of the pathogen, 90 to 95% of the expanded CD8$^+$ T cells pool undergo apoptosis (contraction phase, Figure 11) (Cui and Kaech, 2010) and a population of memory CD8$^+$ T cells persists (memory phase, Figure 11). Memory T cells possess longterm survival potential and self-renewal capacities retaining a multipotent state with high proliferative and effector potential

(Kaech and Wherry, 2007). As for naive T cells, memory T cells have a stem cell-like behaviour by their ability to regenerate effector population diversity and provide immune-competence during secondary responses (Buchholz et al., 2016; Graef et al., 2014). They are more numerous than the initial naive population (Blattman et al., 2002) but are also characterized by altered distribution pattern (Gebhardt et al., 2009; Masopust et al., 2001; Sallusto et al., 1999) and enhanced effector capacities following TCR stimulation compared to naive T cells (Wolint et al., 2004). Thus, memory T cells can give rise to a faster and stronger effector response against a secondary encounter with the same pathogen. However, recent evidence indicates that memory T cells may be less responsive to their cognate antigen but more to inflammatory stimuli (including cytokines), which may lead in some circumstances to innate-like properties and control of pathogens in an antigen non-specific manner (Chu et al., 2013; Mehlhop-Williams and Bevan, 2014).

4.1.2 Diversity within CD8$^+$ T cell responses

Activation and clonal expansion of CD8$^+$ T cells do not produce a homogeneous population of effector cells and transition to memory is not a random process (Figure 11). On the contrary, all activated CD8$^+$ T cells during the acute phase of the infection (expansion phase) do not have an equivalent potential to participate to the memory pool. By focusing mainly on the expression of IL-7 receptor α (CD127) and killer-cell lectin like receptor G1 (KLRG1), short-lived effector cells (SLEC; CD127$^-$ KLRG1$^+$) and memory precursor cells (MPEC; CD127$^+$ KLRG1$^-$) can be differentiated within the clonaly expanded population (Cui and Kaech, 2010; Kaech et al., 2003). Interestingly, effector and memory fate are not strictly separated as evidence indicates that memory precursor cells are able to produce (at least at one point during their ontogeny) the effector molecules IFN-γ or granzyme B (Bannard et al., 2009; Harrington et al., 2008).

Diversity of effector population might represent a continuum of intermediate states between terminally differentiated SLEC and memory precursors; thus a range of cells with high effector capacities but short half-live and cells with lower effector capacities but deeply increased life expectancy (Cui and Kaech, 2010). Memory precursor cells can further generate several subsets of memory cells (Arsenio et al., 2015; Obar and Lefrancois, 2010; Plumlee et al., 2015). Memory CD8$^+$ T cells are usually divided in cell subsets based on surface antigen expression, longevity and effector, proliferative and migration characteristics. Central memory T cells (T_{CM} ; CD62L$^+$ CCR7$^+$) are located in secondary lymphoid tissues, effector memory T cells (T_{EM} ; CD62L$^-$ CCR7$^-$) migrate through non-lymphoid tissues and tissue-resident memory T cells (T_{RM} ; CD62L$^-$ CCR7$^-$ CD103^{hi} CD69^{hi} CD27^{lo}) are present within the tissue and do not recirculate (Gebhardt et al., 2009; Halle et al., 2017; Jameson and Masopust, 2018; Masopust et al., 2010; Masopust et al., 2001; Mueller et al., 2013; Reinhardt et al., 2001; Sallusto et al.,

1999). T_{EM} and T_{RM} act as a first line of defence against secondary infections as they can express immediate lytic functions (Masopust et al., 2001), as opposed to central memory T cells that do not show direct effector functions but rather present longer half-life and higher proliferative potential, thus are important for optimal secondary $CD8^+$ T cell responses (Bachmann et al., 2005). Here again, with description of an increasing number of memory T cell subsets, it was recently proposed that it may be better represented as a continuum (Jameson and Masopust, 2018; Newell et al., 2012).

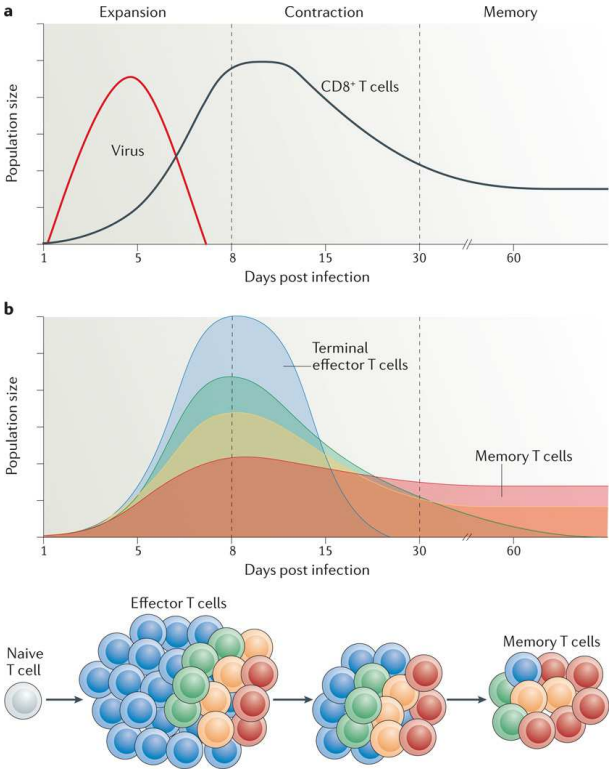

Figure 11. Kinetics of a T cell response and distribution of memory cell potential. a. During an acute viral infection, antigen-specific T cells rapidly proliferate (expansion phase) and differentiate into cytotoxic T lymphocytes that mediate viral clearance. Most of these cells die over the next several weeks (contraction phase). **b**. The pool of effector T cells can be separated into multiple diverse subsets. Some cell-surface markers correlate with distinct effector and memory T cell fates: terminal effector T cells (shown in blue) are $KLRG1^{hi}IL\text{-}7R\alpha^{low}CD27^{low}BCL\text{-}2^{low}$, and long-lived memory (and memory precursor) cells (shown in red) are $KLRG1^{low}IL\text{-}7R\alpha^{hi}CD27^{hi}BCL\text{-}2^{hi}$. However, other T cell subsets with intermediate differentiation states also exist that have mixed phenotypes as depicted by the yellow and green populations. Over time, there may also be some interconversion between these subsets. From (Kaech and Cui, 2012).

4.1.3 Actors of memory formation and maintenance

Several **models** were proposed concerning the mechanisms leading to the functionnal diversity of the T cell response. Despite the existence of the theory “one cell, one fate” suggesting that fate of T cells is already predetermined in naive cells, naive $CD8^+$ T cells were shown to have a “stem-like” feature. Indeed, a single naive $CD8^+$ T cell has been able to generate a phenotypically and functionnaly diverse offspring containing both effector and memory cells (Gerlach et al., 2010; Stemberger et al., 2007). However, optimal response still requires recruitment of several naive cells of the same specificity as individual cell does not always fully translate its diverse potential upon activation (Buchholz et al., 2016). It is still unclear which and how elements of the immune response are integrated in the fate decision process and several models are proposed such as: strength and duration of TCR stimulation, inflammatory cytokines, transcriptional regulations, metabolic switches and uneven segregation of lineage-determining factors during division (Cui and Kaech, 2010). Prolonged exposure to antigen is not required for effective activation of $CD8^+$ T cells (van Stipdonk et al., 2001), but strong cumulative

signals from antigen stimulation (depending on binding affinity to TCR and duration of TCR stimulation), costimulation and inflammation are important favouring factors for the expansion associated with increased short-lived fate (Joshi et al., 2007). Importantly, increased activation of T cells following excessive inflammation or TCR/costimulation signal may be associated with a deficient memory formation as more cells acquire terminaly differentiated states (Kaech and Cui, 2012). Integration of the overall strength of the signals received by $CD8^+$ T cells is proposed to respond to one of the following models. First, in the "decreasing-potential" model, those signals are continuously integrated after initial priming, prolonged signals promoting terminally differentiated effector cells. Second, the "progressive differentiation" or "signal-strength" model suggests that those signals are integrated during initial priming and influence the phenotype at later timepoints. Besides, the "asymmetric cell fate" model proposes that assymetric cell division generates one cell that will adopt an effector fate and the other a memory fate (Buchholz et al., 2016; Kaech and Cui, 2012). Although these models propose that fate decision occurs following antigen stimulation, with all naive $CD8^+$ T cell having the same differentiation potential, recent data indicate a diversity even within naive $CD8^+$ T cells with a partially "pre-programmed" fate that is influenced by the life stage at which the cell was produced (Smith et al., 2018). To add another level of complexity, recent reports suggested that effector $CD8^+$ T cells can dedifferentiate into long-lived memory cells (Herndler-Brandstetter et al., 2018; Youngblood et al., 2017).

Several **transcription factors** have been shown to influence the fate decision process in $CD8^+$ T cells. The T-box factors **T-bet** (T-box expressed in T cells) and **Eomes** (eomesodermin) act in concert to regulate the SLEC/MPEC fate (Cui and Kaech, 2010). Reports highlighted that they both participate to the formation of the effector response with partially redundant roles (Intlekofer et al., 2005; Pearce et al., 2003; Sullivan et al., 2003) and the presence of at least one of them was essential to avoid uncontrolled and deleterious type 17-like activation of $CD8^+$ T cells (Intlekofer et al., 2008). T-bet expression peaked during acute infection, was associated with efficient formation of effector cells and declined after resolution of infection (Takemoto et al., 2006; Wiesel et al., 2012). Eomes expression was upregulated during the effector phase but increased further during the memory phase. In term of memory formation, it appeared that Eomes has a crucial role for optimal formation of T_{CM} (Banerjee et al., 2010). In return, overexpression of T-bet was shown to be responsible for defective T_{CM} formation (Intlekofer et al., 2007). However, both T-bet and Eomes enhanced IL-2/IL-15Rβ (CD122) expression, allowing cells to better respond to IL-15 which is important for the maintenance of memory cell population (Intlekofer et al., 2005). In accordance to a role for inflammation in promoting SLEC formation at the expense of memory formation, IL-12 enhanced T-bet but repressed Eomes expression in effector $CD8^+$ T cells (Joshi et al., 2007; Takemoto et al., 2006). This mechanism appeared to by dependent on mTOR kinase activity. Indeed, when mTOR activity was blocked, IL-12 treatment of $CD8^+$ T cells induced

Eomes expression and formation of memory precursors (Rao et al., 2010). Other inflammatory cytokines like type I IFN are implicated in T-bet upregulation and efficient production of effector cells (Wiesel et al., 2012).

Other transcription factors like B lymphocyte-induced maturation protein-1 (Blimp-1), inhibitor of DNA binding (ID) 2 and STAT-4 are associated with terminal differentiation of SLEC in opposition to B-cell lymphoma (BCL) 6, ID3, T cell factor (TCF) 1, STAT-3 and frokhead box O (FOXO) 1 which are implicated in the maintenance of memory cells. These transcription factors regulate each other in a complexe network of interactions (Kaech and Cui, 2012).

Although **maintenance of memory CD8$^+$ T cells** is independent of antigen or tonic stimulation from self-antigen/MHC (Murali-Krishna et al., 1999) it requires cytokine signals. Both IL-7 and IL-15 have been involved in the optimal CD8$^+$ T cell memory formation and maintenance by cooperatively regulating survival and proliferation of these cells (Becker et al., 2002; Buentke et al., 2006; Judge et al., 2002; Ku et al., 2000; Osborne et al., 2007; Schluns et al., 2000). **IL-7** sustains survival of memory CD8$^+$ T cells. As previously discussed, CD127 is used to differentiate SLEC and MPEC fate as CD127$^+$ CD8$^+$ T cells better survive when transferred in uninfected host than their CD127$^-$ counterparts (Kaech et al., 2003). CD127 is downregulated in the early time of the infection when a population of early effector CD8$^+$ T cells (EEC; KLRG1$^-$ CD127$^-$) is observed. EECs conserve the ability to give rise to both SLEC and MPEC (Obar et al., 2011). At the peak of the immune response, to majority of CD8$^+$ T cells express low levels of CD127 but following resolution of infection, CD127 expression is upregulated within the population of activated cells, which can be explained by the fact that cells expressing higher levels of CD127 will better survive the contraction phase (Cui and Kaech, 2010; Kaech et al., 2003; Schluns et al., 2000). Concerning **IL-15**, it was proved to be an important factor to sustain memory CD8$^+$ T cell proliferation (Goldrath et al., 2002; Ku et al., 2000). IL-7 and IL-15 have a complementary role and differential migratory capacities of memory T cell subset may allow them to reach niche were either of these signals are available (Judge et al., 2002; Jung et al., 2016). Other cytokines signalling through the common gamma chain (γc), like IL-21 and IL-2, have also been implicated in the maintenance of memory CD8$^+$ T cells (Mitchell et al., 2010; Zeng et al., 2005).

Effector and memory CD8$^+$ T cells are most commonly identified by their high expression of CD44, whereas naive CD8$^+$ T cells are CD44^{low}. While CD44 is widely acknowledged in mice to report activated/effector T cells, several other surface molecules (CD122, CXCR3, Ly6C or CD49d) or transcription factors (T-bet and Eomes) are also differentialy expressed between naive and activated CD8$^+$ T cells (Figure 12, first two columns).

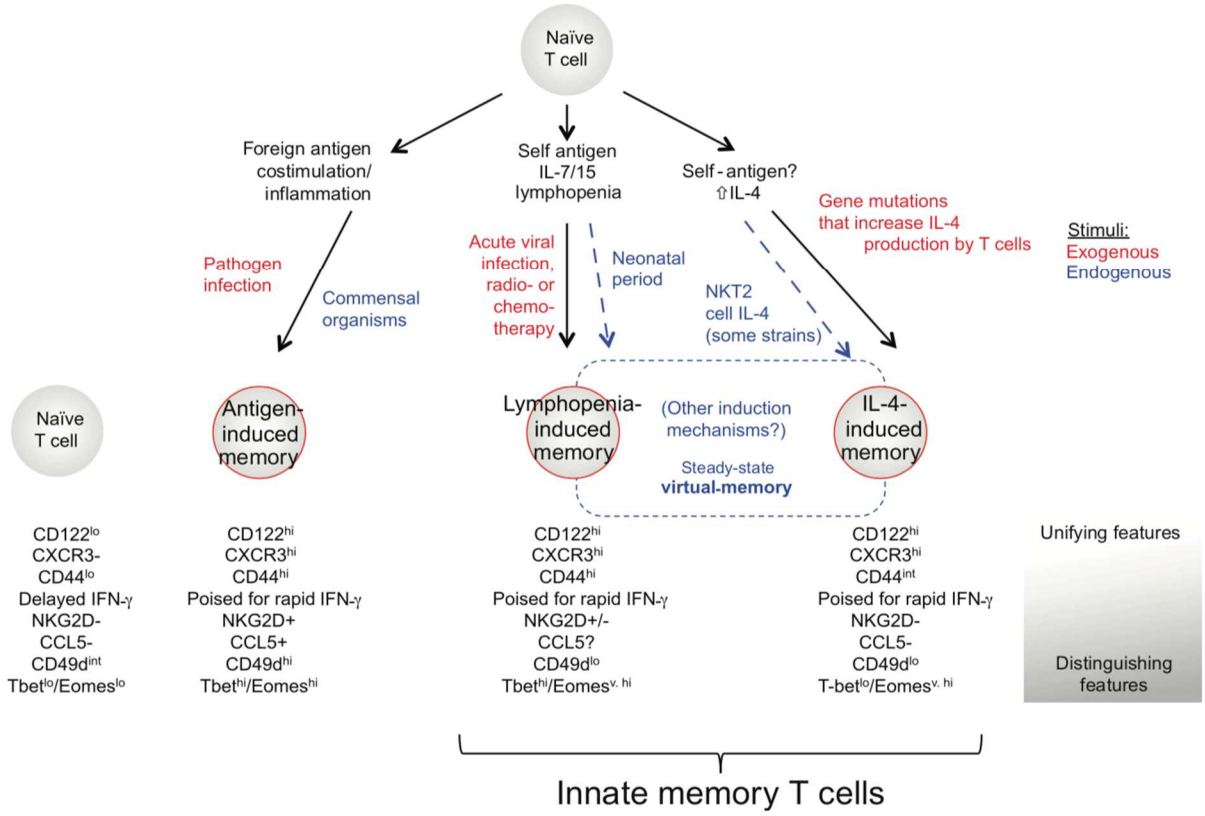

Figure 12. Overview of generation pathways and characteristics of innate and conventional memory T cell populations. Naive T cells can respond to a variety of endogenous and exogenous (or experimental) signals to produce memory-phenotype cells. Stimulation by foreign antigens, in a suitably immunogenic way, will produce "antigen- induced memory", while there are two pathways that produce "Innate memory" T cells: these pathways involve the response to lymphopenia or the response to IL-4. Populations of T cells with innate memory properties are found in normal animals at steady state—these are termed virtual memory cells. Key factors involved in generation of these cells and major phenotypic characteristics that are shared or distinguished these different populations are indicated. From (Jameson et al., 2015).

4.2 Antigen-inexperienced memory $CD8^+$ T cells

According to the conventional definition of T cell memory outlined in the previous section, memory $CD8^+$ T cells were thought to be only present as the result of an immune reaction against a specific antigenic peptide. However, a number of studies over the last decade have comprehensively described the existence of "**antigen-inexperienced" memory-like $CD8^+$ T cells** which highlighted alternative mechanisms that could be involved in the formation of T cell memory (Figure 12). As suggested by their name, these cells share most of functions with "true memory" cells (corresponding to antigen-experienced memory T cells), including increased effector capacities against pathogens (Lee et al., 2013a), independently of the encounter of a specific antigen (Jameson et al., 2015).

Jameson and colleagues (2015) identified two main immunological contexts in which formation of antigen-inexperienced memory T cells could be observed in mice (Figure 12). First, "homeostatic" proliferation of T lymphocytes in a T-cell lymphopenic environment was associated with the acquisition

of memory characteristics. These cells were termed "**innate memory T cells**". Second, several gene-deficiency models associated with IL-4-dominated environments favoured the appearance of memory-like T cells also called "**bystander memory T cells**". Besides these biased immunological contexts of deficiencies, memory-like T cells are also observed at steady-state in normal unimmunized mice and were given the name of "**virtual memory T cells**" (T_{VM}). One possible explanation for the presence of memory T cells in naive animal is that they could arise following a response against environmental antigens. But the existence of alternative mechanisms leading to production of memory-like T cells is conforted by several observations. First, T_{VM} were notably described in pathogen-free, germ-free or even antigen-free mice (Haluszczak et al., 2009). Moreover, enrichment of epitope-specific T cells allowed identification of memory-like T cells in numerous epitope-specific T cell populations making the hypothesis of a previous encounter with these various epitopes unlikely (Akue et al., 2012). A recent comparison between functional capabilities of "true memory" subsets and T_{VM} cells has recently been published and is depicted in Figure 13.

These antigen-inexperienced memory $CD8^+$ T cell populations have to be distinguished from other innate T cell populations that also exhibit a memory-like/activated phenotype with ability to raise a rapid effector response upon activation, such as rapid cytokine secretion and cytotoxic activitiy. Indeed, unconventional T lymphocytes undergo a limited antigen receptor rearrangement process and therefore bear a restricted diversity of antigen receptors. Innate T cells include intraepithelial γδ T cells, mucosal-associated invariant T cells (MAIT cells) and natural killer T cells (NKT cells). These cells are present in the periphery and are abundant compared to the limited number of antigen-specific naive conventional $CD8^+$ T cells (Godfrey et al., 2015). According to these characteristics, innate T cells can take part in the first line of defense similarly to innate immune cells. Despite these confunding attributes, evidence indicates that bystander memory $CD8^+$ T cells differ from innate T cells. For instance, absence of MHC Ia molecules greatly impedes the development of bystander memory $CD8^+$ T cells, indicating that this population is unlikely to belong to a population of innate T cells whose low diversity TCR that rather recognize MHC Ib molecules. Additionally, unlike NKT cells, bystander memory $CD8^+$ T cells do not bind CD1d tetramers (Atherly et al., 2006; Broussard et al., 2006).

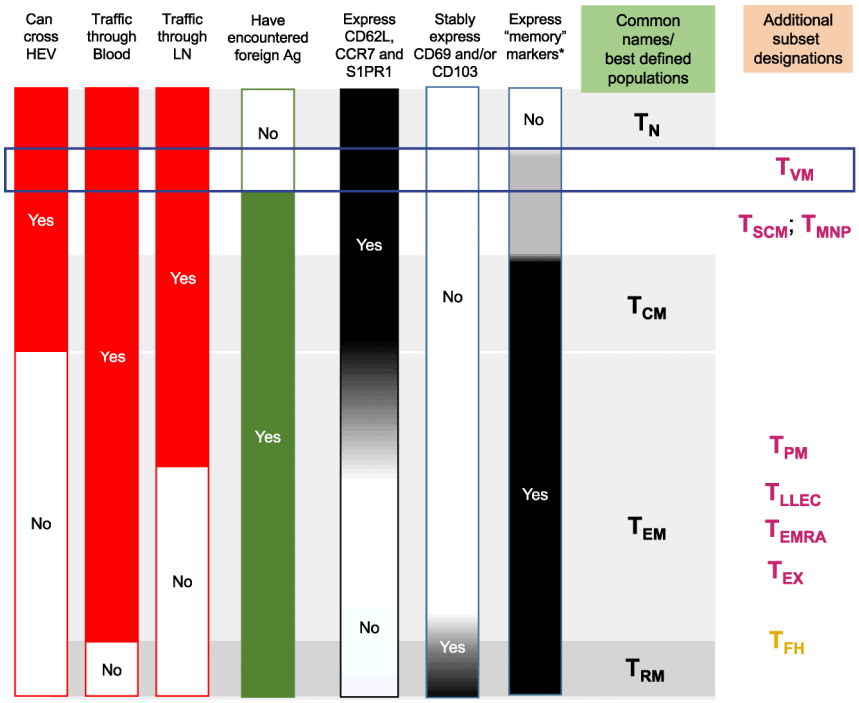

Figure 13. Traits that distinguish naive and major memory T cell populations. The bars on the left indicate various characteristics, which can be used to distinguish the T cell subsets listed on the right. The first four bars indicate trafficking capabilities and stimulation history of the cells, providing rigid distinctions that can be used to define T cell populations, but note that there is only limited concordance between these traits. The other bars indicate gene expression or phenotypic characteristics, focused on molecules associated with trafficking, tissue retention, and "memory markers". Grey shading in these bars indicates where phenotypic/gene-expression characteristics fail to clearly correlate with the red and green bars on the left. At the far right are T cell subsets typically associated with these combinations of traits and phenotypic/gene expression characteristics, note that the position of these identifiers is inherently vague, since the typical criteria for defining "subsets" use markers that may not faithfully correlate with the cells' stimulation history or migration potential. The position of virtual memory T cells (T_{VM}) in this classification is highlighted in blue.
Abbreviations for T cells: Naive, Tn; Central Memory, Tcm; Effector Memory, Tem; Tissue-Resident Memory, Trm; Virtual Memory (also encompassing "Innate" memory), Tvm; Stem Cell Memory, Tscm; Memory T cells with Naive Phenotype, Tmnp; Peripheral Memory, Tpm; Long-Lived Effector Cells, Tllec; CD45RA$^+$ Effector Memory (defined in humans), Temra; Exhausted T cells, Tex; Tfh Follicular Helpers). Color coding of the T cell subsets indicates whether they have been primarily described for CD8$^+$ T cells (maroon), CD4$^+$ T cells (gold) or both populations (black). From (Jameson and Masopust, 2018).

4.2.1 Innate memory CD8$^+$ T cells : lymphopenia-induced memory-like CD8$^+$ T cells

T cell formation process includes negative (elimination of cells with high self peptide/MHC affinity) and positive (survival of cells with lower but significant affinity to self peptide/MHC) selection in the thymus. At steady state, survival of resting naive CD8$^+$ T cells still depends on the presence of self-peptide/MHC signal, known as "tonic signal", along with IL-7 stimulation (Sprent and Surh, 2011; Tanchot et al., 1997). The size of the T cell compartment occured to be tightly regulated and the number of cells is kept constant, apart from circumstance of immune reaction. Therefore, when CD8$^+$ T cells are transfered in a T lymphocytopenic environment (induced notably by irraditation, Rag deficiency, or T cell antibody-based depletion), they undergo a slow homeostatic proliferation to regenerate the pool (Bell et al., 1987; Ernst et al., 1999; Rocha et al., 1989). The slow pace of "homeostatic" proliferation

is one of the parameters that differentiate it from true effector response that exhibit much higher rate of proliferation (Murali-Krishna and Ahmed, 2000). Homeostatic proliferation requires specific, low-affinity interaction between TCR and self-peptide-MHC complexes (Goldrath and Bevan, 1999) and IL-7 coming from non-hematopoietic cells (Goldrath et al., 2002; Schluns et al., 2000; Sprent and Surh, 2011). Thus, the same stimuli sustaining survival of $CD8^+$ T cells in a physiological environment can stimulate proliferation when the number of T cells is abnormally low. Proliferation induced by a depleted T cell compartment will ultimately stop if a normal number a T cell can be restored, indicating that this phenomenon is drove by the existence of an "empty space" in the T cell compartment (Goldrath et al., 2000). The common explanation is that T lymphocytes compete for the factor sustaining their survival. In a lymphopenic environment, the competition for those factors will be reduced and individual lymphocytes will receive increased signals, notably from IL-7, leading to their proliferation (Jameson et al., 2015). Homeostatic proliferation is not observed homogeneously in the T cell pool as some TCR transgenic $CD8^+$ T cells were shown to be more prone to homeostatic proliferation compared to others, and even within a same TCR transgenic cell population, only a proportion of them will actually undergo homeostatic proliferation. Thus, only a portion of the T cell pool proliferates in response to T-cell immunodeficiency (Ernst et al., 1999; Surh and Sprent, 2000). The extent of proliferation appeared to be correlated to the strength of the tonic TCR signal received by T cell, which is directly proportional to its CD5 expression level (Jameson et al., 2015; Kieper et al., 2004). CD5 expression level could also be correlated to CD127 expression level, thus to the capacity of the cell to proliferate in response to IL-7 (Palmer et al., 2011)

Strikingly, homeostatic proliferation of $CD8^+$ T cells is associated with acquisition of a memory phenotype with upregulation of some memory markers (CD44, CD122, CD132) but maintain a naive phenotype for other markers of activation (CD49d, CD62L, CD69, CD71 or CD25), with CD49d often used as a discriminating marker (Ernst et al., 1999; Goldrath and Bevan, 1999; Kieper and Jameson, 1999; Murali-Krishna and Ahmed, 2000) Most importantly, these lymphopenia-induced memory-like $CD8^+$ T cells are also characterized by increased effector functions (including cytotoxic activities, IFN-γ production and enhance response against their cognate antigen) compared to naive cells (Goldrath et al., 2000; Murali-Krishna and Ahmed, 2000; Oehen and Brduscha-Riem, 1999) although they are still less effector than conventional memory $CD8^+$ T cells (Cheung et al., 2009; Goldrath and Bevan, 1999; Murali-Krishna and Ahmed, 2000).

As explain above, IL-7 has a key role in homeostatic proliferation of $CD8^+$ T cells and therefore in lymphopenia-induced memory formation. Supporting this concept, artificially increased levels of IL-7 did not only accelerate homeostatic proliferation in lymphopenic environments but more importantly drove proliferation and memory conversion of naive $CD8^+$ T cells in a lymphoreplete environment. This

was very similar to lymphopenia-induced proliferation and memory formation also required the presence of MHC molecules (Boyman et al., 2008). In addition, other cytokines like IL-2, IL-15, IL-4 also promoted proliferation and memory conversion of naive $CD8^+$ T cells in lymphorepleted environment (Boyman et al., 2006; Kamimura and Bevan, 2007; Li et al., 2011; Morris et al., 2009).

4.2.2 Bystander memory $CD8^+$ T cells : IL-4-induced memory-like $CD8^+$ T cells (gene-deficiency setting)

Lymphopenia-induced memory $CD8^+$ T cells form in the periphery and originate from mature naive $CD8^+$ T cells. In addition, deficiencies of various T cell development-associated genes have been shown to influence the phenotype of $CD8^+$ T cells before they exit the thymus and increase the occurence of single positive $CD8^+$ thymocytes with a memory phenotype. Memory-like $CD8^+$ T cells developing in this mutant mouse models were given the name of "bystander memory $CD8^+$ T cells" (Jameson et al., 2015). A number of mouse strains deficient for genes like *Itk, Klf2, Id3, Cbp, Tbet, Ndf1p, Ly9, Tcf1, Elk1* and *4*, bearing gene mutations in *Slp-76* or transgenic mice (*plck-CIITA*^{Tg}*pIV*-/- mice) have all been associated with an altered thymic development of $CD8^+$ T cells and emergence of bystander memory $CD8^+$ thymocytes (Atherly et al., 2006; Broussard et al., 2006; Fukuyama et al., 2009; Lee et al., 2013b; Maurice et al., 2018; Min et al., 2011; Sharma et al., 2012; Sintes et al., 2013; Verykokakis et al., 2010b; Weinreich et al., 2009). These bystander memory $CD8^+$ T cells display an impressively uniform phenotype in all the different conditions, with upregulation of CD44 and CD122, expression of the transcription factor Eomes but not Tbet and enhanced ability to produce IFN-γ upon restimulation. High expression of Eomes but low expression of T-bet is a chacarteristic feature of bystander memory $CD8^+$ T cells, while innate memory $CD8^+$ T cells rather express high levels of both transcription factors (Figure 12) (Jameson et al., 2015). Initially arising from the thymus, bystander memory T cells have been shown to exit and contribute to peripheral memory-like $CD8^+$ T cells (Gugasyan et al., 2012). Work by Weinreich and colleagues (2009 and 2010) highlighted the mechanisms underlying this recurrent change in $CD8^+$ thymocyte phenotype. Using Kruppel-like factor(KLF) 2 deficient mice, they observed that the emergence of bystander memory $CD8^+$ thymocytes was dependent on KLF2 deficient environment but independent of their intrinsic expression of KLF2. Such observation warranted the name of "bystander" memory $CD8^+$ T cells. In addition, they identified increased production of IL-4 by an expanding promyelocytic leukemia zinc finger(PLZF)-expressing thymocyte population induced by KLF2 deficiency. Such increase in IL-4 and expression of PZLF were both shown to be essential for the expansion of bystander memory $CD8^+$ T cells. Phenotypic changes on $CD8^+$ thymocytes due to KLF2 deficiency were abrogated in absence of IL-4Rα expression or if truncated form of the PLZF protein was expressed. $CD8^+$ T cells can directly respond to IL-4 and need Eomes to upregulate memory markers (Weinreich et al., 2010; Weinreich et al., 2009). Other models of bystander $CD8^+$ T cells expansion were

confirmed to involve a cell extrinsic process crucially depending on the expansion or activation of an IL-4-secreting PLZF$^+$ thymocytes (Felices et al., 2009; Gordon et al., 2011; Kurzweil et al., 2014; Lee et al., 2013b; Sintes et al., 2013; Verykokakis et al., 2010a). The majority of PLZF$^+$ thymocytes expressed CD4 and were identified as invariant (*i*)NKT, γδT cells or αβ T cells (Felices et al., 2009; Lee et al., 2013b; Prince et al., 2014; Weinreich et al., 2010) depending on the model. Interestingly, PLZF is an essential transcription factor for normal development of *i*NKT cells (Kovalovsky et al., 2008), and regulate gene expression in *i*NKT cells, including a role in IL-4 production (Gleimer et al., 2012; Pereira and Boucontet, 2012).

The induction of bystander memory CD8$^+$ T cells is mostly described in the thymus. Yet, in a model involving Nedd4-family interacting protein 1 (Ndfip1) deficiency, memory-like CD8$^+$ T cells with the same characteristics (increased CD44, CD122 and Eomes expression) were induced in the periphery without change neither in CD8$^+$ thymocytes nor in *i*NKT cells or γδT cells. Nonetheless, the observed increased bystander memory T cells was associated with increased IL-4 production but originating from conventional peripheral CD4$^+$ T cells (Kurzweil et al., 2014).

CD8$^+$ T cell intrinsic pathways have also been involved in the emergence of thymic memory-like CD8$^+$ T cells, independently of IL-4 secreting PLZF$^+$ cells but depending on *Elk1* and *4*, *Nfκb1* or *Bcl11b* (Gugasyan et al., 2012; Hirose et al., 2015; Maurice et al., 2018).

A number of these genes were shown to have profound impact on innate T cell populations, influencing development or commitement of *i*NKT towards IFN-, IL-4 or IL-17-producing *i*NTK cells that were subsequently identified as *i*NKT1, *i*NKT 2 or *i*NKT17 (as for CD4$^+$ T lymphocytes Th1, Th2 or Th17) (Lee et al., 2013b). Other targeted genes were also likely involved in post-TCR signalling (*Cbp*, *Itk*, *Id3*, *Slp-76*, *Elk1* and *4*) indicating that generation of bystander memory CD8$^+$ T cells could be associated with an altered TCR signalling pathway (Jameson et al., 2015; Maurice et al., 2018). Consistent with that, CD8$^+$ T cells susceptibility to engage a bystander memory phenotype was likely associated with the strength of positive selection signal. Indeed, differentiation of CD8$^+$ T cells arising from strong positive selection signal are less impacted by *Itk* deficiency. Therefore, as in lymphopenia-induced homeostatic proliferation, every CD8$^+$ T cell clones did not seem to equally respond to this biaised environment (Atherly et al., 2006).

4.2.3 Virtual memory CD8$^+$ T cells : antigen-inexperienced memory-like CD8$^+$ T cells in normal physiology

Following description of memory-like CD8$^+$ T cell generation in transgenic/deficient contexts, a similar population has been described in the thymus of unimmunized wildtype mice, in particular in BALB/c mice (Weinreich et al., 2010). Existence of memory-like CD8$^+$ T cells in the periphery of antigen-inexperienced mice had already been described for some time but pivotal work from Haluszczak and colleagues (2009) clarified the phenotype of these cells. They showed that like innate memory CD8$^+$ T cells but unlike conventional memory CD8$^+$ T cells, memory-like CD8$^+$ T cells present in antigen-inexperienced mice homogeneously express low level of the integrin α4 subunit (CD49d). They were also shown to express high level of CD44 and levels of CD122 that was even higher than antigen-experienced memory CD8$^+$ T cells (Sosinowski et al., 2013). Strikingly, antigen-inexperienced memory T cells can be found at the same frequency in germ-free mice compared to specific pathogen free (SPF) mice, among several TCR clones albeit a great variation in proportions can be observed in-between clones (Akue et al., 2012; Drobek et al., 2018; Haluszczak et al., 2009; Renkema et al., 2016). These observations therefore confirm that memory-like CD8$^+$ T cells could arise independently of cognate antigen stimulation and present a diverse TCR repertoire (Rafei et al., 2011). In this unbiaised context and as introduced in the first section of this chapter, memory-like CD8$^+$ T cells are given the name of "virtual memory CD8$^+$ T cells" (T_{VM}).

T_{VM} could originate from a combination of lymphopenia- and IL-4-induced mechanisms (Jameson et al., 2015). First, immune environment in neonatal mice is characterized as lymphopenic supporting lymphopenia-induced proliferation and acquisition of memory characteristics (Le Campion et al., 2002; Min et al., 2003; Schüler et al., 2004). Consistent with a role for lymphopenia-induced mechanisms for the emergence of T_{VM} cells, these cells are absent at birth but progressively accumulate in the periphery during the period of neonatal lymphopenia. Their emergence in the thymus only occurs later and at lower proportion than in periphery (Akue et al., 2012). Second, IL-4-secreting PLZF$^+$ innate CD4$^+$ T cells population are found in unbiaised wildtype mice and could support the expansion of memory-like CD8$^+$ T cell population (Lee et al., 2013b). Indeed, the role of IL-4-induced mechanims is evidenced by the significantly reduced proportions of T_{VM} in *Il4*$^{-/-}$, *Il4ra*$^{-/-}$ or *i*NKT-deficient mice. Similarly to bystander memory CD8$^+$ T cells, direct signalling of IL-4 on CD8$^+$ T cells was required. However, a population of T_{VM} persist in *Il4*$^{-/-}$, *Il4ra*$^{-/-}$ or *i*NKT-deficient mice mice, supporting the existence of complementary mechanisms (Akue et al., 2012; Renkema et al., 2016; Sosinowski et al., 2013; Weinreich et al., 2010). Development of T_{VM} also required Eomes and IL-15 signalling (IL-15 and its transpresentation by CD8α$^+$ dendritic cells). Furthermore, injection of IL-15 or IL-4 *in vivo* resulted in expansion of T_{VM} cells (Park et al., 2016; Sosinowski et al., 2013; Ventre et al., 2012; White et al.,

2016). Importantly, deficiency in both IL-4 and IL-15 did not lead to a complete abolition of the T_{VM} compartment and other cytokines like type I IFN or IL-7 were also shown to be involved (Martinet et al., 2015; Tripathi et al., 2016).

Virtual memory commitement may not be a stochastic event. Similar to a different propensity to respond to lymphopenia by homeostatic proliferation, $CD8^+$ T cell affinity for self-ligands (tonic signal), proportional to its CD5 expression, correlates with its propensity to convert to virtual memory $CD8^+$ T cell, probably through an increased sensitivity to IL-15 (White et al., 2016). In a recent study, this relation was shown to be cell intrinsic and observed only above a certain treshold of CD5 expression, indicating that cells must experienced a minimum level of self-reactivity to be able to form virtual memory (Drobek et al., 2018). This model is illustrated in figure 14.

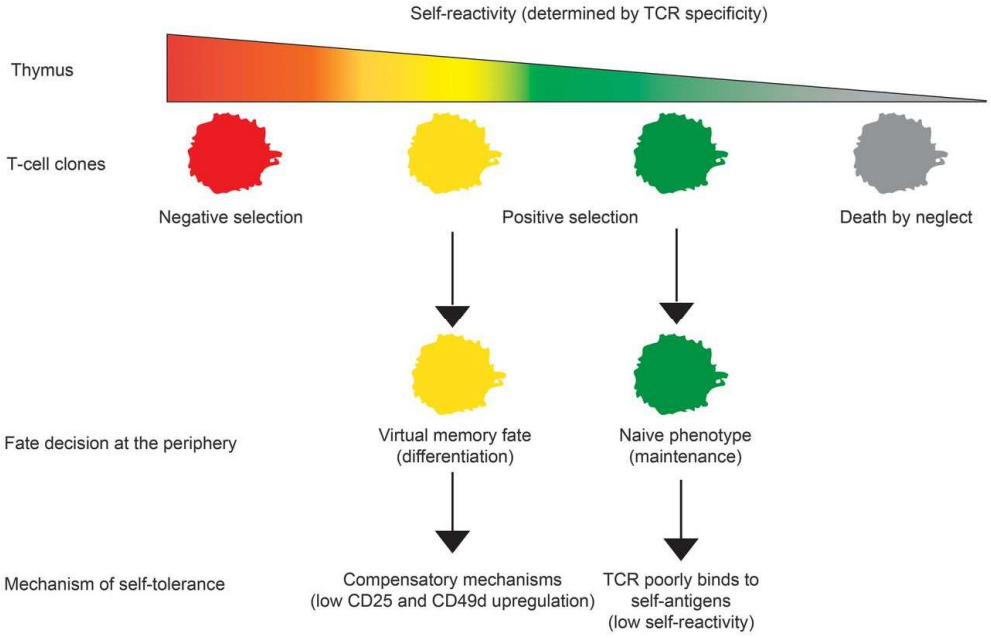

Figure 14 : Level of self-reactivity influence $CD8^+$ T cell fate. Negative and positive selection occuring in the thymus is dependent on self-reactivity of T cells. A low level of self recognition is required for positive selection. Although highly self-reactive cells are eliminated (negative selection), cells displaying an increased level of self reactivity might acquire memory properties. From (Drobek et al., 2018)

CD5 expression also correlates with TCR avidity to foreign antigens. Thus, the T_{VM} TCR repertoire might be skewed towards higher avidity for foreign antigens. This is coherent with the existence of variation in the proportion of T_{VM} cells among diverse antigen-specific T cell populations and with a difference of T cell clones among naive and T_{VM} (Akue et al., 2012; Drobek et al., 2018).

As memory-like $CD8^+$ T cells, T_{VM} displayed heightened effector capacities compared to naive $CD8^+$ T cells (Lee et al., 2013a). Nonetheless, some of their functions turned out to be impaired compared to

conventional ("true") memory $CD8^+$ T cells. For example, they expressed much lower level of IFN-γ in response to *in vivo* or *in vitro* stimulation with their cognate antigen. IFN-γ production levels being similar in T_{VM} compared to naive $CD8^+$ T cells after infection with a pathogen bearing their cognate antigen. Still, T_{VM} expansion following infection did not differ from conventional memory $CD8^+$ T cells but occured earlier and to a greater extent than their naive counterpart. In addition, control of pathogen infection was as efficient by virtual memory T cells than by conventional memory T cells, and both outcompeted naive T cells (Haluszczak et al., 2009; Lee et al., 2013a; Sosinowski et al., 2013). Moreover, signals associated with promotion of virtual memory population, notably IL-4, also impact conventional effector and memory response (Tripathi et al., 2016). Strikingly, virtual memory $CD8^+$ T cells also appear to raise unspecific, bystander effector response against pathogen in absence of cognate antigen recognition, a mechanism described as dependent on IL-15 (White et al., 2016).

4.2.4 IL-15 or IL-4 shape virtual memory T cell responses according to the mouse strain

Immunological differences exist between inbred mouse strains. Already mentioned in the section about bystander memory $CD8^+$ T lymphocytes, a difference in thymic $PLZF^+$ cells proportion can be observed at the steady-state between BALB/c and C57BL/6 mice. BALB/c mice spontaneously produce an important population of IL-4-secreting $PLZF^+$ *i*NKT that is absent from C57BL/6 mice. Such strain effect on physiological abundance of IL-4 secreting $PLZF^+$ population directly correlates with the observed proportion of memory-like $CD8^+$ T cells in the thymus of wildtype mice (Lee et al., 2013b; Pereira and Boucontet, 2012; Weinreich et al., 2010). Interestingly, KLF13 deficiency in BALB/c mice brought *i*NKT and memory-like $CD8^+$ T cells down to levels comparable to C57BL/6 mice (Lai et al., 2011).

In parallel to these physiological differences of IL-4-induced virtual memory formation, several studies have noted discrepancies in cytokine-dependency of T_{VM} cells. While some highlighted an essential role for IL-4 (Weinreich et al., 2010), others concluded for its limited function in this process and rather proved IL-15 to be the main driver of T_{VM} formation (Akue et al., 2012; Sosinowski et al., 2013). Strain-dependent variability could actually explain these conflicting observations. Indeed, when comparing T_{VM} dependency on IL-4 or IL-15 in BALB/c *vs.* C57BL/6 mice, it came out that BALB/c T_{VM} relied on IL-4 while IL-15 played a crucial role in C57BL/6 T_{VM} (Tripathi et al., 2016). Such strain effect could also be translated by potential inconsistencies between studies regarding the kinetics of memory-like $CD8^+$ T cells appearance after birth. As stated in the previous section, some studies reported that memory-like $CD8^+$ T cells first appeared in the periphery during neonatal period, potentially excluding a role for bystander memory $CD8^+$ T cells in the origin of T_{VM} cells (Akue et al., 2012). However, these studies were conducted with C57BL/6 mice that have scarce bystander $CD8^+$ T

cells at steady state (Weinreich et al., 2010). Given their important dependency on IL-4, T_{VM} of BALB/c mice could however mainly originate from bystander memory T cells (Renkema et al., 2016), while C57BL/6 T_{VM} cells would rather be related to innate memory T cells, responding to IL-15 by homeostatic proliferation (Sosinowski et al., 2013). In addition, an important difference between these two subset lies in the T-box transcription factors induced. While homeostatic proliferation could be associated with upregulation of both T-bet and Eomes (Li et al., 2011). IL-4 responding $CD8^+$ T cells upregulate Eomes and not T-bet (Renkema et al., 2016; Weinreich et al., 2009).

Hence, when studying the functional behaviour of T_{VM} cells, one must take into account the potential mouse strain effect in the interpretation. For instance, inflammatory settings where type 2 immunity is induced with high levels of IL-4 are produced could potentially have distinct effects on IL-4-responsive BALB/c T_{VM} when compared to C57BL/6 mice

Objectives

Objectives

Two separate studies are presented in the context of this thesis. Although they both aimed to investigate the impact of helminth infection on their host's immune system, they pursued independent specific objectives.

Although the role of type 2 immunity in helminthiasis and particularly in schistosomiasis is well described, how IL-4Rα-dependent alternatively activated macrophages (aaMφ) are involved in host protection remains uncertain. Therefore, the main objective of this study was to provide additional information on the functions of IL-4Rα-dependent aaMφ and the dynamics of the monocyte/macrophage responses after *S. mansoni* infection in the light of IL-4/IL-13 responsiveness. To help us in that purpose, we have used two mouse models: (*i*) *Il4ra*$^{-/-}$ mice unable to respond to IL-4/IL-13 and thus unable to mount typical type 2 immune responses, and (*ii*) conditional knockdown *Il4ra*$^{-/lox}$*Lyz2*^{Cre} mice lacking sensitivity to IL-4/IL-13 specifically on myeloid cells including lysozyme M-producing macrophages and neutrophils and thus unable to generate aaMφ. We also further investigated IL-4Rα deletion efficiency as some controversy existed concerning the efficiency of IL-4Rα deletion in different macrophage populations in *Il4ra*$^{-/lox}$*Lyz2*^{Cre} mice. Finally, we aimed to investigate the contribution of monocyte-derived macrophages *vs.* resident macrophages in the response to *S. mansoni* infection.

Virtual memory CD8$^+$ T cells (T_{VM}) are antigen-inexperienced memory-like CD8$^+$ T cells. These cells display heightened effector function and can be induced through IL-4Rα signalling. Therefore, we hypothesized that helminth-induced IL-4-dominated immune response could expand the population of T_{VM} responses. We used natural infection with different helminth species (*S. mansoni*, *N. brasiliensis* and *H. polygyrus*) or exposure to helminth-derived antigens to determine whether helminth-induced type 2 inflammation with IL-4, could affect T_{VM} responses. The potential expansion of T_{VM} cells after helminth infection could result in a conditioning of CD8$^+$ T cells to respond more effectively to a subsequent viral infection. Thus, we took advantage of a murine model of γ-herpesvirus infection: the murid herpesvirus 4 (MuHV-4) to address the impact of helminth-induced type 2 inflammation on subsequent anti-viral control by CD8$^+$ T cells. Indeed, MuHV-4 provided a good model as the immune control of acute infection directly depends on effector CD8$^+$ T cell responses.

Experimental section

Experimental section

1st study :

Recruitment of hepatic granuloma macrophages from monocytes is independent of IL-4Rα but is associated with ablation of resident macrophages in schistosomiasis

---

Marion Rolot, Annette Dougall, Justine Javaux, François Lallemand, Bénédicte Machiels, Philippe Martinive, Laurent Gillet, Benjamin G. Dewals

Manuscript under revision in *European Journal of Immunology*

Abstract

Alternatively-activated macrophages (aaMφs) accumulate in hepatic granulomas during schistosomiasis and have been suggested to have a bone marrow origin. What is less understood is how these macrophage responses are regulated after *S. mansoni* infection. Here, we have investigated the role of IL-4 receptor α-chain (IL-4Rα)-signalling in the dynamics of liver macrophage responses. We observed that IL-4Rα signalling was dispensable for the recruitment and proliferation of Ly6C^{hi} monocytes and for their conversion into F4/80^{+}CD64^{+}CD11b^{hi} macrophages. Moreover, while *lyz2*-dependent IL-4Rα provided an aaMφs phenotype to liver F4/80^{+}CD64^{+}CD11b^{hi} macrophages that was associated with regulation of granuloma formation, it was dispensable for host survival. Resident F4/80^{+}CD64^{+}CD11b^{lo} macrophages did not upregulate signature genes of aaMφs. Rather, resident macrophages nearly disappeared by week 8 after infection and artificial ablation of resident macrophages in CD169^{DTR} mice did not affect the response to *S. mansoni* infection. Interestingly, ablation of CD169^{+} cells in naive mice resulted in the accumulation of F4/80^{+}CD64^{+}CD11b^{hi} macrophages, which was amplified when ablation occurred during schistosomiasis. Altogether, our results suggest the ablation of resident KCs after *S. mansoni* infection is associated with the recruitment and accumulation of F4/80^{+}CD64^{+}CD11b^{hi} macrophages with *lyz2*-dependent IL-4Rα contributing to regulate granuloma inflammation but dispensable for host survival.

Introduction

Schistosomiasis is a severe parasitic disease with almost 240 million people infected worldwide and more than 200,000 deaths yearly in sub-Saharan Africa alone (Colley et al., 2014). In the murine model, mice infected with *Schistosoma mansoni* develop a severe liver pathology with granulomatous inflammatory responses directed towards the parasite eggs. During chronic infections, type 2 inflammation in the liver results in fibrosis, which leads to portal hypertension, bleeding from collateral vessels and ultimately death (Barron and Wynn, 2011; Pearce and MacDonald, 2002). Macrophages accumulate in the liver and are a key cellular component in granuloma formation and host protection (Barron and Wynn, 2011; Gieseck et al., 2018).

Macrophages are plastic cells that can be alternatively activated by IL-4 and IL-13 *via* the type I or type II IL-4 receptor, respectively (Van Dyken and Locksley, 2013). Both IL-4 receptors share the IL-4 receptor α chain (IL-4Rα) and it has been demonstrated that mice deficient for IL-4Rα are highly

susceptible to *Schistosoma mansoni* infection (Herbert et al., 2004). *Il4ra*$^{-/-}$ mice develop uncontrolled type 1-biased intestinal inflammation in response to *S. mansoni* eggs, do not develop granulomas in the liver and quickly succumb the acute phase of the infection when the parasite egg production reaches a peak by week 7-8 post-infection. In 2004, Herbert and colleagues generated *Il4ra*$^{-/lox}$*lyz2*^{Cre} mice to conditionally knockdown *Il4ra* expression in lysozyme M-expressing cells such as neutrophils and macrophages (Herbert et al., 2004). These mice produced bigger liver granulomas and succumbed to high dose *S. mansoni* acute infection due to a putative impaired control of type 1-biased gut inflammation similar to that observed in *Il4ra*$^{-/-}$ mice. However, a more recent report by Vannella and colleagues reported that while *Il4ra*$^{-/lox}$*lyz2*^{Cre} mice developed increased liver inflammation upon low or high dose *S. mansoni* infection, the survival kinetics and gut inflammation was not significantly different to hemizygous *Il4ra*$^{-/lox}$ littermate control mice (Vannella et al., 2014). Instead, the macrophages population in liver granulomas was diverse with mature and immature cells expressing high or low levels of *lyz2*, respectively. These contradicting results left the role of IL-4Rα-dependent alternatively-activated macrophages (aaMφs or M(IL-4)) unappreciated in schistosomiasis; although macrophages-specific arginase 1 (Arg1) and resistin-like molecule α (Relm-α), two aaMφ signature genes, controlled type 2 inflammation and deleterious liver fibrosis during chronic schistosomiasis (Nair et al., 2009; Pesce et al., 2009a; Pesce et al., 2009b). IL-4 has been shown to induce local proliferation of resident macrophages after infection with the nematodes *Litomosoides sigmodontis* or *Heligmosomoides polygyrus* (Jenkins et al., 2011), and these cells acquired an aaMφ phenotype. However, this turned out not to be the case in schistosomiasis where the majority of granuloma aaMφs had a signature of recruited Ly6C^{hi} monocytes (Girgis et al., 2014; Gundra et al., 2014; Nascimento et al., 2014). However, the role of IL-4Rα signalling on recruited or resident macrophages during type 2 cell-mediated immune responses to *S. mansoni* infection remains unknown. In the present study, the dynamics of monocytes/macrophages recruitment and activation in the liver during the first weeks after *S. mansoni* infection were investigated in relation to IL-4 signalling in *lyz2*-expressing cells. Our findings demonstrate that while *Il4ra*$^{-/lox}$*lyz2*^{Cre} were not more susceptible to *S. mansoni* infection than *Il4ra*$^{-/lox}$ mice, liver cell-mediated inflammation was significantly increased. We further observed that Ly6C^{hi} monocytes severely proliferated and were recruited to the liver independently of IL-4Rα signalling by week 8 after infection; where they differentiated into CD11b^{hi} aaMφs while CD11b^{lo} resident KCs nearly disappeared.

Results

Ly6C^{hi} monocytes recruitment to the liver is associated with the accumulation of CD11b^{hi} macrophages independently of IL-4Rα.

We used flow cytometry and the gating strategy depicted in **Fig. S1** to investigate liver cellular-mediated responses of *Il4ra*$^{-/lox}$*lyz2*^{Cre}, *Il4ra*$^{-/lox}$ or *Il4ra*$^{-/-}$ mice after *S. mansoni* infection. At 0, 4, 6 and 8 weeks post-infection, proportions of siglecF^{+}CD11b^{+} eosinophils, Ly6G^{+}CD11b^{+} neutrophils, CD3^{+} T cells, CD19^{+}MHCII^{+} B cells, F4/80^{-}CD11c^{+} dendritic cells, Ly6C^{hi}CD11b^{+} monocytes and F4/80^{+}CD64^{+} macrophages were analysed (**Fig. 1A**). Eosinophils were the main cell population expanding by week 6 post-infection and did not expand in *Il4ra*$^{-/-}$ mice. Consequently, other cell populations like neutrophils, lymphocytes and Ly6C^{hi} monocytes, were proportionally increased in *Il4ra*$^{-/-}$ mice at week 6 post-infection despite delayed response of T cells and Ly6C^{hi} monocytes. Hence, the dynamics of the Ly6C^{hi} monocytes and F4/80^{+}CD64^{+} macrophages responses were investigated (**Fig. 1B-C**). We observed that the number of Ly6C^{hi} monocytes significantly increased after infection in all mouse strains by week 8 post-infection, with a delay in *Il4ra*$^{-/-}$ mice. F4/80^{+}CD64^{+} macrophages tended to decrease in *Il4ra*$^{-/lox}$ mice but were not significantly affected in *Il4ra*$^{-/lox}$*lyz2*^{Cre} or *Il4ra*$^{-/-}$ mice (**Fig. 1B-C**). As expected, resident liver F4/80^{+}CD64^{+} macrophages in naive mice expressed low levels of CD11b. Thus, resident KCs were referred as CD11b^{lo} macrophages. However, a population expressing higher levels of CD11b progressively appeared and accumulated from week 4 post-infection in all mouse strains. The numbers and proportions of CD11b^{lo} macrophages were significantly reduced upon infection while a population of CD11b^{hi} cells constituted the main F4/80^{+}CD64^{+} macrophage population by week 8 post-infection (**Fig. 1B-C**). Although the numbers of CD11b^{hi} macrophages were heightened in *Il4ra*$^{-/lox}$*lyz2*^{Cre} mice at week 8 post-infection, the lack of IL-4Rα did not affect the enrichment of these cells after *S. mansoni* infection (**Fig. 1C-D**). No data was available for *Il4ra*$^{-/-}$ at week 8 post-infection as these mice succumbed the infection. Thus, recruitment of Ly6C^{hi} monocytes to the liver after *S. mansoni* infection was associated with an accumulation of CD11b^{hi} macrophages independently of IL-4Rα signalling.

Ly6C^{hi} monocytes convert into CD11b^{hi} macrophages after *S. mansoni* infection

As previously reported, granuloma macrophages in schistosomiasis have a signature of monocyte-derived cells (Girgis et al., 2014; Gundra et al., 2014; Nascimento et al., 2014). We observed that Ly6C^{hi} monocytes indeed overexpressed the macrophage marker CD64 independently of IL-4Rα-responsiveness upon *S. mansoni* infection, and CD11b^{hi} macrophages transiently expressed higher levels

of Ly6C (**Fig. 2A-B**). These results suggested that Ly6C^{hi} monocytes are recruited to the liver upon infection and convert into CD11b^{hi} macrophages. To address this hypothesis, we produced partial chimeric mice by shielding the liver during total body irradiation and engrafting congenic CD45.1.2^{+} bone marrow (BM) cells (**Fig. 2C**). Eight weeks later, mice were left uninfected or subjected to percutaneous infection with *S. mansoni* cercariae. Blood Ly6C^{hi} monocytes were enriched in CD45.1^{+} cells in chimeric mice (mean chimerism of 46%) (**Fig. 2D**) and *S. mansoni* infection of these mice induced the appearance of CD11b^{hi} macrophages in the liver (**Fig. 2E**). When analysing chimerism of CD11b^{lo} resident macrophages or CD11b^{hi} macrophages in the liver of mice at week 0, 4, 6, 8 or 10 post-infection (**Fig. 2F-G**), we observed that whereas resident CD11b^{lo} macrophages cells mainly retained a chimerism of resident liver cells, CD11b^{hi} macrophages displayed a chimerism similar to blood Ly6C^{hi} monocytes. Thus, these results demonstrated that liver CD11b^{hi} macrophages have a BM origin, therefore emerging from recruited Ly6C^{hi} monocytes. Interestingly, a small but significant fraction of CD11b^{lo} resident macrophages acquired a chimerism of BM origin which suggests, as recently proposed, that some recruited CD11b^{hi} macrophages could convert into resident macrophages (Gundra et al., 2017).

S. mansoni infection induces IL-4/13-independent proliferation of recruited Ly6C^{hi} monocytes but not CD11b^{hi} macrophages.

IL-4 can induce proliferation of resident macrophages and *H. polygyrus* infection induced proliferation of KCs (Jenkins et al., 2011; Jenkins et al., 2013). To determine the dynamics of IL-4Rα-dependent proliferation after *S. mansoni* infection, EdU was injected to *Il4ra*$^{-/lox}$*lyz2*^{Cre}, *Il4ra*$^{-/lox}$ or *Il4ra*$^{-/-}$ mice at week 0, 4, 6 or 8 post-infection and the proportion of liver cells having undergone division and incorporated EdU was determined 4h later (**Fig. 3A and B**). We observed very low levels of cell division in Ly6C^{hi} monocytes or F4/80^{+}CD64^{+} macrophages in naive mice. Proliferation remained at basal levels for the first 6 weeks of infection in all mouse strains. By week 8 post-infection however, about 25 to 28% of liver Ly6C^{hi} monocytes from both *Il4ra*$^{-/lox}$*lyz2*^{Cre} and *Il4ra*$^{-/lox}$ mice were actively proliferating. In addition, low but significant increased EdU incorporation in CD11b^{lo} resident macrophages was detected while no increased proliferation could be observed in CD11b^{hi} macrophages after *S. mansoni* infection, suggesting that IL-4 does not induce strong macrophage proliferation in granulomas. Because CD11b^{hi} macrophages are the most abundant population in the liver by week 8 post-infection and are originating from Ly6C^{hi} monocytes, it is likely that Ly6C^{hi} monocytes stop dividing once differentiated into CD11b^{hi} macrophages.

Il4ra$^{-/lox}$*lyz2*^{Cre} mice have increased liver inflammation but survive schistosomiasis.

To revisit the susceptibility of *Il4ra*$^{-/lox}$*lyz2*^{Cre} BALB/c mice to schistosomiasis, mice were infected with either 100, 35 or 20 cercariae percutaneously. Clinical monitoring was performed and survival recorded over time. Compared to hemizygous *Il4ra*$^{-/lox}$ littermate controls, we did not detect increased susceptibility of *Il4ra*$^{-/lox}$*lyz2*^{Cre} mice to *S. mansoni* infection (**Fig. 4A**). Nonetheless, to further investigate the dynamics of IL-4Rα-dependent cellular responses in the liver during the first weeks after *S. mansoni* infection, leukocytes were isolated from livers of *Il4ra*$^{-/lox}$*lyz2*^{Cre} or *Il4ra*$^{-/lox}$ mice before infection and at weeks 4, 6 and 8 post-infection. We observed increased numbers of CD45^{+} leukocytes in the liver of *Il4ra*$^{-/lox}$*lyz2*^{Cre} by week 8 post-infection (**Fig. 4B**). Increased liver cellularity in *Il4ra*$^{-/lox}$*lyz2*^{Cre} mice was associated with the development of larger liver granulomas compared to *Il4ra*$^{-/lox}$ littermate controls (**Fig. 4C-D**). Nonetheless, increased granuloma size did not affect the cytokine responses with similar IL-4, IL-13, IL-5 and IFN-γ responses in liver and hepatic-draining LN after SEA restimulation (**Fig. 4E**). These results confirmed that *lyz2*-dependent IL-4Rα has no significant impact on host survival to schistosomiasis while regulating granuloma formation in the liver.

S. mansoni infection induces an IL-4Rα-dependent aaMφ phenotype in CD11b^{hi} macrophages.

Vannella and colleagues suggested inefficient deletion of the *Il4ra* locus in 'immature' populations of F4/80^{+}CD64^{+} macrophages in *Il4ra*$^{-/lox}$*lyz2*^{Cre} mice after *S. mansoni* infection (Vannella et al., 2014). Moreover, IL-4-driven proliferation in *Il4ra*$^{-/lox}$*lyz2*^{Cre} mice resulted in the positive selection of IL-4Rα-expressing macrophages in these mice (Jenkins et al., 2013). Thus, we investigated the efficacy of Cre recombinase expression under the control of the *lyz2* promoter by crossing *lyz2*^{Cre} mice with lineage *Rosa*^{tdRFP} reporter mice (Luche et al., 2007). These mice express the reported red fluorescent protein tdRFP following Cre-mediated excision of the floxed stop codon (**Fig. S2A**). Using the gating strategy as depicted in **Fig. S1**, the efficacy and selective expression of the tdRFP from naive or *S. mansoni*-infected mice was analysed in liver lymphocytes, eosinophils, dendritic cells, neutrophils, monocytes and macrophages. We observed no expression in T or B cells, basal expression in some eosinophils (<7%) or dendritic cells (<25%) and around 30% of Ly6C^{hi} monocytes expressing tdRFP irrespective of the infection with *S. mansoni* or not (**Fig. S2B**). As expected, we observed that the highest proportion of tdRFP^{+} cells were neutrophils and F4/80^{+}CD64^{+} macrophages with 60 to 70% of the cells effectively expressing the reporter protein in naive and *S. mansoni* infected mice (**Fig. S2B**). Importantly, CD11b^{lo} and CD11b^{hi} macrophages expressed significant levels of tdRFP (**Fig. 5A**). We further observed that IL-4Rα (CD124) protein expression was significantly impaired in neutrophils, CD11b^{lo} macrophages and CD11b^{hi} macrophages of *S. mansoni*-infected *Il4ra*$^{-/lox}$*lyz2*^{Cre} mice (**Fig. 5B**), confirming our previous

observations (Dewals et al., 2010). Thus, deletion of IL-4Rα in *Il4ra*$^{-/lox}$*lyz2*^{Cre} mice is similar between naive and *S. mansoni*-infected mice in term of efficacy and specificity.

We further investigated protein expression levels of the chitinase-like molecule Ym1 over time after *S. mansoni* infection. Proportions of Ym1^{+} cells significantly increased after infection in CD11b^{hi} macrophages whereas proportions of CD11b^{lo} macrophages expressing Ym1 remained low (**Fig. 5C-D**). Thus, the majority of aaMφ expressing Ym1 were of BM origin in the liver of *S. mansoni* infected mice. Proportions of Ym1^{+} CD11b^{hi} macrophages was significantly lower in *Il4ra*$^{-/lox}$*lyz2*^{Cre} mice compared to *Il4ra*$^{-/lox}$ mice but higher than in *Il4ra*$^{-/-}$ mice. Likewise, upregulation of Relm-α was mainly observed in CD11b^{hi} macrophages from *Il4ra*$^{-/lox}$ mice (**Fig. 5E**). These results demonstrate impaired aaMφs in the liver of *S. mansoni* infected *Il4ra*$^{-/lox}$*lyz2*^{Cre} mice and further suggest CD11b^{hi} macrophages to be a main effector population in the liver for controlling granuloma formation.

Resident liver CD11b^{lo} macrophages almost disappear after *S. mansoni* infection and are dispensable against schistosomiasis.

We observed that monocyte-derived CD11b^{hi} macrophages accumulate in the liver after *S. mansoni* infection and contribute to the majority of F4/80^{+}CD64^{+} macrophages in the liver by week 8 post-infection (**Fig. 1**). Nascimento and colleagues highlighted the protective role of CCR2-dependent recruitment of monocytes to the liver to control egg-induced inflammation (Nascimento et al., 2014), which further suggest that CD11b^{hi} macrophages are recruited to the liver from blood monocytes and acquire an aaMφ phenotype for regulating granuloma formation. Although CD11b^{hi} macrophages accumulated, we also observed that resident CD11b^{lo} macrophages nearly disappeared in term of proportion and numbers in the liver from week 6 post-infection (**Fig. 1B-C**). This observation was unexpected and could suggest resident CD11b^{lo} macrophages to be dispensable in schistosomiasis. Most resident macrophages express sialoadhesin (siglec-1 or CD169) (Gupta et al., 2016b) and diphtheria toxin (DT) treatment of CD169$^{DTR/+}$ mice successfully depleted liver resident macrophages (Gupta et al., 2016b). Thus, we induced the depletion of resident macrophages in CD169$^{DTR/+}$ mice by injecting DT at regular intervals from week 5.5 after *S. mansoni* infection (**Fig. 6A**). DT treatment successfully depleted F4/80^{+}CD64^{+} CD11b^{lo} macrophages in naive (**Fig. S3**) and *S. mansoni*-infected (**Fig. 6D**) CD169$^{DTR/+}$ mice but did not significantly affect survival, weight change, liver granuloma volumes (**Fig. 6B-C**) or cellular responses in the liver (**Fig. S4A**). In addition, restimulation with soluble egg antigen (SEA) of hepatic LN and liver cells did not highlight significant differences in the liver although CD169^{+} cell depletion was associated with increased IL-5 and IL-13 responses in the draining LN at week 7 post-

infection (**Fig. S4B**). Altogether, these results suggest resident CD11b^{lo} macrophages to be dispensable in the control of schistosomiasis.

Ablation of resident CD11b^{lo} macrophages during *S. mansoni* infection results in recruitment of monocytes to the liver.

Induction of KC death resulted in the recruitment of monocytes from the BM and these cells differentiated in KCs, filling in the empty niche (Scott et al., 2016). DT-mediated depletion of CD169^{+} cells induced the ablation of CD11b^{lo} macrophages after DT treatment (Chow et al., 2013; Gupta et al., 2016b), and resulted in the recruitment of Ly6C^{hi} monocytes expressing high levels of CD64 in the liver (**Fig. S3B**). In addition, the small population of F4/80^{+}CD64^{+} macrophages in the liver of DT-treated mice displayed high levels of CD11b expression, suggesting that these cells might represent newly differentiated macrophages of monocyte origin (**Fig. S3C**). When mice were treated at 3-4 days interval from week 5.5 after *S. mansoni* infection (**Fig. 6**), recruited Ly6C^{hi} monocytes displayed similar CD64 expression in both CD169$^{DTR/+}$ and WT (CD169$^{+/+}$) mice at week 7 post-infection (**Fig. 6F**). Likewise, the majority of F4/80^{+}CD64^{+} macrophages were CD11b^{hi} after DT treatment of both CD169$^{DTR/+}$ and WT (CD169$^{+/+}$) mice (**Fig. 6D and F**). Taken together, these results suggest that recruitment of Ly6C^{hi} monocytes after *S. mansoni* infection could results from the ablation of resident CD11b^{lo} macrophages.

Figures

Figure 1

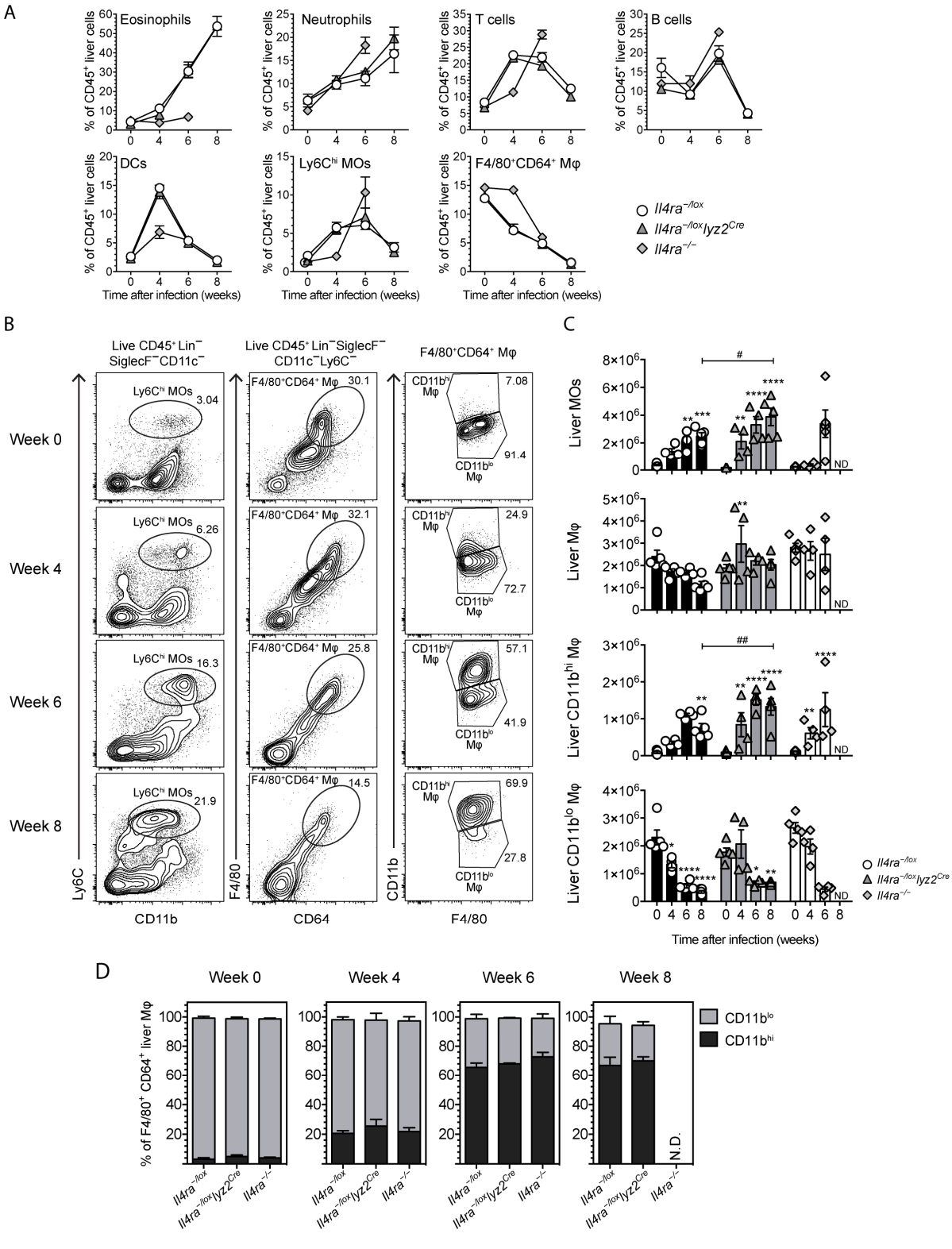

Figure 1. *S. mansoni* infection induces Ly6C^{hi} monocytes recruitment to the liver and expansion of a CD11b^{hi} liver macrophages population independently of IL-4Rα signalling.
Il4ra$^{-/lox}$, *Il4ra*$^{-/lox}$*lyz2*^{Cre}, or *Il4ra*$^{-/-}$ BALB/c mice were percutaneously infected with 35 *S. mansoni* cercariae. Liver leukocytes were analysed by flow cytometry at week 0, 4, 6 and 8 after *S. mansoni* infection. The gating strategy is outlined in **Fig S1**.
(**A**) Flow cytometric quantification (as percentage of total CD45$^+$ leukocytes) of liver eosinophils (SiglecF$^+$), neutrophils (Ly6G$^+$ CD11b$^+$), T cells (CD3$^+$), B cells (CD19$^+$ MHCII$^+$), dendritic cells (CD11c$^+$F4/80$^-$; DCs), monocytes (Ly6C^{hi}CD11b$^+$; MOs) and macrophages (F4/80^{hi} CD64^{hi} ; Mφ).
(**B**) Representative contour plots of Ly6C^{hi} liver monocytes and F4/80$^+$CD64$^+$ liver macrophages obtained by flow cytometric analysis at the given time-points post-infection. Numbers on contour plot correspond to percent of positive events in each gate.
(**C**) Numbers of Ly6C^{hi} monocytes, F4/80$^+$CD64$^+$ macrophages, CD11b^{lo} or CD11b^{hi} F4/80$^+$CD64$^+$ macrophages (from top to bottom) in the liver analysed by flow cytometry as in A and B. Symbols represent values from individual mice and bars show mean ± SEM from one experiment representative of two independent experiment (n=4 to 5). Two-way ANOVA with Sidak's post-test. **P*<0.05, ***P*<0.01, ****P*<0.001 and *****P*<0.0001 compared to naive mice of the same genotype; $^{\#}$*P*<0.05, $^{\#\#}$*P*<0.01, $^{\#\#\#}$*P*<0.001 compared to *Il4ra*$^{-/lox}$ mice at the same infection stage.
(**D**) Proportions of CD11b^{lo} or CD11b^{hi} cells in F4/80$^+$CD64$^+$ liver macrophages overtime after *S. mansoni* infection, analysed by flow cytometry as in A and B. Bars show mean ± SEM of one experiment representative of two independent experiment (n=4 to 5).

Figure 2

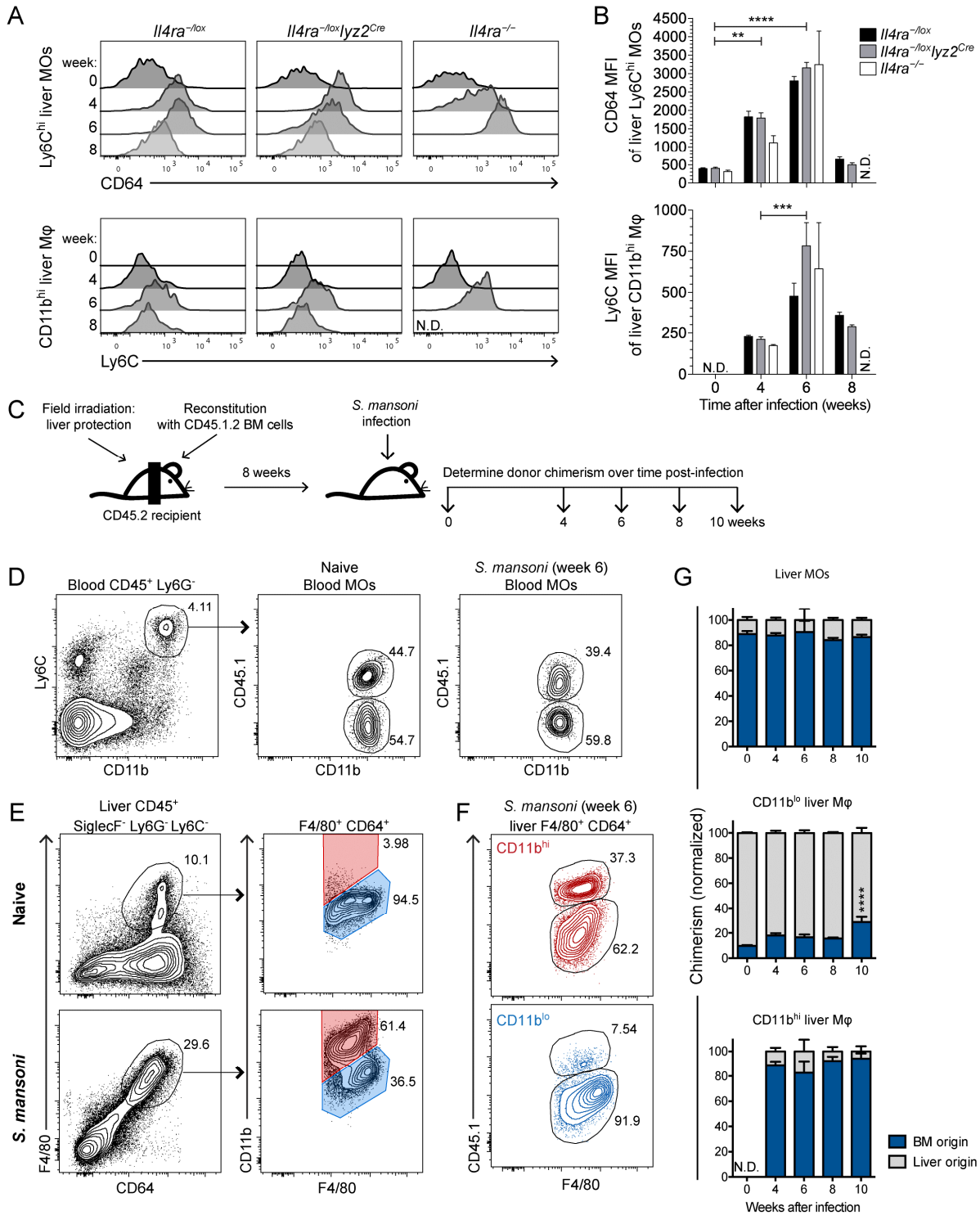
A
Il4ra−/lox
Il4ra−/loxlyz2Cre
Il4ra−/−
week:
0
4
6
8
Ly6Chi liver MOs
CD64
CD11bhi liver Mφ
N.D.
Ly6C
B
CD64 MFI of liver Ly6Chi MOs
Ly6C MFI of liver CD11bhi Mφ
Time after infection (weeks)
C
Field irradiation: liver protection
Reconstitution with CD45.1.2 BM cells
CD45.2 recipient
8 weeks
S. mansoni infection
Determine donor chimerism over time post-infection
10 weeks
D
Blood CD45+ Ly6G-
Naive Blood MOs
S. mansoni (week 6) Blood MOs
Ly6C
CD11b
CD45.1
4.11
44.7
54.7
39.4
59.8
E
Liver CD45+ SiglecF- Ly6G- Ly6C-
F4/80+ CD64+
Naive
S. mansoni
F4/80
CD64
10.1
29.6
3.98
94.5
61.4
36.5
F
S. mansoni (week 6) liver F4/80+ CD64+
CD11bhi
CD11blo
37.3
62.2
7.54
91.9
G
Liver MOs
CD11blo liver Mφ
CD11bhi liver Mφ
Chimerism (normalized)
BM origin
Liver origin
Weeks after infection

Figure 2. Liver CD11b^{hi} macrophages arise from recruited Ly6C^{hi} blood monocytes during *S. mansoni* infection.
(**A and B**) *Il4ra*$^{-/lox}$, *Il4ra*$^{-/lox}$*lyz2*^{Cre}, or *Il4ra*$^{-/-}$ BALB/c mice were percutaneously infected with 35 *S. mansoni* cercariae. Liver leukocytes were analysed by flow cytometry at week 0, 4, 6 and 8 after *S. mansoni* infection. The gating strategy is outlined in **Fig S1**.
(**A**) Half offset representative histograms of CD64 and Ly6C expression in Ly6C^{hi} liver monocytes and CD11b^{hi} F4/80^{+}CD64^{+} liver macrophages, respectively, as analysed by flow cytometry.
(**B**) CD64 and Ly6C median fluorescence intensity (MFI) of Ly6C^{hi} liver monocytes and CD11b^{hi} F4/80^{+}CD64^{+} liver macrophages respectively, as analysed by flow cytometry. Bars show mean ± SEM from one experiment representative of two independent experiment (n=4-5). Two-way ANOVA with Sidak's post-test. ***P*<0.01, ****P*<0.001 and *****P*<0.0001 compared to naive mice of the same genotype.
(**C-G**) Field irradiation with protection of the liver area was performed on recipient CD45.2 BALB/c mice that were reconstituted with CD45.1.2 bone marrow (BM) cells. Chimeric mice were percutaneously infected with 35 *S. mansoni* cercariae and liver leukocytes were analysed by flow cytometry at week 0, 4, 6, 8 and 10 after *S. mansoni* infection. Donor cells were identified based on CD45.1 expression.
(**C**) Experimental design.
(**D**) Representative flow cytometry contour plots of the chimerism in blood Ly6C^{hi} monocytes in naive and *S. mansoni* infected mice.
(**E**) Representative flow cytometry contour plots of liver F4/80^{+}CD64^{+} macrophages analysis by flow cytometry.
(**F**) Representative flow cytometry contour plots of the chimerism in CD11b^{hi} or CD11b^{lo} liver F4/80^{+}CD64^{+} macrophages as gated in E.
(**G**) Chimerism in Ly6C^{hi} liver monocytes and CD11b^{hi} or CD11b^{lo} F4/80^{+}CD64^{+} liver macrophages analysed by flow cytometry as in F. Normalized chimerism is presented as CD45.1^{+}:CD45.1^{-} ratios of the population in the liver over CD45.1^{+}:CD45.1^{-} ratios of blood monocytes. Bars show mean ± SEM (n=4-5). Two-way ANOVA with Sidak's post-test. *****P*<0.0001 compared to naive mice.

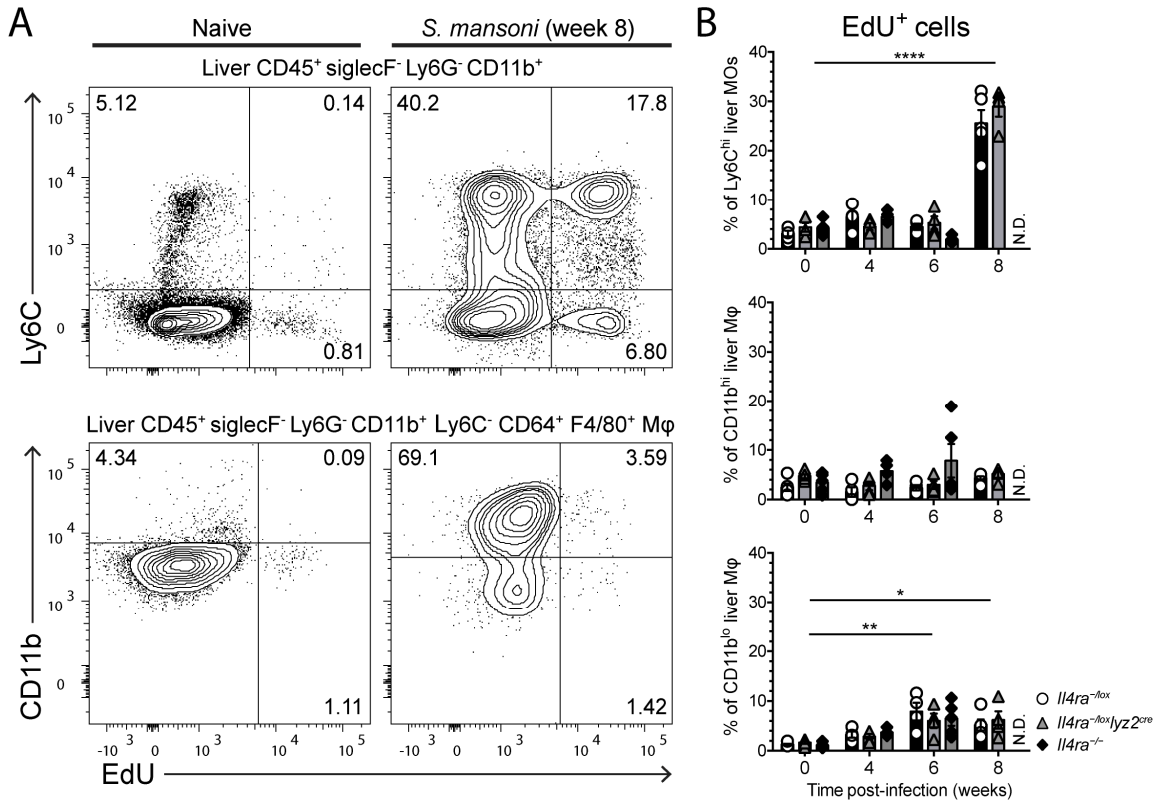

Figure 3. Proliferation of Ly6C^{hi} liver monocytes independently of IL-4 receptor signalling.
Il4ra$^{-/lox}$, *Il4ra*$^{-/lox}$*lyz2*^{Cre}, or *Il4ra*$^{-/-}$ BALB/c mice were percutaneously infected with 35 *S. mansoni* cercariae. Intraperitoneal injection of EdU (500 µg/mouse in PBS) was performed 4 hours before endpoint and liver leukocytes were analysed by flow cytometry at week 0, 4, 6 and 8 after *S. mansoni* infection. The gating strategy is outlined in **Fig S1**.
(**A**) Representative flow cytometry contour plots of EdU incorporation in Ly6C^{hi} liver monocytes (top) and F4/80^{+}CD64^{+} liver macrophages (bottom) in naive and *S. mansoni* infected mice.
(**B**) Proportion of EdU^{+} cells in Ly6C^{hi} liver monocytes (MOs) and CD11b^{hi} or CD11b^{lo} F4/80^{+}CD64^{+} liver macrophages (Mφ) analysed by flow cytometry as in A. Symbols represent values from individual mice and bars show mean ± SEM (n=4-5). **P*<0.05, ***P*<0.01, *****P*<0.0001 compared to naive mice of the same genotype.

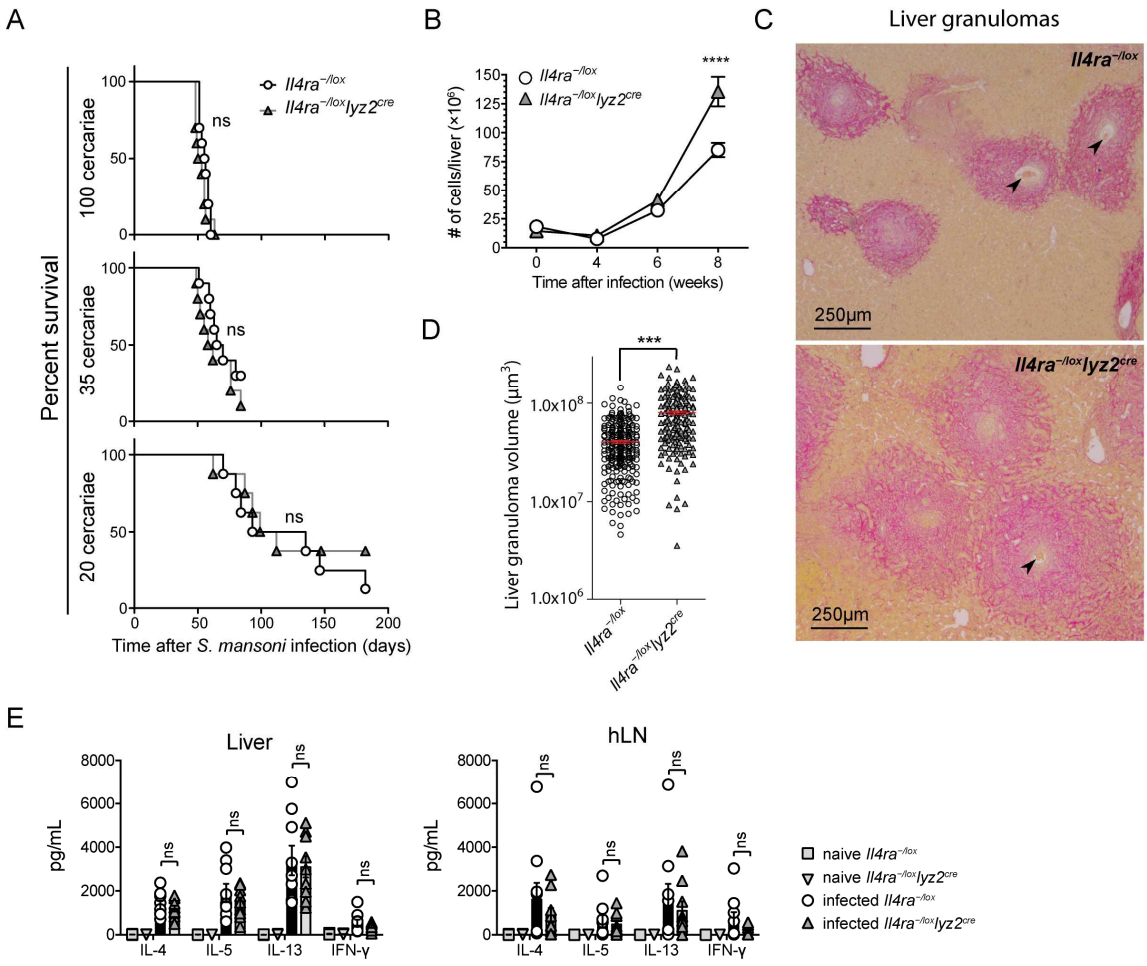

Figure 4. Increased granuloma size after *S. mansoni* infection in *Il4ra*$^{-/lox}$*lyz2*^{cre} mice.
Il4ra$^{-/lox}$ or *Il4ra*$^{-/lox}$*lyz2*^{Cre} BALB/c mice were percutaneously infected with 35 (unless otherwise specified) *S. mansoni* cercariae. Survival and liver inflammation were characterized.
(**A**) Survival rate of *Il4ra*$^{-/lox}$ and *Il4ra*$^{-/lox}$*lyz2*^{Cre} mice for different infectious doses. $P>0.05$ (n=8-10); Log-rank (Mantel-Cox) test
(**B**) Total numbers of CD45^{+} leukocytes per liver. Results are shown as pooled data from two independent experiments (n=4-5 per experiment). Two-way ANOVA with Sidak's post-test.
(**C**) Picrosirius red staining of liver histological section showing representative at 10 weeks post-*S. mansoni* infection. Arrows indicate *S. mansoni* eggs
(**D**) Granulomas volumes as measured on picrosirius red-stained liver sections from mice at 10 weeks post-*S. mansoni* infection. Symbols represent individual granuloma volumes and bars show mean ± SEM (n=4). Mann-Whitney test.
(**E**) Cytokines production as quantified by ELISA on supernatant after 72h *S. mansoni* soluble egg antigen (SEA) *ex vivo* restimulation of cells from liver or hepatic LN (hLN). Symbols and bars show mean ± SEM from one experiment representative of two independent experiments with 4 to 5 mice per group.
**P*<0.05, ***P*<0.01, ****P*<0.001, *****P*<0.0001

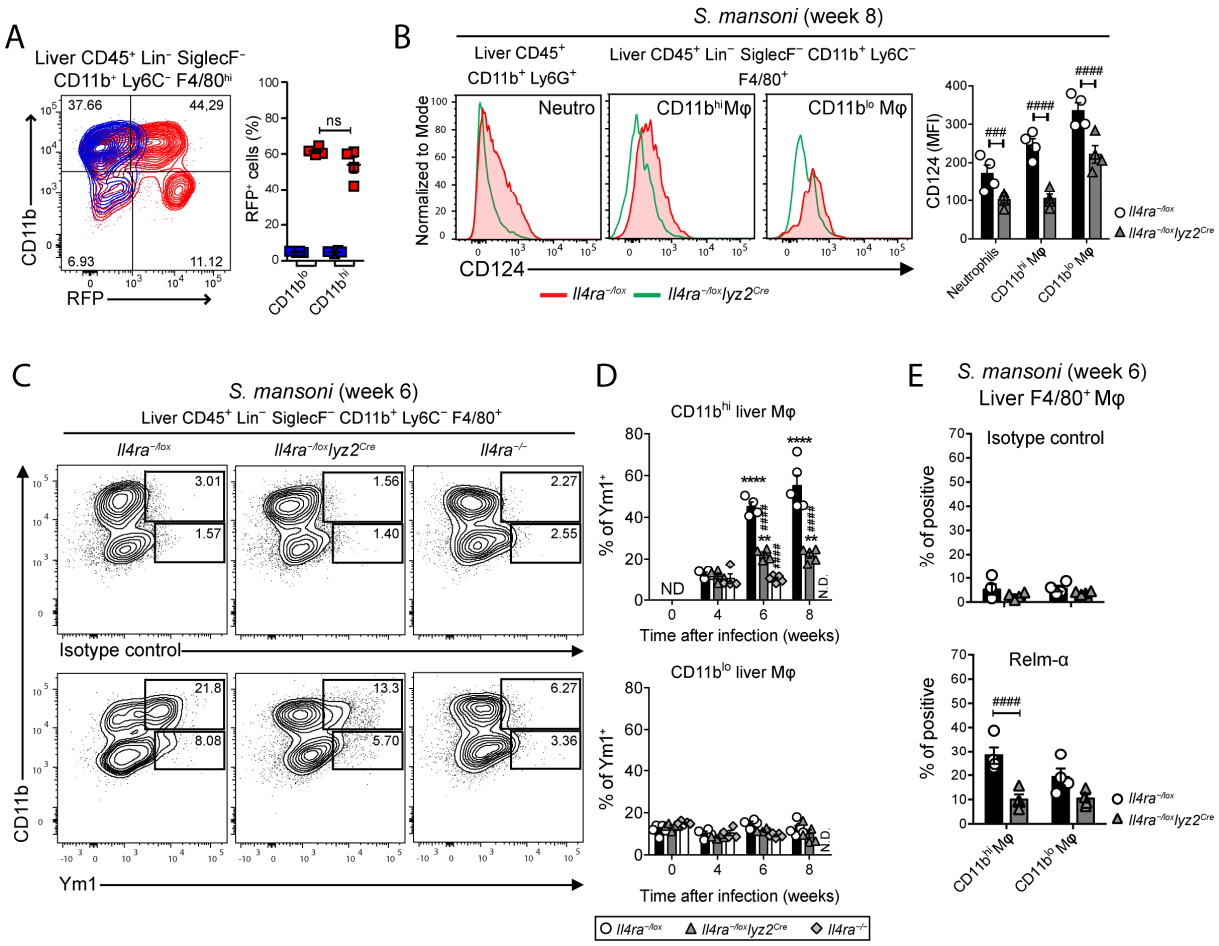

Figure 5. Impaired alternative activation of CD11b^{hi} liver macrophages in *S. mansoni*-infected *Il4ra*$^{-/lox}$*lyz2*^{Cre} mice

(**A**) *Rosa*^{tdRFP}*lyz2*^{Cre} reporter mice and littermate controls were percutaneously infected with 35 *S. mansoni* cercariae. Liver leukocytes were analysed and tdRFP expression in liver CD11b^{hi} or CD11b^{lo} F4/80^{+} macrophages was detected by flow cytometry at week 7 post-infection. Overlays of representative contour plots from *Rosa*^{tdRFP}*lyz2*^{Cre} mice (red) or littermate control (blue) and quantification of tdRFP^{+} cells in the gated populations. Numbers on contour plot correspond to mean percentage of cells in each quadrant of *Rosa*^{tdRFP}*lyz2*^{Cre} mice. Symbols represent values from individual mice and bars show mean ± SEM (n=3 to 4 mice).

(**B-E**) *Il4ra*$^{-/lox}$, *Il4ra*$^{-/lox}$*lyz2*^{Cre}, or *Il4ra*$^{-/-}$ BALB/c mice were percutaneously infected with 35 *S. mansoni* cercariae and liver leukocytes were analysed at the given time-point.

(**B**) Representative histogram and median fluorescence intensity (MFI) of CD124 (IL-4Rα) in Ly6G^{+}CD11b^{+} liver neutrophils and CD11b^{hi} or CD11b^{lo} F4/80^{+} liver macrophages at week 8 post-infection.

(**C**) Representative flow cytometry contour plots of Ym1 expression in F4/80^{+} liver macrophages at week 6 post-infection.

(**D**) Proportion of Ym1^{+} cells in CD11b^{hi} or CD11b^{lo} F4/80^{+} liver macrophages analysed by flow cytometry as in C.

(**E**) Proportion of Relm-α^{+} cells in CD11b^{hi} or CD11b^{lo} F4/80^{+} liver macrophages at week 6 post-infection, as detected by flow cytometry.

Symbols represent values from individual mice and bars show mean ± SEM (n= 4-5). Two-way ANOVA with Sidak's post-test. ****P<0.0001 compared to naive mice of the same genotype; $^{###}P$<0.001, $^{####}P$<0.001 compared to *Il4ra*$^{-/lox}$ mice at the same infection time-point.

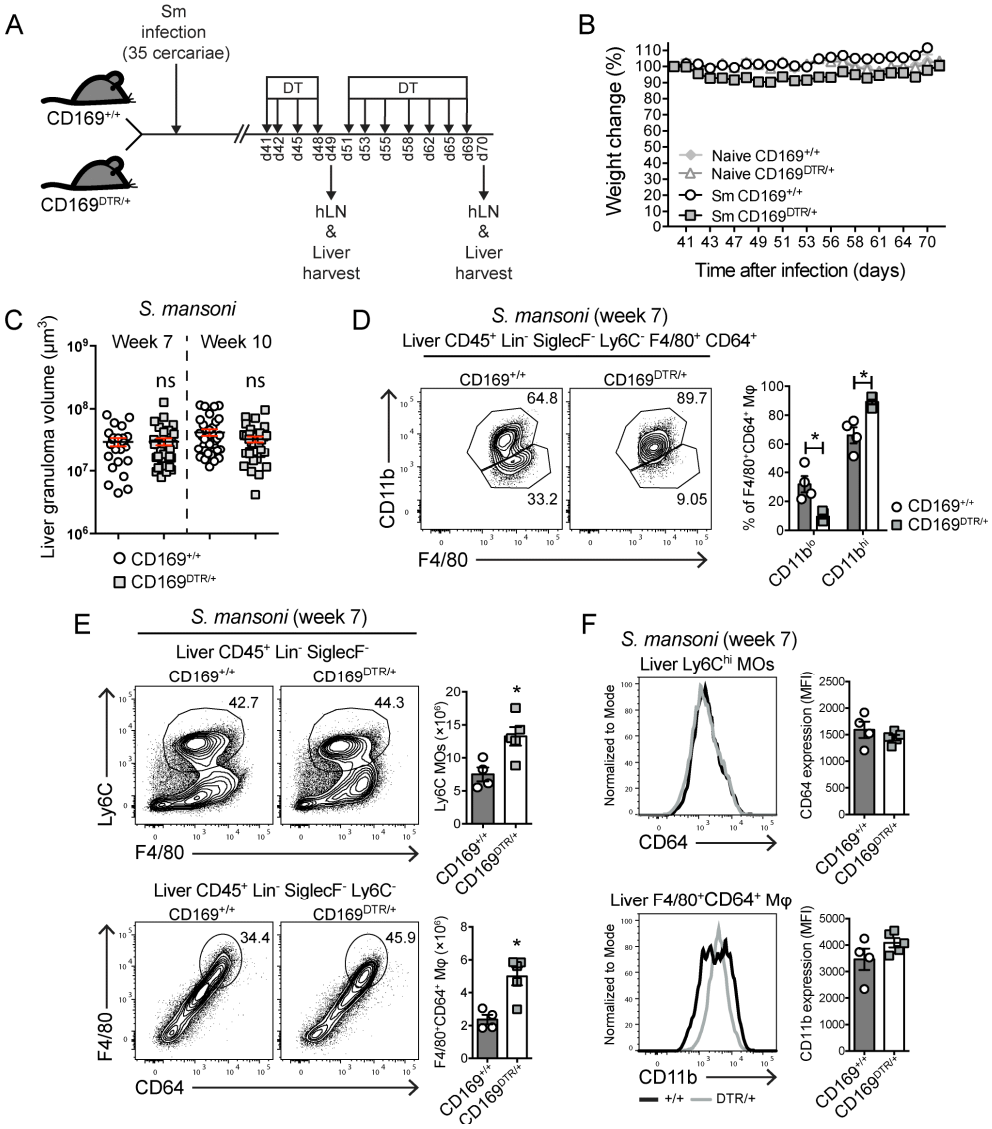

Figure 6. Depletion of CD169^{+} cells in *S. mansoni* infected CD169$^{DTR/+}$ mice.
CD169$^{DTR/+}$ and CD169$^{+/+}$ littermate control C57BL/6 mice were percutaneously infected with 35 *S. mansoni* cercariae and received DT by i.p. injection (250 ng/mouse) at regular intervals.
(**A**) Experimental design.
(**B**) Weight change after first administration of DT.
(**C**) Liver granuloma volumes measured on picrosirius red-stained liver histological section at 7 and 10 weeks post-*S. mansoni* infection. Symbols represent individual granuloma volumes and bars show mean ± SEM (n=4).
(**D**) Representative flow cytometry contour plot gated on liver F4/80^{+}CD64^{+} macrophages and quantification of the proportion of CD11b^{hi} and CD11b^{lo} macrophages 7 weeks after *S. mansoni* infection.
(**E**) Representative flow cytometry contour plot and total number of Ly6C^{hi} liver monocytes and F4/80^{+}CD64^{+} liver macrophages 7 weeks after *S. mansoni* infection.
(**F**) Representative overlaid histogram and median fluorescence intensity (MFI) of CD64 and CD11b expression by Ly6C^{hi} liver monocytes and F4/80^{+}CD64^{+} liver macrophages respectively, 7 weeks after *S. mansoni* infection, as determined by flow cytometry.
Numbers on contour plots correspond to percent in each gate. Symbols represent values from individual mice and bars show mean ± SEM (n=4-5). Mann Whitney test (C, E-F) or two-way ANOVA with Sidak's post-test (B and D)

Supplemental figures

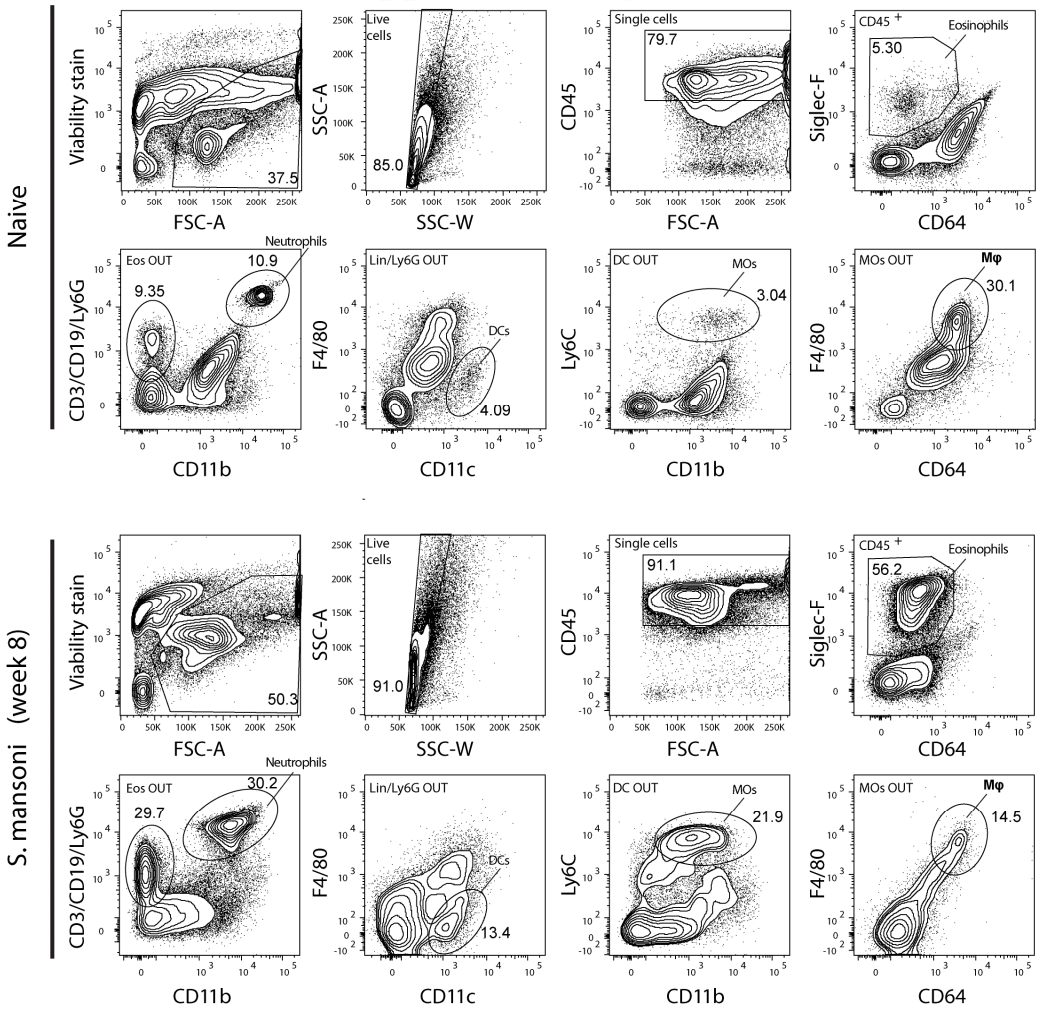

Figure S1. Gating strategy for flow cytometry analysis of liver leukocytes.
Representative contour plot of mice at week 0 (naive) or week 8 after infection with 35 *S. mansoni* cercariae demonstrating the gating strategy for flow cytometric analysis of liver leukocytes. Single cell suspension was obtained from livers as described in the materials and methods and stained with fluorochrome-conjugated antibodies against CD45 (PE-Cy7), SiglecF (PE-CF594), CD3 (APC), CD19 (APC), Ly6G (APC), F4/80 (BV711), CD11c (Alexa-Fluor 700), CD11b (FITC), Ly6C (BV786), CD64 a and b alloantigens (PE) and MHCII (eF450) and stained with fixable viability stain 510. Lineage (Lin) chanel (APC): antibodies against CD3, CD19 and Ly6G were all used conjugated with the same fluorochrome (APC). Viable cells were selected based on their FSC-A properties and low viability dye staining and doublets were excluded by gating on SSC-A/SSC-W plot. Leukocytes were then identified by their CD45 expression, eosinophils (siglecF$^+$), neutrophils (Lin$^+$CD11b$^+$), B and T cells (Lin$^+$CD11b$^-$) and dendritic cells (CD11c$^+$F4/80$^-$) were identified and sequentially excluded from analysis. T and B cells were differentiated based on CD3 or CD19 and MHCII expression, respectively. Monocytes (CD11b$^+$Ly6C^{hi}) were identified and excluded from the remaining cells then macrophages were gated as F4/80$^+$CD64$^+$ cells. For each contour plot, represented population is specified in the upper left corner. When PE channel was used to analyse CD124 expression or when tdRFP expressing cells were present in the sample, CD64 antibody was omitted and the same gating strategy was used except for identification of macrophages which were gated as F4/80$^+$. When PE-CF594 channels were used to detect tdRFP-expressing cells, the same gating strategy was used with Alexa Fluor 647 conjugated-antibody against SiglecF and APC-Cy7 or APC-H7 conjugated antibodies against CD3, CD19 and Ly6G. In chimeric mice experiments, antibodies CD45.1 (BV421) and CD45.2 (PE-Cy7) were used and the same gating strategy was applied.

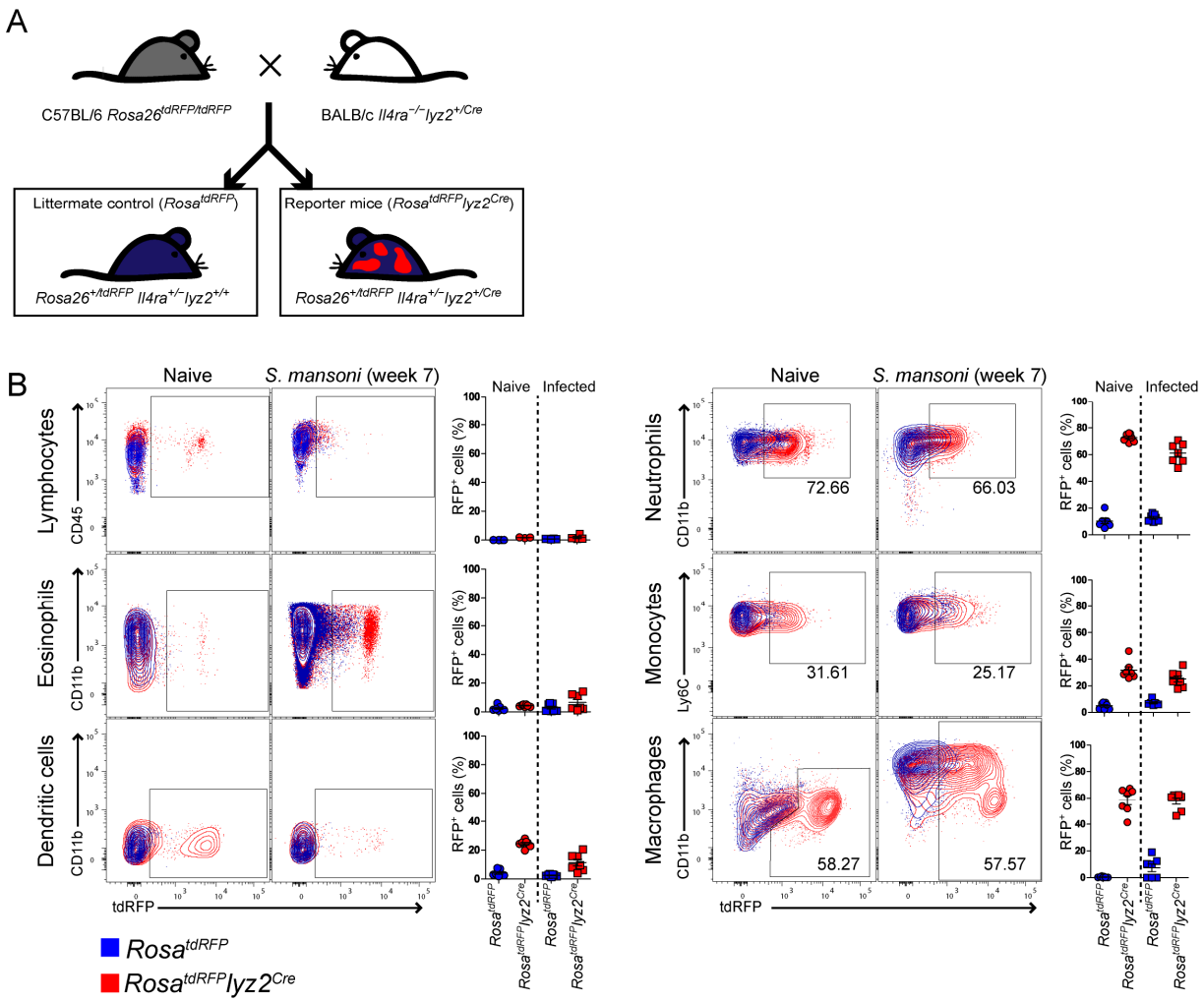

Figure S2. Cre expression in *Rosa^{tdRFP}lyz2^{Cre}* mice after *S. mansoni* infection.
Rosa$^{+/tdRFP}$lyz2$^{+/Cre}$ reporter mice and littermate control were percutaneously infected with 35 *S. mansoni* cercariae or left untreated and tdRFP expression measured in liver leukocytes populations by flow cytometry at 7 weeks post-infection.
(**A**) Breeding strategy to obtain *Rosa$^{+/tdRFP}$lyz2$^{+/Cre}$* reporter mice.
(**B**) Overlap of representative flow cytometry contour plots from *Rosa$^{+/tdRFP}$lyz2$^{+/Cre}$* mice (red) or littermate control (blue) and quantification of RFP^{+} cells in the different populations of liver leukocytes. Numbers on contour plot correspond to mean percentage of RFP^{+} cells in the corresponding leukocyte population of *Rosa$^{+/tdRFP}$lyz2$^{+/Cre}$* mice. Results are shown as pooled data from two independent experiments (n=3-4). Symbols represent values from individual mice and bars show mean +- SEM.

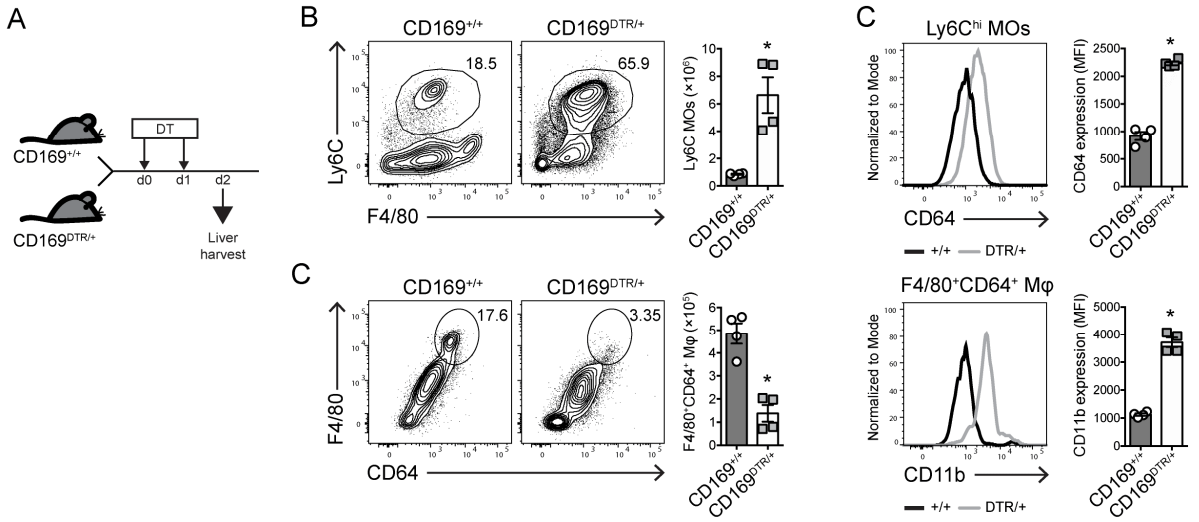

Figure S3. S. mansoni infection mimics artificial deletion of KCs in recruiting Ly6C^{hi} monocytes to the liver.

Naive CD169$^{DTR/+}$ and CD169$^{+/+}$ littermate control C57BL/6 mice were injected intraperitoneally (i.p.) with DT (250ng/mouse) on day 0 and 1 and liver leukocytes were analysed by flow cytometry on day 2. The gating strategy is outlined in Fig S1.

(**A**) Experimental design.

(**B**) Representative flow cytometry contour plot and total number of Ly6C^{hi} liver monocytes and F4/80^{+}CD64^{+} liver macrophages.

(**C**) Representative overlaid histogram and median fluorescence intensity (MFI) of CD64 and CD11b expression from Ly6C^{hi} liver monocytes and F4/80^{+}CD64^{+} liver macrophages, respectively, as detected by flow cytometry.

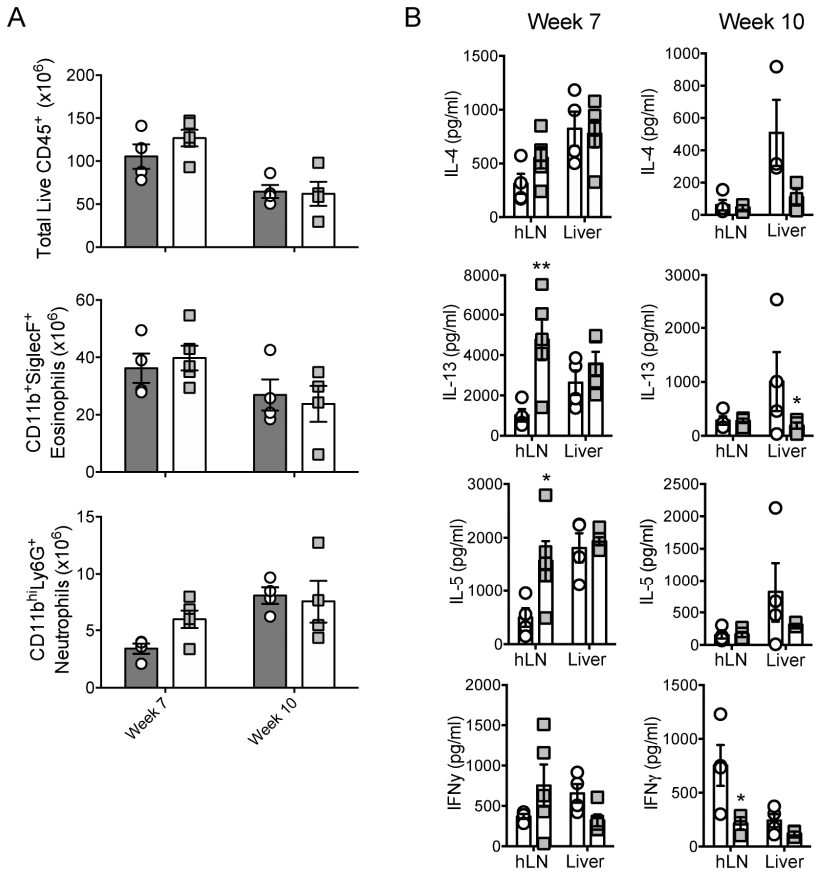

Figure S4. Liver response in DT-treated *S. mansoni* infected CD169^{DTR} mice.
CD169$^{DTR/+}$ and CD169$^{+/+}$ littermate control C57BL/6 mice were percutaneously with 35 *S. mansoni* cercariae and received DT by i.p. injection (250ng/mouse) at regular intervals as depicted in Fig. 6A.
(A) Liver leukocyte responses at 7 and 10 weeks post-*S. mansoni* infection according to the gating strategy in Fig. S1.
(B) Cytokine production as quantified by ELISA on supernatant after 72h of *S. mansoni* soluble egg antigen (SEA) *ex vivo* restimulation of hepatic LN (hLN) and liver cells. Symbols represent values from individual mice and bars show mean +- SEM. Two-way ANOVA with Sidak's post-test.

Discussion

Macrophages are highly plastic and polyfunctional cells that can adopt an array of phenotypes and functions according to the inflammatory environment and the tissue they reside in (Murray et al., 2014). It is now clear that inflammatory stimuli, such as in helminth infection, lead to an array of macrophage responses going from local proliferation and activation of resident macrophages to the recruitment of BM derived monocytes to the inflamed tissue where they differentiate into resident cells (Ruckerl and Allen, 2014), leaving an underestimated complexity to the macrophages responses to helminth infection.

During helminth infection, type 2 cell-mediated responses dominate with high production of cytokines IL-4 and IL-13 that leads to the polarization of macrophages into aaMφs. aaMφs have been at the foresight in helminth immunology for the last two decades as being essential for immunity against nematode infections (Anthony et al., 2007; Turner et al., 2018), but also modulate parasite egg-driven inflammation during schistosomiasis (Horsnell and Brombacher, 2007). Immunomodulation by aaMφs was described either during the peak of egg production to regulate intestinal inflammation during acute schistosomiasis (Herbert et al., 2004), or during the chronic phase of the infection by down-modulating pro-fibrotic type 2 responses (Nair et al., 2009; Pesce et al., 2009a; Pesce et al., 2009b). But while liver fibrosis was modulated by Relm-α- and Arg1-producing aaMφs, the role of IL-4Rα-responsive macrophages during acute or chronic schistosomiasis still remains unappreciated. Indeed, conflicting results exist after infection of conditional knockdown *Il4ra*$^{-/lox}$*lyz2*^{Cre} mice that use lysozyme M (*lyz2*)-dependent Cre expression for cell-specific deletion of the *Il4ra* locus (Herbert et al., 2004; Vannella et al., 2014); which left a number of questions unanswered. In the present study, we aimed to investigate the IL-4Rα dynamics of monocyte/macrophage responses in the liver during schistosomiasis. Whereas infection with filarial or gastrointestinal nematodes such as *L. sigmodontis* or *H. polygyrus* induced IL-4-dependent local proliferation of resident macrophages through IL-4Rα-responsiveness (Jenkins et al., 2011; Jenkins et al., 2013; Ruckerl et al., 2017), liver granuloma formation during schistosomiasis was rather associated with recruitment of Ly6C^{hi} monocytes giving rise to macrophages of a resident phenotype (Girgis et al., 2014; Gundra et al., 2017; Nascimento et al., 2014). But the role of IL-4/IL-13-dependent responses in the dynamics of liver responses to *S. mansoni* remained unknown, as well as the role of liver KCs. Here we comprehensively showed that Ly6C^{hi} monocytes of BM origin progressively upregulated the macrophage marker CD64 and strongly proliferated by week 8 post-infection to populate the liver and give rise to CD11b^{hi} F4/80^{+}CD64^{+} macrophages independently of IL-4Rα-responsiveness. From that time point CD11b^{hi} macrophages were the main macrophage population in the liver while KCs almost disappeared.

By looking at the susceptibility to *S. mansoni* infection after a range of low to high dose of infectious cercariae, we observed that *Il4ra*$^{-/lox}$*lyz2*^{Cre} mice were not dying at a different rate than littermate control mice, which was similar to the results described by Vannella and colleagues (Vannella et al., 2014). Granulomatous inflammation was however affected with *Il4ra*$^{-/lox}$*lyz2*^{Cre} mice developing bigger liver granulomas containing significantly more CD45^{+} leukocytes by week 8 post-infection, without significant effect on the proportion of immune cells composing the granulomas nor cytokine responses. These results suggested that *lyz2*-specific knockdown of IL-4Rα results in heightened liver inflammation globally at the peak of egg production as previously suggested (Herbert et al., 2004; Vannella et al., 2014). But it remained unclear how *S. mansoni* infection affected the selective excision of IL-4Rα in *Il4ra*$^{-/lox}$*lyz2*^{Cre} mice. A previous report investigated the efficiency and specificity of *lyz2*-driven Cre expression using Rosa-EYFP reporter mice (Abram et al., 2014). While YFP expression was mainly specific to neutrophils and macrophages, the efficacy was variable according to the tissue with the majority of alveolar and peritoneal macrophages expressing YFP but less than 40% of spleen macrophages expressed the reporter protein. We used a similar approach to investigate the efficacy and specificity of *lyz2*-driven Cre expression in the liver using reporter Rosa-tdRFP mice. Our results validated the specificity of Cre expression on neutrophils and macrophages with only minimal leaking in T or B lymphocytes, eosinophils or DCs. But the efficacy of Cre expression was not absolute with a significant proportion of neutrophils or macrophages that did not express the reporter protein. Nevertheless *Il4ra*$^{-/lox}$*lyz2*^{Cre} mice developed heightened liver inflammation, which confirm that even though these mice did not achieve 100% expression of Cre recombinase in neutrophils and macrophages, it was sufficient to affect their response to *S. mansoni* infection and significantly impair IL-4/13-driven Ym1 and Relm-α expression. An important additional observation was that *S. mansoni* infection did not significantly affect Cre expression in macrophages in term of percent of RFP-expressing cells, suggesting that *S. mansoni* infection does not necessarily induce positive selection of IL-4Rα^{+} macrophages as previously shown in IL-4-induced local proliferation of resident macrophages (Jenkins et al., 2013). Thus, we provide a more comprehensive view of the cell-specific Cre expression in *lyz2*^{Cre} mice and how it is affected during schistosomiasis.

Importantly, CD11b^{hi} macrophages were the main IL-4Rα-responsive cells producing large amounts of Ym1 and Relm-α whereas the expression of these aaMφ signature proteins was significantly reduced in *S. mansoni*-infected *Il4ra*$^{-/lox}$*lyz2*^{Cre} mice throughout the course of the infection; but Ym1 or Relm-α were not upregulated in CD11b^{lo} KCs. Ablation of CCR2-dependent monocytes after DT treatment of CCR2^{DTR} mice during schistosomiasis resulted in impaired granuloma formation, weight loss and death (Nascimento et al., 2014), further highlighting the essential role of recruited CD11b^{hi} macrophages to the liver to regulate inflammation. We observed that alternative activation was impaired in liver CD11b^{hi} macrophages of *Il4ra*$^{-/lox}$*lyz2*^{Cre} mice after *S. mansoni* infection whereas these mice developed increased

granulomatous inflammation, which suggest that these cells contribute to regulating granuloma formation in the liver while signalling through IL-4Rα is probably not determinant in the protective functions of CD11b^{hi} macrophages.

Resident CD11b^{lo} KCs nearly disappeared progressively after *S. mansoni* infection as early as week 4 p.i and was independent of IL-4Rα. Ablation of KCs is reminiscent of the macrophage disappearance reaction phenomenon of peritoneal macrophages (Barth et al., 1995). This observation was interesting as it questioned the role of CD11b^{lo} KCs during schistosomiasis. Depletion of CD169^{+} cells resulted in the depletion of CD11b^{lo} KCs but did not significantly impact on host survival, granuloma volumes or cytokine responses in the liver after *S. mansoni* infection. Such result was unexpected and could suggest that monocyte-derived aaMφs recruited to the liver fill the empty KC niche and mediate immune regulatory functions as well as the metabolic functions of KCs. Whether KC disappearance is the cause or the consequence of monocyte recruitment is not clear but we observed that inducing KCs death in CD169^{DTR} mice resulted in a severe expansion of Ly6C^{hi} monocytes upregulating CD64 whereas the few F4/80^{+}CD64^{+} macrophages in the liver expressed high levels of CD11b, signing their monocyte origin. These results correlate with a recent report showing that KC death induction in Clec4f^{DTR} mice specifically targeting KCs resulted in their replacement by macrophages of BM origin (Scott et al., 2016). DT treatment of CD169^{DTR} from week 5.5 after *S. mansoni* infection further enhanced the recruitment of Ly6C^{hi} monocytes and their differentiation into macrophages. But during *S. mansoni*, these macrophages maintained a high expression of CD11b, suggesting that their phenotype is divergent to KCs of naive mice. Thus, our results suggest that *S. mansoni* infection induces the contraction of KCs that is associated with repopulating CD11b^{hi} macrophages of BM origin in the liver.

In conclusion, our findings further highlight the role of monocyte-derived aaMφs in regulating liver inflammation after *S. mansoni* infection while demonstrate that CD169^{+} cells, including resident CD11b^{lo} macrophages, are dispensable to control schistosomiasis.

Materials and Methods

Parasites and infection

S. mansoni-exposed snails were provided by the Schistosome Research Reagent Resource Center for distribution by BEI Resources, NIAID, NIH: *S. mansoni*, Strain NMRI exposed *Biomphalaria glabrata*, Strain NMRI (NR-21962). *S. mansoni* cercariae were collected from *S. mansoni*-exposed *B. glabrata*, counted and used for percutaneous infection as described (Tucker et al., 2013). Briefly, every mouse abdomen was shaved using a disposable razor and mice anesthetized by intraperitoneal injection of 16 mg/kg of xylazine and 100 mg/kg of ketamine. Anaesthetized mice were maintained on the back and a metal ring placed on the shaved abdomen before 1 mL of water containing the desired number of cercariae was applied to the skin during 30 min to allow the attachment and penetration of cercariae. Inocula were checked for the absence of cercariae after the incubation period of percutaneous exposure.

Animals

The experiments, maintenance and care of mice complied with the guidelines of the European Convention for the Protection of Vertebrate Animals used for Experimental and other Scientific Purposes (CETS n° 123). The protocol was approved by the Committee on the Ethics of Animal Experiments of the University of Liège, Belgium (Permit Number: 1357, 1713 and 1849). All efforts were made to minimize suffering. Female BALB/cOlaHsd wild-type mice, 6–8 weeks old were purchased from Envigo (Venray, Netherlands). BALB/c Cd45.1^{+} genitor mice were generously provided by Prof. U. Eriksson (Center for Molecular Cardiology, University of Zurich). BALB/c Cd45.1^{+}Cd45.2^{+} were obtained by crossing Cd45.1^{+} BALB/c mice with wild-type BALBc/OlaHsd (Cd45.2^{+}). BALB/c *Il4ra*$^{-/-}$*lyz2*^{Cre}, *Il4ra*$^{lox/lox}$ and *Il4ra*$^{-/-}$ genitor mice were obtained from the Prof. F. Brombacher (University of Cape Town, South Africa). BALB/c *Il4ra*$^{-/lox}$*lyz2*^{Cre} and littermate control *Il4ra*$^{-/lox}$ were obtained by crossing *Il4ra*$^{-/-}$*lyz2*^{Cre} and *Il4ra*$^{lox/lox}$ genitors. C57BL/6 Rosa26$^{\text{flSTOP-tdRFP}}$ were obtained from Prof. H.J. Fehling (University of Ulm, Germany) were crossed to BALB/c *Il4ra*$^{-/-}$*lyz2*^{Cre} to obtain *Il4ra*$^{-/+}$*lyz2*^{Cre}*Rosa26*$^{flSTOP\text{-}tdRFP}$ and littermate control *Il4ra*$^{-/+}$*Rosa26*$^{flSTOP\text{-}tdRFP}$. CD169$^{\text{DTR}}$ (*B6;129-Siglec1<tm1(HBEGF)Mtka>*) mice (Miyake et al., 2007; Saito et al., 2001) were provided by Prof. F. Bureau (GIGA institute, ULiege, Belgium). Six to 8 weeks old female littermates were randomly assigned to experimental groups. During experiments, 4 to 5 female mice were cohoused per cage, food and water was provided *ad libitum*. All the animals were bred and/or housed in the University of Liège, Department of Infectious Diseases.

	Description	**Use**
CD45.1 BALB/c mice	BALB/c mice normally bear the *b* allele of the protein tyrosine phosphatase receptor type C gene (*Ptprc* or *Cd45*). These mice are designated as CD45.2 as opposed to congenic CD45.1 mice bear the *a* variant of *Ptprc*. The transmembrane protein CD45 is expressed on nucleated cells of hematopoietic origin (Raschke et al., 1995).	Expression of the *a* and *b* alleles of *Ptprc* does not affect the function of the expressed protein but can be differentiated using specific antibodies. This allows tracking of cells from a given origin in experiments involving adoptive transfer of cells to mice or production of chimeric mice (for example when transfering cells from CD45.1 mice to CD45.2 mice).
Il4ra$^{-/-}$ mice	These mice lake the α chain of the type I and type II IL-4 receptors (IL-4Rα) on all cells (hematopoietic and non hematopoietic). By consequence, signaling for both IL-4 and IL-13 is impaired (see Introduction Figure 6).	IL-4 and IL-13 are two canonical cytokines of type 2 immune responses, therefore *Il4ra*$^{-/-}$ mice have a diminished type 2 immune. These mice are used to study the role of type 2 immunity during helminth infections.
Lyz2^{Cre} mice	The Cre recombinase (Cre) is a tyrosine recombinase that mediates recombination through palindromic recombinase target sites (loxP sites here) (Anastassiadis et al., 2010). The Cre-loxP system is used to carry out conditional mutagenesis in mice : the control of Cre expression by a specific promoter determine the cell types that will be impacted by the recombination.	Expression of Cre recombinase under the control of the Lyz2 promoter is described in neutrophils, macrophages, monocytes and neurons (Abram et al., 2014; McCubbrey et al., 2017; Orthgiess et al., 2016) and *Lyz2*^{Cre} mice are commonly used to perform mutagenesis in myeloid cells.
Il4ra$^{lox/lox}$ mice	LoxP sites flank exons 7-9 of the *Il4ra* locus (Herbert et al., 2004).	These mice are crossed with mice expressing the Cre to produce mice that are knockdown for IL-4Rα in specific cell types, which therefore have impaired IL-4 and IL-13 responses.
Rosa26$^{flSTOP\text{-}tdRFP}$	These mice bear a stop sequence flanked by loxP sites (flSTOP) followed by a sequence coding for tandem-dimer red fluorscent protein (tdRFP), under the control of ROSA26 promoter. The ROSA26 promoter is ubiquitously expressed in mice cells.	When crossed with Cre-expressing mice, these mice are used as reporter mice to identify the cell types in which the Cre is expressed. Cre expression induce the deletion of a stop codon to allow the expression of tdRFP.
Cd169^{DTR}	These mice bear a sequence coding for the human diphteria toxin receptor (DTR) in exon 1 of the gene coding for CD169 (Miyake et al., 2007).	Diptheria toxin administration induces the depletion of CD169^{+} cells. These mice have been used to induce the depletion of resident macrophages in several organs (Gupta et al., 2016a).
Partial bone marrow chimeras	Partial body irradiation was performed on CD45.2 BALBc mice sparing liver area to achieve destruction of the majority of hematopoietic cells with exception of liver resident cells. Mice were reconstituted with bone marrow cells of CD45.1.2 congenic mice.	Flow cytometric analysis of CD45.2 and CD45.1 expression on liver leukocytes allow to define the origin of the cells. Donor origin (CD45.1.2 cells) indicates that cells have infiltrated the liver from the periphery while recipient origin (CD45.2 cells) indicates that cells originate from liver resident cells.

Table 1. Description of mouse models used

Partial BM chimeric mouse model

Partial BM chimeric mice were produced by exposing CD45.2^{+} BALB/c mice to partial body lethal irradiation as described elsewhere (Machiels et al., 2017). Briefly, mice received a dose of 7 Gy in one

fraction delivered to the whole body except on the liver with a dedicated small animal radiotherapy device (SmART Irradiator from Precision X-Ray Inc). Radiation was delivered using a photon beam (maximum energy of 225 kV and 13 mA), which provided a dose rate of 3 Gy/min. The planning system SmART-plan (version 1.3.9 Precision X-ray, North Branford, CT) was used to plan, to calculate and to deliver the treatment. The dose delivered was almost 0 Gy to the liver, 7.5 Gy to the soft tissue and 20.5 Gy to the bone. Prior to irradiation, mice received continuous isoflurane gas anaesthesia *via* induction in a chamber (0.5 L/min oxygen with 4.0% isoflurane). During irradiation, mice received continuous isoflurane anaesthesia gas *via* a nose cone (0.4 L/min oxygen with 1.5% isoflurane). The next day, mice were reconstituted by intravenous injection of a total of 5×10^6 BM cells isolated from femurs and tibias of BALB/c donor mice. From 1 week before to 3 weeks after irradiation, mice were given broad-spectrum antibiotherapy (0.27g Trimethoprimum and 1.33g Sulfadiazinum per liter of drinking water, Emdotrim 10%, Ecuphar). Mice were left untreated for 8 weeks to allow complete reconstitution and chimerism of the different blood leukocytes populations was then confirmed by flow cytometry.

Tissue processing and cell preparation

After euthanasia, portal vein was sectioned and livers were perfused by injection of 10ml of ice-cold PBS through the left heart ventricle. Livers were removed, cut into pieces with scissors and incubated in DMEM containing 3mg/ml of collagenase IV (Sigma) for 20 (naive mice) to 40 (infected mice) minutes at 37°C and mashed through metallic sieve. All the tissue was then incubated at 37°C for a second period of 15 (naive mice) to 30 (infected mice) minutes and filtered on a 100µm cell strainer (Falcon). The resulting suspension was washed with DMEM and erythrocytes were lysed in red cell lysis solution (155mM NH_4CL, 0.12mM EDTA, 10mM $KHCO_3$).

Flow cytometry

Incubations were performed in FACS buffer (PBS containing 0.5% BSA and 0.1% NaN_3) at 4°C. Cells were first incubated with anti-mouse CD16/32 antibody (clone 93, BioLegend) before fluorochrome-conjugated antibodies against surface antigens were added and incubated during 20 min at 4°C. Panels included antibodies to mouse CD11b (clone M1/70; FITC conjugated), F4/80 (BM8; BV711), Ly6C (HK1.4; BV786), CD3 (145-2C11; APC or APCCy7), CD45.1 (A20; BV421) and CD45.2 (104; PECy7) all from Biolegend; antibodies to mouse CD19 (1D3; APCC7), Ly6G (1A8; APC or APCH7), CD64 a and b alloantigens (X54-5/7.1; PE), SiglecF (E50-2440; PECF594 or AF647) and CD124 (mIL4R-M1; PE), all from BD biosciences and antibodies to mouse CD11c (N418; AF700), CD45 (30-F11; PECy7), CD19 (MB19-1; APC) and MHCII (M5/114.15.2; eF450), all from eBioscience. Dead cells were stained using Fixable Viability Stain 510 (BD Biosciences). In experiments in which intracellular staining was needed, cells were fixed in 2% paraformaldehyde

overnight and washed with Permeabilization Buffer (eBioscience) before being incubated with biotinylated antibodies against mouse-Ym1/Chitinase 3-like 3 (polyclonal goat IgG) or isotype control (goat IgG control) from R&D Systems or biotinylated antibody against mouse Relm-α (polyclonal rabbit) from Peprotech in Permeabilization Buffer for 20 min at 4°C, detected with BV650-conjugated streptavidin (BD Biosciences). Samples were analysed on a BD LSR Fortessa X-20 flow cytometer, cell sorting was performed on a FACS Aria IIIu (BD biosciences).

In vivo EdU incorporation

Mice were injected ip with EdU (500 µg/mouse in PBS, ThermoFisher Scientific) 4 hours before endpoint. Mice were euthanized and livers were processed as described above. Surface staining was performed and cells were fixed, permeabilized and stained for EdU using Click-it Plus EdU Pacific Blue Flow Cytometry Assay Kit (Invitrogen) following manufacturer instructions. Samples were analysed on a BD LSR Fortessa X-20 flow cytometer (BD Biosciences).

Histology

Liver were collected from PBS-perfused animals and immediately fixed in 10% neutral buffered formalin. Tissues were embedded, sectioned and stained with Picrosirius Red. Granulomas area were delimited on ImageJ software v1.8. Granulomas volumes were estimated by the volume of the corresponding sphere ($V=4/3\pi r^3$), with r being half of the geometric mean between Feret and MinFeret diameters of the delimited area.

Cytokine ELISA

Single-cell suspensions were prepared from hLN (Barbier et al., 2012) and livers and cultured at 2×10^6 cells/ml with or without 20 µg/ml SEA in Iscove's modified Dulbecco's medium supplemented with 10% fetal calf serum (Gibco). Culture supernatants were harvested at 72h for cytokine analysis using by specific ELISA (Ready-SET-Go, eBioscience).

Statistical analyses

Statistical evaluation of different groups was performed either by analysis of variance (ANOVA) followed by the Dunnett or Sidak multiple-comparison test or by non-parametric Mann-Whitney test, as indicated. A p-value < 0.05 was considered significant. Statistical analyses were performed using Prism v6 (Graphpad, La Jolla, CA).

Experimental section

2nd study :

Helminth-induced IL-4 expands bystander memory CD8$^+$ T cells for early control of viral infection

Marion Rolot, Annette Dougall, Alisha Chetty, Justine Javaux, Ting Chen, Xue Xiao, Bénédicte Machiels, Murray E. Selkirk, Rick M. Maizels, Cornelis Hokke, Olivier Denis, Frank Brombacher, Alain Vanderplasschen, Laurent Gillet, William G. Horsnell, Benjamin G. Dewals

Nature communications, **9**-4516 (2018) ; doi *:* 10.1038/s41467-018-06978-5

Abstract

Infection with parasitic helminths can imprint the immune system to modulate bystander inflammatory processes. Bystander or virtual memory $CD8^+$ T cells (T_{VM}) are non-conventional T cells displaying memory properties that can be generated through responsiveness to interleukin (IL)-4. However, it is not clear if helminth-induced type 2 immunity functionally affects the T_{VM} compartment. Here, we show that helminths expand $CD44^{hi}CD62L^{hi}CXCR3^{hi}CD49d^{lo}$ T_{VM} cells through direct IL-4 signaling in $CD8^+$ T cells. Importantly, helminth-mediated conditioning of T_{VM} cells provided enhanced control of acute respiratory infection with the murid gammaherpesvirus 4 (MuHV-4). This enhanced control of MuHV-4 infection could further be explained by an increase in antigen-specific $CD8^+$ T cell effector responses in the lung and was directly dependent on IL-4 signaling. These results demonstrate that IL-4 during helminth infection can non-specifically condition $CD8^+$ T cells, leading to a subsequently raised antigen-specific $CD8^+$ T cell activation that enhanced control of viral infection.

Introduction

Soil-transmitted helminths and schistosomes infect more than a quarter of the world population, essentially afflicting people who live in areas of poverty in the developing world (Pullan et al., 2014). Heavy parasite infections cause morbidity and mortality that can occur at levels high enough to delay socio-economic development (Hotez et al., 2006). Low burden infections with helminths while mostly asymptomatic can still have bystander effects on other diseases, especially in the case of autoimmunity and allergy (Osbourn et al., 2017; Ramanan et al., 2016), thus advocating the use of specific helminths or derived products as therapeutic strategies while encouraging guided deworming campaigns (Wammes et al., 2014). However, how bystander helminth infections modulate the control of heterologous pathogens such as viruses is understood in only a limited number of contexts and reports of both beneficial and detrimental effects on viral pathology exist (Furze et al., 2006; McFarlane et al., 2017; Osborne et al., 2014; Reese et al., 2014; Scheer et al., 2014).

Memory establishment and maintenance is the hallmark of the adaptive immune system and essential for ultimate control of many pathogens. B and T lymphocytes are unique in their ability to acquire immune memory against specific antigens (Ag) in order to provide these high levels of protection. However, these lymphocytes can also launch less stringent but still effective responses to either antigen or host immune responses (Guo et al., 2015; Horsnell et al., 2013). Furthermore, conditioning of T cells can impart memory-like properties and functions in absence of encounter of their cognate Ag (White et

al., 2016), and also be important for priming $CD4^+$ T cells for subsequent type 2 immunity (Minutti et al., 2017a). This is also the case for $CD8^+$ T cells; "bystander" or "virtual memory" $CD8^+$ T cells (T_{VM}) emerge from early in life in naive mice (Jameson et al., 2015; Smith et al., 2018; White et al., 2017) and also humans (Jacomet et al., 2015; Min et al., 2011) in the absence of specific Ag stimulation and are thus Ag-inexperienced. T_{VM} cells have a memory-like phenotype with more effective responses to Ag encounter compared to naïve cells and characterized by expression of high levels of CD44 and also CD62L but low levels of CD49d (α4 integrin). T_{VM} emerge in naive mice with an unrestricted TCR repertoire and in response to various stimuli including IL-15, IFN-I and IL-4 (Martinet et al., 2015; Renkema et al., 2016; White et al., 2016). While TCR involvement remains to be fully deciphered, recent data suggest that T_{VM} are favored by stronger TCR signals against self-antigens but maintain self-tolerance (Drobek et al., 2018; Lee et al., 2013b; Martinet et al., 2015; Renkema et al., 2016; White et al., 2016). Whereas T_{VM} development in C57BL/6 mice mostly depend on IL-15, IL-4 is the main driver of T_{VM} expansion in BALB/c mice (Tripathi et al., 2016).

Parasitic helminths induce type 2 immunity characterized by high levels of IL-4 (Harris and Loke, 2017). Bystander consequences of this strong induction of IL-4 on memory $CD8^+$ T cells is not well understood. In this study, we show that infection with helminths (*Schistosoma mansoni*, *Nippostongylus brasiliensis* and *Heligmosomoides polygyrus*) or immunization with *S. mansoni* Ags, expands bystander T_{VM} cells in secondary lymphoid tissues *via* IL-4. This Ag-nonspecific conditioning of $CD8^+$ T cells prior to encounter of their specific Ag provides early and enhanced control of a subsequent gammaherpesvirus acute infection. This enhanced protection was the result of higher levels of virus-specific $CD8^+$ T cell effector responses. Thus, during helminth infection IL-4 expands and conditions T_{VM} cells for more rapid CD8 responses against subsequent cognate Ag encounter.

Results

Immunization with *S. mansoni* eggs alters the memory CD8$^+$ T cell response in peripheral lymphoid tissue by increased CD44^{hi}CD49d^{lo} T_{VM} cells.

To investigate how the T_{VM} cellular compartment is affected by helminth-induced inflammation, we first used a well-characterized experimental model for inducing type 2 inflammation by helminth Ags, in which eggs of the trematode parasite *S. mansoni* are injected intra-peritoneally (i.p.) to 6-8 week-old female BALB/c mice before intra-venous challenge (i.v.) 2 weeks later, and responses measured at d22 after the first injection (Figure S1a) (Joyce et al., 2012). We confirmed that *S. mansoni* eggs induced eosinophilic granulomas in the lung (Figure S1b) and typical type 2 inflammation with high levels of soluble schistosome egg Ag (SEA)-specific IgG1 (Figure S1c) and IL-4 production upon SEA restimulation of the dLN (Figure S1d).

The CD8$^+$ T cell populations were initially compared from lung, dLN and spleen of BALB/c mice subjected to *S. mansoni* egg immunization or not and according to their expression of CD44, CD62L and CD49d (Figure S1e). *S. mansoni*-driven type 2 inflammation did not induce significant increase of lung or spleen cellularity while cell numbers in the dLN were increased (Figure 1a). There was no overt response in the lung, despite increased true memory CD44^{hi}CD49d^{hi} T cell (T_{TM}) proportions (Figure 1b-d). However, responses in dLN and spleen were significantly affected with strikingly increased numbers and proportions of CD44^{hi}CD49d^{lo} T cells, corresponding to the T_{VM} compartment. Increased levels of eomesodermin (Eomes) were also found in T_{VM} cells after *S. mansoni* egg immunization whereas T_{VM} retained low expression levels of T-bet (Figure 1e-f), a typical feature of T_{VM} cells (Renkema et al., 2016).

Interleukin 4 directs the expansion of T_{VM} cells after exposure to helminths.

We then investigated the implication of IL-4 responsiveness in the expansion of the T_{VM} pool after *S. mansoni* egg immunization. We confirmed that treatment with IL-4 complexes (IL-4c) strikingly induced CD44^{hi}CD49d^{lo} T_{VM} cells (Ventre et al., 2012) expressing high levels of Eomes (Figure 2a and b). IL-4 drives the expansion of T_{VM} cells expressing CXCR3 (Weinreich et al., 2009). Thus, we further included CXCR3 surface expression in our analyses and observed that the main part of CD44^{hi}CXCR3^{hi} cells expressed high levels of CD62L and that population expressed low levels of CD49d, corresponding to T_{VM} cells (Figure 2c). The expansion of CXCR3^{hi} T_{VM} cells was further observed after *S. mansoni* egg immunization restricted to i.p. injection (Figure S2a) or immunization with SEA or the Th2-driving

schistosome egg recombinant protein omega-1 (Figure S2b). T_{VM} expansion and Eomes upregulation was also observed in mice at later time points after *S. mansoni* egg immunization (d29 and d43 after initial ip), suggesting that conditioning of T_{VM} is long lasting (Figure S2c). Furthermore, we also observed T_{VM} expansion during other helminth-driven IL-4 dominated responses such as natural infection with *N. brasiliensis* at d10 pi (Figure S2d), and a significant T_{VM} expansion and Eomes upregulation could also be observed by d35 pi (Figure S2e). In addition, natural infection with *H. polygyrus* at d15 pi (Figure S2f and g), and *S. mansoni* at week 7 pi (Figure S2h) also caused increased T_{VM} cell responses. These results further indicated that IL-4-dominated responses to helminth Ags can drive a long-lasting expansion of T_{VM} cells in peripheral lymphoid tissue.

S. mansoni egg injection to *Il4ra*$^{-/-}$ BALB/c mice did not result in the expansion of T_{VM} cells (Figure 2d) and unbiased restimulation of splenocytes with PMA and ionomycin resulted in increased IFN-γ production by $CD8^+$ T cells that was dependent on IL-4 receptor expression (Figure 2e). We further sought to determine whether T_{VM} expansion was directly dependent upon IL-4 responsiveness of $CD8^+$ T cells. Mixed chimeras were generated with congenically distinct BM from WT or *Il4ra*$^{-/-}$ BALB/c mice and subjected to *S. mansoni* egg immunization (Figure 2f) or *S. mansoni* natural infection (Figure S2i). Similar chimerism was observed in both *S. mansoni* egg- or PBS-treated mice. As in the intact mice, the frequency of T_{VM} cells and Eomes expression levels in T_{VM} cells were significantly increased in the WT compartment after exposure to the parasite (Figure 2f and S2g). However, $CXCR3^{hi}CD49d^{lo}$ T_{VM} cells of the *Il4ra*$^{-/-}$ genotype were significantly reduced in naive mice compared to WT compartment and did not expand after helminth exposure. These results demonstrated that IL-4 responsiveness of $CD8^+$ T cells conditions and expands T_{VM} cells after *S. mansoni* egg immunization or natural infection.

Next, in order to examine whether IL-4-dependent T_{VM} expansion would not also result from an Ag-specific response to *S. mansoni* eggs, a tetramer-based enrichment was performed on an unrelated and randomly chosen population of $CD8^+$ T cells expressing a TCR specific to the H-$2K^d$-restricted SYVPSAEQI peptide of the circumsporozoite protein ($CSP^{280-288}$) of *Plamodium yoelii* (Figure S2j). We observed that exposure to *S. mansoni* eggs also caused increased proportions of $CD44^{hi}CXCR3^{hi}$ $CSP^{280-288}$-specific $CD8^+$ T cells (Figure 2g). These results further support that expansion of T_{VM} induced by helminth exposure is Ag-nonspecific.

Helminth exposure ameliorates the control of respiratory MuHV-4 lytic infection.

Ag-inexperienced T_{VM} cells respond more quickly to their cognate Ag than naive T cells (Lee et al., 2013a) and IL-4 signaling in memory $CD8^+$ T cells were previously suggested to reduce effector responses (Ventre et al., 2012). Thus, we investigated whether expanding the T_{VM} pool through helminth exposure would affect effector $CD8^+$ T cell responses against heterologous Ags.

Murid herpesvirus 4 (MuHV-4) is a gammaherpesvirus that infects the laboratory mouse and establishes long term persistence (Barton et al., 2011). Interestingly, levels of primary MuHV-4 lytic infection are directly dependent on effective development of effector $CD8^+$ T cells (Tan et al., 2017). MuHV-4 was therefore used to assess virus-specific $CD8^+$ T cell responses after exposure to helminth Ags. We first immunized 8-week-old female BALB/c mice with *S. mansoni* eggs before their infection with 1×10^4 plaque-forming units (PFU) of MuHV-4 intranasally under general anesthesia (Figure 3a). A control group consisted of PBS-treated mice. Immunization with *S. mansoni* eggs protected against transient weight loss caused by MuHV-4 respiratory infection (Figure 3b) and was associated with reduced levels of infection at d7 post-viral infection (pvi) as determined by immunostaining on lung tissue (Figure 3c) and plaque assay (Figure 3e). We next measured the levels of infection over time using MuHV-4-luc recombinant virus for live imaging of light emission centered on the thorax at day 2, 5, 7 and 9 pvi (Francois et al., 2013). *S. mansoni* egg treatment resulted in significantly reduced levels of light emission by d7 pvi (Figure 3d). There was a similar early control of respiratory MuHV-4 infection when BALB/c mice were infected 49 days after percutaneous exposure to *S. mansoni* cercariae, a time point corresponding to the peak of the response against the parasite eggs (Figure S3a), whereas enhanced control of viral infection was not apparent when mice were coinfected at earlier time points of the parasite life cycle. Likewise, enhanced control of viral infection was also observed when mice were infected with MuHV-4 at d6 or d35 after infection with *N. brasiliensis* (Figure S3b and c).

Colonization of the host by MuHV-4 after lytic respiratory infection was not significantly affected by prior exposure to *S. mansoni* eggs as attested by live imaging of light emission centered on the superficial cervical LN (scLN, Figure 3f) and qPCR for viral genome detection in the spleen at d5, 7, 11 and 20 pvi (Figure 3g). These observations further supported a role of CD8-dependent viral control during lytic replication as effective MuHV-4-specific $CD8^+$ T cell responses were shown to be unable to control the establishment of viral latency (Stevenson et al., 1999b). We further observed that increasing MuHV-4 infectious dose resulted in enhanced control (Figure 3h) and daily imaging of mice infected with 1×10^4 PFU showed similar infection levels up to d5-6 pvi before being controlled in *S. mansoni*-exposed mice (Figure 3i), suggesting enhanced adaptive immune responses rather than impaired viral growth.

Helminths augment CD8$^+$ T cell responses in the respiratory tract after MuHV-4 infection.

We next assessed the immune response against MuHV-4 in BALB/c mice that were exposed to *S. mansoni* eggs or not. We observed no significant difference in the antibody responses against MuHV-4 (Figure S4a) and global cellularity in lungs at d7 pvi was not affected (Figure S4b). Whereas eosinophils and DC numbers were significantly increased in mice exposed to *S. mansoni* eggs, numbers of neutrophils, macrophages, monocytes, B or CD4$^+$ T cells were not affected (Figure S4b). Strikingly, the frequency and number of lung CD8$^+$ T cells was significantly increased at d7 pvi in mice immunized with *S. mansoni* eggs (Figure 4a-c) and mice infected percutaneously with *S. mansoni* cercariae 7 weeks before MuHV-4 infection (Figure 4d). Such enhanced CD8$^+$ T cell response was associated with increased proportions of CD44^{hi}CD62L^{lo} effector T cells (Figure 4e). We further observed that effector CD44^{hi}CD62L^{lo}CD49d^{hi} CD8$^+$ T cell responses were transiently but significantly increased by d7 pvi in the bronchoalveolar lavage fluid (BALF) and lungs of mice prior exposed to *S. mansoni* eggs (Figure 4f), as well as short-lived effector T cells (KLRG1$^+$CD127$^-$) (Figure 4g). These results suggest that prior exposure to helminths enhances CD8$^+$ T cell responses after MuHV-4 infection.

Virus-specific effector CD8$^+$ T cells responses are enhanced after exposure to helminths.

We further sought to evaluate the effector role of CD8$^+$ T cell responses against MuHV-4 infection in BALB/c mice after exposure to *S. mansoni* eggs. Interferon (IFN)-γ and granzyme B (GzmB) expression levels in BAL were significantly increased by d7 pvi (Figure 5a) and unbiased restimulation of lung cells with PMA and ionomycin caused significantly increased co-production of IFN-γ and TNF-α by CD8$^+$ T cells (Figure S5a and b).

In order to assess the MuHV-4-specific CD8$^+$ T cell response, we took advantage of H-2^b congenic BALB/B mice in which the response against the well-established MuHV-4 immunodominant H-2D^b-restricted AGPHNDMEI (ORF6$^{487-495}$) and H-2K^b-restricted SVYGFTGV (ORF61$^{524-531}$) epitopes could be measured (Stevenson et al., 1999a). We initially measured thoracic light emission after MuHV-4-luc infection of BALB/B mice and observed similar enhanced control of viral infection at d7 pvi (Figure 5b). Strikingly, tetramer staining (Figure 5c-d) and peptide restimulation (Figure 5e-f) revealed significantly increased MuHV-4-specific responses in the BALF and lung in BALB/B mice that were initially exposed to *S. mansoni* eggs. Similar increased MuHV-4-specific responses by d7 pvi were observed when mice where infected at d29 or d43 after the initial ip injection of *S. mansoni* eggs (Figure S5c). Moreover, infection of BALB/B mice with 1×10^4 PFU of MuHV-4 intranasally after their initial

infection with *N. brasiliensis* resulted in higher MuHV-4-specific $CD8^+$ T cell responses at d7 pvi (Figure S5d-h).

The results in Figure 2e showed that *S. mansoni* eggs induced expansion of T_{VM} cells expressing a TCR able to recognize MHC tetramers presenting the *P. yoelii* $CSP^{280-288}$ peptide, absent from *S. mansoni* Ags. In order to examine the development of effector Ag-specific responses from $CSP^{280-288}$-specific $CD8^+$ T cells, we infected BALB/c mice with a MuHV-4-luc-CSP virus expressing a modified luciferase protein in which the H-$2K^d$-restricted $CSP^{280-288}$ peptide was inserted in-frame (Figure S5i). We observed enhanced control of MuHV-4-luc-CSP infection in the lung by d7 pvi which was associated with an increased response of effector $CSP^{280-288}$-specific $CD8^+$ T responses (Figure 5g), further supporting that T_{VM} are conditioned by exposure to helminths, which could explain the enhanced effector responses against their cognate Ag.

To further investigate whether the enhanced Ag-specific $CD8^+$ T cell response against MuHV-4 was responsible for the early viral control observed in mice treated with *S. mansoni* eggs, mice were treated with depleting antibodies against CD8 or CD4 one day before MuHV-4 infection and then at d1 and d4 pvi (Figure 5h). While depletion of CD4 did not inhibit the early control of MuHV-4 infection observed in mice exposed to *S. mansoni* eggs, the absence of $CD8^+$ cells resulted the total loss of such early control. These results demonstrate a CD8-dependent mechanism of enhanced control of viral infection and strongly suggest that *S. mansoni* egg immunization rendered $CD8^+$ T cell responses more efficient to clear MuHV-4 infection, independently of $CD4^+$ T cells.

Exposure to helminths expands T_{VM} compartment with discrete phenotypic changes.

To further investigate T_{VM} phenotypic changes after exposure to *S. mansoni* eggs, we compared gene expression profiles between PBS- or *S. mansoni* egg-treated T_{VM} cells by RNA sequencing of FACsorted T_{VM} cells from the spleen (Figure S6). In total, we observed 29 differentially expressed (DE) genes (log_2-fold change > ±0.5, $P < 0.1$) (Figure 6a and 6b) and principal-component analysis (PCA) revealed clustering of PBS- or *S. mansoni* egg-treated T_{VM} cells (Figure 6c). Among genes upregulated in *S. mansoni* egg-induced T_{VM} cells, we observed some genes related to cytotoxicity functions (Gzma, Ctla2a, Slc16a2), cytokine-cytokine receptor interaction (Ccr2, Ccr5) or IFN-I responses (Mx1) (Figure 6b). Further analysis of molecular signatures with BubbleGUM (Spinelli et al., 2015), a tool allowing gene-set enrichment analysis of transcriptomic data, revealed that among the selected gene-sets exposure to *S. mansoni* eggs induced a shift toward higher expression of genes implicated in IFN-γ and IFN-I responses whereas reduced expression of genes involved in cholesterol homeostasis (Figure 6d). These

data demonstrate that naive or *S. mansoni* egg-induced T_{VM} cells are phenotypically distinct and further suggest that this memory T cell population has enhanced capacity to initiate an anti-viral response. Besides affecting their transcriptomics phenotype, exposure to *S. mansoni* eggs leads to T_{VM} expansion that could be due to IL-4 provoking their proliferation. However, EdU incorporation *in vivo* after *S. mansoni* egg immunization did not show overt proliferation in T_{VM} cells but did so in T_{TM} cells after a single EdU administration 4h before harvest (Figure 6e). After a single injection of *S. mansoni* eggs, we observed that levels of IL-4 response to SEA increased by day 4 after injection associated with the expansion of T_{VM} cells (Figure 6f). However, only T_{TM} cells showed significant proliferation and EdU incorporation over time after *S. mansoni* egg injection remained low in T_N and T_{VM} (Figure 6g). T_{VM} expansion could also result from a recruitment to the secondary lymphoid organs. To address this hypothesis, we treated mice with the sphingosine-1 phosphate receptor signaling FTY720 to inhibit recruitment of lymphocytes to the spleen. FTY720 treatment did not impair the IL-4-dependent expansion of T_{VM} in the spleen (Figure 6h), although the extent of the expansion was slightly affected by inhibition of lymphocyte trafficking. In addition, bulk $CD8^+$ T lymphocytes isolated from the spleen of naive mice were transferred to congenic naive BALB/c mice before immunization with *S. mansoni* eggs. T_{VM} expansion occurred irrespective of their donor or recipient origin (Figure 6i), further suggesting that helminth-induced T_{VM} expansion can occur in peripheral $CD8^+$ T lymphocytes. Thus, these results suggest that the observed T_{VM} expansion likely result from the conversion from naive T cells rather than proliferation or recruitment of T_{VM} cells.

IL-4 signaling in $CD8^+$ T cells drives the early control of MuHV-4 acute respiratory infection.

Next, we investigated the role of IL-4 responsiveness in the early control mediated by $CD8^+$ T cells after exposure to helminth Ags. We first used *S. mansoni* eggs to immunize WT or *Il4ra*$^{-/-}$ BALB/c mice before subjecting them to intranasal MuHV-4 infection (Figure 7a). *Il4ra*$^{-/-}$ mice did not display the enhanced control of MuHV-4 infection observed in WT mice, with *Il4ra*$^{-/-}$ mice exposed to *S. mansoni* eggs displaying similar to higher thoracic light signals. The lack of helminth-mediated early control of MuHV-4 infection in *Il4ra*$^{-/-}$ mice was further associated with the absence of increased $CD8^+$ T cells in the lung at d7 pvi (Figure 7b). These results suggest that IL-4 signaling during helminth-elicited inflammation governs the early capacity of BALB/c mice to generate effector $CD8^+$ T cells and control viral infection.

To examine whether the presence of *S. mansoni* eggs in the pulmonary niche conditions the early control of MuHV-4 infection after exposure to helminth Ag, we injected *S. mansoni* eggs to 8-week-old female BALB/c mice twice via the i.p. route at 2 weeks interval before MuHV-4-luc infection

intranasally at d22 (Figure S7a). We found that the presence of *S. mansoni* eggs in the lung was dispensable for the early control of viral infection, with significantly reduced light emission signals by d7 pvi. In addition, treatment with IL-4c at 2 days interval (d0 and d2) before MuHV-4-luc infection intranasally at d4 reduced the levels of light emission reporting infection (Figure 7c), which was associated with enhanced effector $CD8^+$ T cell responses in the lung after MuHV-4 infection (Figure 7d and e). These results further suggest the role of IL-4-induced T_{VM} cells in contributing to the early effector $CD8^+$ T cell responses against MuHV-4 infection.

The impact of IL-4 sensitivity of $CD8^+$ T cells after immunization with *S. mansoni* eggs on subsequent responses against MuHV-4 infection was further investigated by co-transfer of "T_{VM}-rich" WT and "T_{VM}-poor" *Il4ra*$^{-/-}$ purified $CD8^+$ T cells from PBS- or *S. mansoni* egg-treated mice cells in equivalent numbers to congenic PBS- or *S. mansoni* egg-treated BALB/c mice (Figure S7b). Mice were then infected or not with MuHV-4. The absolute numbers of donor WT and *Il4ra*$^{-/-}$ $CD8^+$ T cells localizing to the lung tended to increase at 7 day pvi (Figure 7f), and analysis of WT:*Il4ra*$^{-/-}$ donor cell ratios normalized to uninfected mice demonstrated significant enrichment of donor WT $CD8^+$ T cells compared to donor *Il4ra*$^{-/-}$ $CD8^+$ T cells when the mice were initially treated with *S. mansoni* eggs (Figure 7g). Importantly, IL-4 signaling in $CD8^+$ T cells resulted in significantly increased IFN-γ production after unbiased restimulation of lung cells from *S. mansoni* egg-treated mice after MuHV-4 infection, compared to the donor *Il4ra*$^{-/-}$ $CD8^+$ T cell compartment (Figure 7h). These results demonstrated that IL-4 signaling in $CD8^+$ T cells, probably through expansion of T_{VM} cells, contributes significantly to condition effective anti-viral $CD8^+$ T cell responses and that IL-4Rα-dependent *S. mansoni* egg-induced inflammation in the lung environment alone is not sufficient to significantly enhance $CD8^+$ T cell responses. Nonetheless, it was unclear whether *S. mansoni* egg-induced T_{VM} cells could outcompete their naive counterparts. Thus, we adoptively co-transferred T_{VM} cells FACsorted from PBS- and *S. mansoni* egg-treated mice cells in equivalent numbers to congenic naive BALB/c mice (Figure S7d). At d7 after MuHV-4 infection, effector T cells originating from transferred T_{VM} cells could be detected in lungs and BALF demonstrating the contribution of T_{VM} cells to the effector anti-viral CD8 response (Figure 7i). However, no significant differences could be observed between naive or Sm egg-induced T_{VM} compartments (Figure 7j). Thus, although phenotypically distinct to naive T_{VM} cells, preliminary expansion of T_{VM} cells contributes to the early control of MuHV-4 infection.

Figures

Figure 1

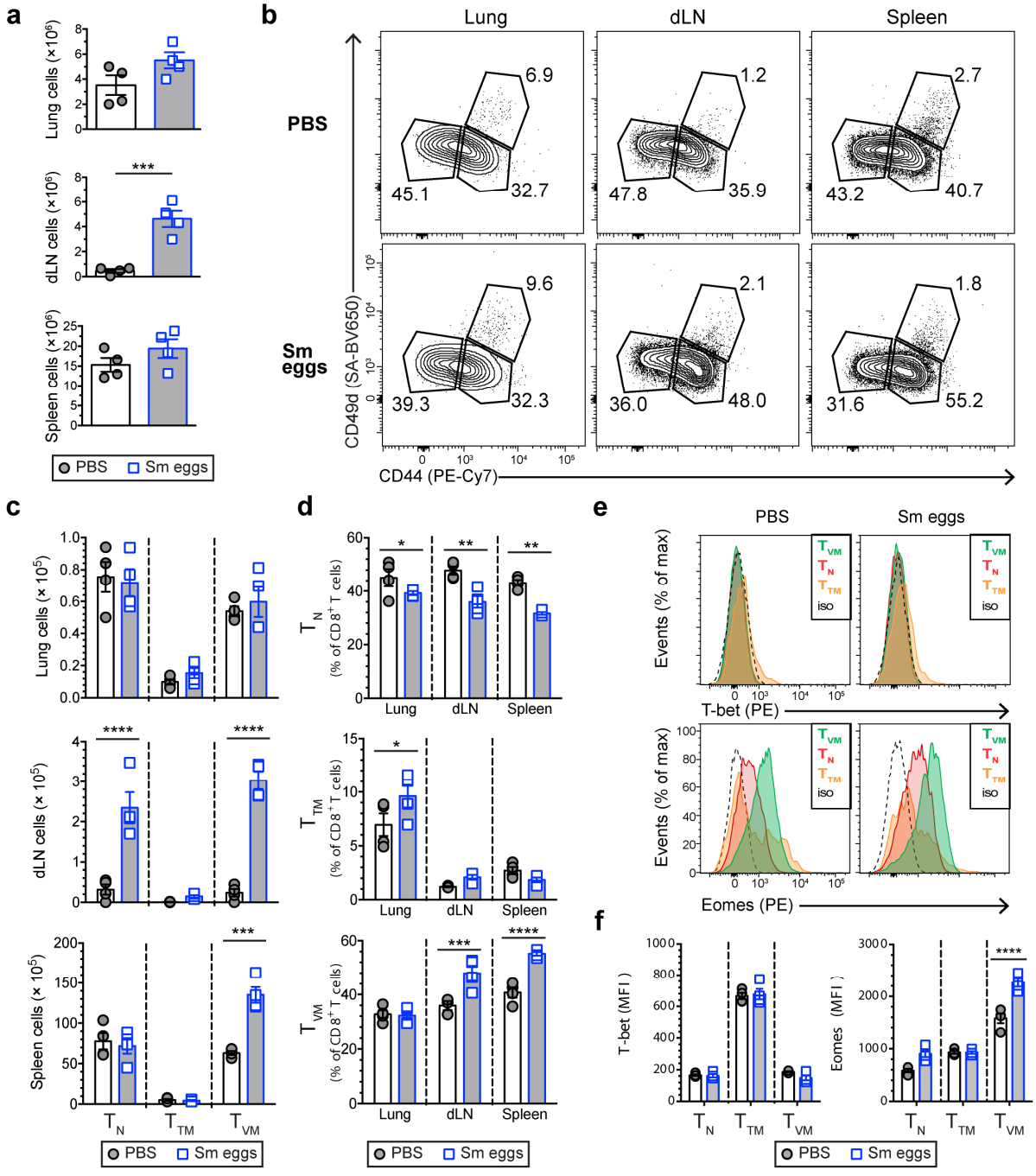

Figure 1. *S. mansoni* eggs induce type 2 inflammation and CD44^{hi}CD49d^{lo} CD8^{+} T cell expansion in the draining LN and spleen.
BALB/c mice were injected with *S. mansoni* (Sm) eggs i.p. and challenged i.v. (5,000/injection) at d14 before analysis at d22 (experimental design outlined in Fig S1a ; gating strategy for flow cytometry analysis outlined in Fig S1e).
(**a**) Absolute cell number at d22 in the indicated tissue.
(**b**) Representative flow cytometry contour plots of gated CD8^{+} T cells from the indicated tissue at d22. Numbers indicate events percent in each gate.
(**c**) Cell number of CD44^{lo} (naive T cells, T_N), CD44^{hi}CD49d^{hi} (true memory T cells, T_{TM}) and CD44^{hi}CD49d^{lo} (virtual memory, T_{VM}) CD8^{+} T cells in the indicated organ at d22, as determined by flow cytometry.
(**d**) Percentage of CD44^{lo} T_N, CD44^{hi}CD49d^{hi} T_{TM} and CD44^{hi}CD49d^{lo} T_{VM} cells in CD8^{+} T cells in the indicated organ at d22, as determined by flow cytometry.
(**e**) Representative flow cytometry histograms of Eomes and T-bet expression of PBS- or Sm egg-treated spleen CD8^{+} T cells populations, as analysed by flow cytometry. Gates were placed on CD44^{lo} T_N, CD44^{hi}CD49d^{hi} T_{TM} and CD44^{hi}CD49d^{lo} T_{VM} cells.
(**f**) Median fluorescence intensities (MFI) of T-bet and Eomes at d22 from the indicated spleen CD8^{+} T cell populations.
Statistical significance calculated using two-way analysis of variance (ANOVA) and Dunnett's (PBS as reference mean) or Sidak's multiple comparison-test (**P < 0.01, ***P < 0.001, ****P < 0.0001).
Data are representative of three independent experiments with 4 mice per group (mean ± s.e.m. in **a, c-d, f**).

Figure 2

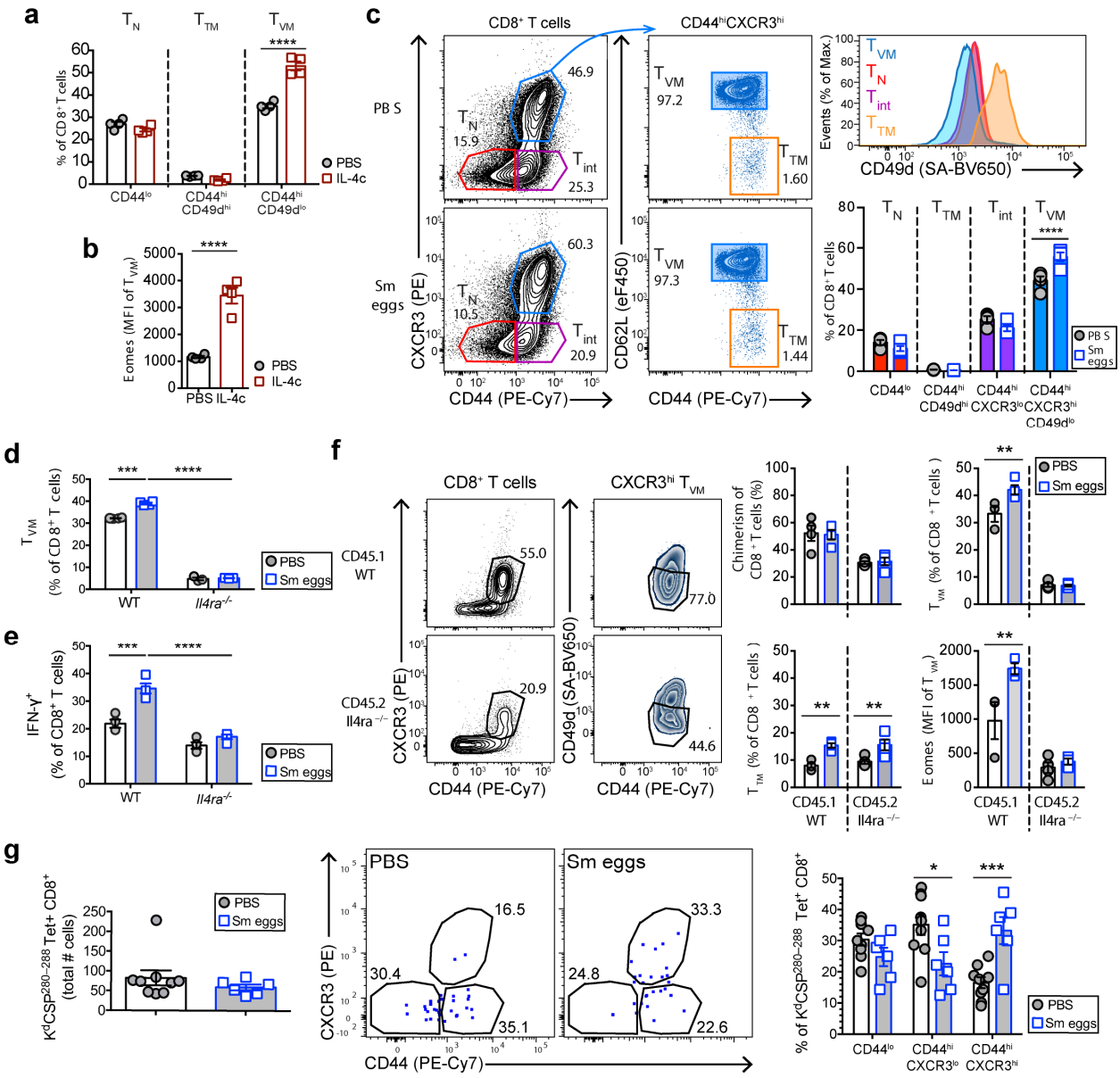
a
b
c
d
e
f
g
PBS
IL-4c
Sm eggs
CD8⁺ T cells
CD44ʰⁱCXCR3ʰⁱ
CXCR3 (PE)
CD62L (eF450)
CD44 (PE-Cy7)
CD49d (SA-BV650)
WT
Il4ra⁻/⁻
CD45.1 WT
CD45.2 Il4ra⁻/⁻
CXCR3ʰⁱ T_VM

Figure 2. IL-4 signaling in CD8$^+$ T cells drives CXCR3^{hi} T_{VM} expansion after *S. mansoni* egg immunization.
(**a-b**) IL-4c were injected to BALB/c mice at d0 and d2 before analysis at d4 (gating strategy outlined in Fig S1e).
(**a**) Percentages of naive T cells (T_N, CD44^{lo}), true memory (T_{TM}, CD44^{hi}CD49d^{hi}) and virtual memory (T_{VM}, CD44^{hi}CD49d^{lo}) cell populations in spleen CD8$^+$ T cells, as determined by flow cytometry.
(**b**) Median fluorescent intensity (MFI) of Eomes in spleen T_{VM} cells, as determined by flow cytometry.
(**c**) BALB/c mice were injected with *S. mansoni* (Sm) eggs i.p. and challenged i.v. (5,000/injection) at d14 before analysis at d22. Representative flow cytometry contour plots gated on CD8$^+$ T cells from the spleen. Gates were placed depending on CD44 and CXCR3 expression to define CD44^{lo}CXCR3^{lo} T_N, CD44^{hi}CXCR3^{lo} T_{int}, CD44^{hi}CXCR3^{hi}CD62L^{lo}CD49d^{hi} T_{TM} and CD44^{hi}CXCR3^{hi}CD62L^{hi}CD49d^{lo} T_{VM} cells and the percentage of each population was graphed. Flow cytometry histogram overlay shows respective CD49d expression in each population.
(**d-e**) WT and *Il4ra*$^{-/-}$ BALB/c mice received one single i.p. injection of *S. mansoni* (Sm) eggs before analysis at d7.
(**d**) Percentages of spleen CD44^{hi}CXCR3^{hi}CD49d^{lo} T_{VM} cells in WT and *Il4ra*$^{-/-}$ mice, as determined by flow cytometry.
(**e**) Percentage of IFN-γ producing splenic CD8$^+$ T cells from WT and *Il4ra*$^{-/-}$ mice following *ex vivo* restimulation with PMA and ionomycin, as determined by flow cytometric analysis.
(**f**) Mixed BM chimeras were generated by introducing WT CD45.1 and *Il4ra*$^{-/-}$ CD45.2 BALB/c donor bone marrow into lethally irradiated WT CD45.1.2 BALB/c hosts. Eight weeks later, chimeric mice were injected with *S. mansoni* (Sm) eggs i.p. and challenged i.v. (5,000/injection) at d14 before analysis at d22. Representative flow cytometry contour plots of both WT and *Il4ra*$^{-/-}$ compartment of the spleen of a Sm egg-treated mice are shown. Percentage of chimerism; percentage of CD44^{hi}CD49d^{hi} T_{TM} and CXCR3^{hi}CD49d^{lo} T_{VM} in CD8$^+$ T cells; median fluorescent intensity (MFI) of Eomes in T_{VM} for both donor populations in spleen are shown.
(**g**) BALB/c mice were injected with *S. mansoni* (Sm) eggs i.p. and challenged i.v. (5,000/injection) at d14 before analysis at d22. Tetramer-based enrichment of *P. yoelii* CSP$^{280\text{-}288}$-specific CD8$^+$ T cells (K^b CSP$^{280\text{-}288}$ tetramer) was performed on pooled spleen and lymph nodes from individual BALB/c mice. Total tetramer$^+$ cells numbers, representative flow cytometry dot plots of tetramer$^+$ cells (numbers indicating mean percent of each gated population) and percentages of the indicated populations from tetramer$^+$ cells in the enriched fraction are shown.
Statistical significance calculated using two-way analysis of variance (ANOVA) and Dunnett's (PBS as reference mean) or Sidak's multiple comparison-test (**$P < 0.01$, ***$P < 0.001$, ****$P < 0.0001$). Data are representative of two to three independent experiments with three to nine mice per group (mean ± s.e.m.).

Figure 3

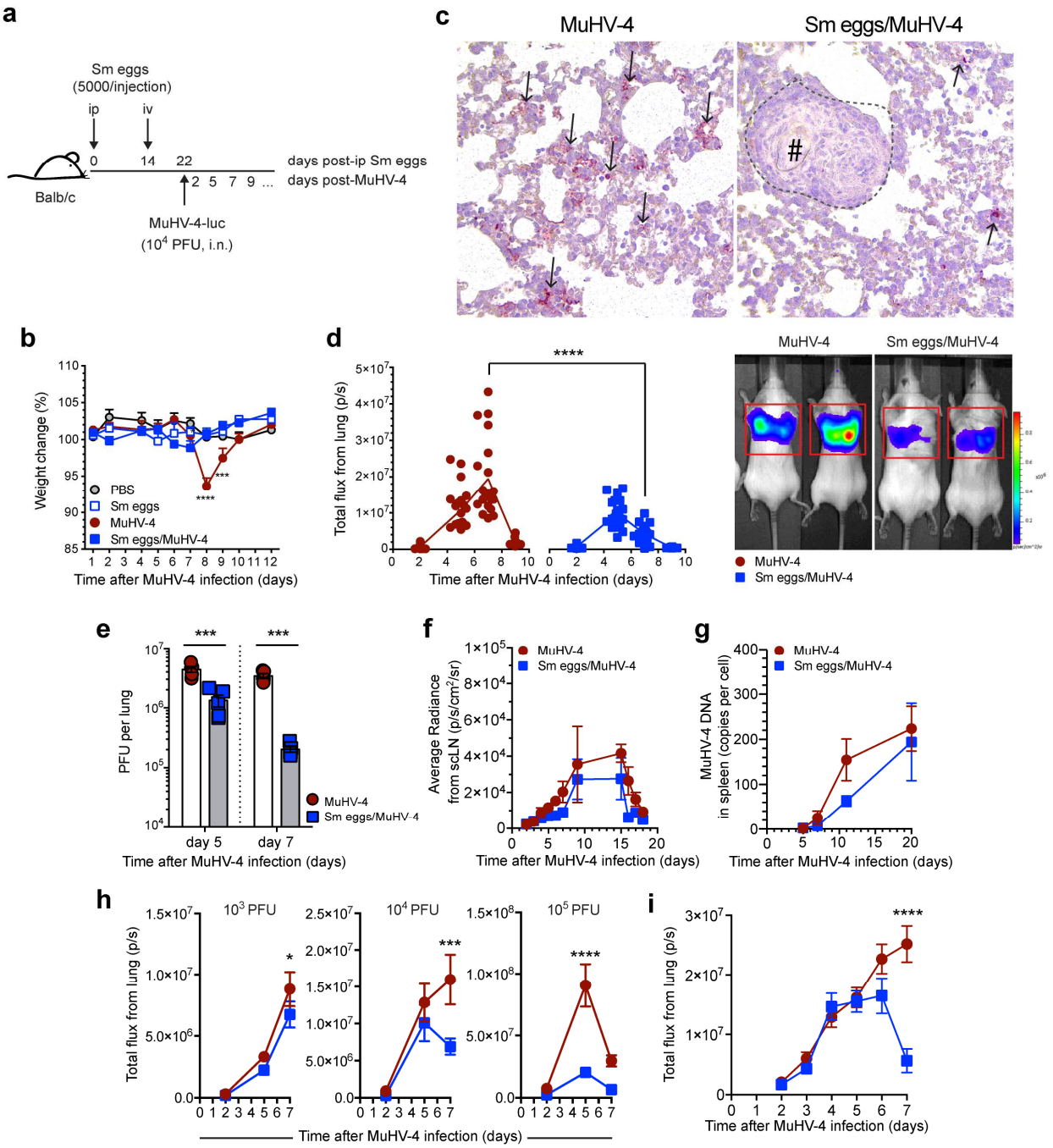
a
Sm eggs
(5000/injection)
ip
iv
0
14
22
days post-ip Sm eggs
2 5 7 9 ...
days post-MuHV-4
Balb/c
MuHV-4-luc
(10^4 PFU, i.n.)
c
MuHV-4
Sm eggs/MuHV-4
#
b
Weight change (%)
PBS
Sm eggs
MuHV-4
Sm eggs/MuHV-4
Time after MuHV-4 infection (days)
d
Total flux from lung (p/s)
****
Time after MuHV-4 infection (days)
MuHV-4
Sm eggs/MuHV-4
e
PFU per lung
***
***
day 5
day 7
MuHV-4
Sm eggs/MuHV-4
Time after MuHV-4 infection (days)
f
Average Radiance from scLN (p/s/cm²/sr)
MuHV-4
Sm eggs/MuHV-4
Time after MuHV-4 infection (days)
g
MuHV-4 DNA in spleen (copies per cell)
MuHV-4
Sm eggs/MuHV-4
Time after MuHV-4 infection (days)
h
10³ PFU
10⁴ PFU
10⁵ PFU
Total flux from lung (p/s)
Time after MuHV-4 infection (days)
i
Total flux from lung (p/s)
****
Time after MuHV-4 infection (days)

Figure 3. *S. mansoni* egg immunization ameliorates the control of MuHV-4 lung infection.
BALB/c mice were injected with *S. mansoni* (Sm) eggs i.p. and challenged i.v. (5,000/injection) at d14. At d22, MuHV-4-luc virus was administered i.n. (**b-g** and **I**: 10^4 PFU per mouse; **h**: 10^3, 10^4 or 10^5 PFU per mouse in 30 µL PBS).
(**a**) Experimental design.
(**b**) Body weight change as percentage of initial weight at d0 of the viral infection.
(**c**) Immunostaining of lung section from MuHV-4-infected cells in a representative PBS- or Sm egg-treated mouse at d7 post-MuHV-4 infection. Arrows indicate positive AEC signal. Dotted line shows boundaries of an egg-centered (#) granuloma.
(**d**) Combined dorsal and ventral measurements by live imaging of thoracic light emission following D-luciferin injection, overtime post-MuHV-4 infection. p/s = photons per second. Representative photographs of bioluminescence signals of two mice per group at d7 post-MuHV-4 infection are shown.
(**e**) Lung viral titers at d7 post-MuHV-4 infection, as determined by plaque assay.
(**f**) Ventral measurements by live imaging of superficial cervical lymph nodes (scLN) region light emission following D-luciferin injection, overtime post-MuHV-4 infection. p/s = photons per second.
(**g**) Splenic MuHV-4 DNA copy numbers overtime post-MuHV-4 infection, as determined by qPCR.
(**h**) Combined dorsal and ventral measurements by live imaging of thoracic light emission following D-luciferin injection, overtime post-MuHV-4 infection with 3 different infectious dose. p/s = photons per second.
(**i**) Combined dorsal and ventral measurements by daily live imaging of thoracic light emission following D-luciferin injection, overtime post-MuHV-4 infection. p/s = photons per second.
Statistical significance calculated using two-way analysis of variance (ANOVA) and Sidak's multiple comparison-test (***P* < 0.01, ****P* < 0.001, *****P* < 0.0001). Data are representative of three independent experiments with five to ten mice per group (mean ± s.e.m. in **b, e-i**).

Figure 4

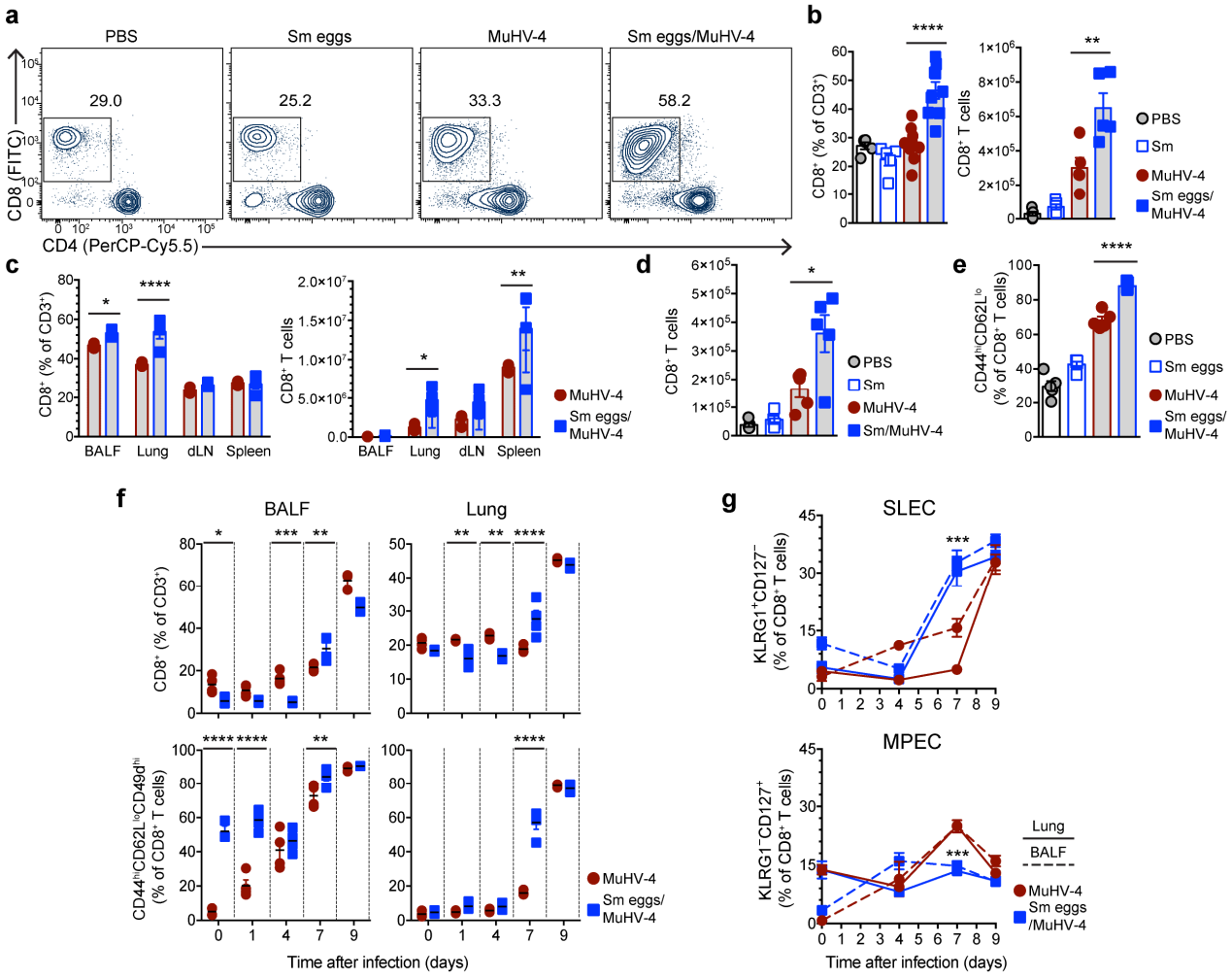
a
PBS
Sm eggs
MuHV-4
Sm eggs/MuHV-4
29.0
25.2
33.3
58.2
CD8 (FITC)
CD4 (PerCP-Cy5.5)
b
CD8+ (% of CD3+)
CD8+ T cells
PBS
Sm
MuHV-4
Sm eggs/ MuHV-4
c
CD8+ (% of CD3+)
CD8+ T cells
BALF
Lung
dLN
Spleen
MuHV-4
Sm eggs/ MuHV-4
d
CD8+ T cells
PBS
Sm
MuHV-4
Sm/MuHV-4
e
CD44hiCD62Llo (% of CD8+ T cells)
PBS
Sm eggs
MuHV-4
Sm eggs/ MuHV-4
f
BALF
Lung
CD8+ (% of CD3+)
CD44hiCD62LloCD49dhi (% of CD8+ T cells)
MuHV-4
Sm eggs/ MuHV-4
Time after infection (days)
g
SLEC
MPEC
KLRG1+CD127- (% of CD8+ T cells)
KLRG1-CD127+ (% of CD8+ T cells)
Lung
BALF
MuHV-4
Sm eggs /MuHV-4
Time after infection (days)

Figure 4. *S. mansoni* egg immunization augments effector/memory CD8$^+$ T cell responses to MuHV-4 infection.
BALB/c mice were injected with *S. mansoni* (Sm) eggs i.p. and challenged i.v. (5,000/injection) at d14 as outlined in Figure 3**a** (**a-c** and **e-g**) or infected with *S. mansoni* cercariae (35 cercariae per mouse, percutaneous infection; **d**) before being infected i.n. with MuHV-4-luc virus at d22 (**a-c** and **e-g**) or d49 (**d**) (10^4PFU per mouse in 30µl of PBS).
(**a**) Representative flow cytometry contour plots of gated lung CD3$^+$ T cells at d7 post-MuHV-4 infection. Gated population and numbers indicates the percentage of CD8$^+$ T cells.
(**b**) Percentage and numbers of lung CD8$^+$ T cells at d7 post-MuHV-4 infection, as determined by flow cytometry.
(**c**) Percentage and numbers of CD8$^+$ T cells at d7 post-MuHV-4 infection in the indicated organs, as determined by flow cytometry.
(**d**) Number of lung CD8$^+$ T cells at d7 post-MuHV-4 infection, of mice previously infected with *S. mansoni* cercariae, as determined by flow cytometry.
(**e**) Percentage of lung effector/memory CD8$^+$ T cells (CD44^{hi}CD62L^{lo}) as determined by flow cytometry.
(**f**) Percentage of broncho-alveolar lavage fluid (BALF) and lung CD8$^+$ T cells and effector/memory (CD44^{hi}CD62L^{lo}CD49d^{hi}) CD8$^+$ T cells at the indicated time points after MuHV-4 infection, as determined by flow cytometry.
(**g**) Percentage of broncho-alveolar lavage fluid (BALF) and lung short-lived (SLEC, KLRG1$^+$CD127$^-$) and memory precursor (MPEC, KLRG1$^-$CD127$^+$) effector CD8$^+$ T cells after MuHV-4 infection.
Statistical significance calculated using two-way analysis of variance (ANOVA) and Sidak's multiple comparison-test (**P < 0.01, ***P < 0.001, ****P < 0.0001). Data are representative of two to three independent experiments with four to five mice per group (mean ± s.e.m. in **b-g**).

Figure 5

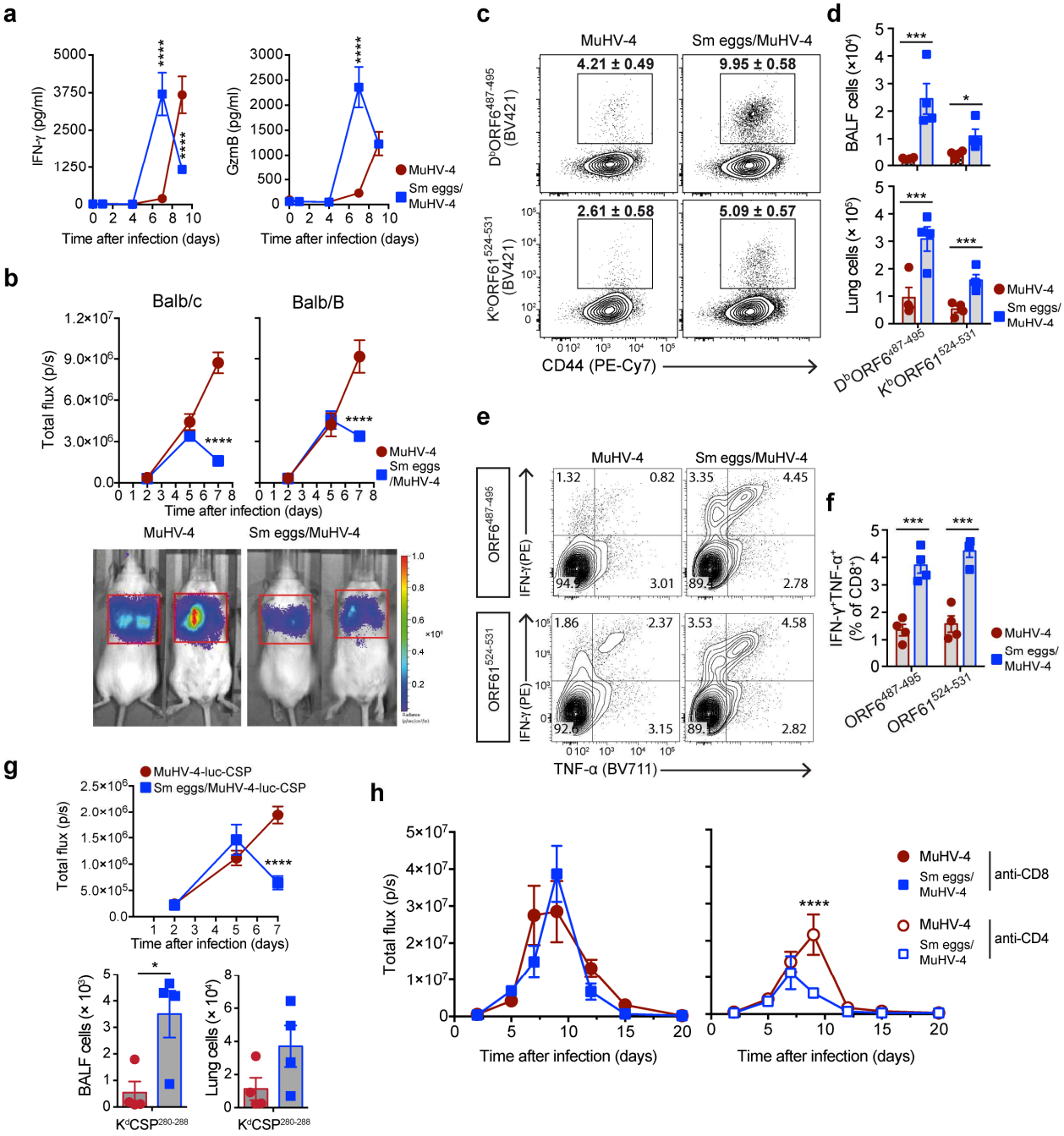
a
IFN-γ (pg/ml)
GzmB (pg/ml)
Time after infection (days)
MuHV-4
Sm eggs/ MuHV-4
b
Balb/c
Balb/B
Total flux (p/s)
Time after infection (days)
MuHV-4
Sm eggs /MuHV-4
Sm eggs/MuHV-4
c
MuHV-4
Sm eggs/MuHV-4
4.21 ± 0.49
9.95 ± 0.58
2.61 ± 0.58
5.09 ± 0.57
CD44 (PE-Cy7)
d
BALF cells (×10⁴)
Lung cells (× 10⁵)
e
1.32
0.82
3.35
4.45
94.9
3.01
89.2
2.78
1.86
2.37
3.53
4.58
92.6
3.15
89.1
2.82
IFN-γ(PE)
TNF-α (BV711)
f
IFN-γ⁺TNF-α⁺ (% of CD8⁺)
g
MuHV-4-luc-CSP
Sm eggs/MuHV-4-luc-CSP
BALF cells (× 10⁵)
Lung cells (× 10⁴)
h
anti-CD8
anti-CD4

Figure 5. *S. mansoni* immunization augments specific anti-viral CD8$^+$ T cell responses to control lytic MuHV-4 infection.

BALB/c (**a**, **b**, **g** and **h**) or BALB/B (**b-f**) mice were injected with *S. mansoni* (Sm) eggs i.p. and challenged i.v. (5,000/injection) at d14 before being infected i.n. with MuHV-4-luc (**a-f**, **h**) or MuHV-4-luc-CSP (**g**) virus at d22 (10^4PFU per mouse in 30µl of PBS) as outlined in Figure 3**a**.

(**a**) IFN-γ and GzmB concentrations in the BALF overtime after MuHV-4 infection, as determined by ELISA.

(**b**) Combined dorsal and ventral measurements by live imaging of thoracic light emission following D-luciferin injection, of BALB/c and BALB/b mice, overtime post-MuHV-4 infection. p/s = photons per second. Representative photographs of bioluminescence signals of two mice per group at d7 post-MuHV-4 infection are shown.

(**c**) Representative flow cytometry contour plots of $D^bORF6^{487-495}$ and $K^bORF61^{524-531}$ MuHV-4-specific tetramer stainings of lung CD8$^+$ T cells, at d7 post-MuHV-4 infection. Numbers in gate indicate percentage of tetramer-positive in CD8$^+$ T cells. Mean ± s.e.m. are shown.

(**d**) Number of tetramer$^+$ ($D^bORF6^{487-495}$ or $K^bORF61^{524-531}$) MuHV-4-specific CD8$^+$ T cells in the broncho-alveolar lavage fluid (BALF) and lung at d7 post-MuHV-4 infection, based on flow cytometry analysis as in **c**.

(**e**) Representative flow cytometry contour plots of gated lung CD8$^+$ T cells at day 7 post-MuHV-4 infection showing IFN-γ and TNF-α production following *ex vivo* MuHV-4 $ORF6^{487-495}$ or $ORF61^{524-531}$ peptide restimulation. Numbers indicate percentage in each quadrant.

(**f**) Percentage of IFN-γ and TNF-α co-producing lung CD8$^+$ T cells after MuHV-4 $ORF6^{487-495}$ or $ORF61^{524-531}$ peptide *ex vivo* restimulation, determined by flow cytometry analysis as in **e**.

(**g**) Combined dorsal and ventral measurements by live imaging of thoracic light emission following D-luciferin injection, overtime post-MuHV-4-luc-CSP infection and number of tetramer$^+$ ($K^dCSP^{280-288}$) CD8$^+$ T cells in the broncho-alveoler lavage fluid (BALF) and lung at d7 post-MuHV-4 infection. p/s = photons per second.

(**h**) Anti-CD8 (YTS-169.4) or anti-CD4 (GK1.5) antibodies were injected i.p. at d-1, d1 and d4 after MuHV-4 infection. Combined dorsal and ventral measurements by live imaging of thoracic light emission following D-luciferin injection, overtime post-MuHV-4 infection. p/s = photons per second.

Statistical significance calculated using two-way analysis of variance (ANOVA) and Sidak's multiple comparison-test (*$P < 0.05$, **$P < 0.01$, ***$P < 0.001$, ****$P < 0.0001$). Data are representative of two independent experiments with four to five mice per group (mean ± s.e.m. in **a, b, d-h**).

Figure 6

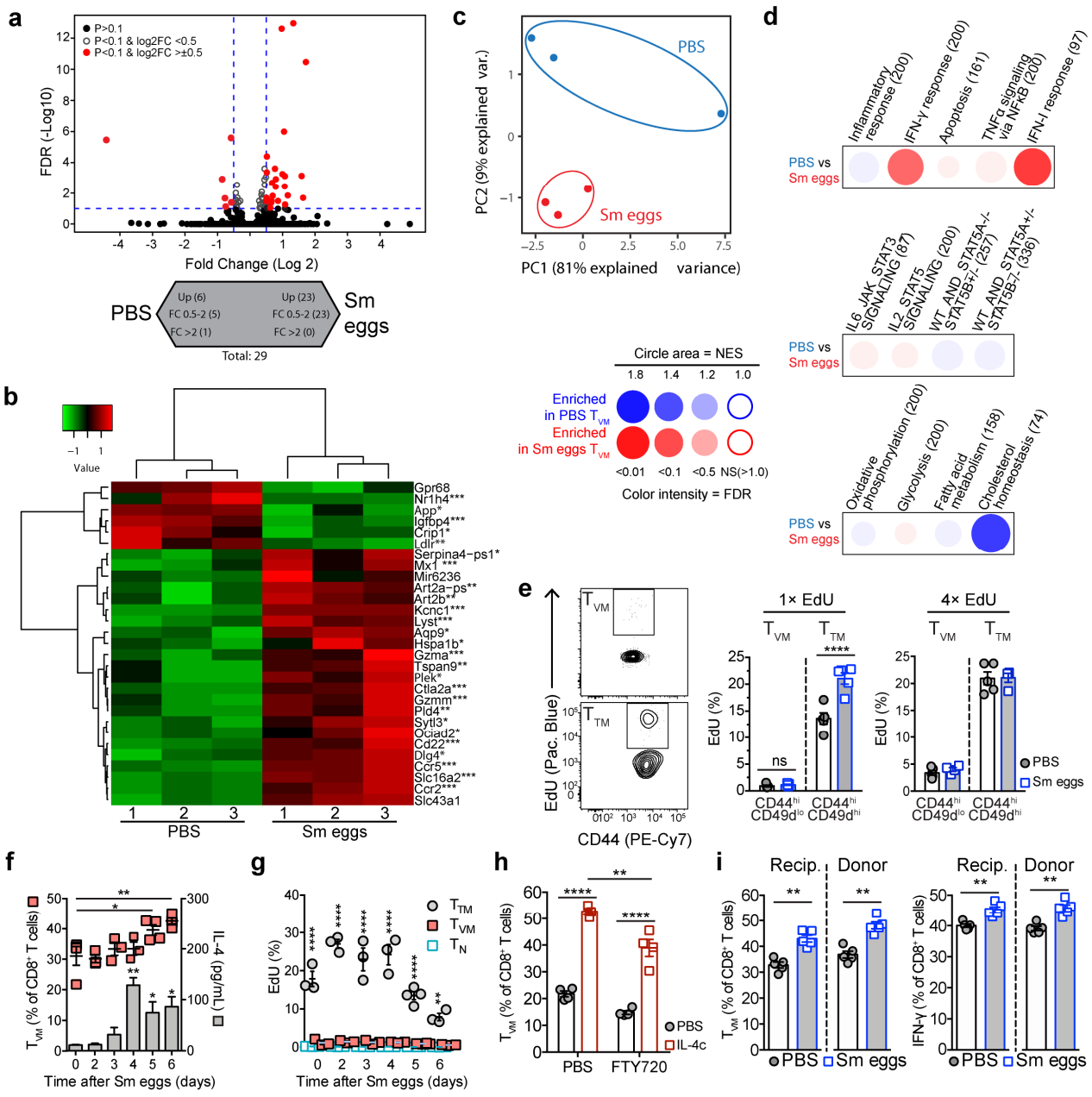
a
P>0.1
P<0.1 & log2FC <0.5
P<0.1 & log2FC >±0.5
FDR (-Log10)
Fold Change (Log 2)
PBS
Sm eggs
Up (6)
FC 0.5-2 (5)
FC >2 (1)
Up (23)
FC 0.5-2 (23)
FC >2 (0)
Total: 29
b
Value
Gpr68
Nr1h4***
App*
Igfbp4***
Crip1*
Ldlr**
Serpina4-ps1*
Mx1***
Mir6236
Art2a-ps**
Art2b**
Kcnc1***
Lyst***
Aqp9*
Hspa1b*
Gzma***
Tspan9**
Plek*
Ctla2a***
Gzmm***
Pld4**
Sytl3*
Ociad2*
Cd22***
Dlg4*
Ccr5***
Slc16a2***
Ccr2***
Slc43a1
PBS
Sm eggs
c
PC2 (9% explained var.)
PC1 (81% explained variance)
PBS
Sm eggs
Circle area = NES
Enriched in PBS TVM
Enriched in Sm eggs TVM
Color intensity = FDR
d
Inflammatory response (200)
IFN-γ response (200)
Apoptosis (161)
TNFα signaling via NFκB (200)
IFN-I response (97)
IL6 JAK STAT3 SIGNALING (87)
IL2 STAT5 SIGNALING (200)
WT AND STAT5A-/- STAT5B+/- (257)
WT AND STAT5A+/- STAT5B-/- (336)
Oxidative phosphorylation (200)
Glycolysis (200)
Fatty acid metabolism (158)
Cholesterol homeostasis (74)
PBS vs Sm eggs
e
EdU (Pac. Blue)
CD44 (PE-Cy7)
1× EdU
4× EdU
EdU (%)
ns
PBS
Sm eggs
f
TVM (% of CD8+ T cells)
IL-4 (pg/mL)
Time after Sm eggs (days)
g
EdU (%)
TTM
TVM
TN
Time after Sm eggs (days)
h
TVM (% of CD8+ T cells)
PBS
IL-4c
PBS
FTY720
i
Recip.
Donor
TVM (% of CD8+ T cells)
IFN-γ (% of CD8+ T cells)
PBS
Sm eggs

Figure 6. Phenotypic changes in helminth-driven T_{VM} cells.
(**a-d**) BALB/c mice were injected with *S. mansoni* (Sm) eggs i.p. and challenged i.v. (5,000/injection) at d14 before analysis at d22 (experimental design outlined in Fig S1a). Transcriptomics analysis was realized on FACS sorted spleen T_{VM}.
(**a**) Summary of differentially expressed (DE) genes (P<0.1) showing DE genes in red in volcano plot, showing the total number of DE genes outside the bidirectional arrows, and showing in the arrowheads the direction of upregulated expression for all, moderately (log 2-fold change ± 0.5-2) and highly (log 2-fold change > 2) DE genes.
(**b**) Heatmap of DE genes (P<0.1, change in expression of over 1.5-fold). Left margin shows hierarchical clustering and right annotation indicate gene symbols.
(**c**) Principal component analysis.
(**d**) Enrichment for transcriptomic fingerprints for selected hallmark gene sets from the MSigDB by gene-set-enrichment analysis with BubbleGUM software. WT_AND_STAT5A-/-_STAT5B+/- and WT_AND_STAT5A-/-_STAT5B+/- gene-sets were obtained from published data(Villarino et al., 2016). Key color indicates cell subset showing enrichment for the gene set, and size of symbols and color intensity indicate significance of enrichment (surface area proportional to absolute value of the normalized enrichment score (NES); color intensity indicates the false-discovery rate (FDR)). Numbers in parentheses (above) indicate number of genes). NS, not significant.
(**e**) BALB/c mice were injected with *S. mansoni* (Sm) eggs i.p. and challenged i.v. (5,000/injection) at d14 before analysis at d22 (experimental design outlined in Fig S1a). Mice were injected i.p. with EdU 4h before harvest (1× EdU) or at d18, 19, 20 and 21 after Sm egg i.p. injection (4× EdU). Representative flow cytometry contour plot showing EdU incorporation in spleen $CXCR3^{hi}CD49d^{lo}$ T_{VM} and $CD49d^{hi}$ T_{TM} cells and bar plot showing percentage of EdU^+ cells from each population.
(**f,g**) BALB/c mice received one single i.p. injection with *S. mansoni* (Sm) eggs (5,000 per injection, i.p.).
(**f**) Percentages of T_{VM} cells in the spleen, as determined by flow cytometry, and IL-4 levels in supernatant after SEA *ex vivo* restimulation of splenocytes as determined by ELISA, at the indicated time points post-Sm egg i.p. injection.
(**g**) Mice were injected i.p. with EdU 4h before harvest. Percentage of EdU^+ T_{TM}, T_{VM}, or T_N cells in the spleen at the indicated time points post-Sm egg i.p. injection, as determined by flow cytometry.
(**h**) IL-4c were injected at d0 and d2 and FTY720 was injected daily from d0 to BALB/c mice, before analysis at d4. Percentages of T_{VM} cells in the spleen as determined by flow cytometry.
(**i**) Spleen $CD8^+$ T cells were adoptively transferred to congenic mice on d-1 before a single injection of Sm eggs (5,000/injection, i.p.) on d0 and analysis on d7. Percentages of spleen T_{VM} cells and IFN-γ-producing $CD8^+$ T cells upon *ex vivo* restimulation with PMA and ionomycin of splenocytes are shown in recipient and donor cells.
Statistical significance calculated using two-way analysis of variance (ANOVA) and Sidak's multiple comparison-test (*P < 0.05, **P < 0.01, ***P < 0.001, ****P < 0.0001). Data are representative of two independent experiments with three to five mice per group (mean ± s.e.m. in **e,f**).

Figure 7

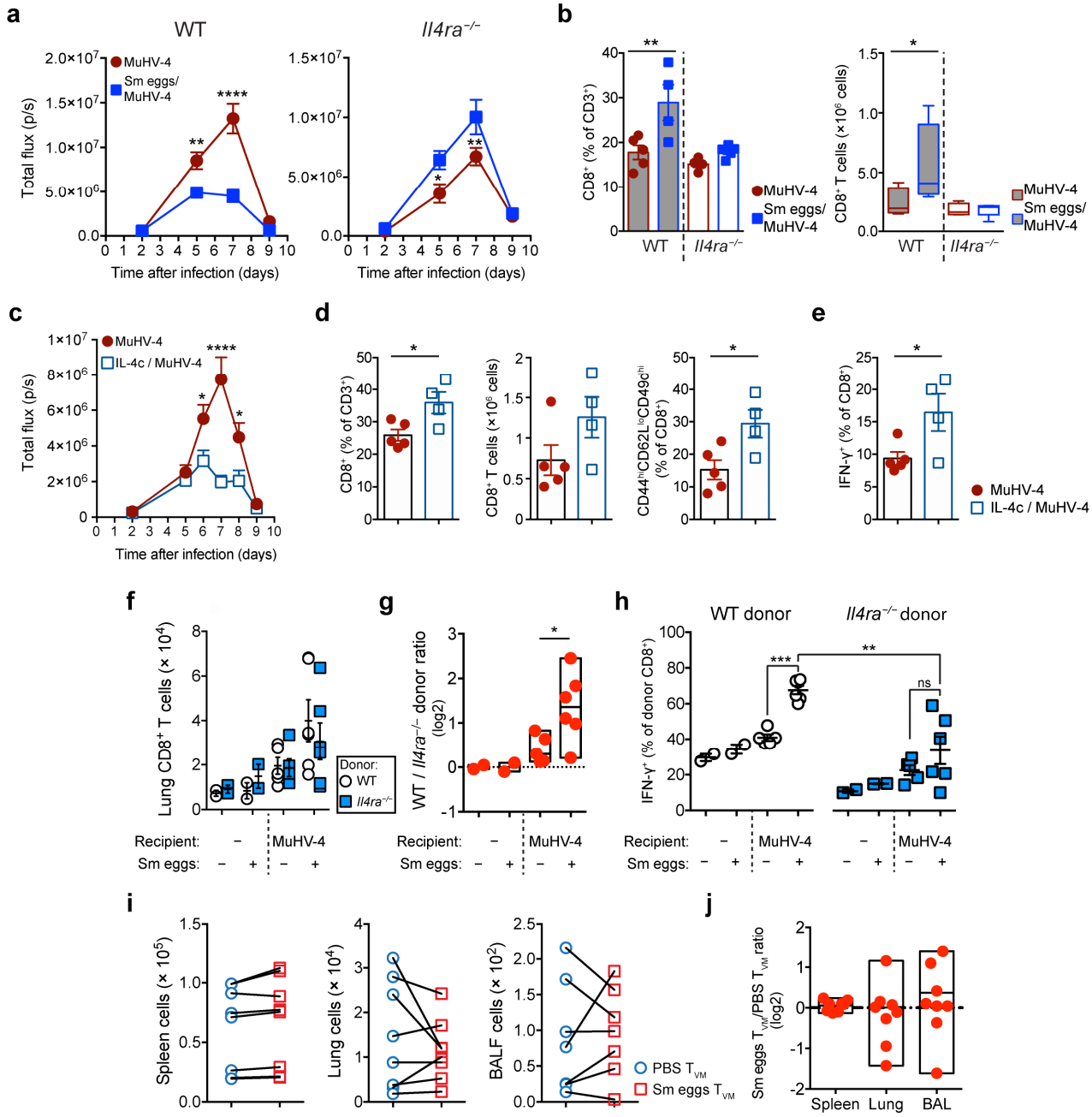
a
WT
Il4ra−/−
MuHV-4
Sm eggs/ MuHV-4
Total flux (p/s)
Time after infection (days)
b
CD8+ (% of CD3+)
CD8+ T cells (×10^6 cells)
MuHV-4
Sm eggs/ MuHV-4
c
IL-4c / MuHV-4
d
CD44hiCD62LloCD49ehi (% of CD8+)
e
IFN-γ+ (% of CD8+)
f
Lung CD8+ T cells (× 10^4)
Donor: WT Il4ra−/−
Recipient:
Sm eggs:
g
WT / Il4ra−/− donor ratio (log2)
h
WT donor
Il4ra−/− donor
IFN-γ+ (% of donor CD8+)
ns
i
Spleen cells (× 10^5)
Lung cells (× 10^4)
BALF cells (× 10^2)
PBS TVM
Sm eggs TVM
j
Sm eggs TVM/PBS TVM ratio (log2)
Spleen
Lung
BAL

Figure 7. Helminth-induced IL-4 conditions CD8$^+$ T cells for early control of MuHV-4 infection.
(**a,b**) WT or *Il4ra*$^{-/-}$ BALB/c mice were injected with *S. mansoni* (Sm) eggs i.p. and challenged i.v. (5,000/injection) at d14. At d22, MuHV-4-luc virus was administered i.n. (10^4PFU per mouse in 30µl of PBS).
(**a**) Combined dorsal and ventral measurements by live imaging of thoracic light emission following D-luciferin injection, overtime post-MuHV-4 infection. p/s = photons per second.
(**b**) Percentage and numbers of lung CD8$^+$ T cells at d7 post-MuHV-4 infection, as determined by flow cytometry.
(**c-e**) BALB/c mice were injected i.p. with IL-4c at d0 and d2 and infected with MuHV-4-luc at d4 (10^4PFU per mouse in 30µl of PBS).
(**c**) Combined dorsal and ventral measurements by live imaging of thoracic light emission following D-luciferin injection, overtime post-MuHV-4 infection. p/s = photons per second.
(**d**) Percentage and numbers of lung CD8$^+$ T cells and proportions of lung CD44^{hi}CD62L^{lo}CD49d^{hi} effector CD8$^+$ T cells at d7 post-MuHV-4 infection, as determined by flow cytometry.
(**e**) Percentage of IFN-γ producing lung CD8$^+$ T cells after *ex vivo* estimulation with PMA and ionomycin at d7 post-MuHV-4 infection, as determined by flow cytometry.
(**f-h**) BALB/c mice were injected with *S. mansoni* (Sm) eggs i.p. and challenged i.v. (5,000/injection) at d14. At d22, CD8$^+$ T cells were enriched by negative magnetic selection from spleen of WT CD45.1 or *Il4ra*$^{-/-}$ CD45.2 mice treated with PBS or Sm eggs before co-transfer in PBS- or Sm egg-treated congenic CD45.1.2 WT recipient mice, followed by MuHV-4-luc i.n. infection (10^4PFU per mouse in 30µl of PBS) as outlined in Figure S7b.
(**f**) Numbers of donor cells from each origin recovered from lungs at d7 post-MuHV-4 infection, as determined by flow cytometry.
(**g**) Ratio of WT over *Il4ra*$^{-/-}$ donor cells in lungs at d7 post-MuHV-4 infection, normalized on uninfected control group (PBS or Sm egg-treated uninfected mice respectively for PBS or Sm egg-treated MuHV-4 infected mice), as determined by flow cytometry.
(**h**) Percentage of IFN-γ producing donor CD8$^+$ T cells following *ex vivo* restimulation with PMA and ionomycin as determined by flow cytometry.
(**i-j**) BALB/c mice were injected with *S. mansoni* (Sm) eggs i.p. and challenged i.v. (5,000/injection) at d14. At d22, CD44^{hi}CXCR3^{hi}CD62L^{hi}CD49d^{lo} T_{VM} cells were FACS-sorted from spleen of PBS-treated BALB/c CD45.1.2 and Sm egg-treated CD45.1 mice, and equal numbers of cells were co-transferred into naive CD45.2 recipients. 1 d after adoptive transfer, recipients were infected i.n. with MuHV-4-luc (10^4PFU per mouse in 30µl of PBS).
(**i**) Total numbers of donor cells of both origins recovered from spleen, lung and BALF at d7 post-MuHV-4 infection, as determined by flow cytometry. Data from the same mice are connected.
(**j**) Ratio of T_{VM} originated from Sm egg-exposed mice (CD45.1) over T_{VM} originated from PBS-injected mice (CD45.1.2) in the indicated organs at d7 post-MuHV-4 infection, as determined in i.
Statistical significance calculated using two-way analysis of variance (ANOVA) and Sidak's multiple comparison-test (*$P < 0.05$, **$P < 0.01$, ***$P < 0.001$, ****$P < 0.0001$). Data are representative of two to three independent experiments with three to eight mice per group (mean ± s.e.m. in **a-f,h**). Each symbol represents an individual mouse; small horizontal lines indicate the mean.

Supplemental figures

Figure S1

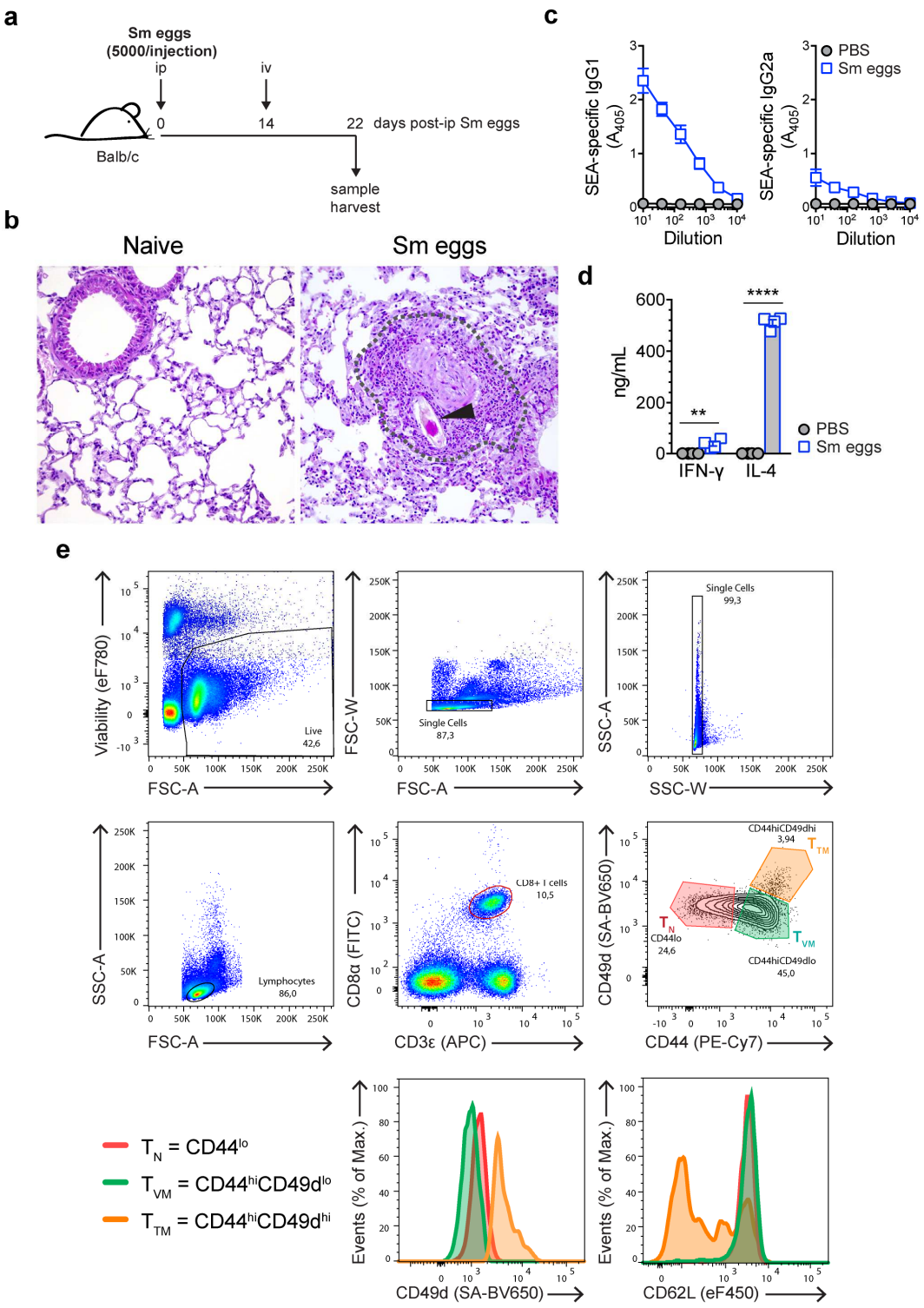

Figure S1. *S. mansoni* egg treatment and gating strategy
BALB/c mice were injected with *S. mansoni* (Sm) eggs i.p. and challenged i.v. (5,000/injection) at d14 before analysis at d22
(**a**) Experimental design.
(**b**) H&E staining of lung section with representative eosinophilic granuloma. Arrows show *S. mansoni* egg and dotted line the boundaries of the granuloma.
(**c**) Antibody ELISA for detection of serum SEA-specific IgG1 and IgG2a.
(**d**) IFN-γ and IL-4 levels in the supernatant after 72h of SEA *ex vivo* restimulation of mediastinal LN cells (20µg/mL), as determined by ELISA.
(**e**) Gating strategy for flow cytometric analysis of memory $CD8^+$ T cell responses

Figure S2

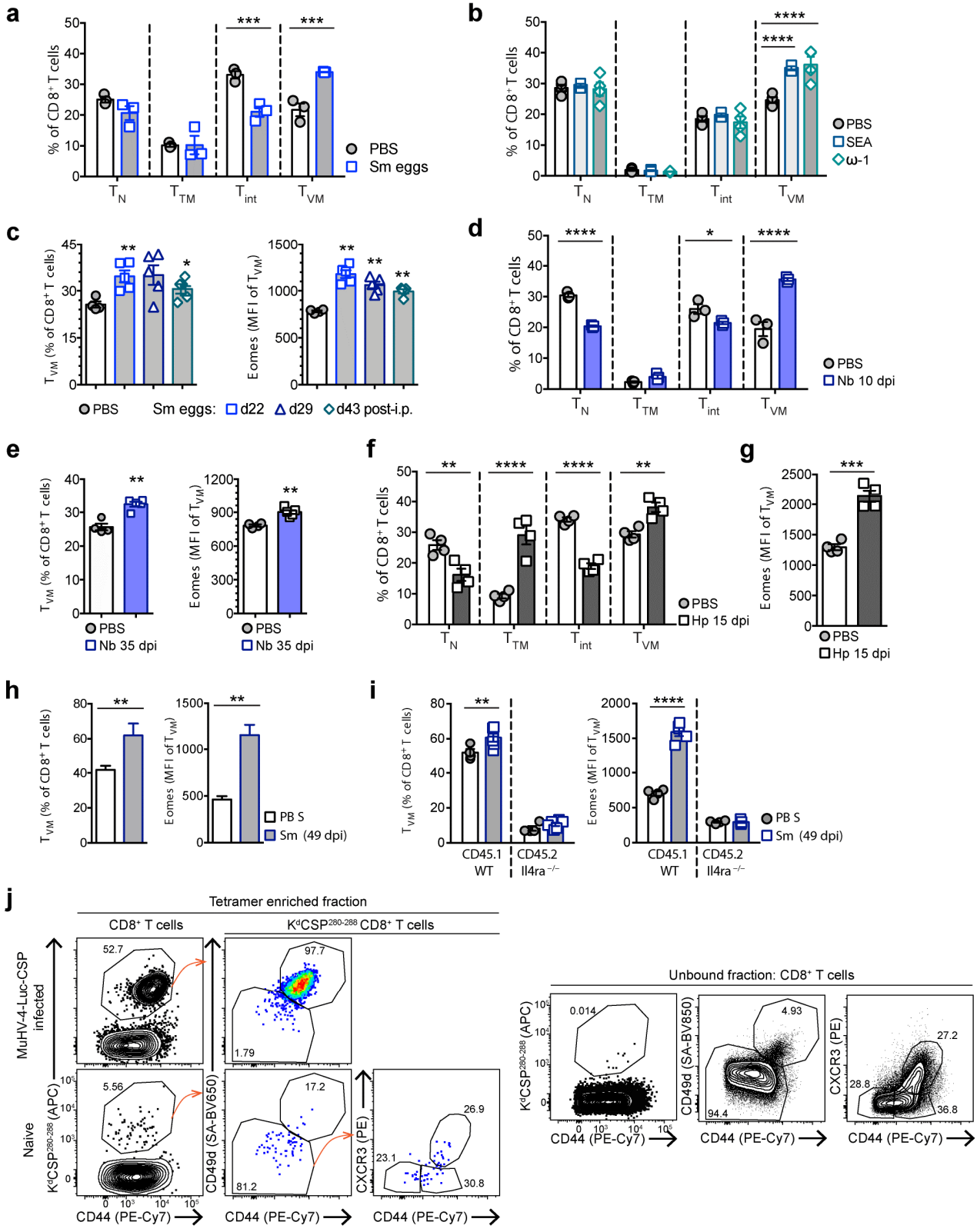
a
% of CD 8+ T cells
PBS
Sm eggs
b
PBS
SEA
ω-1
c
PBS
Sm eggs: d22 d29 d43 post-i.p.
d
PBS
Nb 10 dpi
e
PBS
Nb 35 dpi
f
PBS
Hp 15 dpi
g
PBS
Hp 15 dpi
h
PB S
Sm (49 dpi)
i
CD45.1 WT
CD45.2 Il4ra−/−
PB S
Sm (49 dpi)
j
Tetramer enriched fraction
CD8+ T cells
KdCSP280-288 CD8+ T cells
MuHV-4-Luc-CSP infected
Naive
CD44 (PE-Cy7)
CD49d (SA-BV650)
CXCR3 (PE)
Unbound fraction: CD8+ T cells

Figure S2. Induction of T_{VM} in response to helminth antigens or helminth infection.
(**a-i**) Analysis of spleen $CD8^+$ T cell populationby flow cytometry after different treatments, as gated in Figure 2c : naïve $CD8^+$ T cells (T_N $CD44^{lo}CXCR3^{lo}$), true memory (T_{TM}, $CD44^{hi}CD62L^{lo}CD49d^{hi}$), intermediate memory ($T_{Int}$, $CD44^{hi}CXCR3^{lo}$) and virtual memory (T_{VM}, $CD44^{hi}CXCR3^{hi}CD62L^{hi}CD49d^{lo}$).
(**a**) *S. mansoni* eggs (5,000 per injection) were injected to BALB/c mice i.p. at d0 and d14 and analyses performed at d22.
(**b**) *S. mansoni* soluble egg antigens (SEA) and omega-1 (ω-1) were injected i.p. at d0 and d14 and analysis performed at d22.
(**c**) *S. mansoni* eggs (5,000 per injection) were injected i.p. at d0 and i.v. at d14 (as in Fig. S1a) and analysis performed at d22, 29 or 43 for spleen T_{VM} ($CD44^{hi}CXCR3^{hi}CD62L^{hi}CD49d^{lo}$) and Eomes median fluorescence intensity (MFI) in T_{VM} cells.
(**d**) Mice were infected with *N. brasiliensis* (Nb, 500xL3 s.c.) and analysis performed at d10 post-infection (dpi).
(**e**) Mice were infected with *N. brasiliensis* (Nb, 500xL3 s.c.) and analysis performed at d35 post-infection (dpi) for spleen T_{VM} ($CD44^{hi}CXCR3^{hi}CD62L^{hi}CD49d^{lo}$) and Eomes median fluorescence intensity (MFI) in T_{VM}.
(**f**) Mice were infected with *H. polygyrus bakeri* (Hp, 200xL3, per os) and analysis performed at 15 dpi.
(**g**) Median fluorescence intensity (MFI) of Eomes in T_{VM} cells at 15 dpi with *H. polygyrus*.
(**h**) Mice were infected with *S. mansoni* (35 cercariae, percutaneous infection) and analysis performed at 49dpi for $CXCR3^{hi}$ T_{VM} and Eomes median fluorescence intensity (MFI) in T_{VM} cells.
(**i**) Mixed bone marrow chimeras were generated by introducing WT CD45.1 and *Il4ra*$^{-/-}$ CD45.2 BALB/c donor bone marrow cells into lethally irradiated CD45.1.2 BALB/c hosts. Chimeric mice were infected with *S. mansoni* (35 cercariae, percutaneous infection) 8 weeks later and analysis performed at 49 dpi. Percentage of $CXCR3^{hi}$ T_{VM} and Eomes median fluorescence intensity (MFI) in T_{VM} cells for both donor populations are shown.
(**j**) BALB/c mice were infected i.n. with MuHV-4-luc-CSP (10^4PFU per mouse in 30µl of PBS). Tetramer-based enrichment of *P. yoelii* $CSP^{280-288}$-specific $CD8^+$ T cells (K^b $CSP^{280-288}$ tetramer) was performed on pooled spleen and lymph nodes from individual BALB/c mice at d7 post-MuHV-4 infection. Flow cytometry gating strategy to analyze $CD8^+$ T cells populations in K^d-$CSP^{280-288}$ $tetramer^+$ cells is shown.
Statistical significance calculated using unpaired two-tailed Student's *t* test (c, e, g, h) or two-way analysis of variance (ANOVA) and Sidak's multiple-comparison test (**P<0.01, ***P<0.001, ****P<0.0001). Data are representative of two to three independent experiments with three to five mice per group (mean +- s.e.m. in a-g)

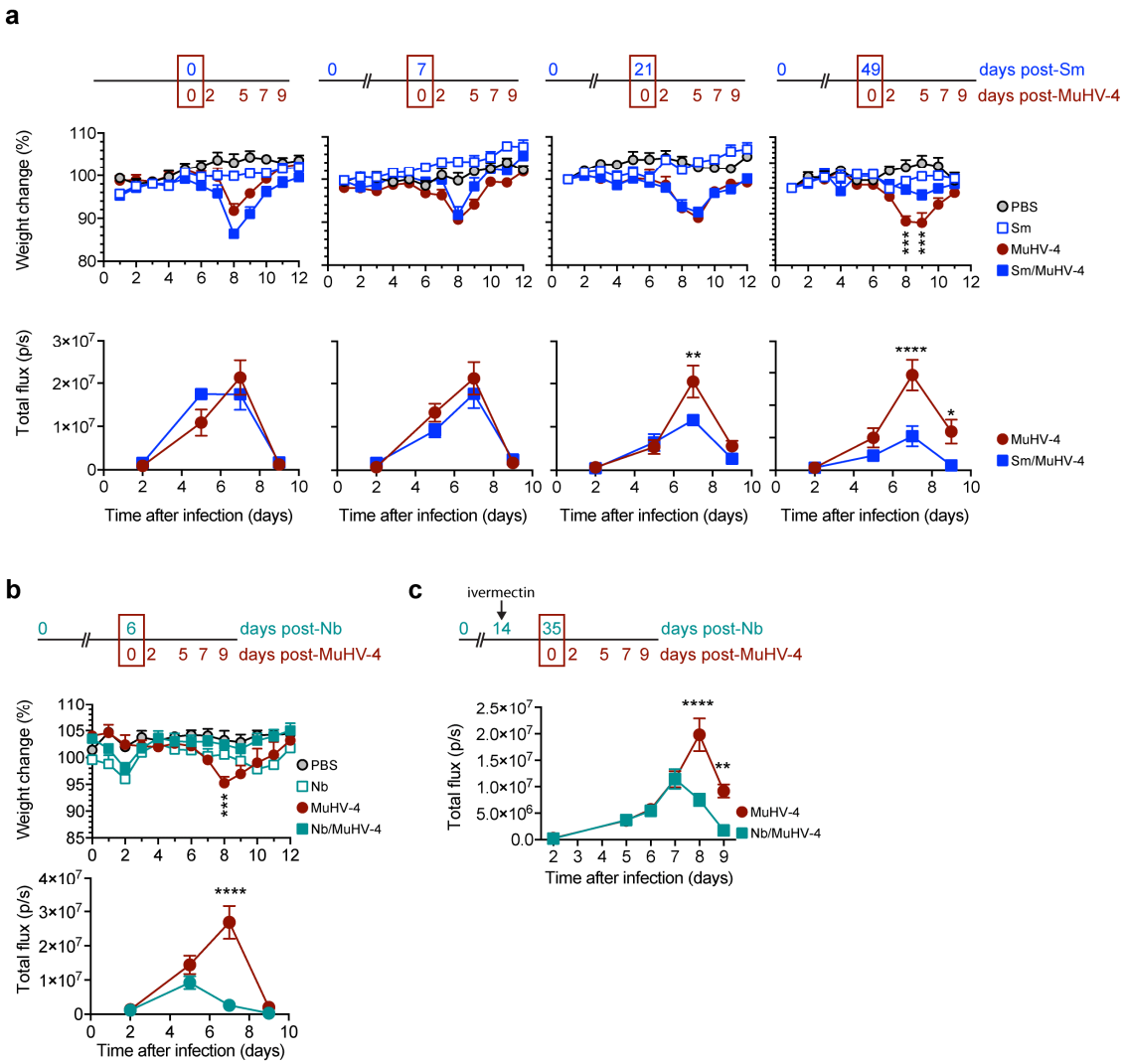

Figure S3. Helminth infections ameliorates the control of MuHV-4 lung infection.
(**a**) BALB/c mice were infected with *S. mansoni* (Sm, 35 cercariae, percutaneous infection) before being infected with MuHV-4-luc virus (10^4 PFU per mouse in 30 µL PBS i.n.) at the indicated time points after Sm infection. Experimental designs (top), body weight changes after viral infection (middle) and combined dorsal and ventral measurements by live imaging of thoracic light emission following D-luciferin injection (bottom) are shown.
(**b**) BALB/c mice were infected with *N. brasiliensis* (Nb, 500xL3, s.c.) before being infected with MuHV-4-luc virus (10^4 PFU per mouse in 30 µL PBS i.n.) after 6 days of Nb infection. Experimental design (top), body weight change after viral infection (middle) and combined dorsal and ventral measurements by live imaging of thoracic light emission following D-luciferin injection (bottom) are shown.
(**c**) BALB/c mice were infected with *N. brasiliensis* (Nb, 500xL3, s.c.), treated with ivermectin between 14 and 21 dpi before being infected with MuHV-4-luc virus (10^4 PFU per mouse in 30 µL PBS i.n.) 35 days after Nb infection. Experimental design (top) and combined dorsal and ventral measurements by live imaging of thoracic light emission following D-luciferin injection (bottom) are shown.
p/s = photon per second
Statistical significance calculated using two-way analysis of variance (ANOVA) and Sidak's multiple-comparison test (*P<0.05, **P<0.01, ***P<0.001, ****P<0.0001). Data are representative of two to three independent experiments with three to five mice per group (mean +- s.e.m.).

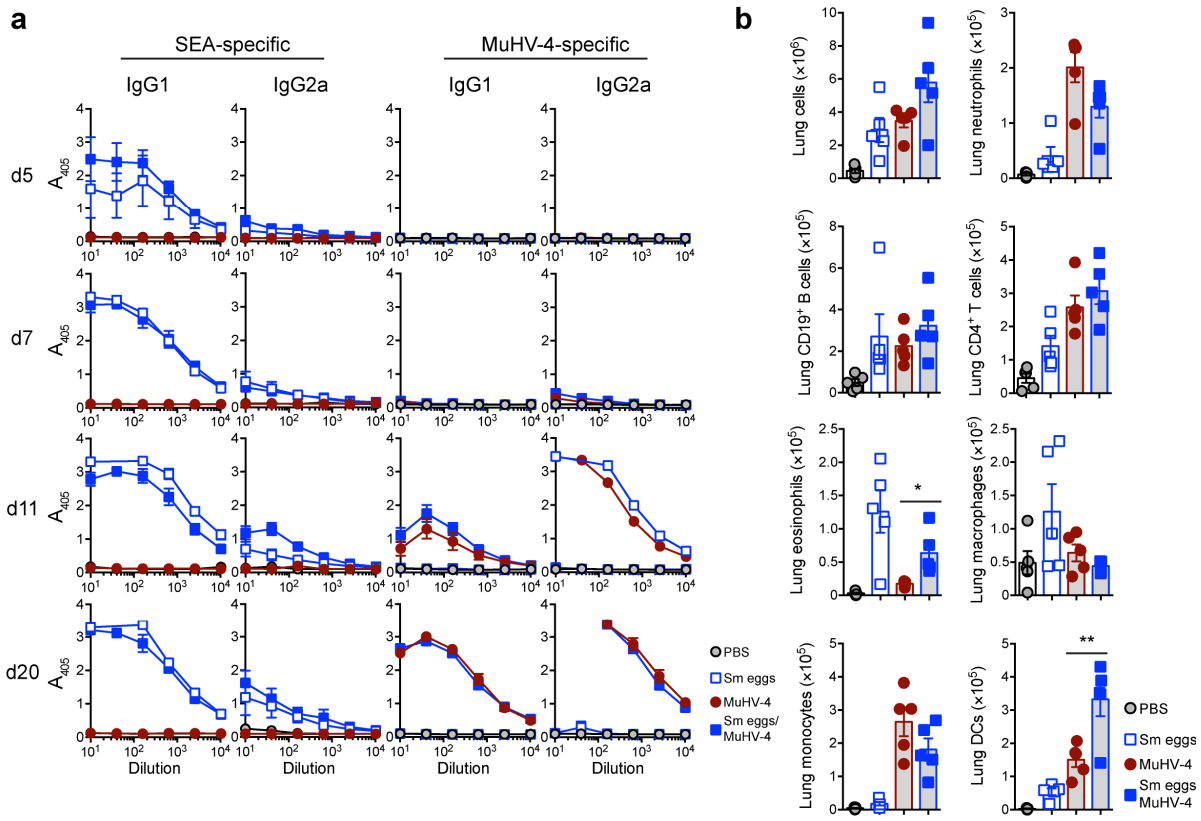

Figure S4. Antibody and lung cell responses.
BALB/c mice were injected with *S. mansoni* (Sm) eggs i.p. and challenged i.v. (5,000/injection) at d14 before being infected i.n. with MuHV-4-luc virus at d22 (10^4PFU per mouse in 30µl of PBS) as outlined in Figure 3**a**.
(**a**) Antibody ELISA for detection of serum SEA- and MuHV-4-specific IgG1 and IgG2a overtime after MuHV-4 infection.
(**b**) Number of cells in the lung at d7 post-MuHV-4 infection, as determined by flow cytometry. Neutrophils : $CD11b^{hi}Ly6G^{+}$, eosinophils: $CD11c^{-}SiglecF^{+}$, macrophages; $CD11c^{+}SiglecF^{+}$, monocytes: $CD11b^{hi}Ly6C^{hi}$, DCs: $CD11c^{+}MHC\text{-}II^{hi}$.
Statistical significance calculated using two-way analysis of variance (ANOVA) and Sidak's multiple-comparison test (**P<0.01, ***P<0.001, ****P<0.0001). Data are representative of two to three independent experiments with three to five mice per group (mean +- s.e.m.)

Figure S5

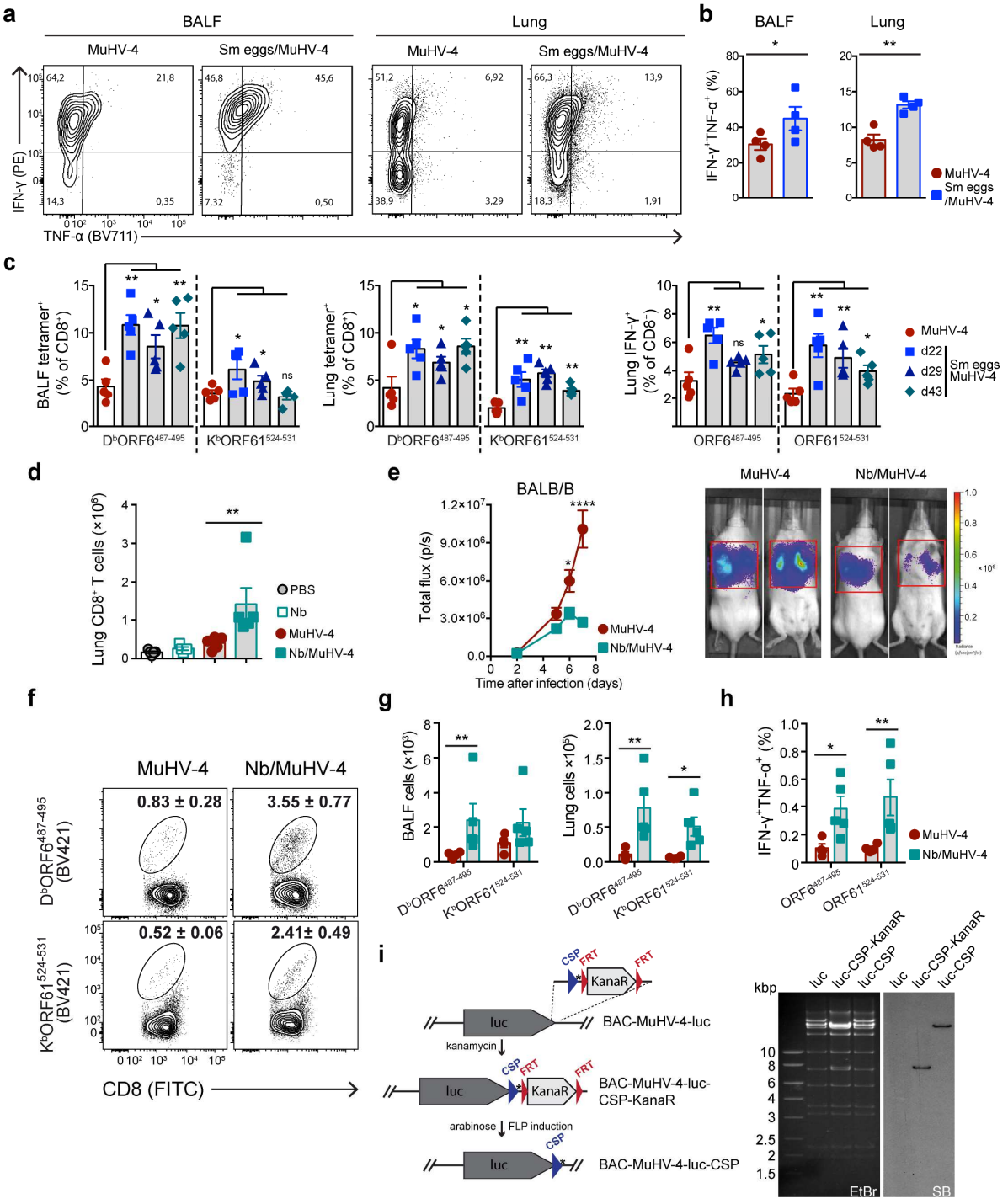
a
BALF
Lung
MuHV-4
Sm eggs/MuHV-4
IFN-γ (PE)
TNF-α (BV711)
b
BALF
Lung
IFN-γ+TNF-α+ (%)
MuHV-4
Sm eggs /MuHV-4
c
BALF tetramer+ (% of CD8+)
Lung tetramer+ (% of CD8+)
Lung IFN-γ+ (% of CD8+)
DbORF6487-495
KbORF61524-531
ORF6487-495
ORF61524-531
MuHV-4
d22
d29
d43
Sm eggs MuHV-4
d
Lung CD8+ T cells (×10⁶)
PBS
Nb
MuHV-4
Nb/MuHV-4
e
BALB/B
Total flux (p/s)
Time after infection (days)
MuHV-4
Nb/MuHV-4
f
MuHV-4
Nb/MuHV-4
0.83 ± 0.28
3.55 ± 0.77
0.52 ± 0.06
2.41± 0.49
CD8 (FITC)
g
BALF cells (×10³)
Lung cells ×10⁵
h
IFN-γ+TNF-α+ (%)
i
CSP
FRT
KanaR
luc
BAC-MuHV-4-luc
kanamycin
BAC-MuHV-4-luc-CSP-KanaR
arabinose
FLP induction
BAC-MuHV-4-luc-CSP
kbp
luc
luc-CSP-KanaR
luc-CSP
EtBr
SB

Figure S5. *S. mansoni* egg immunization and *N. brasiliensis* infection augment anti-viral CD8+ T cell responses.
(**a-h**) BALB/c (**a-b**) or BALB/B (**c-h**) mice were injected with *S. mansoni* (Sm) eggs i.p. and challenged i.v. (5,000/injection) at d14 before being infected i.n. with MuHV-4-luc at d22, unless stated otherwise (10^4PFU per mouse in 30µl of PBS) (**a-c**) as outlined in Fig. 3a or infected with *N. brasiliensis* (Nb, 500xL3, s.c.) being infected i.n. with MuHV-4-luc at d6 (10^4PFU per mouse in 30µl of PBS) (**d-h**) as outlined in Fig. S3b.
(**a**) Representative contour plots of $CD8^+$ T cells showing IFN-γ and TNF-α intracellular stainings following PMA and ionomycin *ex vivo* restimulation of lung or broncho-alveolar lavage fluid (BALF) cells at d7 post-MuHV-4 infection, as determined by flow cytometry. Numbers indicate percentage in each quadrant.
(**b**) Percentage of IFN-γ and TNF-α co-producing $CD8^+$ T cells determined by flow cytometric analysis as in (**a**).
(**c**) MuHV-4 intranasal infection was performed 22, 29 or 43 days after the first *S. mansoni* egg i.p. injection. Percentage of broncho-alveolar lavage fluid (BALF) and lung $tetramer^+$ $CD8^+$ T cells and percentage of IFN-γ-producing $CD8^+$ T cells after $ORF6^{487-495}$ and $ORF61^{524-531}$ peptide *ex vivo* restimulation and intracellular staining of lung cells of BALB/B mice at d7 post-MuHV-4 infection, as determined by flow cytometry.
(**d**) Number of lung $CD8^+$ T cells at d7 post-MuHV-4 infection, as determined by flow cytometry.
(**e**) Combined dorsal and ventral measurements by live imaging of thoracic light emission following D-luciferin injection, overtime post-MuHV-4 infection. p/s = photons per second. Representative photographs of bioluminescence signals of two mice per group are shown.
(**f**) Representative flow cytometry contour plots of $D^bORF6^{487-495}$ and $K^bORF61^{524-531}$ MuHV-4-specific tetramer stainings of lung cells at d7 post-MuHV-4 infection. Numbers in gate indicate percentage of tetramer-positive cells in $CD8^+$ T cells. Mean +- s.e.m. are shown.
(**g**) Number of MuHV-4-specific CD8+ T cells in the broncho-alveolar lavage (BALF) and lung at d7 post-MuHV-4 infection, based on flow cytometric analysis of tetramer stainings as in (**f**).
(**h**) Percentage of IFN-γ and TNF-α co-producing $CD8^+$ T cells after $ORF6^{487-495}$ and $ORF61^{524-531}$ peptide *ex vivo* restimulation at d7 post-MuHV-4 infection, as determined by flow cytometry.
(**i**) Strategy to insert the H-2d-restricted $CSP^{280-288}$ sequence in-frame to the luciferase coding sequence in the MuHV-4-luc BAC clone. Endonuclease restriction profile (SpeI, EtBr) and southern blotting (SB) approach using CSP nucleotide sequence as probe. Kbp, kilobase pair; *, stop codon.
Statistical significance calculated using Mann-Withney test (**b**,**c**) or two-way analysis of variance (ANOVA) and Sidak's multiple-comparison test (**c**,**d**,**f**,**g**) (*P<0.05, **P<0.01, ***P<0.001, ****P<0.0001). Data are representative of two to three independent experiments with four to five mice per group (mean +- s.e.m. in b-e,g,h)

a.

Treatment	Repeat	Total Reads	No. unique mapped Reads	% mapped	No. reads in UCSC mm10 annotation	% Reads in UCSC mm10 annotation
PBS	1	31111257	25531697	82	24194339	77.7671535
PBS	2	30197255	24913806	83	23226334	76.9153819
PBS	3	31303555	24792520	79	25532703	81.564867
Sm eggs	1	35153236	28928185	82	26040023	74.0757494
Sm eggs	2	30238693	24657512	82	23724067	78.4559935
Sm eggs	3	31613985	25578151	81	24620208	77.8775849

b.

			PBS			Sm eggs		
Subset marker	Lineage	Entrezid	Repl. #1	Repl. #2	Repl. #3	Repl. #1	Repl. #2	Repl. #3
Cd19	B cells	12478	0.00	0.00	0.08	0.14	0.08	0.04
Itgax (CD11c)	Dendritic cells	16411	0.51	0.84	0.69	0.41	0.45	0.31
Lyz2	Macrophage	17105	0.04	0.00	0.04	0.03	0.04	0.00
Epx	Eosinophils	13861	0.27	0.40	0.36	0.10	0.24	0.12
Cd3d	T cells	12500	471.57	421.73	595.18	435.01	504.02	517.39
Cd3e	T cells	12501	460.37	429.36	543.23	405.69	441.53	414.38
CD8a	CD8+ T cells	12525	1365.60	1359.85	1534.78	1434.97	1432.46	1359.48
CD8b1	CD8+ T cells	12526	1261.22	1187.69	1650.50	1213.66	1276.24	1276.99
Sell (CD62L)	Naïve T cells	20343	1712.42	1681.44	2080.83	1761.53	2021.70	1982.47
Cd4	CD4+ T cells	12504	0.04	0.16	0.20	0.14	0.16	0.31
Ncr1	Natural killer	17086	0.00	0.00	0.12	0.03	0.04	0.04

*Gene expression levels are RPM normalized == Read count per gene/ (total mapped reads/1000000)

c.

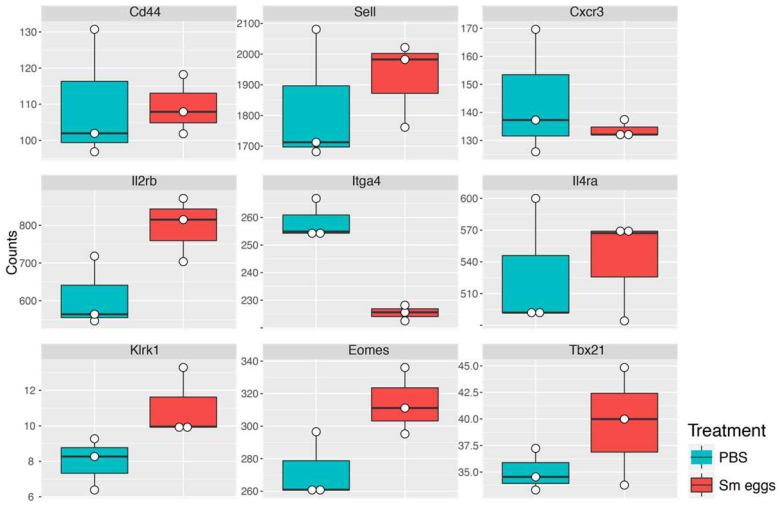

Figure S6.

(**a**) Sequence and mapping statistics for raw Illumina data.

(**b**) Validation of sample purity by assessing the expression of lineage-restricted marker genes for potential contaminants

(**c**). Read count per million mapped reads for selected genes: Cd44, Sell (CD62L), Cxcr3, Il2rb (CD122), Itga4 (CD49d), Il4ra, Klrk1 (NKG2D), Eomes, Tbx21 (T-bet). Each symbol represents an individual mouse: small horizontal lines indicate the mean.

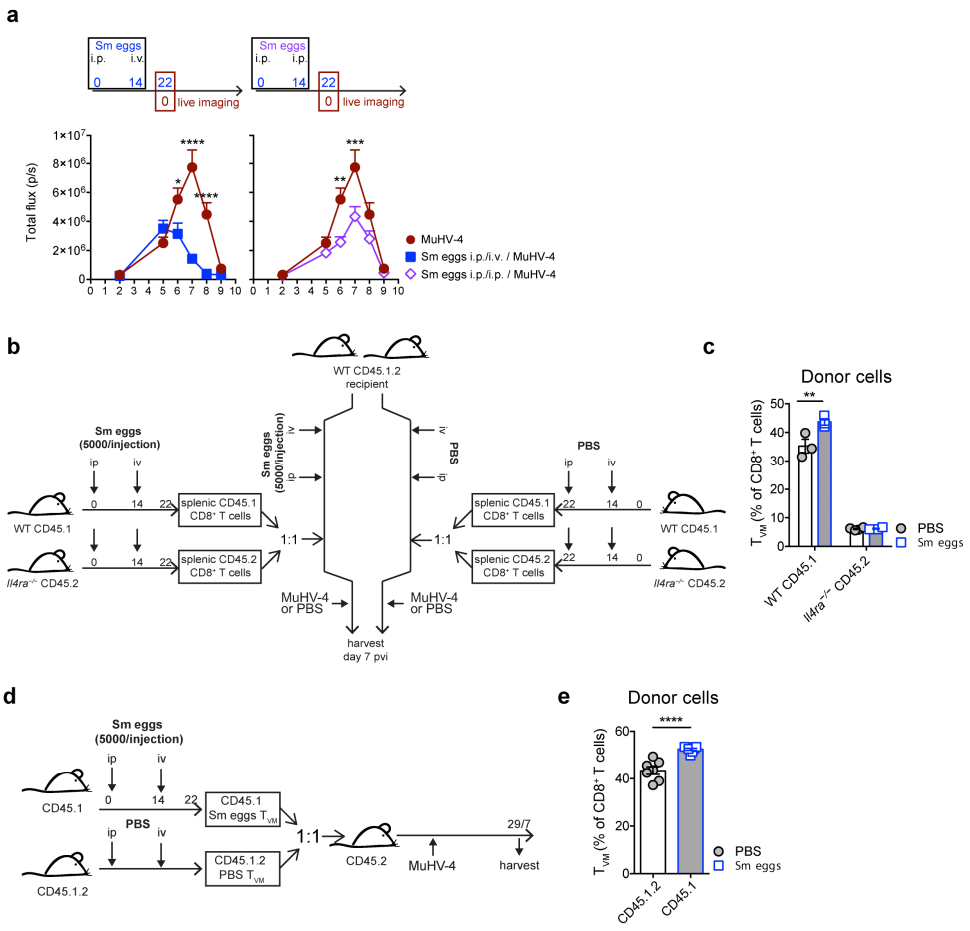

Figure S7. Helminth-induced early control of MuHV-4 infection and in vivo adoptive transfer of CD8$^+$ T cells.

(**a**) BALB/c mice were injected with *S. mansoni* (Sm) eggs i.p. and challenged i.v. or i.p. (5,000/injection) at d14 before being infected i.n. with MuHV-4-luc at d22 (10^4PFU per mouse in 30µl of PBS) as outlined. Combined dorsal and ventral measurements by live imaging of thoracic light emission following D-luciferin infection of BALB/c mice, overtime after MuHV-4 infection. p/s = photon per second

(**b-c**) BALB/c mice were injected with *S. mansoni* (Sm) eggs i.p. and challenged i.v. (5,000/injection) at d14. At d22, CD8$^+$ T cells were enriched by negative magnetic selection from spleen of WT CD45.1 or *Il4ra*$^{-/-}$ CD45.2 mice treated with PBS or Sm eggs before co-transfer in PBS- or Sm egg-treated congenic CD45.1.2 WT recipient mice, followed by MuHV-4-luc i.n. infection (10^4PFU per mouse in 30µl of PBS)

(**b**) Experimental outline.

(**c**) Quantification by flow cytometry of T_{VM} proportion in donor splenic CD8$^+$ T cells used in (**b**).

(**d-e**) BALB/c mice were injected with *S. mansoni* (Sm) eggs i.p. and challenged i.v. (5,000/injection) at d14. At d22, CD44^{hi}CXCR3^{hi}CD62L^{hi}CD49d^{lo} T_{VM} cells were FACS-sorted from spleen of PBS-treated BALB/c CD45.1.2 and Sm egg-treated CD45.1 mice, and equal numbers of cells were co-transferred into naive CD45.2 recipients. 1 d after adoptive transfer, recipients were infected i.n. with MuHV-4-luc (10^4PFU per mouse in 30µl of PBS).

(**d**) Experimental outline.

(**e**) Quantification by flow cytometry of T_{VM} proportion in donor splenic CD8$^+$ T cells used in (**d**).

Statistical significance calculated using non-parametric Mann-Withney test or two-way analysis of variance (ANOVA) and Sidak's multiple-comparison test (*P<0.05, **P<0.01, ***P<0.001, ****P<0.0001). Data are representative of two to three independent experiments with three to seven mice per group (mean +- s.e.m. in a,c,e)

Discussion

Helminth infections are highly prevalent and have been shown to modulate the immune system, sometimes leaving a long-lasting imprint on the ability of the helminth-exposed hosts to respond to heterologous Ags. Indeed, helminth infections can down-modulate allergy or inflammatory bowel disease through various mechanisms (Maizels and McSorley, 2016), but have also been involved in modulating the ability of the infected host to control virus infections. Several groups have shown using C57BL/6 mice that exposure to *H. polygyrus* or *S. mansoni* eggs enhanced reactivation from latency of MuHV-4 through changes in the IL-4/IFN-γ balance (Reese et al., 2014) and also that intestine dwelling helminths could alter effector $CD8^+$ T cell responses against a subsequent viral (Osborne et al., 2014) or protozoal infection (Marple et al., 2016). Nevertheless, these studies did not investigate how helminths could affect bystander memory T cells such as the T_{VM} compartment. Indeed, although T_{VM} development can be highly dependent on IL-4 direct signaling in $CD8^+$ T cells (Renkema et al., 2016; Tripathi et al., 2016), little was known on the ability of this cytokine to drive the expansion of T_{VM} in settings dominated by type 2 immunity such as exposure to helminths. BALB/c mice provide an important opportunity to investigate sensitivity to IL-4 of $CD8^+$ T cells after egress from the thymus as this strain show a particular sensitivity to IL-4 for driving T_{VM} development (Tripathi et al., 2016). This aspect is of great importance as disregarding IL-4-responsive T_{VM} cells could thwart the full understanding of the mechanism involved and how helminths can affect bystander memory T cells such as T_{VM} cells. Our data reveal that exposure to helminths and derived products elicit Ag-nonspecific expansion of the T_{VM} compartment through direct signaling of IL-4. Notably, we observed that such expansion was associated with Eomes upregulation in T_{VM} cells with no alteration of T-bet expression levels, further characterizing these cells as IL-4-induced T_{VM} (Jameson et al., 2015). Such conditioning was observed in several settings involving Th2-dominating responses such as immunization with helminth Ags or infection with systemic or intestinal helminths like *S. mansoni*, *N. brasiliensis*, or *H. polygyrus*. These observations are important as they demonstrated that helminths could actually condition bystander memory $CD8^+$ T cells to respond more effectively to their cognate Ags to the benefit of the infected host.

Indeed, our findings revealed that helminths induced Ag-nonspecific expansion of bystander T_{VM} cells in secondary lymphoid organs *via* direct sensitivity to IL-4 that resulted in increased Ag-specific effector $CD8^+$ T cell responses in the lungs of BALB/c mice to further enhance the control of MuHV-4 lytic replication. These data are supported by previous reports showing that IL-4Rα deficiency compromises the Ag-specific $CD8^+$ T cell response to lymphocytic choriomeningitis virus (LCMV) or influenza virus infections whereas the ability of effector IL-4Rα-deficient $CD8^+$ T cells to kill was unaffected (Marsland et al., 2005; Renkema et al., 2016). Thus, the inability of *Il4ra*$^{-/-}$ mice for early

control of MuHV-4 after *S. mansoni* egg exposure lies in the ineffective development of T_{VM} cells and absence of IL-4 responsiveness of $CD8^+$ T cells in these mice. Although IL-4 signaling in memory T cells was previously associated with downregulation of NKG2D expression and impaired killing capabilities (Ventre et al., 2012), we did not observe significant modulation of NKG2D mRNA expression levels after *S. mansoni* egg treatment in our experimental settings and we observed increased $CD8^+$ antiviral effector responses in the lung. Our transcriptomics data rather indicated that *S. mansoni* egg-induced T_{VM} were phenotypically distinct from naive T_{VM} cells with increased IFN-γ and IFN-α gene signatures. Nonetheless, their ability to react against their cognate Ag and migrate to the infected lungs was not significantly different to naive T_{VM} in a competitive adoptive transfer in naive congenic mice. These observations suggest that both expansion of the T_{VM} compartment after exposure to helminths and alterations of their phenotype can explain the early response to MuHV-4 Ags and subsequent early control. In addition, the low proliferation levels in the T_{VM} population after exposure to *S. mansoni* eggs together with the observation that FTY720 did not inhibit T_{VM} expansion in the spleen after IL-4c treatment and T_{VM} expansion in adoptively transferred congenic $CD8^+$ T lymphocytes suggest that the expansion is likely due to conversion from naive $CD44^{lo}$ T cells while independent of proliferation or recruitment to the spleen. In consequence, expansion of the T_{VM} pool is likely associated with an enrichment of the TCR repertoire in this bystander memory population rather than the proliferation of pre-existing T_{VM} cells, a phenomenon that could significantly augment the probability of effective Ag priming together with the ability of T_{VM} cells to outcompete their naive $CD44^{lo}$ T cell counterpart (Lee et al., 2013a).

Whether helminth-induced bystander T_{VM} cells is also associated with MuHV-4-specific true memory $CD8^+$ T cells after lytic infection remains unknown, but the establishment of effective memory is rather suggested by a previous report demonstrating that establishment of effective memory against malaria requires IL-4Rα on $CD8^+$ T cells (Morrot et al., 2005). This could have important implication for improved vaccination strategies and should further encourage investigators to unravel how T_{VM} cells can be effectively expanded in multiple settings with various types of Ags. Latency during gammaherpesvirus infections such as Kaposi Sarcoma-associated herpesvirus or Epstein-Barr virus, is mainly responsible for malignancies such as lymphomas in human (Mesri et al., 2010; Thorley-Lawson and Gross, 2004), a phase during which virus-infected cells evade $CD8^+$ T cell recognition (Blake, 2010). However, reactivation events of lytic replication occur and are believed to maintain sufficient levels of infection in the host as well as for transmission (Francois et al., 2013). Thus, an effective memory T cell response to control these reactivation events is important. Understanding how helminth-driven expansion of T_{VM} cells impact on long term virus-specific memory is therefore essential.

In conclusion, we provide evidence that helminth-driven type 2 immune responses drives T_{VM} expansion through IL-4 which could in turn positively condition effector Ag-specific $CD8^+$ T cells responses and significantly enhance the control of viral infection such as lytic gammaherpesvirus infections. IL-4 and IFN-γ are usually considered antagonistic as hallmark cytokines of type 2 and type 1 immunity, respectively. Nonetheless, IL-4 can drive Eomes expression in $CD8^+$ T cells and lead to IFN-γ production (Carty et al., 2014; Lee et al., 2013b). We confirm here that this intriguing mechanism has functional consequences *in vivo* by providing evidence that IL-4 induced by helminths can have beneficial bystander consequences on IFN-γ-dependent anti-viral effector responses. Immunity against helminths could therefore have evolved a safety mechanism through induction of highly responding T_{VM} cells to counterbalance negative effects of type 2 immunity on the development of effective anti-viral responses.

Materials and Methods

Cells

Baby Hamster Kidney (BHK)-21 [C13] fibroblasts (ATCC CCL-10) were purchased from ATCC (Manassas, VA, USA) and cultured in Dulbecco's Modified Eagle Medium (DMEM, Sigma-Aldrich) supplemented with 2mM glutamine, 100 U/ml penicillin, 100mg/ml streptomycin and 10% fetal calf serum (FCS) at 37°C under 5% of CO2. Cells were free of mycoplasma contamination (PlasmoTest Mycoplasma Detection Kit, Invivogen).

Viruses

The MHV-68 strain of Murid Herpesvirus-4 (MuHV-4) expressing luciferase under the control of the M3 promoter (MuHV-4-Luc) (Milho et al., 2009) was propagated on BHK-21 cells. Cells and supernatant were harvested at about 4 days post-infection (~85% of lysis) and debris were removed by low-speed centrifugation (1000 × g, 10 min, 4°C). Virions present in the supernatant were harvested by ultracentrifugation (100,000 × g, 2h at 4°C) and purified through a 30% w/v sucrose cushion (100,000 × g, 2h at 4°C), washed in PBS before being stored in PBS at −80°C. Viral titers were determined by plaque assay on BHK-21 cells (de Lima et al., 2004). Briefly, BHK-21 cells monolayers were incubated with 10-fold dilution of viral stock at 37°C, 5% CO_2 for 3 hours. Inoculum was then replaced by semi-solid medium containing 0.6% carboxymethylcellulose. Cells were further incubated for 4 days then fixed in 4% paraformaldehyde and stained for plaques counting.

To assess antigen-specific $CD8^+$ T cells responses in BALB/c mice, we modified the MuHV-4-luc virus to insert the H-$2K^d$-restricted SYVPSAEQI peptide of the circumsporozoite protein of *P. yoelii* ($CSP^{280-288}$) in frame of the luciferase sequence to generate a MuHV-4-luc-CSP virus strain. First, primers PL451-*HindIII*-CSP-STOP-*HindIII*-Fwd (5'−gtcgacggtatcgat*aagctt*-agaggaccagggagagcatttgttacaatatcttatgtcccaagcgcggaacaaatataa*aagctt*gatatcgaattccga−3') and PL451-*HindIII*-STOP-CSP-*HindIII*-Rev (5'−tcggaattcgatatc*aagctt*ttatatttgttccgcgcttggg-acataagatattgtaacaaatgctctccctggtcctct*aagctt*atcgataccgtcgac−3') were annealed and inserted in the HindIII site of the pL451 plasmid vector (http://redrecombineering.ncifcrf.gov/) using inFusion HD kit (Promega) to generate pL451-CSP. Plasmid pL451 contains an FRT-flanked expression cassette of the kanamycin/neomycin resistance gene (KanaR) as selection marker in *Escherichia coli* (Liu et al., 2003; Sorel et al., 2015). Then, the CSP sequence was inserted in frame to the carboxy-terminus of the luciferase coding sequence of the MuHV-4-luc BAC clone using an amplicon generated by PCR with primers MuHV-Luc-CSP-Fwd (5'-agatccgcgagattctcattaaggccaa-gaagggcggcaagatcgccgtgagaggaccagggagagcatt-3') and MuHV-Luc-CSP-Rev (5'-atgtatc-

tatcatgtctgctcgaagcggccggccgccccgactctagaaatattatgtacctgactgat-3') and pL451-CSP as template (Figure S5h). Phage λ-mediated recombineering in SW105 bacteria (http://redrecombineering.ncifcrf.gov/) followed by arabinose-induced FLP expression for excision of FRT-flanked sequence were used (Warming et al., 2005). The generated MuHV-4-luc-CSP BAC construct was verified by an endonuclease restriction and Southern blotting approach and sequencing of the recombination genomic region. The loxP-flanked BAC cassette was removed by virus growth in NIH 3T3-Cre cells to produce MuHV-4-luc-CSP BAC$^-$ virus (Zeippen et al., 2017).

Parasites

S. mansoni-exposed Swiss-Webster mice and snails were provided by the Schistosome Research Reagent Resource Center for distribution by BEI Resources, NIAID, NIH: *Schistosoma mansoni*, Strain NMRI exposed Biomphalaria glabrata, Strain NMRI (NR-21962), *Schistosoma mansoni*, Strain NMRI exposed Swiss-Webster mice (NR-21963). *S. mansoni* cercariae were collected from *S. mansoni* exposed *B. glabrata*, and used for natural infection. *S. mansoni* eggs used for egg immunization, were collected from *S. mansoni*-exposed Swiss-Webster mouse liver and stored in PBS at −80°C, as previously described with minor modifications (Joyce et al., 2012). Briefly, livers were cut into small pieces with scissors and incubated individually in 50-mL tubes overnight in 20 mL of PBS containing 100 µg/ml collagenase IV (Sigma-Aldrich). The homogenates were then slowly poured onto strainers of decreasing mesh sizes (425 µm/180 µm/106 µm and45 µm). Eggs present on top of the 45 µm strainer were collected with PBS and centrifuged for 5 min at 250 × *g* at RT. Pellets were suspended in 10 mL PBS and layered onto 20% Percoll in 0.25 M sucrose (Sigma-Aldrich) and centrifuged at 1850 rpm for 10 min at RT. Pellets were then washed in PBS containing 1 mM EGTA and 1 mM EDTA before layered onto 25% Percoll in 0.25M sucrose and centrifuged at 1850 rpm for 10 min at RT. Pellets were further washed in PBS, counted and resuspended at 50,000 eggs/ml and stored in PBS at -80°C. Soluble Egg Antigen (SEA) from *S. mansoni* were prepared as previously described (Tucker et al., 2013). Eggs were suspended in PBS at a concentration of 100,000 eggs/ml and homogenized with a Potter-Elvehjem hand-held homogenizer and centrifuged (2000 × g, 20 min at 4°C). The supernatant was ultra-centrifuged (100,000 × g, 90 min at 4°C) and the final supernatant was filter-sterilized before being stored at -80°C. Protein concentration was determined by BCA assay (Thermofisher, 23225). Recombinant ω-1 protein was generated in *Nicotiana benthamiana* and purified from the leaf extracellular space using POROS 50 cation resin (Life Technologies) (Wilbers et al., 2017).

N. brasiliensis was maintained in male Sprague-Dawley rats as described (Camberis et al., 2003). *N. brasiliensis* L3 larvae were isolated from d6 to d9 fecal cultures through a Baermann apparatus and used for subcutaneous infection.

H. polygyrus was maintained in male CBA mice as described (Johnston et al., 2015). *H. polygyrus* L3 larvae were isolated from fecal cultures and stored in distilled water at 4°C.

Animals

The experiments, maintenance and care of mice and rats complied with the guidelines of the European Convention for the Protection of Vertebrate Animals used for Experimental and other Scientific Purposes (CETS n° 123). The protocol was approved by the Committee on the Ethics of Animal Experiments of the University of Liège, Belgium (Permit Number: 1357, 1713 and 1849). All efforts were made to minimize suffering. Female BALB/cOlaHsd wild-type mice, 6–8 weeks old and Sprague Dawley male rats were purchased from Envigo (Venray, Netherlands). Female BALB/B mice, congenic for the C57BL/10-derived H-2^b region, were maintained at the Scientific Institute of Public Health, Belgium and transferred to the University of Liege, Department of Infectious Diseases for experiments. BALB/c Cd45.1^+ genitor mice were generously provided by Prof. U. Eriksson (Center for Molecular Cardiology, University of Zurich). BALB/c Cd45.1^+Cd45.2^+ were obtained by crossing Cd45.1^+ BALB/c mice with wild-type BALBc/OlaHsd (Cd45.2^+). *Il4ra*$^{-/-}$ BALB/c mice were bred at the University of Liège, Department of Infectious Diseases. Six to 8 weeks old female littermates were randomly assigned to experimental groups. During experiences, 4 to 5 female mice were cohoused per cage, food and water was provided *ad libitum*. All the animals were bred and/or housed in the University of Liège, Department of Infectious Diseases.

Mixed bone-marrow chimeric mice models

Mixed bone-marrow chimeric mice were produced by exposing CD45.1^+CD45.2^+ BALB/c mice to a whole body lethal irradiation protocol (Gammacell 40 Exactor, 4.5 Gy, two expositions at 3h interval). The next day, mice were reconstituted by intravenous injection of 4.5×10^6 BM cells isolated from femurs and tibias of donor CD45.1^+ WT and CD45.2^+ *Il4ra*$^{-/-}$ mice and mixed at a 1:1 ratio. From 1 week before to 3 weeks after irradiation, mice were given broad-spectrum antibiotherapy (0.27g Trimethoprimum and 1.33g Sulfadiazinum per liter of drinking water, Emdotrim 10%, Ecuphar). Mice were left untreated for 8 weeks to allow complete reconstitution and chimerism of the different blood leukocytes populations was then confirmed by flow cytometry.

	Description	**Use**
CD45.1 BALB/c mice	BALB/c mice normally bear the *b* allele of the protein tyrosine phosphatase receptor type C gene (*Ptprc* or *Cd45*). These mice are designated as CD45.2 as opposed to congenic CD45.1 mice bear the *a* variant of *Ptprc*. The transmembrane protein CD45 is expressed on nucleated cells of hematopoietic origin (Raschke et al., 1995).	Expression of the *a* and *b* alleles of *Ptprc* can be differentiated using specific antibodies. This allow tracking of cells from a given origin in experiments involving adoptive transfer of cells to mice or production of chimeric mice (for example when transfering cells from CD45.1 mice to CD45.2 mice).
Il4ra$^{-/-}$ mice	These mice lake the α chain of the type I and type II IL-4 receptors (IL-4Rα) on all cells (hematopoietic and non hematopoietic). By consequence, signaling for both IL-4 and IL-13 is impaired (see Introduction Figure 6).	IL-4 and IL-13 are two canonical cytokines of type 2 immune response, therefore *Il4ra*$^{-/-}$ mice have a diminished type 2 immune responses. These mice are used to study the role of type 2 immunity during helminth infections.
BALB/B mice	MHC haplotypes differ between mice strains : C57BL/6 express the *b* haplotype while BALB/c mice express the *d* haplotype. BALB/B mice are BALB/c mice expressing the C57BL/10-derived $H2^b$ region	BALB/B mice were used to study MuHV-4-specific $CD8^+$ T cell response on a BALB/c model by taking advantage of the well described $H2^b$-restricted MuHV-4 epitopes AGPHNDMEI and SVYGFTGV.
Mixed bone marrow chimeras	Total body irradiation was performed on CD45.1.2 BALBc mice to achieve destruction of the majority of hematopoietic cells. Mice were reconstituted with a 1 :1 mix of bone marrow cells from CD45.1 WT and CD45.2 *Il4ra*$^{-/-}$ congenic mice.	The hematopoietic cells of these mice are composed of 50% of WT cells and 50% of *Il4ra*$^{-/-}$ cells. Unlike *Il4ra*$^{-/-}$ mice, these mice retain the ability to mount a type 2 immune response and allow to study the direct impact of the absence of the IL-4Rα on the cell itself.
Competitive adoptive transfer of WT and *Il4ra*$^{-/-}$ bulk $CD8^+$ T cells	Spleen $CD8^+$ T cells isolated from CD45.1 and CD45.2 *Il4ra*$^{-/-}$ mice were cotransfered to WT CD45.1.2 congenic mice, after *S. mansoni* egg treatment of both donor and recipient or not.	These mice were used to analyse if *S. mansoni* egg treatment confer a competitive advantage to WT over *Il4ra*$^{-/-}$ $CD8^+$ T cells during MuHV-4 infection.
Competitive adoptive transfer of naive and *S. mansoni* egg-treated WT T_{VM} cells	Spleen T_{VM} from naive CD45.1.2 and *S. mansoni* egg-treated CD45.1 mice were cotransfered to WT CD45.2 congenic mice.	These mice were used to analyse if T_{VM} from *S. mansoni* egg-treated mice display a competitive advantage over T_{VM} from naive mice during MuHV-4 infection.

Table 1. Description of mouse models used

Helminth infections and immunization with helminth Ags

For natural infection with *S. mansoni*, mice were anesthetized by intraperitoneal injection of 16mg/kg of xylazine and 100mg/kg of ketamine and infected by percutaneous exposure to 35 cercariae during 30 min. Treatment with *S. mansoni* eggs consisted of an intraperitoneal immunization on day 0 (5,000 eggs/mouse) followed by one intravenous injection of 5,000 eggs on day 14. In some experiments, mice received *S. mansoni* eggs (5,000 eggs/mouse), SEA (60 μg/mouse) or recombinant ω-1 (10 μg/mouse) intraperitoneally at 2 weeks interval.

Mice anesthetized by isoflurane inhalation were infected with *N. brasiliensis* by subcutaneous injection of 500 × L3 larvae. In some experiments, mice were treated with ivermectin (10mg/L of drinking water, Noromectin, Norbrook) from day 14 to 21 after *N. brasiliensis* infection. Mice were infected with *H. polygyrus* by gavage (200 × L3).

IL-4 complex treatment

Mice received 2 intraperitoneal injections of IL-4c: 5 µg of recombinant IL-4 (BioLegend, carrier-free) and 25 µg of anti-IL-4 antibody (BioLegend, clone 11B11, LEAF purified) per mouse at d0 and d2.

FTY720 treatment.

In order to block lymphocyte trafficking, mice received daily i.p. administration of 1 mg/kg of FTY720 (Sigma-Aldrich) dissolved in 100 ml of sterile water as described elsewhere (Thawer et al., 2014).

Peptide-MHC class I tetramer enrichment

Enrichment of Ag-specific naïve $CD8^+$ T cells or *P. yoelii* circumsporozoite protein peptide after immunization was performed using an established protocol (Renkema et al., 2016). Combined spleen and lymph nodes were digested with collagenase D. Cells were then labeled with APC-conjugated H-$2K^d$-$CSP^{280-288}$ tetramer (SYVPSAEQI, NIH Tetramer Core Facility) for 30min at room temperature, followed by magnetic enrichment over LS columns using anti-APC microbeads (Miltenyi biotec). Enriched samples and unbound fractions were stained with surface antibodies, and Polybead polystyrene microspheres (Polyscience) were used for calculating cell number.

Viral infection and quantification

Mice were anesthetized with isoflurane and 10^4 plaque forming units (PFU) (10^3 or 10^5 PFU for some experiments) of MuHV-4-Luc or MuHV-4-Luc-CSP was administered intranasally in 30 µl of PBS. Light emission was then monitored by *in vivo* bioluminescence imaging using a IVIS Spectrum *In Vivo* Imaging System (Perkin Elmer) after D-luciferin intraperitoneal injection (75mg/kg, Perkin Elmer). Living Image v4.1 software (Perkin Elmer) was used to obtain the total flux (photons/seconds) using a fixed-sized region of interest or average radiance (photons/seconds/cm2/steradiants).

Infectious virus in lungs was quantified after homogenization using glass Potter-Elvehjem hand-held homogenizers after freezing (−80°C) in 6 ml complete medium prior to plaque assay(de Lima et al., 2004).

Viral genome loads were measured using a Taqman-based real-time PCR reaction (CFX) (Latif et al., 2015). DNA was extracted from spleens using Wizard genomic DNA purification kit (Promega) and 100 ng per sample was used in iQ supermix (Biorad) to amplify a MuHV-4-specific sequence (genomic co-ordinates 43,015 to 43,138, NC_001826.2): gene ORF25 with primers ORF25fwd, 5′-atggtatagccgcctttgtg-3′ and ORF25rev 5′-acaagtggatgaagggttgc-3′ and probe 5′-6-carboxyfluorescein [FAM]-caaccactggatcagcataaaacttatgaa-black hole quencher [BHQ1]-3′. Cellular DNA was quantified in parallel by amplifying the interstitial retinoid binding protein (IRBP) gene sequence using iQ SYBR Green supermix (Biorad) and IRBPfwd 5′-atccctatgtcatctcctacytg-3′ and IRBPrev 5′-ccrctgccttcccatgtytg-3′ primers. Standard curves were obtained using pGEMT-easy (Promega) plasmid templates in which MuHV-4 ORF25 or mouse IRBP sequences were cloned, respectively. Amplified products were distinguished from paired primers by melting curve analysis and the correct sizes of the amplified products confirmed by electrophoresis and staining with ethidium bromide.

Histology and immunohistochemistry

Lungs were collected from PBS-perfused animals and immediately fixed in 10% neutral buffered formalin. Tissues were embedded and sectioned, and sections were stained with hematoxylin and eosin. Immunochemistry was performed using EnVision Detection Systems (DAKO) with anti-MHV-68 rabbit polyserum or naive rabbit serum as primary antibodies.

Antigen-specific antibody titers

Nunc Maxisorp ELISA plates (Nalgene Nunc) were coated overnight at 4°C with MuHV-4 virions (10^6 PFU/ml of carbonate buffer pH 9.5 containing 0.1% Triton X-100), or SEA (10 µg/ml in carbonate buffer) before being incubated for 1h in wash/blocking buffer (0.1% Tween-20 and 3% BSA in PBS) at RT. Plates were then incubated with mouse sera (serial dilutions) in wash/blocking buffer for 2h at RT. Detection was performed using alkaline phosphatase-conjugated anti-mouse IgG1 or IgG2a (BD Biosciences) in wash/blocking buffer for 1h at RT. Chromogenic reaction was performed using p-Nitrophenylphosphate (Sigma) and stopped in NaOH 1M before absorbance was read at 405 nm using a iMark ELISA plate reader (Biorad).

BAL cytokines quantification

After euthanasia, airways were flushed twice with 1ml of ice cold PBS containing protease inhibitors (cOmplete, Roche) via catheterization of the trachea. Quantification of IL-4, IFN-γ and granzyme B was performed using specific Ready-SET-Go kits (eBioscience) following the manufacturer's instructions.

Tissue processing and cell preparation

Airways were flushed twice with 1ml of ice cold PBS, cells were harvested by centrifugation of the BAL fluid. After section of the vena cava, lungs were perfused with 5ml of ice-cold PBS through the right ventricule. Lung were dissociated with the gentleMACS dissociator (Miltenyi Biotec) in C-tube (Miltenyi Biotec), incubated in HBSS (Gibco), 5% FCS, 1mg/ml of collagenase D (Roche) and 0.1mg/ml of DNase I (Roche) for 30 min at 37°C under agitation and further dissociated with the gentleMACS dissociator. The resulting suspension was washed in cold PBS/2mM EDTA and filtered on a 100µm cell strainer (Falcon). Spleen and cranial and caudal mediastinal lymph nodes were disrupted using scissors and a sterile syringe plunger and filtered through a 70 µm filter. Erythrocytes were lysed in red cell lysis solution (155mM NH_4CL, 0.12mM EDTA, 10mM $KHCO_3$) and counted in a Neubauer cytometer chamber with trypan blue 0.4% dye exclusion of dead cells.

Flow cytometry and cell sorting

Incubations were performed in FACS buffer (PBS containing 0.5% BSA and 0.1% NaN_3) at 4°C. Cells were first incubated with anti-mouse CD16/32 antibody (clone 93, BioLegend) before fluorochrome-conjugated antibodies against surface antigens were added and incubated during 20 min at 4°C. Various panels were used including antibodies to CD3e (clone 145-2C11, APC), CD19 (MB19-1, APC), CD4 (RM4-5, PerCP-Cy5.5), CD44 (IM7, PE), CD49d (R1-2, biotinylated), CD62L (MEL-14, eFluor 450), MHC class II (M5/114.15.2, PE-Cy7 or eFluor 450), Gr-1 (RB6-8C5, FITC), CD11c (N418, PerCP-Cy5.5 or APC-Alexa Fluor 700), Ly6C (HK1.4, PE-Cy7), CD11b (M1/70, APC-eFluor 780) all from eBioscience/ThermoFisher Scientific ; antibodies to CD3 molecular complexe (17A2, v450), CD19 (1D3, APC-Cy7), CD8a (53-6.7, FITC), CD183 (CXCR3-173, PE), KLRG1 (2F1, PE), CD127 (SB/199, BV786), Siglec-F (E50-2440, PE or PE-CF594), CD45.1 (A20, APC), CD45.2 (104, v500) all from BD Biosciences and antibody to CD44 (IM7, PE-Cy7) from BioLegend. Biotinylated antibodies were detected using BV650-conjugated streptavidin (BD Biosciences). Dead cells were stained using Fixable Viability Stain 510 (BD Bioscience) or Fixable Viability Dye eFluor 780 (eBioscience). In experiments in which intranuclear staining for transcription factors was needed, cells were fixed and permeabilized using Foxp3/Transcription factor staining buffer set (eBioscience) following manufaturer's instruction and incubated 30 min at 4°C with antibody against either T-bet (O4-

46, PE, BD Biosciences) or Eomes (Dan11mag, PE, eBioscience) diluted in permeabilization buffer. Samples were analyzed on a BD LSR Fortessa X-20 flow cytometer, cell sorting was performed on a FACS Aria IIIu (BD biosciences).

In vivo EdU incorporation

To assess the proliferation of virtual memory $CD8^+$ T lymphocytes upon helminth exposure, *S. mansoni* eggs exposed mice were injected ip with EdU (500 µg/mouse in PBS, ThermoFisher Scientific) 4 hours before endpoint (1×) or daily for 4 days before endpoint (4×). Mice were euthanized and spleen were processed as described above. Surface staining was performed with exception of PE-conjugated antibodies. After dead cells staining, cells were fixed for 15 min at room temperature in Click-It Fixative (ThermoFisher Scientific), washed with PBS/1%BSA and incubated 15 min at RT in Click-It Saponine-Based Permeabilization Buffer (ThermoFisher Scientific). Cells were then resuspended in freshly prepared EdU staining cocktail [10µM Pacific Blue-azide, 1mM $CuSO_4$, 10mM sodium ascorbate with 1mM THPTA (tris((1-hydroxy-propyl-1H-1,2,3-triazol-4-yl)methyl)amine) and 10mM amino-guanidine in PBS] and incubated 2h at RT (Wang et al., 2013). Cells were washed with Click-It Saponine-Based Permeabilization Buffer and incubated with PE-conjugated antibodies for 20 min at 4°C. Samples were analyzed on a BD LSR Fortessa X-20 flow cytometer (BD Biosciences).

MHC-tetramer stainings

Lung and BAL cells were processed as described above from BALB/B mice (H-2^b congenic BALB/c). Cells were incubated with BV421-conjugated tetramers H-$2D^b$-$ORF6^{487-495}$ (AGPHNDMEI, 90 nM) or H-$2K^b$-$ORF61^{521-531}$ (TSINFVKI, 45 nM), or APC-conjugated H-$2K^d$-$CSP^{280-288}$ (80 nM) (NIH Tetramer Core Facility), respectively, for 30min at RT before further staining. Samples were analyzed on a BD LSR Fortessa X-20 flow cytometer (BD Biosciences).

Ex vivo restimulation and cytokine production

Cytokine production upon restimulation was assessed by intracellular cytokine staining (ICCS) and flow cytometry or by ELISA on culture supernatants. For ICCS, cells were cultured at 37°C, 5% CO_2 in IMDM complemented with 2 mM glutamine, 100 U penicillin ml^{-1}, 100 mg streptomycin ml^{-1} and 10% fetal calf serum for 4 hours in presence of brefeldin A (10 µg/mL, Sigma-Adlrich), monensin (2 µM, eBioscience) and restimulating agent. For unbiased restimulation, cells were incubated with phorbol 12-myristate 13-acetate (PMA, 20 ng/mL, Sigma-Adlrich) and ionomycin (1 µg/mL, Sigma-Adlrich). For antigen-specific restimulation, cells were incubated with H-2^b-restricted MuHV-4 $ORF6^{487-495}$ (AGPHNDMEI) and $ORF61^{521-531}$ (TSINFVKI) peptides (1 µM). Following surface and

viability stainings, cells were fixed in 2% paraformaldehyde overnight and washed with Permeabilization Buffer (eBioscience) before being incubated with antibodies against IFN-γ (clone XMG1.2, PE, BioLegend) and TNF-α (clone MP6-XT22, BV711, BD Biosciences) in Permeabilization Buffer for 20 min at 4°C. For ELISA, cells were cultured at 37°C, 5% CO_2 in IMDM complemented with 2 mM glutamine, 100 U penicillin ml^{-1}, 100 mg streptomycin ml^{-1} and 10% fetal calf serum for 72 hours with SEA (20 µg/ml). Supernatant were collected and conserved at -20°C. Quantification of cytokines IL-4 and IFN-γ was performed using specific ELISA (Ready-SET-Go, eBioscience) following manufacturer's instructions.

In vivo CD8$^+$ or CD4$^+$ cells depletion

For depletion experiments, mice were injected intraperitoneally with anti-CD8 (clone YTS-169.4, 200 µg/injection) or anti-CD4 (clone GK1.5, 200 µg/injection) both obtained from BioXCell at d-1, 1 and 4 after MuHV-4-Luc infection. Depletion was confirmed by flow cytometry analysis of blood cells on day 6.

T cell enrichment and competitive adoptive transfer

Spleen single-cell suspensions were obtained by forcing through a 70 µm cell strainer (Falcon) before cell counts determined. CD8$^+$ T cells were then enriched using negative magnetic isolation (Miltenyi Biotec) and used either for adoptive transfer of bulk CD8$^+$ T cells or for further T_{VM} purification : enriched CD8$^+$ T cells were then FACsorted to isolate CD44^{hi}CXCR3^{hi}CD62L^{hi}CD49d^{lo} T_{VM} cells to high purity (>97%) before further analysis or adoptive transfer. Competitive adoptive transfer of naive and Sm egg-induced T_{VM} cells consisted in the intravenous administration into WT naive BALB/c congenic recipients of equal numbers (4×10^6 cells total) of naive and Sm egg-induced T_{VM} cells. For competitive transfer of WT and *Il4ra*$^{-/-}$ bulk CD8$^+$ T cells, equal number (4×10^6 cells total) of WT and *Il4ra*$^{-/-}$ enriched CD8$^+$ T cells from naïve or Sm egg-treated BALB/c mice were intravenously administered respectively into naive or Sm egg-treated WT naive BALB/c congenic recipients.

RNA sequencing

T_{VM} cells were extracted as described in the previous section before RNA extraction with on-column DNase treatment (RNeasy Plus mini kit, Qiagen). Integrity of extracted RNAs was controlled on a 2100 Agilent Bioanalyzer and samples with a RIN > 9 were processed for RNA sequencing. Libraries were prepared from 0.5 µg of RNA of three independent replicates per group, using the Illumina TruSeq Stranded mRNA library preparation kit. Libraries were then sequenced and bioinformatics analysis was performed. Approximately 30 million 75-base single-end reads were generated per sample. Quality

control checks on raw sequencing data for each sample were performed using FastQC (Babraham Bioinformatics). Reads were mapped to the mouse reference genome (mm10) using STAR (version 3.4.0) (Dobin et al., 2013). Subsequently the analysis was performed with R Bioconductor packages (Gentleman et al., 2004): Rsamtools (version 1.18.3) and GenomicAlignments (version 1.2.2) were used to count the reads by exons, and gene count datasets were then analyzed to determine differentially expressed genes (DEGs) using DESeq2 (version 1.16.1). A gene was determined to be a DEG by passing FDR<0.1 and log 2-fold change $\geq \pm 0.5$.

Statistical analysis

Statistical evaluation of different groups was performed either by analysis of variance (ANOVA) followed by the Dunnett or Sidak multiple-comparison test or by non-parametric Mann-Whitney test, as indicated. A p-value < 0.05 was considered significant. Statistical analyses were performed using Prism v6 (Graphpad, La Jolla, CA).

Discussion

Discussion

The work presented as part of this thesis investigated mechanisms involved in the broad influence that helminths have on their host's immune system. Two studies, that were not directly related, were performed in this thesis. The first study focused on the immune response to helminth infection itself, in particular on the dynamics of liver macrophages responses and how aaMφ can participate to the immune response against natural infection with *S. mansoni*. The second study investigated how helminth infections can impact subsequent anti-viral responses, in particular *via* conditioning of $CD8^+$ T cell responses. The results generated in these two independent studies are discussed separately.

The role of IL-4Rα-dependent aaMφ in schistosomiasis.

Type 2 immunity is essential for survival during the acute phase of schistosomiasis (Brunet et al., 1997; Herbert et al., 2004; Herbert et al., 2008; Jankovic et al., 1999). In 2004, aaMφ were described as the main cell type responsible for such protection by controlling intestinal egg-induced inflammation and endotoxemia due to increased gut permeability (Herbert et al., 2004). However, these results were recently challenged by Vannella and colleagues (2014) who couldn't find any survival difference between *Il4ra*$^{-/lox}$*Lyz2*^{Cre} mice (used in the first study) and littermate control. They also highlighted that *Il4ra*$^{-/lox}$*Lyz2*^{Cre} mice fail to efficiently delete *Il4ra* in all macrophages population during *S. mansoni* infection precluding any conclusion about the global role of aaMφ in schistosomiasis (see Introduction 2.3.2). Still, subpopulation of aaMφ expressing high levels of *Lyz2* and thus efficiently deleted for *Il4ra* in *Il4ra*$^{-/lox}$*Lyz2*^{Cre} mice play a role in regulation of granulomatous inflammation (Vannella et al., 2014). Our results confirmed those obtained by Vannella and colleagues (2014). Indeed, *Il4ra*$^{-/lox}$*Lyz2*^{Cre} mice had survival rate comparable to control *Il4ra*$^{-/lox}$ mice, whatever the infectious dose used, but increased granulomatous inflammation during *S. mansoni* infection. To better understand which population of aaMφ is responsible for the modulation of liver inflammation, we dissected the dynamics of monocytes/macrophages responses in the liver at the light of IL-4Rα signalling and showed that resident macrophages ($F4/80^+CD64^+$) expressed low levels of CD11b and were progressively replaced by a population of macrophages expressing high levels of CD11b and arising from infiltrating $Ly6C^{hi}$ monocytes independently of IL-4Rα signalling. Proliferation of resident macrophages was observed but limited and was independent of IL-4Rα. The important contribution of $Ly6C^{hi}$ infiltrating monocytes could be anticipated from previous reports (Girgis et al., 2014; Nascimento et al., 2014) but contrary to those studies, we identified the presence of *in situ* proliferation within $Ly6C^{hi}$ monocytes population. This result makes sense in the light of the data from Jenkins and colleagues (2011). Besides their major description of local tissue-resident $F4/80^{hi}$ macrophage proliferation with no contribution of circulating monocytes during canonical type 2 inflammation (IL-4c injections), Jenkins and colleagues used another

model of "mixed" inflammation, using injection of both thioglycollate and IL-4c. Mixed IL-4c and thioglycollate administration induced *in situ* proliferation of inflammatory F4/80^{lo} macrophages originating from circulating monocytes, while thioglycollate alone induced infiltration of monocytes with no proliferation. The presence of both type 1 and type 2 immune triggers is a more faithful reflection of the real situation observed during helminth infection as it is often associated with type 1 immune stimulation, for example from pathogenic bacteria's translocating through helminth-induced tissue damage.

Recently recruited immature macrophages were shown to express insufficient level of *Lyz2* to be efficiently deleted for *Il-4ra* in *Il4ra*$^{-/lox}$*Lyz2*^{Cre} mice (Vannella et al., 2014). Here, the use of *Rosa*^{tdRFP}*Lyz2*^{Cre} lineage reporter mice allowed us to confirm that, consistent with previous report, both CD11b^{hi} and CD11b^{lo} macrophages expressed high levels of cre recombinase but newly recruited Ly6C^{hi} monocytes only expressed low levels. This has important implications for the interpretation of the data since this might imply that a large proportion of Ly6C^{hi} monocytes retained expression of the IL-4Rα. First, *Il4ra*$^{-/lox}$*Lyz2*^{Cre} mice can not give us answers concerning the requirement of IL-4Rα for monocyte infiltration in the liver and differentiation in CD11b^{hi} macrophages during *S. mansoni* infection. However, since similar (but delayed) infiltration of monocytes and differentiation to macrophages was observed in *Il4ra*$^{-/-}$ mice (at least until 6 weeks post-infection, the last timepoint available before mice death), we concluded that IL-4Rα was neither necessary for monocyte infiltration, nor for differentiation. Second, as emphasized by Vannella and colleagues (2014), alternative activation could still be present during *S. mansoni* infection of *Il4ra*$^{-/lox}$*Lyz2*^{Cre} therefore no general conclusion about the role (or absence thereof) of aaMφ could be drawn. Nevertheless, we identified CD11b^{hi} aaMφ as central actors in the modulation of liver granulomatous inflammation during *S. mansoni* infection. Indeed, these cells, on contrary to CD11b^{lo} macrophages, showed signs of alternative activation at week 6 and 8 post-*S. mansoni* infection, that were strongly and significantly reduced in *Il4ra*$^{-/lox}$*Lyz2*^{Cre} mice. Monocyte infiltration was shown to be essential for survival during *S. mansoni* infection (Nascimento et al., 2014) but it remains unknown if their protective role is dependent on alternative activation. Nascimento and colleagues (2014) showed a strong expression of aaMφ markers in hepatic Ly6C^{hi} monocytes during *S. mansoni* infection. Although it has to be confirmed, our data tend to be consistent with the presence of alternative activation within Ly6C^{+} monocytes (data not shown) in both *Il4ra*$^{-/lox}$ and *Il4ra*$^{-/lox}$*Lyz2*^{Cre} mice, highlighting that through these cells, alternative activation of macrophages/monocytes could play additional roles than the role of granulomatous inflammation regulation attributed to CD11b^{hi} aaMφ. Furthermore, a recent study reported the expansion of a population of Ym1-expressing Ly6C^{hi} monocytes in the late phase of LPS-induced inflammation or during the tissue regeneration phase following dextran sodium sulfate administration in drinking water. These cells didn't show other signs of alternative activation but harbour immunoregulatory properties and might play a role in the resolution

of inflammation and in tissue regeneration (Ikeda et al., 2018). Interestingly, Ikeda and colleagues (2018) showed that these cells could arise from maturation of common monocyte progenitor in the bone marrow rather than differentiation of mature monocytes and that granulocyte-macrophage colony-stimulating factor or macrophage colony-stimulating factor and IL-3 rather than IL-4 or IL-10 were involved in this maturation. These data remind us that besides canonical Il-14/IL-13-induced alternative activation of macrophages, monocytes can display features and functions characteristic of aaMφ and participate to mechanisms usually attributed to aaMφ. Although we have identified 3 different populations of monocytes/macrophages in the liver of *S. mansoni* infected mice, the real diversity is likely to be more complex (Thomas et al., 2012). This diversity and role of different populations could be further revealed by single-cell RNAseq. Besides, future work could aim at identifying which effector pathways are elicited by $CD11b^{hi}$ aaMφ to downmodulate liver granulomatous inflammation. A broad and unbiased approach consist of RNAseq of FACS-sorted hepatic $CD11b^{hi}$ macrophages from *Il4ra*$^{-/lox}$*Lyz2*^{Cre} and control *Il4ra*$^{-/lox}$ mice.

We also highlighted that $CD11b^{hi}$ macrophages accumulation during *S. mansoni* infection was associated with the disappearance of hepatic resident $CD11b^{lo}$ macrophages. Although we demonstrated that $CD11b^{lo}$ macrophage population did not play a direct role in the pathology, as its depletion by DT injection in $CD169^{DTR/+}$ mice during ongoing immune response did not influence granuloma formation nor survival, it could be interesting to investigate if their disappearance *per se* takes an active part in the dynamics of the response. Indeed, Blériot and colleagues identify KC death as a trigger to the switch from type 1 to type 2 immune responses following control of *Listeria monocytogenes* infection in the liver, by inducing IL-33 production by hepatocytes. Monocyte-derived macrophages that have contributed to bacterial clearance acquired an alternative activation phenotype through basophil-derived secretion of IL-4, allowing restoration of tissue homeostasis (Blériot et al., 2015). $CD11b^{lo}$ macrophages disappearance might also be a stimulus for monocyte recruitment as their depletion in naive $CD169^{DTR/+}$ mice induced monocyte recruitment (Guilliams and Scott, 2017). Interestingly, changes in hepatic monocyte/macrophage populations was observed as early as 4 weeks post-infection by *S. mansoni*, before the inflow of eggs in the liver and the induction of the dramatic granulomatous inflammation. These results indicates that the presence of worms in the blood circulation can be sufficient to induce liver inflammation and could be investigated using infection with monosexual *S. mansoni* infection.

Within the monocytes/macrophage populations that we identified in the infected liver, $CD11b^{hi}$ cells might represent the part of infiltrating monocytes that differenciate in resident macrophages to replace the loss of $CD11b^{lo}$ macrophages. Indeed, total $F4/80^{+}CD64^{+}$ macrophage number (consisting of both $CD11b^{hi}$ and $CD11b^{lo}$ cells) in the liver remained relatively constant during *S. mansoni* infection, consistant with the concept of “niche”. Behind this concept is the hypothesis that a restricted space is

available for resident macrophages in the tissue, allowing the presence of a restricted and constant number of resident macrophages (Guilliams and Scott, 2017). Monocytes were shown to engraft and differentiate in KCs only when the existing pool of KCs is depleted and, whenever the niche is complete no new engraftment of monocytes is observed. Once established as resident KCs, monocyte-derived macrophages become long-lived and self-renewing cells with transcriptional profiles similar to the original resident KCs (Scott et al., 2016). How this niche concept is affected by inflammation requires further investigation. Still, during *S. mansoni* infection, progressive reduction of $CD11b^{lo}$ macrophage numbers might increase the niche availability, allowing differentiation of infiltrating monocytes to fill the niche. To our knowledge, no reliable marker can differentiate between macrophages of embryonic or monocytic origin but our partial chimera experiments showed that $CD11b^{hi}$ macrophages originate from circulating monocytes while $CD11b^{lo}$ macrophages remain of recipient phenotype during schistosomiasis. In this model monocyte-derived $CD11b^{hi}$ macrophages maintain a distinct phenotype from original tissue-resident macrophages, although our partial chimeras show a slight enrichment of monocyte-derived cells in $CD11b^{lo}$ resident macrophages, indicating that some of the $CD11b^{hi}$ macrophages can further differentiate and acquire full resident phenotype. The investigation of later time points could give us insights concerning the ultimate fate of $CD11b^{hi}$ macrophages but it has to be kept in mind that schistosomiasis is a chronic disease, with new eggs constantly flooding in the liver and continuously eliciting inflammation. This constant inflammatory state might impede terminal differentiation of macrophages. Current view of monocyte contribution to resident macrophages suggest that environment rather than origin shape resident macrophage phenotype. As stated above, the gene-expression profile of monocyte-derived KCs highly resemble that of embryonic-derived resident macrophages (Scott et al., 2016). It could be interesting to investigate if, during schistosomiasis,$CD11b^{hi}$ macrophages acquire a gene-expression profile close to $CD11b^{lo}$ cells and assess their ability to replace $CD11b^{lo}$ macrophages in homeostatic functions like iron or lipid metabolism (Scott et al., 2016).

The investigation of molecular mechanisms underlying the acquisition, by monocytes and macrophages, of particular phenotypes associated with deleterious (e.g. excessive fibrosis) or beneficial (e.g. tissue regeneration) role attributed to aaMφ could bring to light potential therapeutical targets for disease involving macrophages. In that perspective, the identification of moncoyte/macrophage subsets and the understanding of their origin and response dynamics in various inflammatory setting is essential. Such studies for example recently bring more light to the complexity of this response by the identification of specialised population of monocytes involved in resolution of inflammation and tissue regeneration (Ikeda et al., 2018) or fibrosis (Satoh et al., 2017). Liver macrophages were shown to be involved in numerous pathologies (Ritz et al., 2018). *S. mansoni* infection can be used as a model of chronic liver inflammation and fibrosis and bring new understanding of how monocyte/macrophages complexity and plasticity contribute to pathology.

The main issue concerning the study of the role of aaMφ during schistosomiasis is the lack of suitable tools. Most of the tools available failed to efficiently and specifically target aaMφ (see Introduction 2.3.1). Despite that, valuable advances on the understanding of macrophage- and aaMφ-associated molecules functions during schistosomiasis have been made using these tools (Nair et al., 2009; Nascimento et al., 2014; Pesce et al., 2009a; Pesce et al., 2009b; Vannella et al., 2014). In the absence of ubiquitous markers for macrophages populations, single cell RNAseq could help in identifying and targeting populations of interest.

Helminth-induced IL-4 expands functional virtual memory T cells

In the second study, we investigated how helminth infection could influence the pool of virtual memory $CD8^+$ T cells and how this could impact on subsequent anti-viral effector $CD8^+$ T cell responses. Previous reports indicated a role for IL-4 in the development and expansion of T_{VM} cells, a population of non-conventional antigen-inexperienced $CD8^+$ T cells displaying memory properties, particularly in BALB/c mice (Renkema et al., 2016; Weinreich et al., 2010) (see Introduction 4.2.4). Therefore, we hypothesized that helminth infection, through the IL-4-dominated immune response they elicit, might influence T_{VM} compartment. We confirmed this hypothesis using various helminth infection models and provide for the first time evidence that helminth infections or exposure to helminth products induce Ag-nonspecific expansion of $CD8^+$ T_{VM} population through direct IL-4 signaling on $CD8^+$ T cells in BALB/c mice. Moreover, we could directly associate this helminth-induced expansion of T_{VM} with an enhanced virus-specific $CD8^+$ T cell effector responses, resulting in the better control of a subsequent acute infection with the γ-herpesvirus MuHV-4 (figure discussion 1). Importantly, we further demonstrated that IL-4 signaling was required for helminth-induced mediated enhanced viral control.

Our findings were recently consolidated by a study published by Lin and colleagues (2018). They observed a similar mechanism in which *H. polygyrus* infection induces IL-4-dependent T_{VM} expansion associated with increased control of bacterial infection. However, their model slightly differs from ours in that helminth-induced increased control of bacterial load was observed as early as 3 days post-bacterial infection. On the contrary in our model, increased viral control consistently occurs 7 days post-MuHV-4 infection. Lin and colleagues (2018) attributed the protective potential of T_{VM} to their innate bystander function while we hypothetized a contribution of T_{VM} to MuHV-4-specific $CD8^+$ T cell response.

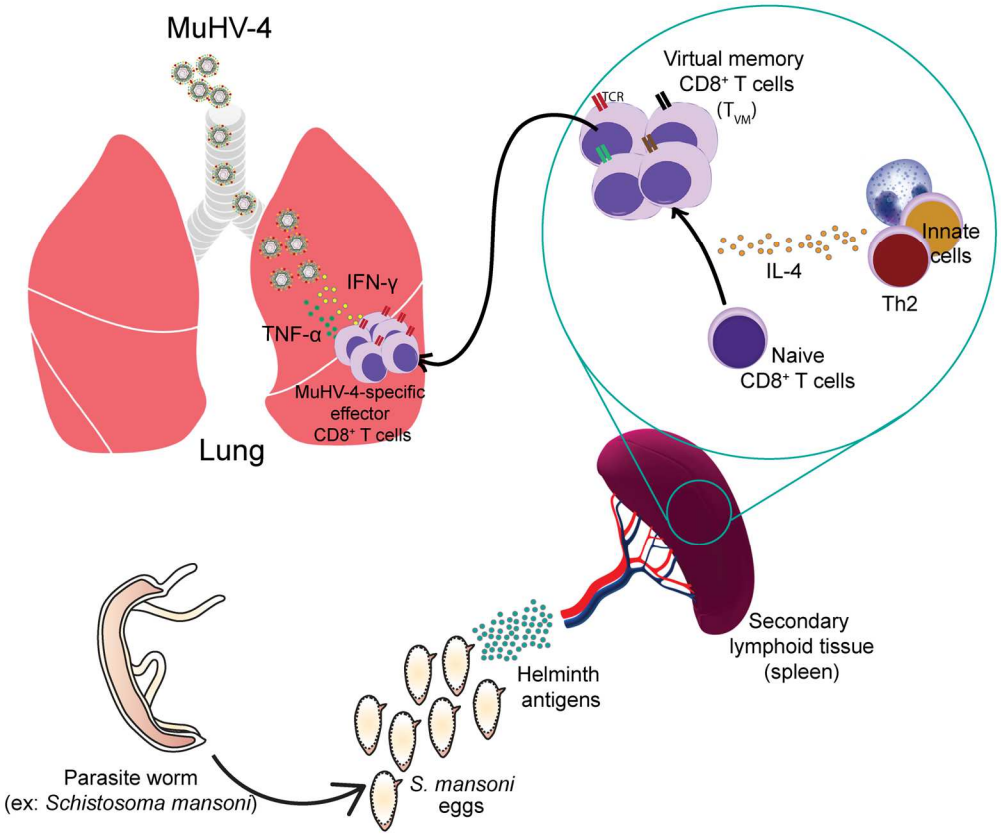

Figure discussion 1: Proposed model of helminth-induced enhanced protection against MuHV-4 acute infection. Immune response elicited by helminth infection is dominated by IL-4 production. IL-4 directly signals on $CD8^+$ T cells to mediate expansion of T_{VM} pool, likely by conversion of naive $CD8^+$ T cells in T_{VM} cells. Upon subsequent MuHV-4 infection, anti-viral $CD8^+$ T cell response is characterized by increased number of specific effector $CD8^+$ T cells with increased effector responses and enhanced control of acute lung infection.

The mechanisms underlying the IL-4-dependent expansion of $CD8^+$ T_{VM} are still not fully understood. Our data corroborate other reports indicating a direct role of IL-4 signaling on $CD8^+$ T cells with a characteristic upregulation of Eomes but not Tbet expression. Subsequent pathways involved need to be further investigated but both STAT-6 and Akt pathways have been involved in IL-4-induced Eomes upregulation (Carty et al., 2014). Although our experiments did not allow us to comprehensively determine the origin of expanded $CD8^+$ T_{VM}, the more likely hypothesis remains conversion from naive T cells. Adoptive transfer of congenic bulk $CD8^+$ T cells isolated from the spleen demonstrated that T_{VM} expansion can occur from peripheral $CD8^+$ T cells, thus potentially independently of cells from the thymus. Supporting this observation, inhibition of S1P-dependent trafficking by FTY720 treatment during IL-4c treatment did not impair T_{VM} expansion. EdU incorporation remained low in T_{VM} cells after *S. mansoni* egg injection, suggesting that *S. mansoni* egg treatment did not cause T_{VM} proliferation. Thus, these observations strongly suggested that the observed expansion of T_{VM} cells is due to conversion from $CD44^{lo}$ naive T cells while independent of proliferation or recruitment to the spleen. In

an attempt to determine whether *S. mansoni* could indeed induce conversion from $CD44^{lo}$ naïve T cells, these cells were FACsorted and adoptively transferred to naive congenic mice before *S. mansoni* egg treatment. Unfortunately, we could not observe significant induction of T_{VM} cells in the transferred cells (data not shown). Previous reports using IL-4c injection in C57BL/6 mice to induce T_{VM} expansion indicated that they can arise from both proliferation of existing T_{VM} pool or conversion of naive cells (Park et al., 2016) while another report using the same model indicates that IL-4-induced upregulation of Eomes expression is observed in pre-existing memory $CD8^+$ T cells but not in naïve cells (Carty et al., 2014). Interestingly, in this latter study, Eomes upregulation in naive $CD8^+$ T cells in response to IL-4 stimulation was observed but only in the presence of low (but not high) TCR stimulation. However, IL-4c treatment does not exactly recapitulates what happens during helminth infection. Furthermore, T_{VM} cells likely behave differently in C57BL/6 or in BALB/c mice.

We observed that increased proportions of T_{VM} are maintained for at least one month after the last *S. mansoni* egg injection. Changes in $CD8^+$ T cells might therefore be longlasting, however, we observed a trend towards a decrease of $CD8^+$ T_{VM} proportion overtime. Data from Park and colleagues (2016) also indicated that IL-4c-induced $CD44^{hi}CXCR3^+$ $CD8^+$ T_{VM} population was maintained overtime, although Eomes expression rapidly declined (Park et al., 2016). This study performed on C57BL/6 mice also identified a non-persistent, intermediate population of $CD44^{lo}CXCR3^+$ $CD8^+$ T_{VM}, which we did not observe in our model.

T_{VM} are known for their enhanced effector functions, and their ability to control pathogens bearing their cognate antigen in a comparable manner to conventional memory $CD8^+$ T cells (Lee et al., 2013a; Weinreich et al., 2010). Here, we showed that IL-4-dependent expansion of bulk, not TCR-transgenic T_{VM} population is associated with a better control of subsequent viral infection. In particular, helminth infection induced increased virus-specific effector $CD8^+$ T cell response probably participating to the enhanced control of MuHV-4 infection. Several hypothesis could explain how expanded T_{VM} contribute to the helminth-induced increased anti-viral response. T_{VM} have been shown to maintain TCR diversity. Thus, an increased number of T_{VM} cells through conversion from naïve cells is potentially associated with an enrichment of the TCR repertoire in this pool of T_{VM} compared to naive T cells, a phenomenon that could significantly augment the probability of effective antigen priming. T_{VM} cells were also shown to outcompete their naïve $CD44^{lo}$ T cell counterpart during response to their cognate antigen and could therefore establish a more rapide $CD8^+$ T cell response (Lee et al., 2013a). Besides, we provided evidence that helminth-conditionned T_{VM} had enhanced effector capacities, as evidenced by increased IFN-γ production from $CD8^+$ T cells after helminth exposure. Consistent with that, RNAseq revealed limited but probably determinant differences between naive and *S. mansoni* egg-induced T_{VM} since *S.*

mansoni egg-induced T_{VM} showed increased IFN-γ and IFN-α gene signatures, evidence of increased effector capacities.

Conditioning of bulk $CD8^+$ T cells by *S. mansoni* eggs conferred migration and effector advantages to wildtype over *Il4ra*$^{-/-}$ $CD8^+$ T cells during MuHV-4 infection, indicating that IL-4Rα-dependent mechanisms underlie enhanced anti-viral $CD8^+$ T cell responses, consistent with the observation that helminth-induced T_{VM} expansion depends on direct IL-4 signaling. However, adoptive transfer experiments did not show any competitive advantage of *S. mansoni* egg-induced T_{VM} over naive T_{VM} at the site of viral infection, indicating that expansion itself, along with altered effector phenotype, might explain the enhanced anti-viral $CD8^+$ T cell response.

In our coinfection model, we clearly identified that increased anti-viral $CD8^+$ T cell responses was associated with an increased virus-specific response. But T_{VM} have also been shown to mediate efficient bystander protective response (White et al., 2016) and this could be further investigated in our model.

Our observations of helminth-induced enhanced protection against MuHV-4 acute infection could have been unexpected as it contrasts with previous reports rather suggesting a deleterious effect of helminth-induced Ym1 on subsequent anti-viral $CD8^+$ T cell responses (Osborne et al., 2014). The most stricking difference between this study and ours, besides using a different viral model, comes from the strain of mouse used. Osborne and colleagues performed their experiments in C57BL/6 mice. Based on known difference between C57BL/6 and BALB/c mice concerning cytokines involved in T_{VM} development, we chose BALB/c mice for our study as they appeared to be to most sensitive to IL-4 (Tripathi et al., 2016). It would be interesting to study on one hand if Ym1 display the same inhibitory function on $CD8^+$ T cells response against MuHV-4 infection, more particularly in BALB/c mice and on the other hand if helminth exposure could induce similar T_{VM} expansion in C57BL/6 mice. Indeed, studies showed expansion of memory-like T cells, either from $CD8^+$ single positive thymocyte or peripheral $CD8^+$ T cells, in response to IL-4c injections in C57BL/6 mice (Carty et al., 2014; Park et al., 2016). Our preliminary experiments showed that, although helminth exposure also induce expansion of T_{VM} in C57BL/6 mice, the percentage of T_{VM} among $CD8^+$ T lymphocytes remain lower than in BALB/c mice. We also performed extensive coinfection experiments in C57BL/6 mice and strickingly observed a reversed phenotype compared to that observed in BALB/c mice (Figure discussion 2). These observations are consistent with a deleterious role of helminth exposure on anti-viral response. Indeed, luminescent signals reporting MuHV-4 lung infection *in vivo* were heavily increased in mice previously exposed with *S. mansoni* eggs. However, these results still differ from those obtained by Osborne and colleagues (2014) as in our experiments increased viral load was observed early during infection, associated with increased migration of antigen-loaded DCs to mediastinal lymph nodes and,

importantly, increased virus-specific CD8$^+$ T cell effector response ultimately leading to similar control of MuHV-4 in mice exposed or not to *S. mansoni* eggs.

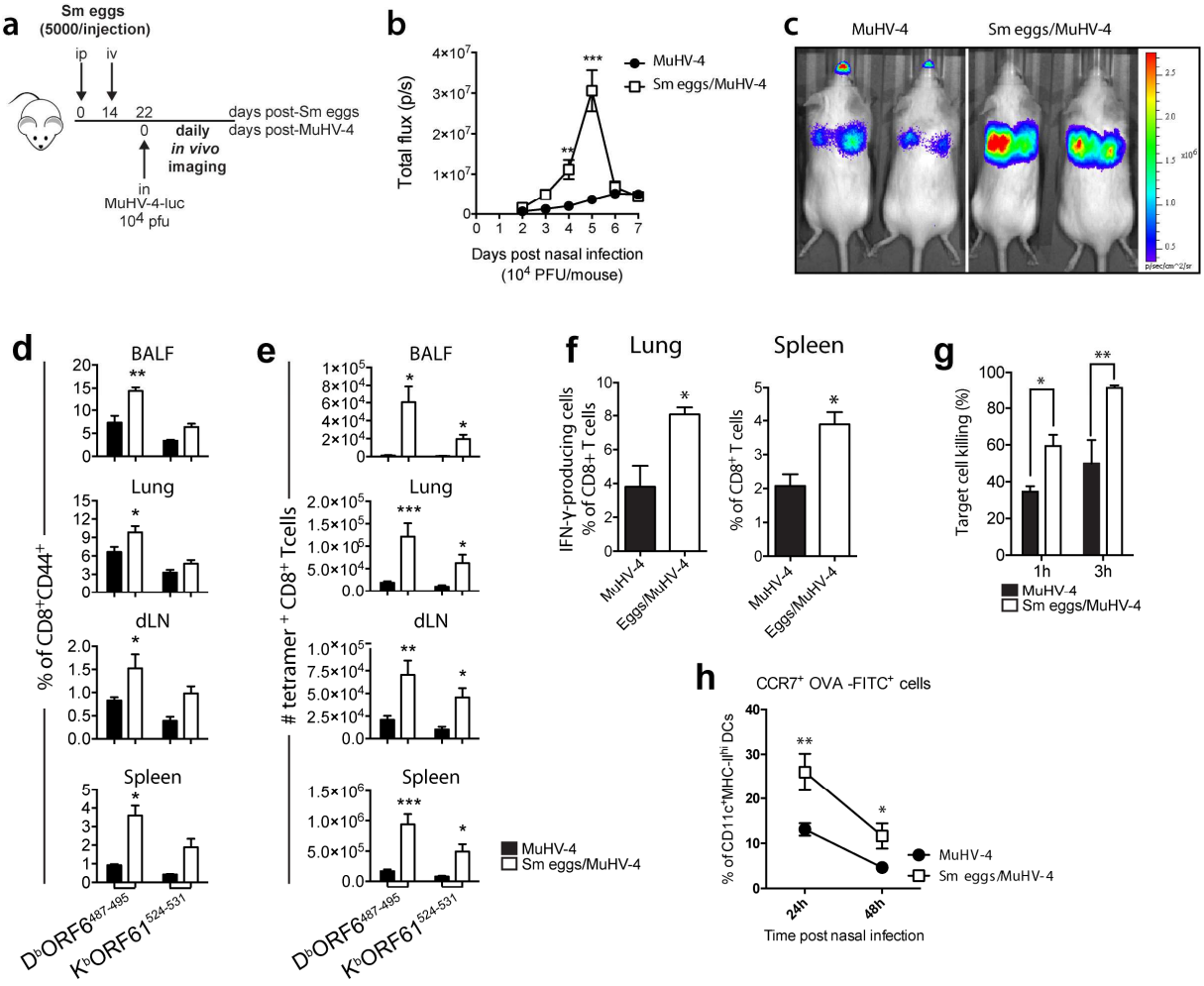

Figure discussion 2 : *S. mansoni* egg immunization of C57BL/6 mice is associated with impaired control of acute infection with MuHV-4 but increased anti-viral CD8$^+$ T cells response.
Albino (**a-c**) or wild-type (**d-h**) C57BL/6 mice were injected with *S. mansoni* eggs i.p. and challenge i.v. (5,000/injection) at d14. At d22, MuHV-4-luc virus was administered i.n. (10^4 PFU per mouse in 30µl PBS)
(**a**) Experimental design.
(**b**) MuHV-4-luc lung infection was monitored daily by *in vivo* imaging following D-luciferine infection. Thoracic dorsal and ventral light emission was measured and combined. p/s = photons per second.
(**c**) Representative photographs of bioluminescence signals of two mice per group at d7 pvi
(**d-e**) D^{b}ORF6$^{487-495}$ and K^{b}ORF61$^{524-531}$ MuHV-4-specific tetramer$^+$ CD8$^+$ T cells percentage (**d**) and total numbers (**e**) in indicated organs at d7 pvi.
(**f**) Percentage of IFN-γ-producing CD8$^+$ T cells after 4h *ex vivo* restimulation with ORF6$^{487-495}$ and ORF61$^{524-531}$ MuHV-4 peptides.
(**g**) In vivo cytotoxic assay: CFSE-labeled peptide pulsed splenocytes were transferred to PBS- or S. mansoni egg-treated mice at d7 pvi and target cell killing efficacy was measured.
(**h**) OVA-FITC was administered in along with MuHV-4 infection. At d1 or d2 pvi, migration of antigen-loaded DCs in mediastinal lymph nodes was assessed.

Thus, although helminth exposure increased C57BL/6 mice susceptibility to MuHV-4 infection, it did not impair CD8$^+$ T cells responses. Furthermore, these results do not exclude a potential role of IL-4-induced T_{VM} in the control of MuHV-4 in C57BL/6 mice as helminth-induced increased viral

colonization occured really early during the infection, before the onset of adaptive immune response. On the contrary, the existence of a similar mechanism in C57BL6 mice was suggested by a recent study (Lin et al., 2018). Interestingly, Lin and colleagues also highlighted that while helminth-induced T_{VM} expansion was strictly dependent on IL-4 signaling in BALB/c mice, this dependency was only partial in C57BL/6 mice and alternative mechanisms should exist, as expected based on available data (see Introduction 4.2). Despite expansion of T_{VM}, other parameters modified by helminth infection in C57BL/6 but not BALB/c mice could explain the strong increased in viral load in helminth-exposed C57BL/6 mice at early timepoints post-infection. The mechanisms underlying the initial increased viral replication in helminth-exposed C57BL/6 mice could involve impaired innate immune responses, for example decreased production of type I IFN (Dutia et al., 1999) or increased MuHV-4 replication in aaMφ (Reese et al., 2014). Helminth-exposed BALB/c mice did not support similar increased viral replication despite alternative macrophage activation in the lung. Genetic variability between BALB/c and C57BL/6 mice have already been shown to influence the ability of *Leishmania major* to replicate in aaMφ (Sans-Fons et al., 2013). Similar phenomenon could explain differences in MuHV-4 susceptibility of helminth-exposed BALB/c or C57BL/6 mice. Difference of MuHV-4 proliferation in aaMφ from BALB/c or C57BL/6 mice could be tested *in vitro*. Interestingly, colonization of C57BL/6 and BALB/c mice by MuHV-4 already differs independently of helminth exposure, BALB/c mice harbour increased viral load compared to C57BL/6 mice during acute lung infection (Weinberg et al., 2004 ; our own data, not shown). The mechanisms implicated in the control of MuHV-4 acute infection was also shown to be different between these two strains, IFN-γ being essential for viral clearance from the lung of BALB/c but not C57BL/6 mice (Tsai et al., 2011). These are just example of the impact of genetic variability on the immune response. In addition, immune responses elicited by helminth infections are highly complex and might vary depending on the context. Discrepancies exist in the litterature concerning coinfection outcomes or mechanisms involved. The high diversity of models used (e.g. mouse strain, pathogens, timing of coinfection, route of infection) at least partially explains these apparently inconsistent results. The difficulty to generalize results obtained from a particular model support the need for the understanding of underlying mechanisms.

We described the possibility that exposure to helminth products condition $CD8^+$ T cells resulting in increased anti-viral $CD8^+$ T cell effector response and enhance control of subsequent viral infection. One obvious application of these findings could therefore be the use of helminths products as vaccine adjuvants. Indeed, despite being described as deleterious for vaccine-induced immunity by several studies, helminth products have already been tested as adjuvant for vaccines (Jiang et al., 2014). In particular, SEA was successfully shown to enhance long-lasting Th1 and cytotoxic $CD8^+$ T cell response to a *Listeria* vector HIV-1 Gag vaccine. However ability to control challenge infection was not evaluated and underlying mechanism was not studied (Bui et al., 2014). Our study did not investigate the influence

of helminth exposure on true memory formation and maintenance after a first encounter with viral antigens, but we observed that during acute anti-viral immune response, percentage of MPEC within $CD8^+$ T cell was transiently lower in mice exposed to helminth than in unexposed mice but reached similar levels by day 9 post-viral infection. How this observation influence memory formation would need to be further explored, especially when considering that IL-4 signaling has already been shown to be essential for efficient memory formation following *Plasmodium yoelii* immunization (Morrot et al., 2005). However, other reports highlighted a deleterious role of IL-4 signaling for effector functions of memory $CD8^+$ T cells (Ventre et al., 2012). Lee and colleagues (2013) described the enhanced effector capacity of T_{VM} compared to naive cells during reaction against their cognate antigenic peptide and mostly attributed it to faster response of T_{VM} cells. But ultimately naive cells expanded to similar numbers compared to T_{VM} cells. This is consistent with our results since, in our study, MuHV-4 infection is ultimately controlled similarly in mice exposed or not to helminths. During a secondary response, expansion of $CD8^+$ T cells originating from T_{VM} or naive precursor cells followed a similar kinetics (Lee et al., 2013a), indicating that there was no improved or impaired true memory formation after antigen-dependent activation of T_{VM} despite observation of increased capacity of naive $CD8^+$ T cells to differentiate in MPEC (Lee et al., 2013a). Importantly, testing the consequence of helminth-induced T_{VM} in vaccine efficacy would only be clinically relevant if similar mechanisms exist in humans. Despite the difficulty to assert that innate memory-like T cells exist and do not arise from previous antigen encounter in humans, studies tend to confirm the existence of a comparable population of antigen-inexperienced memory T cells. Innate memory-like T cells were notably identified in cord blood and spleen of premature children with characteristics that assimilate them to antigen-inexperienced memory $CD8^+$ T cells (Jameson et al., 2015). These cells are being characterized more closely but more work is needed to understand if they respond to similar stimuli as mouse T_{VM} and have similar functions.

In this work, we focused on the impact of helminth infection on $CD8^+$ T cell response against the acute phase of MuHV-4 infection as a model for helminth-induced enhanced anti-viral $CD8^+$ T cell responses. However, when considering γ-herpesvirus infection which are characterized by establishment of latent infection, control of reactivation events is an important parameter. As a consequence, the "quality" of the immune response is assessed less by control of acute infection than by efficient memory formation controlling reactivation events. Helminth exposure have already been shown to induce reactivation of previously established latent MuHV-4 infection (Reese et al., 2014). However, the mechanisms involved in that particular study was a direct effect of STAT-6 on the switch from latency to viral lytic replication. Thus, effect of helminth infection on capacity of memory $CD8^+$ T cells to control latent MuHV-4 infection remains to be investigated.

In conclusion, the first study provides additional data about the dynamics of hepatic monocytes/macrophage responses during *S. mansoni* natural infection at the light of IL-4Rα signalling and showed that IL-4Rα signalling was dispensable for monocyte infiltration and differentiation. Precise comprehension of this response would help understanding the still unelucidated role of aaMφ in *S. mansoni* induced pathology. Thereby, we identified a subpopulation of monocyte-derived aaMφ with a role in the regulation of hepatic granulomatous inflammation. On the contrary, resident macrophages appeared dispensable for the control of *S. mansoni* induced pathology. In the second study, we reported a beneficial outcome of helminth-virus coinfection. Type 2 immune responses initiated by helminth infections or helminth products induced T_{VM} expansion through direct IL-4 signaling on $CD8^+$ T cells that conditionned an increased effector potential of $CD8^+$ T cells. This could in turn positively influence a subsequent anti-viral $CD8^+$ T cell response and enhance the control of acute infection with the γ-herpesvirus MuHV-4. Helminth-induced enhanced effector $CD8^+$ T cell response was also dependent on IL-4Rα-signaling. IL-4 was already known to drive T_{VM} expansion but whether these mechanisms also occur in pathologies dominated by type 2 immune response was not known. Thus, we provided evidence that type 1 and type 2 immune responses do not always antagonize each other and we identified a new mechanism of beneficial helminth-induced modulation of subsequent bystander immune response.

References

Abbate, J.L., Ezenwa, V.O., Guégan, J.F., Choisy, M., Nacher, M., and Roche, B. (2018). Disentangling complex parasite interactions: Protection against cerebral malaria by one helminth species is jeopardized by co-infection with another. PLoS Negl Trop Dis *12*, e0006483.

Abram, C.L., Roberge, G.L., Hu, Y., and Lowell, C.A. (2014). Comparative analysis of the efficiency and specificity of myeloid-Cre deleting strains using ROSA-EYFP reporter mice. J Immunol Methods *408*, 89-100.

Ajami, B., Bennett, J.L., Krieger, C., McNagny, K.M., and Rossi, F.M. (2011). Infiltrating monocytes trigger EAE progression, but do not contribute to the resident microglia pool. Nat Neurosci *14*, 1142-1149.

Ajami, B., Bennett, J.L., Krieger, C., Tetzlaff, W., and Rossi, F.M. (2007). Local self-renewal can sustain CNS microglia maintenance and function throughout adult life. Nat Neurosci *10*, 1538-1543.

Ajendra, J., Specht, S., Neumann, A.L., Gondorf, F., Schmidt, D., Gentil, K., Hoffmann, W.H., Taylor, M.J., Hoerauf, A., and Hübner, M.P. (2014). ST2 deficiency does not impair type 2 immune responses during chronic filarial infection but leads to an increased microfilaremia due to an impaired splenic microfilarial clearance. PLoS One *9*, e93072.

Aksoy, E., Zouain, C.S., Vanhoutte, F., Fontaine, J., Pavelka, N., Thieblemont, N., Willems, F., Ricciardi-Castagnoli, P., Goldman, M., Capron, M.*, et al.* (2005). Double-stranded RNAs from the helminth parasite Schistosoma activate TLR3 in dendritic cells. J Biol Chem *280*, 277-283.

Akue, A.D., Lee, J.Y., and Jameson, S.C. (2012). Derivation and maintenance of virtual memory CD8 T cells. J Immunol *188*, 2516-2523.

Albonico, M., Montresor, A., Crompton, D.W., and Savioli, L. (2006). Intervention for the control of soil-transmitted helminthiasis in the community. Adv Parasitol *61*, 311-348.

Aldridge, A., and O'Neill, S.M. (2016). Fasciola hepatica tegumental antigens induce anergic-like T cells via dendritic cells in a mannose receptor-dependent manner. European journal of immunology *46*, 1180-1192.

Allen, J.E., and Maizels, R.M. (2011). Diversity and dialogue in immunity to helminths. Nat Rev Immunol *11*, 375-388.

Allen, J.E., and Wynn, T.A. (2011). Evolution of Th2 immunity: a rapid repair response to tissue destructive pathogens. PLoS Pathog *7*, e1002003.

Almeida, M.C., Lima, G.S., Cardoso, L.S., de Souza, R.P., Campos, R.A., Cruz, A.A., Figueiredo, J.P., Oliveira, R.R., Carvalho, E.M., and Araujo, M.I. (2012). The effect of antihelminthic treatment on subjects with asthma from an endemic area of schistosomiasis: a randomized, double-blinded, and placebo-controlled trial. J Parasitol Res *2012*, 296856.

Alonso-Trujillo, J., Rivera-Montoya, I., Rodríguez-Sosa, M., and Terrazas, L.I. (2007). Nitric oxide contributes to host resistance against experimental Taenia crassiceps cysticercosis. Parasitol Res *100*, 1341-1350.

Alvarez, J.I., Mishra, B.B., Gundra, U.M., Mishra, P.K., and Teale, J.M. (2010). Mesocestoides corti intracranial infection as a murine model for neurocysticercosis. Parasitology *137*, 359-372.

Anastassiadis, K., Glaser, S., Kranz, A., Berhardt, K., and Stewart, A.F. (2010). A practical summary of site-specific recombination, conditional mutagenesis, and tamoxifen induction of CreERT2. Methods Enzymol *477*, 109-123.

Anthony, R.M., Rutitzky, L.I., Urban, J.F., Jr., Stadecker, M.J., and Gause, W.C. (2007). Protective immune mechanisms in helminth infection. Nature reviews. Immunology *7*, 975-987.

Anthony, R.M., Urban, J.F., Alem, F., Hamed, H.A., Rozo, C.T., Boucher, J.L., Van Rooijen, N., and Gause, W.C. (2006). Memory T(H)2 cells induce alternatively activated macrophages to mediate protection against nematode parasites. Nat Med *12*, 955-960.

Arsenio, J., Metz, P.J., and Chang, J.T. (2015). Asymmetric Cell Division in T Lymphocyte Fate Diversification. Trends Immunol *36*, 670-683.

Artis, D., Kane, C.M., Fiore, J., Zaph, C., Shapira, S., Joyce, K., Macdonald, A., Hunter, C., Scott, P., and Pearce, E.J. (2005). Dendritic cell-intrinsic expression of NF-kappa B1 is required to promote optimal Th2 cell differentiation. J Immunol *174*, 7154-7159.

Artis, D., Wang, M.L., Keilbaugh, S.A., He, W., Brenes, M., Swain, G.P., Knight, P.A., Donaldson, D.D., Lazar, M.A., Miller, H.R.*, et al.* (2004). RELMbeta/FIZZ2 is a goblet cell-specific immune-effector molecule in the gastrointestinal tract. Proc Natl Acad Sci U S A *101*, 13596-13600.

Atherly, L.O., Lucas, J.A., Felices, M., Yin, C.C., Reiner, S.L., and Berg, L.J. (2006). The Tec family tyrosine kinases Itk and Rlk regulate the development of conventional CD8+ T cells. Immunity *25*, 79-91.

Babayan, S., Ungeheuer, M.N., Martin, C., Attout, T., Belnoue, E., Snounou, G., Rénia, L., Korenaga, M., and Bain, O. (2003). Resistance and susceptibility to filarial infection with Litomosoides sigmodontis are associated with early differences in parasite development and in localized immune reactions. Infect Immun *71*, 6820-6829.

Babu, S., Bhat, S.Q., Kumar, N.P., Anuradha, R., Kumaran, P., Gopi, P.G., Kolappan, C., Kumaraswami, V., and Nutman, T.B. (2009). Attenuation of toll-like receptor expression and function in latent tuberculosis by coexistent filarial infection with restoration following antifilarial chemotherapy. PLoS Negl Trop Dis *3*, e489.

Babu, S., and Nutman, T.B. (2016). Helminth-Tuberculosis Co-infection: An Immunologic Perspective. Trends Immunol *37*, 597-607.

Bachmann, M.F., Wolint, P., Schwarz, K., Jäger, P., and Oxenius, A. (2005). Functional properties and lineage relationship of CD8+ T cell subsets identified by expression of IL-7 receptor alpha and CD62L. J Immunol *175*, 4686-4696.

Bager, P., Arnved, J., Rønborg, S., Wohlfahrt, J., Poulsen, L.K., Westergaard, T., Petersen, H.W., Kristensen, B., Thamsborg, S., Roepstorff, A.*, et al.* (2010). Trichuris suis ova therapy for allergic rhinitis: a randomized, double-blind, placebo-controlled clinical trial. J Allergy Clin Immunol *125*, 123-130.e121-123.

Bahgat, M.M., El-Far, M.A., Mesalam, A.A., Ismaeil, A.A., Ibrahim, A.A., Gewaid, H.E., Maghraby, A.S., Ali, M.A., and Abd-Elshafy, D.N. (2010). Schistosoma mansoni soluble egg antigens enhance HCV replication in mammalian cells. J Infect Dev Ctries *4*, 226-234.

Bailer, R.T., Lee, B., and Montaner, L.J. (2000). IL-13 and TNF-alpha inhibit dual-tropic HIV-1 in primary macrophages by reduction of surface expression of CD4, chemokine receptors CCR5, CXCR4 and post-entry viral gene expression. Eur J Immunol *30*, 1340-1349.

Bain, C.C., Bravo-Blas, A., Scott, C.L., Perdiguero, E.G., Geissmann, F., Henri, S., Malissen, B., Osborne, L.C., Artis, D., and Mowat, A.M. (2014). Constant replenishment from circulating monocytes maintains the macrophage pool in the intestine of adult mice. Nat Immunol *15*, 929-937.

Bain, C.C., Hawley, C.A., Garner, H., Scott, C.L., Schridde, A., Steers, N.J., Mack, M., Joshi, A., Guilliams, M., Mowat, A.M.*, et al.* (2016). Long-lived self-renewing bone marrow-derived macrophages displace embryo-derived cells to inhabit adult serous cavities. Nat Commun *7*, ncomms11852.

Balic, A., Harcus, Y., Holland, M.J., and Maizels, R.M. (2004). Selective maturation of dendritic cells by Nippostrongylus brasiliensis-secreted proteins drives Th2 immune responses. Eur J Immunol *34*, 3047-3059.

Bancroft, A.J., McKenzie, A.N., and Grencis, R.K. (1998). A critical role for IL-13 in resistance to intestinal nematode infection. J Immunol *160*, 3453-3461.

Banerjee, A., Gordon, S.M., Intlekofer, A.M., Paley, M.A., Mooney, E.C., Lindsten, T., Wherry, E.J., and Reiner, S.L. (2010). Cutting edge: The transcription factor eomesodermin enables CD8+ T cells to compete for the memory cell niche. J Immunol *185*, 4988-4992.

Bannard, O., Kraman, M., and Fearon, D.T. (2009). Secondary replicative function of CD8+ T cells that had developed an effector phenotype. Science *323*, 505-509.

Bansemir, A.D., and Sukhdeo, M.V. (2001). Intestinal distribution of worms and host ingesta in Nippostrongylus brasiliensis. J Parasitol *87*, 1470-1472.

Barbier, L., Tay, S.S., McGuffog, C., Triccas, J.A., McCaughan, G.W., Bowen, D.G., and Bertolino, P. (2012). Two lymph nodes draining the mouse liver are the preferential site of DC migration and T cell activation. J Hepatol *57*, 352-358.

Barron, L., and Wynn, T.A. (2011). Macrophage activation governs schistosomiasis-induced inflammation and fibrosis. European journal of immunology *41*, 2509-2514.

Barth, M.W., Hendrzak, J.A., Melnicoff, M.J., and Morahan, P.S. (1995). Review of the macrophage disappearance reaction. Journal of leukocyte biology *57*, 361-367.

Barton, E., Mandal, P., and Speck, S.H. (2011). Pathogenesis and host control of gammaherpesviruses: lessons from the mouse. Annual review of immunology *29*, 351-397.

Becker, T.C., Wherry, E.J., Boone, D., Murali-Krishna, K., Antia, R., Ma, A., and Ahmed, R. (2002). Interleukin 15 is required for proliferative renewal of virus-specific memory CD8 T cells. J Exp Med *195*, 1541-1548.

Belkaid, Y., and Hand, T.W. (2014). Role of the microbiota in immunity and inflammation. Cell *157*, 121-141.

Bell, B.D., Kitajima, M., Larson, R.P., Stoklasek, T.A., Dang, K., Sakamoto, K., Wagner, K.U., Kaplan, D.H., Reizis, B., Hennighausen, L., and Ziegler, S.F. (2013). The transcription factor STAT5 is critical in dendritic cells for the development of TH2 but not TH1 responses. Nat Immunol *14*, 364-371.

Bell, E.B., Sparshott, S.M., Drayson, M.T., and Ford, W.L. (1987). The stable and permanent expansion of functional T lymphocytes in athymic nude rats after a single injection of mature T cells. J Immunol *139*, 1379-1384.

Berasain, P., Carmona, C., Frangione, B., Dalton, J.P., and Goñi, F. (2000). Fasciola hepatica: parasite-secreted proteinases degrade all human IgG subclasses: determination of the specific cleavage sites and identification of the immunoglobulin fragments produced. Exp Parasitol *94*, 99-110.

Beyer, M., Mallmann, M.R., Xue, J., Staratschek-Jox, A., Vorholt, D., Krebs, W., Sommer, D., Sander, J., Mertens, C., Nino-Castro, A.*, et al.* (2012). High-resolution transcriptome of human macrophages. PLoS One *7*, e45466.

Blake, N. (2010). Immune evasion by gammaherpesvirus genome maintenance proteins. The Journal of general virology *91*, 829-846.

Blattman, J.N., Antia, R., Sourdive, D.J., Wang, X., Kaech, S.M., Murali-Krishna, K., Altman, J.D., and Ahmed, R. (2002). Estimating the precursor frequency of naive antigen-specific CD8 T cells. J Exp Med *195*, 657-664.

Bleriot, C., Dupuis, T., Jouvion, G., Eberl, G., Disson, O., and Lecuit, M. (2015). Liver-resident macrophage necroptosis orchestrates type 1 microbicidal inflammation and type-2-mediated tissue repair during bacterial infection. Immunity *42*, 145-158.

Blériot, C., Dupuis, T., Jouvion, G., Eberl, G., Disson, O., and Lecuit, M. (2015). Liver-resident macrophage necroptosis orchestrates type 1 microbicidal inflammation and type-2-mediated tissue repair during bacterial infection. Immunity *42*, 145-158.

Boireau, P. (2014). Multicriteria-based Ranking for Risk Management of Food-borne Parasites : report of a joint FAO/WHO meeting (FAO/WHO).

Bonelli, M., Shih, H.Y., Hirahara, K., Singelton, K., Laurence, A., Poholek, A., Hand, T., Mikami, Y., Vahedi, G., Kanno, Y., and O'Shea, J.J. (2014). Helper T cell plasticity: impact of extrinsic and intrinsic signals on transcriptomes and epigenomes. Curr Top Microbiol Immunol *381*, 279-326.

Bonne-Année, S., Kerepesi, L.A., Hess, J.A., Wesolowski, J., Paumet, F., Lok, J.B., Nolan, T.J., and Abraham, D. (2014). Extracellular traps are associated with human and mouse neutrophil and macrophage mediated killing of larval Strongyloides stercoralis. Microbes Infect *16*, 502-511.

Bosurgi, L., Cao, Y.G., Cabeza-Cabrerizo, M., Tucci, A., Hughes, L.D., Kong, Y., Weinstein, J.S., Licona-Limon, P., Schmid, E.T., Pelorosso, F.*, et al.* (2017). Macrophage function in tissue repair and remodeling requires IL-4 or IL-13 with apoptotic cells. Science *356*, 1072-1076.

Bouchery, T., Kyle, R., Camberis, M., Shepherd, A., Filbey, K., Smith, A., Harvie, M., Painter, G., Johnston, K., Ferguson, P.*, et al.* (2015). ILC2s and T cells cooperate to ensure maintenance of M2 macrophages for lung immunity against hookworms. Nat Commun *6*, 6970.

Bouvard, V., Baan, R., Straif, K., Grosse, Y., Secretan, B., El Ghissassi, F., Benbrahim-Tallaa, L., Guha, N., Freeman, C., Galichet, L.*, et al.* (2009). A review of human carcinogens--Part B: biological agents. Lancet Oncol *10*, 321-322.

Boyman, O., Kovar, M., Rubinstein, M.P., Surh, C.D., and Sprent, J. (2006). Selective stimulation of T cell subsets with antibody-cytokine immune complexes. Science *311*, 1924-1927.

Boyman, O., Ramsey, C., Kim, D.M., Sprent, J., and Surh, C.D. (2008). IL-7/anti-IL-7 mAb complexes restore T cell development and induce homeostatic T Cell expansion without lymphopenia. J Immunol *180*, 7265-7275.

Briggs, N., Weatherhead, J., Sastry, K.J., and Hotez, P.J. (2016). The Hygiene Hypothesis and Its Inconvenient Truths about Helminth Infections. PLoS Negl Trop Dis *10*, e0004944.

Bronte, V., Serafini, P., Mazzoni, A., Segal, D.M., and Zanovello, P. (2003). L-arginine metabolism in myeloid cells controls T-lymphocyte functions. Trends Immunol *24*, 302-306.

Broussard, C., Fleischacker, C., Fleischecker, C., Horai, R., Chetana, M., Venegas, A.M., Sharp, L.L., Hedrick, S.M., Fowlkes, B.J., and Schwartzberg, P.L. (2006). Altered development of CD8+ T cell lineages in mice deficient for the Tec kinases Itk and Rlk. Immunity *25*, 93-104.

Brunet, L.R., Finkelman, F.D., Cheever, A.W., Kopf, M.A., and Pearce, E.J. (1997). IL-4 protects against TNF-alpha-mediated cachexia and death during acute schistosomiasis. J Immunol *159*, 777-785.

Buchholz, V.R., Schumacher, T.N., and Busch, D.H. (2016). T Cell Fate at the Single-Cell Level. Annu Rev Immunol *34*, 65-92.

Buck, A.H., Coakley, G., Simbari, F., McSorley, H.J., Quintana, J.F., Le Bihan, T., Kumar, S., Abreu-Goodger, C., Lear, M., Harcus, Y.*, et al.* (2014). Exosomes secreted by nematode parasites transfer small RNAs to mammalian cells and modulate innate immunity. Nat Commun *5*, 5488.

Buentke, E., Mathiot, A., Tolaini, M., Di Santo, J., Zamoyska, R., and Seddon, B. (2006). Do CD8 effector cells need IL-7R expression to become resting memory cells? Blood *108*, 1949-1956.

Bui, C.T., Shollenberger, L.M., Paterson, Y., and Harn, D.A. (2014). Schistosoma mansoni soluble egg antigens enhance Listeria monocytogenes vector HIV-1 vaccine induction of cytotoxic T cells. Clin Vaccine Immunol *21*, 1232-1239.

Bussink, A.P., Speijer, D., Aerts, J.M., and Boot, R.G. (2007). Evolution of mammalian chitinase(-like) members of family 18 glycosyl hydrolases. Genetics *177*, 959-970.

Buys, J., Wever, R., van Stigt, R., and Ruitenberg, E.J. (1981). The killing of newborn larvae of Trichinella spiralis by eosinophil peroxidase in vitro. Eur J Immunol *11*, 843-845.

Cai, Y., Kumar, R.K., Zhou, J., Foster, P.S., and Webb, D.C. (2009). Ym1/2 promotes Th2 cytokine expression by inhibiting 12/15(S)-lipoxygenase: identification of a novel pathway for regulating allergic inflammation. J Immunol *182*, 5393-5399.

Calderon, B., Carrero, J.A., Ferris, S.T., Sojka, D.K., Moore, L., Epelman, S., Murphy, K.M., Yokoyama, W.M., Randolph, G.J., and Unanue, E.R. (2015). The pancreas anatomy conditions the origin and properties of resident macrophages. J Exp Med *212*, 1497-1512.

Camberis, M., Le Gros, G., and Urban, J. (2003). Animal model of Nippostrongylus brasiliensis and Heligmosomoides polygyrus. Curr Protoc Immunol *Chapter 19*, Unit 19.12.

Campbell, S.M., Knipper, J.A., Ruckerl, D., Finlay, C.M., Logan, N., Minutti, C.M., Mack, M., Jenkins, S.J., Taylor, M.D., and Allen, J.E. (2018). Myeloid cell recruitment versus local proliferation differentiates susceptibility from resistance to filarial infection. Elife *7*.

Cardona, A.E., Restrepo, B.I., Jaramillo, J.M., and Teale, J.M. (1999). Development of an animal model for neurocysticercosis: immune response in the central nervous system is characterized by a predominance of gamma delta T cells. J Immunol *162*, 995-1002.

Cardoso, V., Chesné, J., Ribeiro, H., García-Cassani, B., Carvalho, T., Bouchery, T., Shah, K., Barbosa-Morais, N.L., Harris, N., and Veiga-Fernandes, H. (2017). Neuronal regulation of type 2 innate lymphoid cells via neuromedin U. Nature *549*, 277-281.

Carty, S.A., Koretzky, G.A., and Jordan, M.S. (2014). Interleukin-4 regulates eomesodermin in CD8+ T cell development and differentiation. PLoS One *9*, e106659.

Cervi, L., MacDonald, A.S., Kane, C., Dzierszinski, F., and Pearce, E.J. (2004). Cutting edge: dendritic cells copulsed with microbial and helminth antigens undergo modified maturation, segregate the antigens to distinct intracellular compartments, and concurrently induce microbe-specific Th1 and helminth-specific Th2 responses. J Immunol *172*, 2016-2020.

Chang, N.C., Hung, S.I., Hwa, K.Y., Kato, I., Chen, J.E., Liu, C.H., and Chang, A.C. (2001). A macrophage protein, Ym1, transiently expressed during inflammation is a novel mammalian lectin. J Biol Chem *276*, 17497-17506.

Chatterjee, S., Kolappan, C., Subramani, R., Gopi, P.G., Chandrasekaran, V., Fay, M.P., Babu, S., Kumaraswami, V., and Nutman, T.B. (2014). Incidence of active pulmonary tuberculosis in patients with coincident filarial and/or intestinal helminth infections followed longitudinally in South India. PLoS One *9*, e94603.

Chen, F., Liu, Z., Wu, W., Rozo, C., Bowdridge, S., Millman, A., Van Rooijen, N., Urban, J.F., Wynn, T.A., and Gause, W.C. (2012a). An essential role for TH2-type responses in limiting acute tissue damage during experimental helminth infection. Nat Med *18*, 260-266.

Chen, F., Wu, W., Millman, A., Craft, J.F., Chen, E., Patel, N., Boucher, J.L., Urban, J.F., Kim, C.C., and Gause, W.C. (2014a). Neutrophils prime a long-lived effector macrophage phenotype that mediates accelerated helminth expulsion. Nat Immunol *15*, 938-946.

Chen, G., Chan, A.J., Chung, J.I., Jang, J.C., Osborne, L.C., and Nair, M.G. (2014b). Polarizing the T helper 17 response in Citrobacter rodentium infection via expression of resistin-like molecule α. Gut Microbes *5*, 363-368.

Chen, L., Liu, W.Q., Lei, J.H., Guan, F., Li, M.J., Song, W.J., Li, Y.L., and Wang, T. (2012b). Chronic Schistosoma japonicum infection reduces immune response to vaccine against hepatitis B in mice. PLoS One *7*, e51512.

Cherian, T., Wang, S., and Mantel, C. (2012). Rotavirus vaccines in developing countries: the potential impact, implementation challenges, and remaining questions. Vaccine *30 Suppl 1*, A3-6.

Cheung, K.P., Yang, E., and Goldrath, A.W. (2009). Memory-like CD8+ T cells generated during homeostatic proliferation defer to antigen-experienced memory cells. J Immunol *183*, 3364-3372.

Chiaramonte, M.G., Donaldson, D.D., Cheever, A.W., and Wynn, T.A. (1999). An IL-13 inhibitor blocks the development of hepatic fibrosis during a T-helper type 2-dominated inflammatory response. J Clin Invest *104*, 777-785.

Chorro, L., Sarde, A., Li, M., Woollard, K.J., Chambon, P., Malissen, B., Kissenpfennig, A., Barbaroux, J.B., Groves, R., and Geissmann, F. (2009). Langerhans cell (LC) proliferation mediates neonatal development, homeostasis, and inflammation-associated expansion of the epidermal LC network. J Exp Med *206*, 3089-3100.

Chow, A., Huggins, M., Ahmed, J., Hashimoto, D., Lucas, D., Kunisaki, Y., Pinho, S., Leboeuf, M., Noizat, C., van Rooijen, N.*, et al.* (2013). CD169(+) macrophages provide a niche promoting erythropoiesis under homeostasis and stress. Nat Med *19*, 429-436.

Chu, T., Tyznik, A.J., Roepke, S., Berkley, A.M., Woodward-Davis, A., Pattacini, L., Bevan, M.J., Zehn, D., and Prlic, M. (2013). Bystander-activated memory CD8 T cells control early pathogen load in an innate-like, NKG2D-dependent manner. Cell Rep *3*, 701-708.

Cliffe, L.J., Humphreys, N.E., Lane, T.E., Potten, C.S., Booth, C., and Grencis, R.K. (2005). Accelerated intestinal epithelial cell turnover: a new mechanism of parasite expulsion. Science *308*, 1463-1465.

Colley, D.G., Bustinduy, A.L., Secor, W.E., and King, C.H. (2014). Human schistosomiasis. Lancet *383*, 2253-2264.

Colombe, S., Machemba, R., Mtenga, B., Lutonja, P., Kalluvya, S.E., de Dood, C.J., Hoekstra, P.T., van Dam, G.J., Corstjens, P.L.A.M., Urassa, M.*, et al.* (2018). Impact of schistosome infection on long-term HIV/AIDS outcomes. PLoS Negl Trop Dis *12*, e0006613.

Cook, P.C., Jones, L.H., Jenkins, S.J., Wynn, T.A., Allen, J.E., and MacDonald, A.S. (2012). Alternatively activated dendritic cells regulate CD4+ T-cell polarization in vitro and in vivo. Proc Natl Acad Sci U S A *109*, 9977-9982.

Cooper, P.J., Chico, M., Sandoval, C., Espinel, I., Guevara, A., Levine, M.M., Griffin, G.E., and Nutman, T.B. (2001). Human infection with Ascaris lumbricoides is associated with suppression of the interleukin-2 response to recombinant cholera toxin B subunit following vaccination with the live oral cholera vaccine CVD 103-HgR. Infect Immun *69*, 1574-1580.

Correale, J., and Farez, M. (2007). Association between parasite infection and immune responses in multiple sclerosis. Ann Neurol *61*, 97-108.

Cox, F.E.G. (2009). Modern Parasitology: A Textbook of Parasitology, Second Edition (Blackwell Science LTD).

Coyle, C.M., Mahanty, S., Zunt, J.R., Wallin, M.T., Cantey, P.T., White, A.C., O'Neal, S.E., Serpa, J.A., Southern, P.M., Wilkins, P.*, et al.* (2012). Neurocysticercosis: neglected but not forgotten. PLoS Negl Trop Dis *6*, e1500.

Creery, D., Weiss, W., Graziani-Bowering, G., Kumar, R., Aziz, Z., Angel, J.B., and Kumar, A. (2006). Differential regulation of CXCR4 and CCR5 expression by interleukin (IL)-4 and IL-13 is associated with inhibition of chemotaxis and human immunodeficiency Virus (HIV) type 1 replication but not HIV entry into human monocytes. Viral Immunol *19*, 409-423.

Cui, W., and Kaech, S.M. (2010). Generation of effector CD8+ T cells and their conversion to memory T cells. Immunol Rev *236*, 151-166.

D'Elia, R., Behnke, J.M., Bradley, J.E., and Else, K.J. (2009). Regulatory T cells: a role in the control of helminth-driven intestinal pathology and worm survival. J Immunol *182*, 2340-2348.

Daveson, A.J., Jones, D.M., Gaze, S., McSorley, H., Clouston, A., Pascoe, A., Cooke, S., Speare, R., Macdonald, G.A., Anderson, R.*, et al.* (2011). Effect of hookworm infection on wheat challenge in celiac disease--a randomised double-blinded placebo controlled trial. PLoS One *6*, e17366.

de Lima, B.D., May, J.S., and Stevenson, P.G. (2004). Murine gammaherpesvirus 68 lacking gp150 shows defective virion release but establishes normal latency in vivo. J Virol *78*, 5103-5112.

Degarege, A., and Erko, B. (2016). Epidemiology of Plasmodium and Helminth Coinfection and Possible Reasons for Heterogeneity. Biomed Res Int *2016*, 3083568.

Dematteis, S., Baz, A., Rottenberg, M., Fernández, C., Orn, A., and Nieto, A. (1999). Antibody and Th1/Th2-type responses in BALB/c mice inoculated with live or dead Echinococcus granulosus protoscoleces. Parasite Immunol *21*, 19-26.

Denis, M., and Ghadirian, E. (1994). Interleukin 13 and interleukin 4 protect bronchoalveolar macrophages from productive infection with human immunodeficiency virus type 1. AIDS Res Hum Retroviruses *10*, 795-802.

Deplazes, P., Rinaldi, L., Alvarez Rojas, C.A., Torgerson, P.R., Harandi, M.F., Romig, T., Antolova, D., Schurer, J.M., Lahmar, S., Cringoli, G.*, et al.* (2017). Global Distribution of Alveolar and Cystic Echinococcosis. Adv Parasitol *95*, 315-493.

deSchoolmeester, M.L., Martinez-Pomares, L., Gordon, S., and Else, K.J. (2009). The mannose receptor binds Trichuris muris excretory/secretory proteins but is not essential for protective immunity. Immunology *126*, 246-255.

Devleesschauwer, B., Allepuz, A., Dermauw, V., Johansen, M.V., Laranjo-González, M., Smit, G.S., Sotiraki, S., Trevisan, C., Wardrop, N.A., Dorny, P., and Gabriël, S. (2017). Taenia solium in Europe: Still endemic? Acta Trop *165*, 96-99.

Devleesschauwer, B., Praet, N., Speybroeck, N., Torgerson, P.R., Haagsma, J.A., De Smet, K., Murrell, K.D., Pozio, E., and Dorny, P. (2015). The low global burden of trichinellosis: evidence and implications. Int J Parasitol *45*, 95-99.

Dewals, B.G., Marillier, R.G., Hoving, J.C., Leeto, M., Schwegmann, A., and Brombacher, F. (2010). IL-4Ralpha-independent expression of mannose receptor and Ym1 by macrophages depends on their IL-10 responsiveness. PLoS neglected tropical diseases *4*, e689.

Dinarello, C.A., Novick, D., Kim, S., and Kaplanski, G. (2013). Interleukin-18 and IL-18 binding protein. Front Immunol *4*, 289.

Dobin, A., Davis, C.A., Schlesinger, F., Drenkow, J., Zaleski, C., Jha, S., Batut, P., Chaisson, M., and Gingeras, T.R. (2013). STAR: ultrafast universal RNA-seq aligner. Bioinformatics *29*, 15-21.

Downs, J.A., Dupnik, K.M., van Dam, G.J., Urassa, M., Lutonja, P., Kornelis, D., de Dood, C.J., Hoekstra, P., Kanjala, C., Isingo, R.*, et al.* (2017). Effects of schistosomiasis on susceptibility to HIV-1 infection and HIV-1 viral load at HIV-1 seroconversion: A nested case-control study. PLoS Negl Trop Dis *11*, e0005968.

Downs, J.A., Mguta, C., Kaatano, G.M., Mitchell, K.B., Bang, H., Simplice, H., Kalluvya, S.E., Changalucha, J.M., Johnson, W.D., and Fitzgerald, D.W. (2011). Urogenital schistosomiasis in women of reproductive age in Tanzania's Lake Victoria region. Am J Trop Med Hyg *84*, 364-369.

Drobek, A., Moudra, A., Mueller, D., Huranova, M., Horkova, V., Pribikova, M., Ivanek, R., Oberle, S., Zehn, D., McCoy, K.D.*, et al.* (2018). Strong homeostatic TCR signals induce formation of self-tolerant virtual memory CD8 T cells. EMBO J *37*.

Du, L., Tang, H., Ma, Z., Xu, J., Gao, W., Chen, J., Gan, W., Zhang, Z., Yu, X., Zhou, X., and Hu, X. (2011). The protective effect of the recombinant 53-kDa protein of Trichinella spiralis on experimental colitis in mice. Dig Dis Sci *56*, 2810-2817.

Du, L., Wei, H., Li, L., Shan, H., Yu, Y., Wang, Y., and Zhang, G. (2014). Regulation of recombinant Trichinella spiralis 53-kDa protein (rTsP53) on alternatively activated macrophages via STAT6 but not IL-4Rα in vitro. Cell Immunol *288*, 1-7.

du Plessis, N., Kleynhans, L., Thiart, L., van Helden, P.D., Brombacher, F., Horsnell, W.G., and Walzl, G. (2013). Acute helminth infection enhances early macrophage mediated control of mycobacterial infection. Mucosal Immunol *6*, 931-941.

Du, W.Y., Chen, C.W., Lin, F.K., and Chuang, C.C. (2013). IL-33 mediates the expressions of IL-5 and IL-13 in Angiostrongylus cantonensis-infected mice. Exp Parasitol *135*, 587-594.

Dutia, B.M., Allen, D.J., Dyson, H., and Nash, A.A. (1999). Type I interferons and IRF-1 play a critical role in the control of a gammaherpesvirus infection. Virology *261*, 173-179.

Edwards, J.P., Zhang, X., Frauwirth, K.A., and Mosser, D.M. (2006). Biochemical and functional characterization of three activated macrophage populations. J Leukoc Biol *80*, 1298-1307.

Elias, D., Akuffo, H., Pawlowski, A., Haile, M., Schön, T., and Britton, S. (2005). Schistosoma mansoni infection reduces the protective efficacy of BCG vaccination against virulent Mycobacterium tuberculosis. Vaccine *23*, 1326-1334.

Elias, D., Britton, S., Aseffa, A., Engers, H., and Akuffo, H. (2008). Poor immunogenicity of BCG in helminth infected population is associated with increased in vitro TGF-beta production. Vaccine *26*, 3897-3902.

Elias, D., Mengistu, G., Akuffo, H., and Britton, S. (2006). Are intestinal helminths risk factors for developing active tuberculosis? Trop Med Int Health *11*, 551-558.

Ernst, B., Lee, D.S., Chang, J.M., Sprent, J., and Surh, C.D. (1999). The peptide ligands mediating positive selection in the thymus control T cell survival and homeostatic proliferation in the periphery. Immunity *11*, 173-181.

Espinoza-Jiménez, A., De Haro, R., and Terrazas, L.I. (2017). Antigens Control Experimental Type 1 Diabetes by Inducing Alternatively Activated Macrophages. Mediators Inflamm *2017*, 8074329.

Esser-von Bieren, J., Mosconi, I., Guiet, R., Piersgilli, A., Volpe, B., Chen, F., Gause, W.C., Seitz, A., Verbeek, J.S., and Harris, N.L. (2013). Antibodies trap tissue migrating helminth larvae and prevent tissue damage by driving IL-4Rα-independent alternative differentiation of macrophages. PLoS Pathog *9*, e1003771.

Esser-von Bieren, J., Volpe, B., Kulagin, M., Sutherland, D.B., Guiet, R., Seitz, A., Marsland, B.J., Verbeek, J.S., and Harris, N.L. (2015). Antibody-mediated trapping of helminth larvae requires CD11b and Fcγ receptor I. J Immunol *194*, 1154-1163.

Everts, B., Hussaarts, L., Driessen, N.N., Meevissen, M.H., Schramm, G., van der Ham, A.J., van der Hoeven, B., Scholzen, T., Burgdorf, S., Mohrs, M.*, et al.* (2012). Schistosome-derived omega-1 drives Th2 polarization by suppressing protein synthesis following internalization by the mannose receptor. The Journal of experimental medicine *209*, 1753-1767, S1751.

Everts, B., Perona-Wright, G., Smits, H.H., Hokke, C.H., van der Ham, A.J., Fitzsimmons, C.M., Doenhoff, M.J., van der Bosch, J., Mohrs, K., Haas, H.*, et al.* (2009). Omega-1, a glycoprotein secreted by Schistosoma mansoni eggs, drives Th2 responses. The Journal of experimental medicine *206*, 1673-1680.

Fallon, P.G. (2000). Immunopathology of schistosomiasis: a cautionary tale of mice and men. Immunol Today *21*, 29-35.

Fallon, P.G., Ballantyne, S.J., Mangan, N.E., Barlow, J.L., Dasvarma, A., Hewett, D.R., McIlgorm, A., Jolin, H.E., and McKenzie, A.N. (2006). Identification of an interleukin (IL)-25-dependent cell population that provides IL-4, IL-5, and IL-13 at the onset of helminth expulsion. J Exp Med *203*, 1105-1116.

Fallon, P.G., Richardson, E.J., McKenzie, G.J., and McKenzie, A.N. (2000). Schistosome infection of transgenic mice defines distinct and contrasting pathogenic roles for IL-4 and IL-13: IL-13 is a profibrotic agent. J Immunol *164*, 2585-2591.

Feary, J., Britton, J., and Leonardi-Bee, J. (2011). Atopy and current intestinal parasite infection: a systematic review and meta-analysis. Allergy *66*, 569-578.

Feary, J.R., Venn, A.J., Mortimer, K., Brown, A.P., Hooi, D., Falcone, F.H., Pritchard, D.I., and Britton, J.R. (2010). Experimental hookworm infection: a randomized placebo-controlled trial in asthma. Clin Exp Allergy *40*, 299-306.

Felices, M., Yin, C.C., Kosaka, Y., Kang, J., and Berg, L.J. (2009). Tec kinase Itk in gammadeltaT cells is pivotal for controlling IgE production in vivo. Proc Natl Acad Sci U S A *106*, 8308-8313.

Fichtner-Feigl, S., Strober, W., Kawakami, K., Puri, R.K., and Kitani, A. (2006). IL-13 signaling through the IL-13alpha2 receptor is involved in induction of TGF-beta1 production and fibrosis. Nat Med *12*, 99-106.

Finkelman, F.D., Shea-Donohue, T., Morris, S.C., Gildea, L., Strait, R., Madden, K.B., Schopf, L., and Urban, J.F., Jr. (2004). Interleukin-4- and interleukin-13-mediated host protection against intestinal nematode parasites. Immunol Rev *201*, 139-155.

Finney, C.A., Taylor, M.D., Wilson, M.S., and Maizels, R.M. (2007). Expansion and activation of CD4(+)CD25(+) regulatory T cells in Heligmosomoides polygyrus infection. Eur J Immunol *37*, 1874-1886.

Fleming, J.O., Isaak, A., Lee, J.E., Luzzio, C.C., Carrithers, M.D., Cook, T.D., Field, A.S., Boland, J., and Fabry, Z. (2011). Probiotic helminth administration in relapsing-remitting multiple sclerosis: a phase 1 study. Mult Scler *17*, 743-754.

Flohr, C., Quinnell, R.J., and Britton, J. (2009). Do helminth parasites protect against atopy and allergic disease? Clin Exp Allergy *39*, 20-32.

Flohr, C., Tuyen, L.N., Quinnell, R.J., Lewis, S., Minh, T.T., Campbell, J., Simmons, C., Telford, G., Brown, A., Hien, T.T*., et al.* (2010). Reduced helminth burden increases allergen skin sensitization but not clinical allergy: a randomized, double-blind, placebo-controlled trial in Vietnam. Clin Exp Allergy *40*, 131-142.

Fort, M.M., Cheung, J., Yen, D., Li, J., Zurawski, S.M., Lo, S., Menon, S., Clifford, T., Hunte, B., Lesley, R*., et al.* (2001). IL-25 induces IL-4, IL-5, and IL-13 and Th2-associated pathologies in vivo. Immunity *15*, 985-995.

Francois, S., Vidick, S., Sarlet, M., Desmecht, D., Drion, P., Stevenson, P.G., Vanderplasschen, A., and Gillet, L. (2013). Illumination of murine gammaherpesvirus-68 cycle reveals a sexual transmission route from females to males in laboratory mice. PLoS pathogens *9*, e1003292.

Fukuyama, T., Kasper, L.H., Boussouar, F., Jeevan, T., van Deursen, J., and Brindle, P.K. (2009). Histone acetyltransferase CBP is vital to demarcate conventional and innate CD8+ T-cell development. Mol Cell Biol *29*, 3894-3904.

Furze, R.C., Hussell, T., and Selkirk, M.E. (2006). Amelioration of influenza-induced pathology in mice by coinfection with Trichinella spiralis. Infect Immun *74*, 1924-1932.

Fürst, T., Duthaler, U., Sripa, B., Utzinger, J., and Keiser, J. (2012a). Trematode infections: liver and lung flukes. Infect Dis Clin North Am *26*, 399-419.

Fürst, T., Keiser, J., and Utzinger, J. (2012b). Global burden of human food-borne trematodiasis: a systematic review and meta-analysis. Lancet Infect Dis *12*, 210-221.

Gao, Y., Nish, S.A., Jiang, R., Hou, L., Licona-Limón, P., Weinstein, J.S., Zhao, H., and Medzhitov, R. (2013). Control of T helper 2 responses by transcription factor IRF4-dependent dendritic cells. Immunity *39*, 722-732.

Gause, W.C., Wynn, T.A., and Allen, J.E. (2013). Type 2 immunity and wound healing: evolutionary refinement of adaptive immunity by helminths. Nat Rev Immunol *13*, 607-614.

Gautier, E.L., Shay, T., Miller, J., Greter, M., Jakubzick, C., Ivanov, S., Helft, J., Chow, A., Elpek, K.G., Gordonov, S*., et al.* (2012). Gene-expression profiles and transcriptional regulatory pathways that underlie the identity and diversity of mouse tissue macrophages. Nat Immunol *13*, 1118-1128.

Gebhardt, T., Wakim, L.M., Eidsmo, L., Reading, P.C., Heath, W.R., and Carbone, F.R. (2009). Memory T cells in nonlymphoid tissue that provide enhanced local immunity during infection with herpes simplex virus. Nat Immunol *10*, 524-530.

Gebreselassie, N.G., Moorhead, A.R., Fabre, V., Gagliardo, L.F., Lee, N.A., Lee, J.J., and Appleton, J.A. (2012). Eosinophils preserve parasitic nematode larvae by regulating local immunity. J Immunol *188*, 417-425.

Gentleman, R.C., Carey, V.J., Bates, D.M., Bolstad, B., Dettling, M., Dudoit, S., Ellis, B., Gautier, L., Ge, Y., Gentry, J*., et al.* (2004). Bioconductor: open software development for computational biology and bioinformatics. Genome Biol *5*, R80.

Gerbe, F., Sidot, E., Smyth, D.J., Ohmoto, M., Matsumoto, I., Dardalhon, V., Cesses, P., Garnier, L., Pouzolles, M., Brulin, B*., et al.* (2016). Intestinal epithelial tuft cells initiate type 2 mucosal immunity to helminth parasites. Nature *529*, 226-230.

Gerlach, C., van Heijst, J.W., Swart, E., Sie, D., Armstrong, N., Kerkhoven, R.M., Zehn, D., Bevan, M.J., Schepers, K., and Schumacher, T.N. (2010). One naive T cell, multiple fates in CD8+ T cell differentiation. J Exp Med *207*, 1235-1246.

Gessner, A., Mohrs, K., and Mohrs, M. (2005). Mast cells, basophils, and eosinophils acquire constitutive IL-4 and IL-13 transcripts during lineage differentiation that are sufficient for rapid cytokine production. J Immunol *174*, 1063-1072.

Gieseck, R.L., 3rd, Wilson, M.S., and Wynn, T.A. (2018). Type 2 immunity in tissue repair and fibrosis. Nature reviews. Immunology *18*, 62-76.

Gieseck, R.L., Ramalingam, T.R., Hart, K.M., Vannella, K.M., Cantu, D.A., Lu, W.Y., Ferreira-González, S., Forbes, S.J., Vallier, L., and Wynn, T.A. (2016). Interleukin-13 Activates Distinct Cellular Pathways Leading to Ductular Reaction, Steatosis, and Fibrosis. Immunity *45*, 145-158.

Ginhoux, F., and Guilliams, M. (2016). Tissue-Resident Macrophage Ontogeny and Homeostasis. Immunity *44*, 439-449.

Girgis, N.M., Gundra, U.M., Ward, L.N., Cabrera, M., Frevert, U., and Loke, P. (2014). Ly6Chigh monocytes become alternatively activated macrophages in schistosome granulomas with help from CD4+ cells. PLoS Pathog *10*, e1004080.

Gleimer, M., von Boehmer, H., and Kreslavsky, T. (2012). PLZF Controls the Expression of a Limited Number of Genes Essential for NKT Cell Function. Front Immunol *3*, 374.

Godfrey, D.I., Uldrich, A.P., McCluskey, J., Rossjohn, J., and Moody, D.B. (2015). The burgeoning family of unconventional T cells. Nat Immunol *16*, 1114-1123.

Goldrath, A.W., and Bevan, M.J. (1999). Low-affinity ligands for the TCR drive proliferation of mature CD8+ T cells in lymphopenic hosts. Immunity *11*, 183-190.

Goldrath, A.W., Bogatzki, L.Y., and Bevan, M.J. (2000). Naive T cells transiently acquire a memory-like phenotype during homeostasis-driven proliferation. J Exp Med *192*, 557-564.

Goldrath, A.W., Sivakumar, P.V., Glaccum, M., Kennedy, M.K., Bevan, M.J., Benoist, C., Mathis, D., and Butz, E.A. (2002). Cytokine requirements for acute and Basal homeostatic proliferation of naive and memory CD8+ T cells. J Exp Med *195*, 1515-1522.

Gordon, S.M., Carty, S.A., Kim, J.S., Zou, T., Smith-Garvin, J., Alonzo, E.S., Haimm, E., Sant'Angelo, D.B., Koretzky, G.A., Reiner, S.L., and Jordan, M.S. (2011). Requirements for eomesodermin and promyelocytic leukemia zinc finger in the development of innate-like CD8+ T cells. J Immunol *186*, 4573-4578.

Gottstein, B., Pozio, E., and Nöckler, K. (2009). Epidemiology, diagnosis, treatment, and control of trichinellosis. Clin Microbiol Rev *22*, 127-145, Table of Contents.

Gottstein, B., Stojkovic, M., Vuitton, D.A., Millon, L., Marcinkute, A., and Deplazes, P. (2015). Threat of alveolar echinococcosis to public health--a challenge for Europe. Trends Parasitol *31*, 407-412.

Graef, P., Buchholz, V.R., Stemberger, C., Flossdorf, M., Henkel, L., Schiemann, M., Drexler, I., Höfer, T., Riddell, S.R., and Busch, D.H. (2014). Serial transfer of single-cell-derived immunocompetence reveals stemness of CD8(+) central memory T cells. Immunity *41*, 116-126.

Grainger, J.R., Smith, K.A., Hewitson, J.P., McSorley, H.J., Harcus, Y., Filbey, K.J., Finney, C.A., Greenwood, E.J., Knox, D.P., Wilson, M.S*., et al.* (2010). Helminth secretions induce de novo T cell Foxp3 expression and regulatory function through the TGF-β pathway. J Exp Med *207*, 2331-2341.

Grogan, J.L., Kremsner, P.G., Deelder, A.M., and Yazdanbakhsh, M. (1996). Elevated proliferation and interleukin-4 release from CD4+ cells after chemotherapy in human Schistosoma haematobium infection. Eur J Immunol *26*, 1365-1370.

Gruden-Movsesijan, A., and Milosavljevic Lj, S. (2006). The involvement of the macrophage mannose receptor in the innate immune response to infection with parasite Trichinella spiralis. Vet Immunol Immunopathol *109*, 57-67.

Gryseels, B., Polman, K., Clerinx, J., and Kestens, L. (2006). Human schistosomiasis. Lancet *368*, 1106-1118.

Grzych, J.M., Pearce, E., Cheever, A., Caulada, Z.A., Caspar, P., Heiny, S., Lewis, F., and Sher, A. (1991). Egg deposition is the major stimulus for the production of Th2 cytokines in murine schistosomiasis mansoni. J Immunol *146*, 1322-1327.

Guan, F., Hou, X., Nie, G., Xiao, Y., Zhang, Q., Liu, W.Q., Li, Y.L., and Lei, J.H. (2013). Effect of Trichinella spiralis infection on the immune response to HBV vaccine in a mouse model. Foodborne Pathog Dis *10*, 882-887.

Guasconi, L., Serradell, M.C., and Masih, D.T. (2012). Fasciola hepatica products induce apoptosis of peritoneal macrophages. Vet Immunol Immunopathol *148*, 359-363.

Gugasyan, R., Horat, E., Kinkel, S.A., Ross, F., Grigoriadis, G., Gray, D., O'Keeffe, M., Berzins, S.P., Belz, G.T., Grumont, R.J.*, et al.* (2012). The NF-κB1 transcription factor prevents the intrathymic development of CD8 T cells with memory properties. EMBO J *31*, 692-706.

Guilliams, M., and Scott, C.L. (2017). Does niche competition determine the origin of tissue-resident macrophages? Nat Rev Immunol *17*, 451-460.

Gundra, U.M., Girgis, N.M., Gonzalez, M.A., San Tang, M., Van Der Zande, H.J.P., Lin, J.D., Ouimet, M., Ma, L.J., Poles, J., Vozhilla, N.*, et al.* (2017). Vitamin A mediates conversion of monocyte-derived macrophages into tissue-resident macrophages during alternative activation. Nature immunology.

Gundra, U.M., Girgis, N.M., Ruckerl, D., Jenkins, S., Ward, L.N., Kurtz, Z.D., Wiens, K.E., Tang, M.S., Basu-Roy, U., Mansukhani, A.*, et al.* (2014). Alternatively activated macrophages derived from monocytes and tissue macrophages are phenotypically and functionally distinct. Blood *123*, e110-122.

Guo, L., Huang, Y., Chen, X., Hu-Li, J., Urban, J.F., Jr., and Paul, W.E. (2015). Innate immunological function of TH2 cells in vivo. Nature immunology *16*, 1051-1059.

Gupta, P., Lai, S.M., Sheng, J., Tetlak, P., Balachander, A., Claser, C., Renia, L., Karjalainen, K., and Ruedl, C. (2016a). Tissue-Resident CD169(+) Macrophages Form a Crucial Front Line against Plasmodium Infection. Cell Rep *16*, 1749-1761.

Gupta, P., Lai, S.M., Sheng, J., Tetlak, P., Balachander, A., Claser, C., Renia, L., Karjalainen, K., and Ruedl, C. (2016b). Tissue-Resident CD169(+) Macrophages Form a Crucial Front Line against Plasmodium Infection. Cell Rep *16*, 1749-1761.

Halle, S., Halle, O., and Förster, R. (2017). Mechanisms and Dynamics of T Cell-Mediated Cytotoxicity In Vivo. Trends Immunol *38*, 432-443.

Haluszczak, C., Akue, A.D., Hamilton, S.E., Johnson, L.D., Pujanauski, L., Teodorovic, L., Jameson, S.C., and Kedl, R.M. (2009). The antigen-specific CD8+ T cell repertoire in unimmunized mice includes memory phenotype cells bearing markers of homeostatic expansion. J Exp Med *206*, 435-448.

Hammad, H., and Lambrecht, B.N. (2015). Barrier Epithelial Cells and the Control of Type 2 Immunity. Immunity *43*, 29-40.

Hams, E., Aviello, G., and Fallon, P.G. (2013). The schistosoma granuloma: friend or foe? Front Immunol *4*, 89.

Harrington, L.E., Janowski, K.M., Oliver, J.R., Zajac, A.J., and Weaver, C.T. (2008). Memory CD4 T cells emerge from effector T-cell progenitors. Nature *452*, 356-360.

Harris, N.L., and Loke, P. (2017). Recent Advances in Type-2-Cell-Mediated Immunity: Insights from Helminth Infection. Immunity *47*, 1024-1036.

Hashimoto, D., Chow, A., Noizat, C., Teo, P., Beasley, M.B., Leboeuf, M., Becker, C.D., See, P., Price, J., Lucas, D.*, et al.* (2013). Tissue-resident macrophages self-maintain locally throughout adult life with minimal contribution from circulating monocytes. Immunity *38*, 792-804.

Hasnain, S.Z., Evans, C.M., Roy, M., Gallagher, A.L., Kindrachuk, K.N., Barron, L., Dickey, B.F., Wilson, M.S., Wynn, T.A., Grencis, R.K., and Thornton, D.J. (2011). Muc5ac: a critical component mediating the rejection of enteric nematodes. J Exp Med *208*, 893-900.

He, Y., Li, J., Zhuang, W., Yin, L., Chen, C., Chi, F., Bai, Y., and Chen, X.P. (2010). The inhibitory effect against collagen-induced arthritis by Schistosoma japonicum infection is infection stage-dependent. BMC Immunol *11*, 28.

Helmby, H., Kullberg, M., and Troye-Blomberg, M. (1998). Altered immune responses in mice with concomitant Schistosoma mansoni and Plasmodium chabaudi infections. Infect Immun *66*, 5167-5174.

Hepworth, M.R., Daniłowicz-Luebert, E., Rausch, S., Metz, M., Klotz, C., Maurer, M., and Hartmann, S. (2012). Mast cells orchestrate type 2 immunity to helminths through regulation of tissue-derived cytokines. Proc Natl Acad Sci U S A *109*, 6644-6649.

Herbert, D.R., Holscher, C., Mohrs, M., Arendse, B., Schwegmann, A., Radwanska, M., Leeto, M., Kirsch, R., Hall, P., Mossmann, H.*, et al.* (2004). Alternative macrophage activation is essential for survival during schistosomiasis and downmodulates T helper 1 responses and immunopathology. Immunity *20*, 623-635.

Herbert, D.R., Orekov, T., Perkins, C., Rothenberg, M.E., and Finkelman, F.D. (2008). IL-4R alpha expression by bone marrow-derived cells is necessary and sufficient for host protection against acute schistosomiasis. J Immunol *180*, 4948-4955.

Herbert, D.R., Orekov, T., Roloson, A., Ilies, M., Perkins, C., O'Brien, W., Cederbaum, S., Christianson, D.W., Zimmermann, N., Rothenberg, M.E., and Finkelman, F.D. (2010). Arginase I suppresses IL-12/IL-23p40-driven intestinal inflammation during acute schistosomiasis. J Immunol *184*, 6438-6446.

Herbert, D.R., Yang, J.Q., Hogan, S.P., Groschwitz, K., Khodoun, M., Munitz, A., Orekov, T., Perkins, C., Wang, Q., Brombacher, F.*, et al.* (2009). Intestinal epithelial cell secretion of RELM-beta protects against gastrointestinal worm infection. J Exp Med *206*, 2947-2957.

Herndler-Brandstetter, D., Ishigame, H., Shinnakasu, R., Plajer, V., Stecher, C., Zhao, J., Lietzenmayer, M., Kroehling, L., Takumi, A., Kometani, K.*, et al.* (2018). KLRG1. Immunity *48*, 716-729.e718.

Herricks, J.R., Hotez, P.J., Wanga, V., Coffeng, L.E., Haagsma, J.A., Basáñez, M.G., Buckle, G., Budke, C.M., Carabin, H., Fèvre, E.M.*, et al.* (2017). The global burden of disease study 2013: What does it mean for the NTDs? PLoS Negl Trop Dis *11*, e0005424.

Hesse, M., Modolell, M., La Flamme, A.C., Schito, M., Fuentes, J.M., Cheever, A.W., Pearce, E.J., and Wynn, T.A. (2001). Differential regulation of nitric oxide synthase-2 and arginase-1 by type 1/type 2 cytokines in vivo: granulomatous pathology is shaped by the pattern of L-arginine metabolism. J Immunol *167*, 6533-6544.

Hirose, S., Touma, M., Go, R., Katsuragi, Y., Sakuraba, Y., Gondo, Y., Abe, M., Sakimura, K., Mishima, Y., and Kominami, R. (2015). Bcl11b prevents the intrathymic development of innate CD8 T cells in a cell intrinsic manner. Int Immunol *27*, 205-215.

Hoffmann, W., Petit, G., Schulz-Key, H., Taylor, D., Bain, O., and Le Goff, L. (2000). Litomosoides sigmodontis in mice: reappraisal of an old model for filarial research. Parasitol Today *16*, 387-389.

Holgate, S.T. (2012). Trials and tribulations in identifying new biologic treatments for asthma. Trends Immunol *33*, 238-246.

Homer, R.J., Zhu, Z., Cohn, L., Lee, C.G., White, W.I., Chen, S., and Elias, J.A. (2006). Differential expression of chitinases identify subsets of murine airway epithelial cells in allergic inflammation. Am J Physiol Lung Cell Mol Physiol *291*, L502-511.

Horsnell, W.G., and Brombacher, F. (2007). Alternatively activated macrophages in experimental parasitic infections. In Advances in the immunobiology of parasitic diseases, L.I. Terrazas, ed. (Kerala: Research Signpost), pp. 1-19.

Horsnell, W.G., Cutler, A.J., Hoving, J.C., Mearns, H., Myburgh, E., Arendse, B., Finkelman, F.D., Owens, G.K., Erle, D., and Brombacher, F. (2007). Delayed goblet cell hyperplasia, acetylcholine receptor expression, and worm expulsion in SMC-specific IL-4Ralpha-deficient mice. PLoS Pathog *3*, e1.

Horsnell, W.G., Darby, M.G., Hoving, J.C., Nieuwenhuizen, N., McSorley, H.J., Ndlovu, H., Bobat, S., Kimberg, M., Kirstein, F., Cutler, A.J.*, et al.* (2013). IL-4Ralpha-associated antigen processing by B cells promotes immunity in Nippostrongylus brasiliensis infection. PLoS pathogens *9*, e1003662.

Hotez, P.J., Brindley, P.J., Bethony, J.M., King, C.H., Pearce, E.J., and Jacobson, J. (2008). Helminth infections: the great neglected tropical diseases. J Clin Invest *118*, 1311-1321.

Hotez, P.J., Bundy, D.A.P., Beegle, K., Brooker, S., Drake, L., de Silva, N., Montresor, A., Engels, D., Jukes, M., Chitsulo, L*., et al.* (2006). Helminth Infections: Soil-transmitted Helminth Infections and Schistosomiasis. In Disease Control Priorities in Developing Countries, D.T. Jamison, J.G. Breman, A.R. Measham, G. Alleyne, M. Claeson, D.B. Evans, P. Jha, A. Mills, and P. Musgrove, eds. (Washington (DC)).

Howitt, M.R., Lavoie, S., Michaud, M., Blum, A.M., Tran, S.V., Weinstock, J.V., Gallini, C.A., Redding, K., Margolskee, R.F., Osborne, L.C*., et al.* (2016). Tuft cells, taste-chemosensory cells, orchestrate parasite type 2 immunity in the gut. Science *351*, 1329-1333.

Huang, L., Gebreselassie, N.G., Gagliardo, L.F., Ruyechan, M.C., Luber, K.L., Lee, N.A., Lee, J.J., and Appleton, J.A. (2015). Eosinophils mediate protective immunity against secondary nematode infection. J Immunol *194*, 283-290.

Huber, S., Hoffmann, R., Muskens, F., and Voehringer, D. (2010). Alternatively activated macrophages inhibit T-cell proliferation by Stat6-dependent expression of PD-L2. Blood *116*, 3311-3320.

Humphreys, N.E., Xu, D., Hepworth, M.R., Liew, F.Y., and Grencis, R.K. (2008). IL-33, a potent inducer of adaptive immunity to intestinal nematodes. J Immunol *180*, 2443-2449.

Hung, L.Y., Lewkowich, I.P., Dawson, L.A., Downey, J., Yang, Y., Smith, D.E., and Herbert, D.R. (2013). IL-33 drives biphasic IL-13 production for noncanonical Type 2 immunity against hookworms. Proc Natl Acad Sci U S A *110*, 282-287.

Hussaarts, L., Yazdanbakhsh, M., and Guigas, B. (2014). Priming dendritic cells for th2 polarization: lessons learned from helminths and implications for metabolic disorders. Front Immunol *5*, 499.

Ikeda, N., Asano, K., Kikuchi, K., Uchida, Y., Ikegami, H., Takagi, R., Yotsumoto, S., Shibuya, T., Makino-Okamura, C., Fukuyama, H*., et al.* (2018). Emergence of immunoregulatory Ym1+ Ly6Chi monocytes during recovery phase of tissue injury. Sci Immunol *3*.

Ince, M.N., Elliott, D.E., Setiawan, T., Metwali, A., Blum, A., Chen, H.L., Urban, J.F., Flavell, R.A., and Weinstock, J.V. (2009). Role of T cell TGF-beta signaling in intestinal cytokine responses and helminthic immune modulation. Eur J Immunol *39*, 1870-1878.

Intlekofer, A.M., Banerjee, A., Takemoto, N., Gordon, S.M., Dejong, C.S., Shin, H., Hunter, C.A., Wherry, E.J., Lindsten, T., and Reiner, S.L. (2008). Anomalous type 17 response to viral infection by CD8+ T cells lacking T-bet and eomesodermin. Science *321*, 408-411.

Intlekofer, A.M., Takemoto, N., Kao, C., Banerjee, A., Schambach, F., Northrop, J.K., Shen, H., Wherry, E.J., and Reiner, S.L. (2007). Requirement for T-bet in the aberrant differentiation of unhelped memory CD8+ T cells. J Exp Med *204*, 2015-2021.

Intlekofer, A.M., Takemoto, N., Wherry, E.J., Longworth, S.A., Northrup, J.T., Palanivel, V.R., Mullen, A.C., Gasink, C.R., Kaech, S.M., Miller, J.D*., et al.* (2005). Effector and memory CD8+ T cell fate coupled by T-bet and eomesodermin. Nat Immunol *6*, 1236-1244.

Ito, A., Honey, R.D., Scanlon, T., Lightowlers, M.W., and Rickard, M.D. (1988). Analysis of antibody responses to Hymenolepis nana infection in mice by the enzyme-linked immunosorbent assay and immunoprecipitation. Parasite Immunol *10*, 265-277.

Ito, T., Wang, Y.H., Duramad, O., Hori, T., Delespesse, G.J., Watanabe, N., Qin, F.X., Yao, Z., Cao, W., and Liu, Y.J. (2005). TSLP-activated dendritic cells induce an inflammatory T helper type 2 cell response through OX40 ligand. J Exp Med *202*, 1213-1223.

Iwasaki, A., and Medzhitov, R. (2015). Control of adaptive immunity by the innate immune system. Nat Immunol *16*, 343-353.

Jackson-Jones, L.H., Rückerl, D., Svedberg, F., Duncan, S., Maizels, R.M., Sutherland, T.E., Jenkins, S.J., McSorley, H.J., Bénézech, C., MacDonald, A.S., and Allen, J.E. (2016). IL-33 delivery induces serous cavity macrophage proliferation independent of interleukin-4 receptor alpha. Eur J Immunol *46*, 2311-2321.

Jacomet, F., Cayssials, E., Basbous, S., Levescot, A., Piccirilli, N., Desmier, D., Robin, A., Barra, A., Giraud, C., Guilhot, F.*, et al.* (2015). Evidence for eomesodermin-expressing innate-like CD8(+) KIR/NKG2A(+) T cells in human adults and cord blood samples. European journal of immunology *45*, 1926-1933.

Jaguin, M., Houlbert, N., Fardel, O., and Lecureur, V. (2013). Polarization profiles of human M-CSF-generated macrophages and comparison of M1-markers in classically activated macrophages from GM-CSF and M-CSF origin. Cell Immunol *281*, 51-61.

Jakubzick, C., Gautier, E.L., Gibbings, S.L., Sojka, D.K., Schlitzer, A., Johnson, T.E., Ivanov, S., Duan, Q., Bala, S., Condon, T.*, et al.* (2013). Minimal differentiation of classical monocytes as they survey steady-state tissues and transport antigen to lymph nodes. Immunity *39*, 599-610.

Jameson, S.C., Lee, Y.J., and Hogquist, K.A. (2015). Innate memory T cells. Adv Immunol *126*, 173-213.

Jameson, S.C., and Masopust, D. (2018). Understanding Subset Diversity in T Cell Memory. Immunity *48*, 214-226.

Jankovic, D., Kullberg, M.C., Noben-Trauth, N., Caspar, P., Ward, J.M., Cheever, A.W., Paul, W.E., and Sher, A. (1999). Schistosome-infected IL-4 receptor knockout (KO) mice, in contrast to IL-4 KO mice, fail to develop granulomatous pathology while maintaining the same lymphokine expression profile. J Immunol *163*, 337-342.

Jenkins, S.J., and Allen, J.E. (2010). Similarity and diversity in macrophage activation by nematodes, trematodes, and cestodes. J Biomed Biotechnol *2010*, 262609.

Jenkins, S.J., Ruckerl, D., Cook, P.C., Jones, L.H., Finkelman, F.D., van Rooijen, N., MacDonald, A.S., and Allen, J.E. (2011). Local macrophage proliferation, rather than recruitment from the blood, is a signature of TH2 inflammation. Science *332*, 1284-1288.

Jenkins, S.J., Ruckerl, D., Thomas, G.D., Hewitson, J.P., Duncan, S., Brombacher, F., Maizels, R.M., Hume, D.A., and Allen, J.E. (2013). IL-4 directly signals tissue-resident macrophages to proliferate beyond homeostatic levels controlled by CSF-1. The Journal of experimental medicine *210*, 2477-2491.

Jiang, J., Fisher, E.M., Hensley, S.E., Lustigman, S., Murasko, D.M., and Shen, H. (2014). Antigen sparing and enhanced protection using a novel rOv-ASP-1 adjuvant in aqueous formulation with influenza vaccines. Vaccine *32*, 2696-2702.

Joffre, O.P., Segura, E., Savina, A., and Amigorena, S. (2012). Cross-presentation by dendritic cells. Nat Rev Immunol *12*, 557-569.

Johnston, C.J., Robertson, E., Harcus, Y., Grainger, J.R., Coakley, G., Smyth, D.J., McSorley, H.J., and Maizels, R. (2015). Cultivation of Heligmosomoides polygyrus: an immunomodulatory nematode parasite and its secreted products. Journal of visualized experiments : JoVE, e52412.

Johnston, C.J.C., Smyth, D.J., Kodali, R.B., White, M.P.J., Harcus, Y., Filbey, K.J., Hewitson, J.P., Hinck, C.S., Ivens, A., Kemter, A.M*., et al.* (2017). A structurally distinct TGF-β mimic from an intestinal helminth parasite potently induces regulatory T cells. Nat Commun *8*, 1741.

Joshi, N.S., Cui, W., Chandele, A., Lee, H.K., Urso, D.R., Hagman, J., Gapin, L., and Kaech, S.M. (2007). Inflammation directs memory precursor and short-lived effector CD8(+) T cell fates via the graded expression of T-bet transcription factor. Immunity *27*, 281-295.

Jourdan, P.M., Lamberton, P.H.L., Fenwick, A., and Addiss, D.G. (2017). Soil-transmitted helminth infections. Lancet.

Joyce, K.L., Morgan, W., Greenberg, R., and Nair, M.G. (2012). Using eggs from Schistosoma mansoni as an in vivo model of helminth-induced lung inflammation. Journal of visualized experiments : JoVE, e3905.

Judge, A.D., Zhang, X., Fujii, H., Surh, C.D., and Sprent, J. (2002). Interleukin 15 controls both proliferation and survival of a subset of memory-phenotype CD8(+) T cells. J Exp Med *196*, 935-946.

Jung, Y.W., Kim, H.G., Perry, C.J., and Kaech, S.M. (2016). CCR7 expression alters memory CD8 T-cell homeostasis by regulating occupancy in IL-7- and IL-15-dependent niches. Proc Natl Acad Sci U S A *113*, 8278-8283.

Junttila, I.S. (2018). Tuning the Cytokine Responses: An Update on Interleukin (IL)-4 and IL-13 Receptor Complexes. Front Immunol *9*, 888.

Kaech, S.M., and Cui, W. (2012). Transcriptional control of effector and memory CD8+ T cell differentiation. Nat Rev Immunol *12*, 749-761.

Kaech, S.M., Tan, J.T., Wherry, E.J., Konieczny, B.T., Surh, C.D., and Ahmed, R. (2003). Selective expression of the interleukin 7 receptor identifies effector CD8 T cells that give rise to long-lived memory cells. Nat Immunol *4*, 1191-1198.

Kaech, S.M., and Wherry, E.J. (2007). Heterogeneity and cell-fate decisions in effector and memory CD8+ T cell differentiation during viral infection. Immunity *27*, 393-405.

Kambayashi, T., and Laufer, T.M. (2014). Atypical MHC class II-expressing antigen-presenting cells: can anything replace a dendritic cell? Nat Rev Immunol *14*, 719-730.

Kamimura, D., and Bevan, M.J. (2007). Naive CD8+ T cells differentiate into protective memory-like cells after IL-2 anti IL-2 complex treatment in vivo. J Exp Med *204*, 1803-1812.

Kane, C.M., Cervi, L., Sun, J., McKee, A.S., Masek, K.S., Shapira, S., Hunter, C.A., and Pearce, E.J. (2004). Helminth antigens modulate TLR-initiated dendritic cell activation. J Immunol *173*, 7454-7461.

Keiser, J., and Utzinger, J. (2009). Food-borne trematodiases. Clin Microbiol Rev *22*, 466-483.

Kheradmand, F., Kiss, A., Xu, J., Lee, S.H., Kolattukudy, P.E., and Corry, D.B. (2002). A protease-activated pathway underlying Th cell type 2 activation and allergic lung disease. J Immunol *169*, 5904-5911.

Kieper, W.C., Burghardt, J.T., and Surh, C.D. (2004). A role for TCR affinity in regulating naive T cell homeostasis. J Immunol *172*, 40-44.

Kieper, W.C., and Jameson, S.C. (1999). Homeostatic expansion and phenotypic conversion of naïve T cells in response to self peptide/MHC ligands. Proc Natl Acad Sci U S A *96*, 13306-13311.

Kitagaki, K., Businga, T.R., Racila, D., Elliott, D.E., Weinstock, J.V., and Kline, J.N. (2006). Intestinal helminths protect in a murine model of asthma. J Immunol *177*, 1628-1635.

Klose, C.S.N., Mahlakõiv, T., Moeller, J.B., Rankin, L.C., Flamar, A.L., Kabata, H., Monticelli, L.A., Moriyama, S., Putzel, G.G., Rakhilin, N*., et al.* (2017). The neuropeptide neuromedin U stimulates innate lymphoid cells and type 2 inflammation. Nature *549*, 282-286.

Knight, P.A., Wright, S.H., Lawrence, C.E., Paterson, Y.Y., and Miller, H.R. (2000). Delayed expulsion of the nematode Trichinella spiralis in mice lacking the mucosal mast cell-specific granule chymase, mouse mast cell protease-1. J Exp Med *192*, 1849-1856.

Knipper, J.A., Willenborg, S., Brinckmann, J., Bloch, W., Maaß, T., Wagener, R., Krieg, T., Sutherland, T., Munitz, A., Rothenberg, M.E*., et al.* (2015). Interleukin-4 Receptor α Signaling in Myeloid Cells Controls Collagen Fibril Assembly in Skin Repair. Immunity *43*, 803-816.

Kondo, Y., Yoshimoto, T., Yasuda, K., Futatsugi-Yumikura, S., Morimoto, M., Hayashi, N., Hoshino, T., Fujimoto, J., and Nakanishi, K. (2008). Administration of IL-33 induces airway hyperresponsiveness and goblet cell hyperplasia in the lungs in the absence of adaptive immune system. Int Immunol *20*, 791-800.

Kool, M., Willart, M.A., van Nimwegen, M., Bergen, I., Pouliot, P., Virchow, J.C., Rogers, N., Osorio, F., Reis e Sousa, C., Reis E Sousa, C*., et al.* (2011). An unexpected role for uric acid as an inducer of T helper 2 cell immunity to inhaled antigens and inflammatory mediator of allergic asthma. Immunity *34*, 527-540.

Kouzaki, H., Iijima, K., Kobayashi, T., O'Grady, S.M., and Kita, H. (2011). The danger signal, extracellular ATP, is a sensor for an airborne allergen and triggers IL-33 release and innate Th2-type responses. J Immunol *186*, 4375-4387.

Kouzaki, H., O'Grady, S.M., Lawrence, C.B., and Kita, H. (2009). Proteases induce production of thymic stromal lymphopoietin by airway epithelial cells through protease-activated receptor-2. J Immunol *183*, 1427-1434.

Kovalovsky, D., Uche, O.U., Eladad, S., Hobbs, R.M., Yi, W., Alonzo, E., Chua, K., Eidson, M., Kim, H.J., Im, J.S*., et al.* (2008). The BTB-zinc finger transcriptional regulator PLZF controls the development of invariant natural killer T cell effector functions. Nat Immunol *9*, 1055-1064.

Ku, C.C., Murakami, M., Sakamoto, A., Kappler, J., and Marrack, P. (2000). Control of homeostasis of CD8+ memory T cells by opposing cytokines. Science *288*, 675-678.

Kumamoto, Y., Linehan, M., Weinstein, J.S., Laidlaw, B.J., Craft, J.E., and Iwasaki, A. (2013). CD301b^{+} dermal dendritic cells drive T helper 2 cell-mediated immunity. Immunity *39*, 733-743.

Kurzweil, V., LaRoche, A., and Oliver, P.M. (2014). Increased peripheral IL-4 leads to an expanded virtual memory CD8+ population. J Immunol *192*, 5643-5651.

Lai, D., Zhu, J., Wang, T., Hu-Li, J., Terabe, M., Berzofsky, J.A., Clayberger, C., and Krensky, A.M. (2011). KLF13 sustains thymic memory-like CD8(+) T cells in BALB/c mice by regulating IL-4-generating invariant natural killer T cells. J Exp Med *208*, 1093-1103.

Laranjeiras, R.F., Brant, L.C., Lima, A.C., Coelho, P.M., and Braga, E.M. (2008). Reduced protective effect of Plasmodium berghei immunization by concurrent Schistosoma mansoni infection. Mem Inst Oswaldo Cruz *103*, 674-677.

Latif, M.B., Machiels, B., Xiao, X., Mast, J., Vanderplasschen, A., and Gillet, L. (2015). Deletion of Murid Herpesvirus 4 ORF63 Affects the Trafficking of Incoming Capsids toward the Nucleus. Journal of virology *90*, 2455-2472.

Le Campion, A., Bourgeois, C., Lambolez, F., Martin, B., Léaument, S., Dautigny, N., Tanchot, C., Pénit, C., and Lucas, B. (2002). Naive T cells proliferate strongly in neonatal mice in response to self-peptide/self-MHC complexes. Proc Natl Acad Sci U S A *99*, 4538-4543.

Lee, J.Y., Hamilton, S.E., Akue, A.D., Hogquist, K.A., and Jameson, S.C. (2013a). Virtual memory CD8 T cells display unique functional properties. Proc Natl Acad Sci U S A *110*, 13498-13503.

Lee, M.R., Lim, C.J., Lee, Y.H., Park, J.G., Sonn, S.K., Lee, M.N., Jung, I.H., Jeong, S.J., Jeon, S., Lee, M*., et al.* (2014). The adipokine Retnla modulates cholesterol homeostasis in hyperlipidemic mice. Nat Commun *5*, 4410.

Lee, Y.J., Holzapfel, K.L., Zhu, J., Jameson, S.C., and Hogquist, K.A. (2013b). Steady-state production of IL-4 modulates immunity in mouse strains and is determined by lineage diversity of iNKT cells. Nat Immunol *14*, 1146-1154.

Leonardi-Bee, J., Pritchard, D., and Britton, J. (2006). Asthma and current intestinal parasite infection: systematic review and meta-analysis. Am J Respir Crit Care Med *174*, 514-523.

Li, Q., Rao, R.R., Araki, K., Pollizzi, K., Odunsi, K., Powell, J.D., and Shrikant, P.A. (2011). A central role for mTOR kinase in homeostatic proliferation induced CD8+ T cell memory and tumor immunity. Immunity *34*, 541-553.

Lin, J.S., Mohrs, K., Szaba, F.M., Kummer, L.W., Leadbetter, E.A., and Mohrs, M. (2018). Virtual memory CD8 T cells expanded by helminth infection confer broad protection against bacterial infection. Mucosal Immunol.

Linehan, S.A., Coulson, P.S., Wilson, R.A., Mountford, A.P., Brombacher, F., Martinez-Pomares, L., and Gordon, S. (2003). IL-4 receptor signaling is required for mannose receptor expression by macrophages recruited to granulomata but not resident cells in mice infected with Schistosoma mansoni. Lab Invest *83*, 1223-1231.

Liu, P., Jenkins, N.A., and Copeland, N.G. (2003). A highly efficient recombineering-based method for generating conditional knockout mutations. Genome research *13*, 476-484.

Liu, T., Dhanasekaran, S.M., Jin, H., Hu, B., Tomlins, S.A., Chinnaiyan, A.M., and Phan, S.H. (2004). FIZZ1 stimulation of myofibroblast differentiation. Am J Pathol *164*, 1315-1326.

Liu, Y.J., Soumelis, V., Watanabe, N., Ito, T., Wang, Y.H., Malefyt, R.e.W., Omori, M., Zhou, B., and Ziegler, S.F. (2007). TSLP: an epithelial cell cytokine that regulates T cell differentiation by conditioning dendritic cell maturation. Annu Rev Immunol *25*, 193-219.

Loke, P., and Allison, J.P. (2003). PD-L1 and PD-L2 are differentially regulated by Th1 and Th2 cells. Proceedings of the National Academy of Sciences of the United States of America *100*, 5336-5341.

Loke, P., MacDonald, A.S., Robb, A., Maizels, R.M., and Allen, J.E. (2000). Alternatively activated macrophages induced by nematode infection inhibit proliferation via cell-to-cell contact. Eur J Immunol *30*, 2669-2678.

Loke, P., Nair, M.G., Parkinson, J., Guiliano, D., Blaxter, M., and Allen, J.E. (2002). IL-4 dependent alternatively-activated macrophages have a distinctive in vivo gene expression phenotype. BMC Immunol *3*, 7.

Lopez, A.D., Mathers, C.D., Ezzati, M., Jamison, D.T., and Murray, C.J.L. (2006). Chapter 1 - Measuring the Global Burden of Disease and Risk Factors, 1990–2001 in : Global Burden of Disease and Risk Factors (New York: Oxford University Press).

Lott, J.M., Sumpter, T.L., and Turnquist, H.R. (2015). New dog and new tricks: evolving roles for IL-33 in type 2 immunity. J Leukoc Biol *97*, 1037-1048.

Luche, H., Weber, O., Nageswara Rao, T., Blum, C., and Fehling, H.J. (2007). Faithful activation of an extra-bright red fluorescent protein in "knock-in" Cre-reporter mice ideally suited for lineage tracing studies. European journal of immunology *37*, 43-53.

Lynch, N.R., Palenque, M., Hagel, I., and DiPrisco, M.C. (1997). Clinical improvement of asthma after anthelminthic treatment in a tropical situation. Am J Respir Crit Care Med *156*, 50-54.

Ma, X., Zhao, H., Zhang, F., Zhu, Y., Peng, S., Ma, H., Cao, C., Xin, Y., Yimiti, D., Wen, H., and Ding, J. (2016). Activity in mice of recombinant BCG-EgG1Y162 vaccine for Echinococcus granulosus infection. Hum Vaccin Immunother *12*, 170-175.

MacDonald, A.S., Straw, A.D., Bauman, B., and Pearce, E.J. (2001). CD8- dendritic cell activation status plays an integral role in influencing Th2 response development. J Immunol *167*, 1982-1988.

Machiels, B., Dourcy, M., Xiao, X., Javaux, J., Mesnil, C., Sabatel, C., Desmecht, D., Lallemand, F., Martinive, P., Hammad, H.*, et al.* (2017). A gammaherpesvirus provides protection against allergic asthma by inducing the replacement of resident alveolar macrophages with regulatory monocytes. Nature immunology *18*, 1310-1320.

Madden, K.B., Yeung, K.A., Zhao, A., Gause, W.C., Finkelman, F.D., Katona, I.M., Urban, J.F., and Shea-Donohue, T. (2004). Enteric nematodes induce stereotypic STAT6-dependent alterations in intestinal epithelial cell function. J Immunol *172*, 5616-5621.

Maizels, R.M., and Gause, W.C. (2014). Immunology. How helminths go viral. Science *345*, 517-518.

Maizels, R.M., and McSorley, H.J. (2016). Regulation of the host immune system by helminth parasites. J Allergy Clin Immunol *138*, 666-675.

Mangan, N.E., van Rooijen, N., McKenzie, A.N., and Fallon, P.G. (2006). Helminth-modified pulmonary immune response protects mice from allergen-induced airway hyperresponsiveness. J Immunol *176*, 138-147.

Marichal, T., Starkl, P., Reber, L.L., Kalesnikoff, J., Oettgen, H.C., Tsai, M., Metz, M., and Galli, S.J. (2013). A beneficial role for immunoglobulin E in host defense against honeybee venom. Immunity *39*, 963-975.

Marple, A., Wu, W., Shah, S., Zhao, Y., Du, P., Gause, W.C., and Yap, G.S. (2016). Cutting Edge: Helminth Coinfection Blocks Effector Differentiation of CD8 T Cells through Alternate Host Th2- and IL-10-Mediated Responses. J Immunol.

Marsland, B.J., Schmitz, N., and Kopf, M. (2005). IL-4Ralpha signaling is important for CD8+ T cell cytotoxicity in the absence of CD4+ T cell help. European journal of immunology *35*, 1391-1398.

Martinet, V., Tonon, S., Torres, D., Azouz, A., Nguyen, M., Kohler, A., Flamand, V., Mao, C.A., Klein, W.H., Leo, O., and Goriely, S. (2015). Type I interferons regulate eomesodermin expression and the development of unconventional memory CD8(+) T cells. Nature communications *6*, 7089.

Martinez-Pomares, L., Reid, D.M., Brown, G.D., Taylor, P.R., Stillion, R.J., Linehan, S.A., Zamze, S., Gordon, S., and Wong, S.Y. (2003). Analysis of mannose receptor regulation by IL-4, IL-10, and proteolytic processing using novel monoclonal antibodies. Journal of leukocyte biology *73*, 604-613.

Masopust, D., Choo, D., Vezys, V., Wherry, E.J., Duraiswamy, J., Akondy, R., Wang, J., Casey, K.A., Barber, D.L., Kawamura, K.S.*, et al.* (2010). Dynamic T cell migration program provides resident memory within intestinal epithelium. J Exp Med *207*, 553-564.

Masopust, D., Vezys, V., Marzo, A.L., and Lefrançois, L. (2001). Preferential localization of effector memory cells in nonlymphoid tissue. Science *291*, 2413-2417.

Massacand, J.C., Stettler, R.C., Meier, R., Humphreys, N.E., Grencis, R.K., Marsland, B.J., and Harris, N.L. (2009). Helminth products bypass the need for TSLP in Th2 immune responses by directly modulating dendritic cell function. Proc Natl Acad Sci U S A *106*, 13968-13973.

Matisz, C.E., Faz-López, B., Thomson, E., Al Rajabi, A., Lopes, F., Terrazas, L.I., Wang, A., Sharkey, K.A., and McKay, D.M. (2017). Suppression of colitis by adoptive transfer of helminth antigen-treated dendritic cells requires interleukin-4 receptor-α signaling. Sci Rep *7*, 40631.

Matta, B.M., Lott, J.M., Mathews, L.R., Liu, Q., Rosborough, B.R., Blazar, B.R., and Turnquist, H.R. (2014). IL-33 is an unconventional Alarmin that stimulates IL-2 secretion by dendritic cells to selectively expand IL-33R/ST2+ regulatory T cells. J Immunol *193*, 4010-4020.

Maurice, D., Costello, P., Sargent, M., and Treisman, R. (2018). ERK Signaling Controls Innate-like CD8. J Immunol.

McCoy, K., Camberis, M., and Gros, G.L. (1997). Protective immunity to nematode infection is induced by CTLA-4 blockade. J Exp Med *186*, 183-187.

McCubbrey, A.L., Allison, K.C., Lee-Sherick, A.B., Jakubzick, C.V., and Janssen, W.J. (2017). Promoter Specificity and Efficacy in Conditional and Inducible Transgenic Targeting of Lung Macrophages. Front Immunol *8*, 1618.

McDermott, J.R., Bartram, R.E., Knight, P.A., Miller, H.R., Garrod, D.R., and Grencis, R.K. (2003). Mast cells disrupt epithelial barrier function during enteric nematode infection. Proc Natl Acad Sci U S A *100*, 7761-7766.

McFarlane, A.J., McSorley, H.J., Davidson, D.J., Fitch, P.M., Errington, C., Mackenzie, K.J., Gollwitzer, E.S., Johnston, C.J.C., MacDonald, A.S., Edwards, M.R*., et al.* (2017). Enteric helminth-induced type I interferon signaling protects against pulmonary virus infection through interaction with the microbiota. J Allergy Clin Immunol *140*, 1068-1078.e1066.

McKay, D.M., Halton, D.W., McCaigue, M.D., Johnston, C.F., Fairweather, I., and Shaw, C. (1990). Hymenolepis diminuta: intestinal goblet cell response to infection in male C57 mice. Exp Parasitol *71*, 9-20.

McKenzie, G.J., Bancroft, A., Grencis, R.K., and McKenzie, A.N. (1998). A distinct role for interleukin-13 in Th2-cell-mediated immune responses. Curr Biol *8*, 339-342.

McKenzie, G.J., Fallon, P.G., Emson, C.L., Grencis, R.K., and McKenzie, A.N. (1999). Simultaneous disruption of interleukin (IL)-4 and IL-13 defines individual roles in T helper cell type 2-mediated responses. J Exp Med *189*, 1565-1572.

McSorley, H.J., Blair, N.F., Smith, K.A., McKenzie, A.N., and Maizels, R.M. (2014). Blockade of IL-33 release and suppression of type 2 innate lymphoid cell responses by helminth secreted products in airway allergy. Mucosal Immunol *7*, 1068-1078.

McSorley, H.J., and Maizels, R.M. (2012). Helminth infections and host immune regulation. Clin Microbiol Rev *25*, 585-608.

McSorley, H.J., O'Gorman, M.T., Blair, N., Sutherland, T.E., Filbey, K.J., and Maizels, R.M. (2012). Suppression of type 2 immunity and allergic airway inflammation by secreted products of the helminth Heligmosomoides polygyrus. Eur J Immunol *42*, 2667-2682.

Means, A.R., Burns, P., Sinclair, D., and Walson, J.L. (2016). Antihelminthics in helminth-endemic areas: effects on HIV disease progression. Cochrane Database Syst Rev *4*, CD006419.

Mehlhop-Williams, E.R., and Bevan, M.J. (2014). Memory CD8+ T cells exhibit increased antigen threshold requirements for recall proliferation. J Exp Med *211*, 345-356.

Melendez, A.J., Harnett, M.M., Pushparaj, P.N., Wong, W.S., Tay, H.K., McSharry, C.P., and Harnett, W. (2007). Inhibition of Fc epsilon RI-mediated mast cell responses by ES-62, a product of parasitic filarial nematodes. Nat Med *13*, 1375-1381.

Merad, M., Manz, M.G., Karsunky, H., Wagers, A., Peters, W., Charo, I., Weissman, I.L., Cyster, J.G., and Engleman, E.G. (2002). Langerhans cells renew in the skin throughout life under steady-state conditions. Nat Immunol *3*, 1135-1141.

Mesri, E.A., Cesarman, E., and Boshoff, C. (2010). Kaposi's sarcoma and its associated herpesvirus. Nat Rev Cancer *10*, 707-719.

Metenou, S., Kovacs, M., Dembele, B., Coulibaly, Y.I., Klion, A.D., and Nutman, T.B. (2012). Interferon regulatory factor modulation underlies the bystander suppression of malaria antigen-driven IL-12 and IFN-γ in filaria-malaria co-infection. Eur J Immunol *42*, 641-650.

Milho, R., Smith, C.M., Marques, S., Alenquer, M., May, J.S., Gillet, L., Gaspar, M., Efstathiou, S., Simas, J.P., and Stevenson, P.G. (2009). In vivo imaging of murid herpesvirus-4 infection. The Journal of general virology *90*, 21-32.

Min, B., McHugh, R., Sempowski, G.D., Mackall, C., Foucras, G., and Paul, W.E. (2003). Neonates support lymphopenia-induced proliferation. Immunity *18*, 131-140.

Min, H.S., Lee, Y.J., Jeon, Y.K., Kim, E.J., Kang, B.H., Jung, K.C., Chang, C.H., and Park, S.H. (2011). MHC class II-restricted interaction between thymocytes plays an essential role in the production of innate CD8+ T cells. J Immunol *186*, 5749-5757.

Minutti, C.M., Drube, S., Blair, N., Schwartz, C., McCrae, J.C., McKenzie, A.N., Kamradt, T., Mokry, M., Coffer, P.J., Sibilia, M.*, et al.* (2017a). Epidermal Growth Factor Receptor Expression Licenses Type-2 Helper T Cells to Function in a T Cell Receptor-Independent Fashion. Immunity *47*, 710-722 e716.

Minutti, C.M., Jackson-Jones, L.H., Garcia-Fojeda, B., Knipper, J.A., Sutherland, T.E., Logan, N., Rinqvist, E., Guillamat-Prats, R., Ferenbach, D.A., Artigas, A.*, et al.* (2017b). Local amplifiers of IL-4Ralpha-mediated macrophage activation promote repair in lung and liver. Science.

Mirchandani, A.S., Salmond, R.J., and Liew, F.Y. (2012). Interleukin-33 and the function of innate lymphoid cells. Trends Immunol *33*, 389-396.

Misharin, A.V., Morales-Nebreda, L., Reyfman, P.A., Cuda, C.M., Walter, J.M., McQuattie-Pimentel, A.C., Chen, C.I., Anekalla, K.R., Joshi, N., Williams, K.J.N.*, et al.* (2017). Monocyte-derived alveolar macrophages drive lung fibrosis and persist in the lung over the life span. J Exp Med *214*, 2387-2404.

Mishra, B.B., Gundra, U.M., and Teale, J.M. (2011a). STAT6^{-}/$^{-}$ mice exhibit decreased cells with alternatively activated macrophage phenotypes and enhanced disease severity in murine neurocysticercosis. J Neuroimmunol *232*, 26-34.

Mishra, P.K., Wu, W., Rozo, C., Hallab, N.J., Benevenia, J., and Gause, W.C. (2011b). Micrometer-sized titanium particles can induce potent Th2-type responses through TLR4-independent pathways. J Immunol *187*, 6491-6498.

Mitchell, D.M., Ravkov, E.V., and Williams, M.A. (2010). Distinct roles for IL-2 and IL-15 in the differentiation and survival of CD8+ effector and memory T cells. J Immunol *184*, 6719-6730.

Miyake, Y., Asano, K., Kaise, H., Uemura, M., Nakayama, M., and Tanaka, M. (2007). Critical role of macrophages in the marginal zone in the suppression of immune responses to apoptotic cell-associated antigens. J Clin Invest *117*, 2268-2278.

Molawi, K., Wolf, Y., Kandalla, P.K., Favret, J., Hagemeyer, N., Frenzel, K., Pinto, A.R., Klapproth, K., Henri, S., Malissen, B.*, et al.* (2014). Progressive replacement of embryo-derived cardiac macrophages with age. J Exp Med *211*, 2151-2158.

Monticelli, L.A., Sonnenberg, G.F., Abt, M.C., Alenghat, T., Ziegler, C.G., Doering, T.A., Angelosanto, J.M., Laidlaw, B.J., Yang, C.Y., Sathaliyawala, T.*, et al.* (2011). Innate lymphoid cells promote lung-tissue homeostasis after infection with influenza virus. Nat Immunol *12*, 1045-1054.

Moriyasu, T., Nakamura, R., Deloer, S., Senba, M., Kubo, M., Inoue, M., Culleton, R., and Hamano, S. (2018). Schistosoma mansoni infection suppresses the growth of Plasmodium yoelii parasites in the liver and reduces gametocyte infectivity to mosquitoes. PLoS Negl Trop Dis *12*, e0006197.

Moro, K., Yamada, T., Tanabe, M., Takeuchi, T., Ikawa, T., Kawamoto, H., Furusawa, J., Ohtani, M., Fujii, H., and Koyasu, S. (2010). Innate production of T(H)2 cytokines by adipose tissue-associated c-Kit(+)Sca-1(+) lymphoid cells. Nature *463*, 540-544.

Morris, S.C., Heidorn, S.M., Herbert, D.R., Perkins, C., Hildeman, D.A., Khodoun, M.V., and Finkelman, F.D. (2009). Endogenously produced IL-4 nonredundantly stimulates CD8+ T cell proliferation. J Immunol *182*, 1429-1438.

Morrot, A., Hafalla, J.C., Cockburn, I.A., Carvalho, L.H., and Zavala, F. (2005). IL-4 receptor expression on CD8+ T cells is required for the development of protective memory responses against liver stages of malaria parasites. The Journal of experimental medicine *202*, 551-560.

Mueller, S.N., Gebhardt, T., Carbone, F.R., and Heath, W.R. (2013). Memory T cell subsets, migration patterns, and tissue residence. Annu Rev Immunol *31*, 137-161.

Munder, M., Eichmann, K., and Modolell, M. (1998). Alternative metabolic states in murine macrophages reflected by the nitric oxide synthase/arginase balance: competitive regulation by CD4+ T cells correlates with Th1/Th2 phenotype. J Immunol *160*, 5347-5354.

Munitz, A., Seidu, L., Cole, E.T., Ahrens, R., Hogan, S.P., and Rothenberg, M.E. (2009). Resistin-like molecule alpha decreases glucose tolerance during intestinal inflammation. J Immunol *182*, 2357-2363.

Murali-Krishna, K., and Ahmed, R. (2000). Cutting edge: naive T cells masquerading as memory cells. J Immunol *165*, 1733-1737.

Murali-Krishna, K., Lau, L.L., Sambhara, S., Lemonnier, F., Altman, J., and Ahmed, R. (1999). Persistence of memory CD8 T cells in MHC class I-deficient mice. Science *286*, 1377-1381.

Murray, P.J., Allen, J.E., Biswas, S.K., Fisher, E.A., Gilroy, D.W., Goerdt, S., Gordon, S., Hamilton, J.A., Ivashkiv, L.B., Lawrence, T.*, et al.* (2014). Macrophage activation and polarization: nomenclature and experimental guidelines. Immunity *41*, 14-20.

Murrell, K.D., and Pozio, E. (2011). Worldwide occurrence and impact of human trichinellosis, 1986-2009. Emerg Infect Dis *17*, 2194-2202.

Mutapi, F., Imai, N., Nausch, N., Bourke, C.D., Rujeni, N., Mitchell, K.M., Midzi, N., Woolhouse, M.E., Maizels, R.M., and Mduluza, T. (2011). Schistosome infection intensity is inversely related to auto-reactive antibody levels. PLoS One *6*, e19149.

Muñoz-Antoli, C., Cortés, A., Santano, R., Sotillo, J., Esteban, J.G., and Toledo, R. (2016). Interleukin-25 Induces Resistance Against Intestinal Trematodes. Sci Rep *6*, 34142.

Nadjsombati, M.S., McGinty, J.W., Lyons-Cohen, M.R., Jaffe, J.B., DiPeso, L., Schneider, C., Miller, C.N., Pollack, J.L., Nagana Gowda, G.A., Fontana, M.F.*, et al.* (2018). Detection of Succinate by Intestinal Tuft Cells Triggers a Type 2 Innate Immune Circuit. Immunity *49*, 33-41.e37.

Nair, M.G., Du, Y., Perrigoue, J.G., Zaph, C., Taylor, J.J., Goldschmidt, M., Swain, G.P., Yancopoulos, G.D., Valenzuela, D.M., Murphy, A.*, et al.* (2009). Alternatively activated macrophage-derived RELM-{alpha} is a negative regulator of type 2 inflammation in the lung. J Exp Med *206*, 937-952.

Nair, M.G., Gallagher, I.J., Taylor, M.D., Loke, P., Coulson, P.S., Wilson, R.A., Maizels, R.M., and Allen, J.E. (2005). Chitinase and Fizz family members are a generalized feature of nematode infection with selective upregulation of Ym1 and Fizz1 by antigen-presenting cells. Infect Immun *73*, 385-394.

Nascimento, M., Huang, S.C., Smith, A., Everts, B., Lam, W., Bassity, E., Gautier, E.L., Randolph, G.J., and Pearce, E.J. (2014). Ly6Chi Monocyte Recruitment Is Responsible for Th2 Associated Host-Protective Macrophage Accumulation in Liver Inflammation due to Schistosomiasis. PLoS pathogens *10*, e1004282.

Nausch, N., and Mutapi, F. (2018). Group 2 ILCs: A way of enhancing immune protection against human helminths? Parasite Immunol *40*.

Neill, D.R., Wong, S.H., Bellosi, A., Flynn, R.J., Daly, M., Langford, T.K., Bucks, C., Kane, C.M., Fallon, P.G., Pannell, R.*, et al.* (2010). Nuocytes represent a new innate effector leukocyte that mediates type-2 immunity. Nature *464*, 1367-1370.

Newell, E.W., Sigal, N., Bendall, S.C., Nolan, G.P., and Davis, M.M. (2012). Cytometry by time-of-flight shows combinatorial cytokine expression and virus-specific cell niches within a continuum of CD8+ T cell phenotypes. Immunity *36*, 142-152.

Nogueira, D.S., Gazzinelli-Guimarães, P.H., Barbosa, F.S., Resende, N.M., Silva, C.C., de Oliveira, L.M., Amorim, C.C., Oliveira, F.M., Mattos, M.S., Kraemer, L.R.*, et al.* (2016). Multiple Exposures to Ascaris suum Induce Tissue Injury and Mixed Th2/Th17 Immune Response in Mice. PLoS Negl Trop Dis *10*, e0004382.

Noland, G.S., Chowdhury, D.R., Urban, J.F., Zavala, F., and Kumar, N. (2010). Helminth infection impairs the immunogenicity of a Plasmodium falciparum DNA vaccine, but not irradiated sporozoites, in mice. Vaccine *28*, 2917-2923.

Nookala, S., Srinivasan, S., Kaliraj, P., Narayanan, R.B., and Nutman, T.B. (2004). Impairment of tetanus-specific cellular and humoral responses following tetanus vaccination in human lymphatic filariasis. Infect Immun *72*, 2598-2604.

Nutman, T.B. (2013). Insights into the pathogenesis of disease in human lymphatic filariasis. Lymphat Res Biol *11*, 144-148.

O'Connell, A.E., Hess, J.A., Santiago, G.A., Nolan, T.J., Lok, J.B., Lee, J.J., and Abraham, D. (2011). Major basic protein from eosinophils and myeloperoxidase from neutrophils are required for protective immunity to Strongyloides stercoralis in mice. Infect Immun *79*, 2770-2778.

O'Connell, A.E., Kerepesi, L.A., Vandergrift, G.L., Herbert, D.R., VAN Winkle, T.J., Hooper, D.C., Pearce, E.J., and Abraham, D. (2009). IL-4(-/-) mice with lethal Mesocestoides corti infections--reduced Th2 cytokines and alternatively activated macrophages. Parasite Immunol *31*, 741-749.

Obar, J.J., Jellison, E.R., Sheridan, B.S., Blair, D.A., Pham, Q.M., Zickovich, J.M., and Lefrançois, L. (2011). Pathogen-induced inflammatory environment controls effector and memory CD8+ T cell differentiation. J Immunol *187*, 4967-4978.

Obar, J.J., and Lefrancois, L. (2010). Memory CD8+ T cell differentiation. Ann N Y Acad Sci *1183*, 251-266.

Oehen, S., and Brduscha-Riem, K. (1999). Naïve cytotoxic T lymphocytes spontaneously acquire effector function in lymphocytopenic recipients: A pitfall for T cell memory studies? Eur J Immunol *29*, 608-614.

Ohno, T., Oboki, K., Kajiwara, N., Morii, E., Aozasa, K., Flavell, R.A., Okumura, K., Saito, H., and Nakae, S. (2009). Caspase-1, caspase-8, and calpain are dispensable for IL-33 release by macrophages. J Immunol *183*, 7890-7897.

Okano, M., Satoskar, A.R., Nishizaki, K., Abe, M., and Harn, D.A. (1999). Induction of Th2 responses and IgE is largely due to carbohydrates functioning as adjuvants on Schistosoma mansoni egg antigens. J Immunol *163*, 6712-6717.

Oksanen, A., Siles-Lucas, M., Karamon, J., Possenti, A., Conraths, F.J., Romig, T., Wysocki, P., Mannocci, A., Mipatrini, D., La Torre, G.*, et al.* (2016). The geographical distribution and prevalence of

Echinococcus multilocularis in animals in the European Union and adjacent countries: a systematic review and meta-analysis. Parasit Vectors *9*, 519.

Omori, M., and Ziegler, S. (2007). Induction of IL-4 expression in CD4(+) T cells by thymic stromal lymphopoietin. J Immunol *178*, 1396-1404.

Orthgiess, J., Gericke, M., Immig, K., Schulz, A., Hirrlinger, J., Bechmann, I., and Eilers, J. (2016). Neurons exhibit Lyz2 promoter activity in vivo: Implications for using LysM-Cre mice in myeloid cell research. Eur J Immunol *46*, 1529-1532.

Osborne, L.C., Dhanji, S., Snow, J.W., Priatel, J.J., Ma, M.C., Miners, M.J., Teh, H.S., Goldsmith, M.A., and Abraham, N. (2007). Impaired CD8 T cell memory and CD4 T cell primary responses in IL-7R alpha mutant mice. J Exp Med *204*, 619-631.

Osborne, L.C., Monticelli, L.A., Nice, T.J., Sutherland, T.E., Siracusa, M.C., Hepworth, M.R., Tomov, V.T., Kobuley, D., Tran, S.V., Bittinger, K.*, et al.* (2014). Coinfection. Virus-helminth coinfection reveals a microbiota-independent mechanism of immunomodulation. Science *345*, 578-582.

Osbourn, M., Soares, D.C., Vacca, F., Cohen, E.S., Scott, I.C., Gregory, W.F., Smyth, D.J., Toivakka, M., Kemter, A.M., le Bihan, T.*, et al.* (2017). HpARI Protein Secreted by a Helminth Parasite Suppresses Interleukin-33. Immunity *47*, 739-751.e735.

Owhashi, M., Arita, H., and Hayai, N. (2000). Identification of a novel eosinophil chemotactic cytokine (ECF-L) as a chitinase family protein. J Biol Chem *275*, 1279-1286.

Owyang, A.M., Zaph, C., Wilson, E.H., Guild, K.J., McClanahan, T., Miller, H.R., Cua, D.J., Goldschmidt, M., Hunter, C.A., Kastelein, R.A., and Artis, D. (2006). Interleukin 25 regulates type 2 cytokine-dependent immunity and limits chronic inflammation in the gastrointestinal tract. J Exp Med *203*, 843-849.

Oyoshi, M.K., Larson, R.P., Ziegler, S.F., and Geha, R.S. (2010). Mechanical injury polarizes skin dendritic cells to elicit a T(H)2 response by inducing cutaneous thymic stromal lymphopoietin expression. J Allergy Clin Immunol *126*, 976-984, 984.e971-975.

Palm, N.W., Rosenstein, R.K., Yu, S., Schenten, D.D., Florsheim, E., and Medzhitov, R. (2013). Bee venom phospholipase A2 induces a primary type 2 response that is dependent on the receptor ST2 and confers protective immunity. Immunity *39*, 976-985.

Palmer, M.J., Mahajan, V.S., Chen, J., Irvine, D.J., and Lauffenburger, D.A. (2011). Signaling thresholds govern heterogeneity in IL-7-receptor-mediated responses of naïve CD8(+) T cells. Immunol Cell Biol *89*, 581-594.

Park, H.J., Lee, A., Lee, J.I., Park, S.H., Ha, S.J., and Jung, K.C. (2016). Effect of IL-4 on the Development and Function of Memory-like CD8 T Cells in the Peripheral Lymphoid Tissues. Immune Netw *16*, 126-133.

Passeri, B., Vismarra, A., Cricri, G., Bazzocchi, C., Kramer, L., and Bacci, C. (2014). The adulticide effect of a combination of doxycycline and ivermectin in Dirofilaria immitis-experimentally infected dogs is associated with reduction in local T regulatory cell populations. Vet Parasitol *205*, 208-210.

Pastille, E., Frede, A., McSorley, H.J., Gräb, J., Adamczyk, A., Kollenda, S., Hansen, W., Epple, M., Buer, J., Maizels, R.M.*, et al.* (2017). Intestinal helminth infection drives carcinogenesis in colitis-associated colon cancer. PLoS Pathog *13*, e1006649.

Patnode, M.L., Bando, J.K., Krummel, M.F., Locksley, R.M., and Rosen, S.D. (2014). Leukotriene B4 amplifies eosinophil accumulation in response to nematodes. J Exp Med *211*, 1281-1288.

Pearce, E.J., Caspar, P., Grzych, J.M., Lewis, F.A., and Sher, A. (1991). Downregulation of Th1 cytokine production accompanies induction of Th2 responses by a parasitic helminth, Schistosoma mansoni. J Exp Med *173*, 159-166.

Pearce, E.J., and MacDonald, A.S. (2002). The immunobiology of schistosomiasis. Nat Rev Immunol *2*, 499-511.

Pearce, E.L., Mullen, A.C., Martins, G.A., Krawczyk, C.M., Hutchins, A.S., Zediak, V.P., Banica, M., DiCioccio, C.B., Gross, D.A., Mao, C.A.*, et al.* (2003). Control of effector CD8+ T cell function by the transcription factor Eomesodermin. Science *302*, 1041-1043.

Pei, C., Zhao, C., Wang, A.J., Fan, A.X., Grinchuk, V., Smith, A., Sun, R., Xie, Y., Lu, N., Urban, J.F.*, et al.* (2016). Critical Role for Interleukin-25 in Host Protective Th2 Memory Response against Heligmosomoides polygyrus bakeri. Infect Immun *84*, 3328-3337.

Pellefigues, C., Tang, S.C., Schmidt, A., White, R.F., Lamiable, O., Connor, L.M., Ruedl, C., Dobrucki, J., Le Gros, G., and Ronchese, F. (2017). Toll-Like Receptor 4, but Not Neutrophil Extracellular Traps, Promote IFN Type I Expression to Enhance Th2 Responses to. Front Immunol *8*, 1575.

Perdiguero, E.G., Klapproth, K., Schulz, C., Busch, K., de Bruijn, M., Rodewald, H.R., and Geissmann, F. (2015). The Origin of Tissue-Resident Macrophages: When an Erythro-myeloid Progenitor Is an Erythro-myeloid Progenitor. Immunity *43*, 1023-1024.

Pereira, P., and Boucontet, L. (2012). Innate NKTγδ and NKTαβ cells exert similar functions and compete for a thymic niche. Eur J Immunol *42*, 1272-1281.

Pesce, J., Kaviratne, M., Ramalingam, T.R., Thompson, R.W., Urban, J.F., Jr., Cheever, A.W., Young, D.A., Collins, M., Grusby, M.J., and Wynn, T.A. (2006). The IL-21 receptor augments Th2 effector function and alternative macrophage activation. J Clin Invest *116*, 2044-2055.

Pesce, J.T., Ramalingam, T.R., Mentink-Kane, M.M., Wilson, M.S., El Kasmi, K.C., Smith, A.M., Thompson, R.W., Cheever, A.W., Murray, P.J., and Wynn, T.A. (2009a). Arginase-1-expressing macrophages suppress Th2 cytokine-driven inflammation and fibrosis. PLoS pathogens *5*, e1000371.

Pesce, J.T., Ramalingam, T.R., Wilson, M.S., Mentink-Kane, M.M., Thompson, R.W., Cheever, A.W., Urban, J.F., Jr., and Wynn, T.A. (2009b). Retnla (relmalpha/fizz1) suppresses helminth-induced Th2-type immunity. PLoS Pathog *5*, e1000393.

Pfeiffer, J.K., and Virgin, H.W. (2016). Viral immunity. Transkingdom control of viral infection and immunity in the mammalian intestine. Science *351*.

Phillips, C., Coward, W.R., Pritchard, D.I., and Hewitt, C.R. (2003). Basophils express a type 2 cytokine profile on exposure to proteases from helminths and house dust mites. J Leukoc Biol *73*, 165-171.

Phythian-Adams, A.T., Cook, P.C., Lundie, R.J., Jones, L.H., Smith, K.A., Barr, T.A., Hochweller, K., Anderton, S.M., Hämmerling, G.J., Maizels, R.M., and MacDonald, A.S. (2010). CD11c depletion severely disrupts Th2 induction and development in vivo. J Exp Med *207*, 2089-2096.

Plumlee, C.R., Obar, J.J., Colpitts, S.L., Jellison, E.R., Haining, W.N., Lefrancois, L., and Khanna, K.M. (2015). Early Effector CD8 T Cells Display Plasticity in Populating the Short-Lived Effector and Memory-Precursor Pools Following Bacterial or Viral Infection. Sci Rep *5*, 12264.

Pozio, E., and Darwin Murrell, K. (2006). Systematics and epidemiology of trichinella. Adv Parasitol *63*, 367-439.

Prasanphanich, N.S., Mickum, M.L., Heimburg-Molinaro, J., and Cummings, R.D. (2013). Glycoconjugates in host-helminth interactions. Front Immunol *4*, 240.

Price, A.E., Liang, H.E., Sullivan, B.M., Reinhardt, R.L., Eisley, C.J., Erle, D.J., and Locksley, R.M. (2010). Systemically dispersed innate IL-13-expressing cells in type 2 immunity. Proc Natl Acad Sci U S A *107*, 11489-11494.

Prince, A.L., Watkin, L.B., Yin, C.C., Selin, L.K., Kang, J., Schwartzberg, P.L., and Berg, L.J. (2014). Innate PLZF+CD4+ αβ T cells develop and expand in the absence of Itk. J Immunol *193*, 673-687.

Pullan, R.L., Smith, J.L., Jasrasaria, R., and Brooker, S.J. (2014). Global numbers of infection and disease burden of soil transmitted helminth infections in 2010. Parasit Vectors *7*, 37.

Raes, G., Brys, L., Dahal, B.K., Brandt, J., Grooten, J., Brombacher, F., Vanham, G., Noel, W., Bogaert, P., Boonefaes, T.*, et al.* (2005). Macrophage galactose-type C-type lectins as novel markers for alternatively activated macrophages elicited by parasitic infections and allergic airway inflammation. J Leukoc Biol *77*, 321-327.

Rafei, M., Hardy, M.P., Williams, P., Vanegas, J.R., Forner, K.A., Dulude, G., Labrecque, N., Galipeau, J., and Perreault, C. (2011). Development and function of innate polyclonal TCRalphabeta+ CD8+ thymocytes. J Immunol *187*, 3133-3144.

Rafi, W., Bhatt, K., Gause, W.C., and Salgame, P. (2015). Neither primary nor memory immunity to Mycobacterium tuberculosis infection is compromised in mice with chronic enteric helminth infection. Infect Immun *83*, 1217-1223.

Ramalingam, T.R., Gieseck, R.L., Acciani, T.H., M Hart, K., Cheever, A.W., Mentink-Kane, M.M., Vannella, K.M., and Wynn, T.A. (2016). Enhanced protection from fibrosis and inflammation in the combined absence of IL-13 and IFN-γ. J Pathol *239*, 344-354.

Ramalingam, T.R., Pesce, J.T., Sheikh, F., Cheever, A.W., Mentink-Kane, M.M., Wilson, M.S., Stevens, S., Valenzuela, D.M., Murphy, A.J., Yancopoulos, G.D.*, et al.* (2008). Unique functions of the type II interleukin 4 receptor identified in mice lacking the interleukin 13 receptor alpha1 chain. Nat Immunol *9*, 25-33.

Ramanan, D., Bowcutt, R., Lee, S.C., Tang, M.S., Kurtz, Z.D., Ding, Y., Honda, K., Gause, W.C., Blaser, M.J., Bonneau, R.A*., et al.* (2016). Helminth infection promotes colonization resistance via type 2 immunity. Science *352*, 608-612.

Rank, M.A., Kobayashi, T., Kozaki, H., Bartemes, K.R., Squillace, D.L., and Kita, H. (2009). IL-33-activated dendritic cells induce an atypical TH2-type response. J Allergy Clin Immunol *123*, 1047-1054.

Rao, R.R., Li, Q., Odunsi, K., and Shrikant, P.A. (2010). The mTOR kinase determines effector versus memory CD8+ T cell fate by regulating the expression of transcription factors T-bet and Eomesodermin. Immunity *32*, 67-78.

Raschke, W.C., Hendricks, M., and Chen, C.M. (1995). Genetic basis of antigenic differences between three alleles of Ly5 (CD45) in mice. Immunogenetics *41*, 144-147.

Reese, T.A., Bi, K., Kambal, A., Filali-Mouhim, A., Beura, L.K., Bürger, M.C., Pulendran, B., Sekaly, R.P., Jameson, S.C., Masopust, D*., et al.* (2016). Sequential Infection with Common Pathogens Promotes Human-like Immune Gene Expression and Altered Vaccine Response. Cell Host Microbe *19*, 713-719.

Reese, T.A., Liang, H.E., Tager, A.M., Luster, A.D., Van Rooijen, N., Voehringer, D., and Locksley, R.M. (2007). Chitin induces accumulation in tissue of innate immune cells associated with allergy. Nature *447*, 92-96.

Reese, T.A., Wakeman, B.S., Choi, H.S., Hufford, M.M., Huang, S.C., Zhang, X., Buck, M.D., Jezewski, A., Kambal, A., Liu, C.Y*., et al.* (2014). Helminth infection reactivates latent gamma-herpesvirus via cytokine competition at a viral promoter. Science.

Reinhardt, R.L., Khoruts, A., Merica, R., Zell, T., and Jenkins, M.K. (2001). Visualizing the generation of memory CD4 T cells in the whole body. Nature *410*, 101-105.

Renkema, K.R., Lee, J.Y., Lee, Y.J., Hamilton, S.E., Hogquist, K.A., and Jameson, S.C. (2016). IL-4 sensitivity shapes the peripheral CD8+ T cell pool and response to infection. The Journal of experimental medicine *213*, 1319-1329.

Resende Co, T., Hirsch, C.S., Toossi, Z., Dietze, R., and Ribeiro-Rodrigues, R. (2007). Intestinal helminth co-infection has a negative impact on both anti-Mycobacterium tuberculosis immunity and clinical response to tuberculosis therapy. Clin Exp Immunol *147*, 45-52.

Reyes, J.L., Terrazas, C.A., Alonso-Trujillo, J., van Rooijen, N., Satoskar, A.R., and Terrazas, L.I. (2010). Early removal of alternatively activated macrophages leads to Taenia crassiceps cysticercosis clearance in vivo. Int J Parasitol *40*, 731-742.

Reyes, J.L., and Terrazas, L.I. (2007). The divergent roles of alternatively activated macrophages in helminthic infections. Parasite Immunol *29*, 609-619.

Reynolds, L.A., Filbey, K.J., and Maizels, R.M. (2012). Immunity to the model intestinal helminth parasite Heligmosomoides polygyrus. Semin Immunopathol *34*, 829-846.

Ritz, T., Krenkel, O., and Tacke, F. (2018). Dynamic plasticity of macrophage functions in diseased liver. Cell Immunol *330*, 175-182.

Robinson, M.W., Alvarado, R., To, J., Hutchinson, A.T., Dowdell, S.N., Lund, M., Turnbull, L., Whitchurch, C.B., O'Brien, B.A., Dalton, J.P., and Donnelly, S. (2012). A helminth cathelicidin-like protein suppresses antigen processing and presentation in macrophages via inhibition of lysosomal vATPase. FASEB J *26*, 4614-4627.

Rocha, B., Dautigny, N., and Pereira, P. (1989). Peripheral T lymphocytes: expansion potential and homeostatic regulation of pool sizes and CD4/CD8 ratios in vivo. Eur J Immunol *19*, 905-911.

Rodrigo, M.B., Schulz, S., Krupp, V., Ritter, M., Wiszniewsky, K., Arndts, K., Tamadaho, R.S., Endl, E., Hoerauf, A., and Layland, L.E. (2016). Patency of Litomosoides sigmodontis infection depends on Toll-like receptor 4 whereas Toll-like receptor 2 signalling influences filarial-specific CD4(+) T-cell responses. Immunology *147*, 429-442.

Rodríguez, E., Carasi, P., Frigerio, S., da Costa, V., van Vliet, S., Noya, V., Brossard, N., van Kooyk, Y., García-Vallejo, J.J., and Freire, T. (2017a). Immune Regulates CD11c. Front Immunol *8*, 264.

Rodríguez, E., Kalay, H., Noya, V., Brossard, N., Giacomini, C., van Kooyk, Y., García-Vallejo, J.J., and Freire, T. (2017b). Fasciola hepatica glycoconjugates immuneregulate dendritic cells through the Dendritic Cell-Specific Intercellular adhesion molecule-3-Grabbing Non-integrin inducing T cell anergy. Sci Rep *7*, 46748.

Rodríguez, E., Noya, V., Cervi, L., Chiribao, M.L., Brossard, N., Chiale, C., Carmona, C., Giacomini, C., and Freire, T. (2015). Glycans from Fasciola hepatica Modulate the Host Immune Response and TLR-Induced Maturation of Dendritic Cells. PLoS Negl Trop Dis *9*, e0004234.

Rodríguez-Sosa, M., Rosas, L.E., David, J.R., Bojalil, R., Satoskar, A.R., and Terrazas, L.I. (2003). Macrophage migration inhibitory factor plays a critical role in mediating protection against the helminth parasite Taenia crassiceps. Infect Immun *71*, 1247-1254.

Rodríguez-Sosa, M., Saavedra, R., Tenorio, E.P., Rosas, L.E., Satoskar, A.R., and Terrazas, L.I. (2004). A STAT4-dependent Th1 response is required for resistance to the helminth parasite Taenia crassiceps. Infect Immun *72*, 4552-4560.

Rolot, M., and Dewals, B.G. (2018). Macrophage Activation and Functions during Helminth Infection: Recent Advances from the Laboratory Mouse. J Immunol Res *2018*, 2790627.

Ruckerl, D., and Allen, J.E. (2014). Macrophage proliferation, provenance, and plasticity in macroparasite infection. Immunological reviews *262*, 113-133.

Ruckerl, D., Campbell, S.M., Duncan, S., Sutherland, T.E., Jenkins, S.J., Hewitson, J.P., Barr, T.A., Jackson-Jones, L.H., Maizels, R.M., and Allen, J.E. (2017). Macrophage origin limits functional plasticity in helminth-bacterial co-infection. PLoS pathogens *13*, e1006233.

Saito, M., Iwawaki, T., Taya, C., Yonekawa, H., Noda, M., Inui, Y., Mekada, E., Kimata, Y., Tsuru, A., and Kohno, K. (2001). Diphtheria toxin receptor-mediated conditional and targeted cell ablation in transgenic mice. Nat Biotechnol *19*, 746-750.

Salazar-Castañon, V.H., Legorreta-Herrera, M., and Rodriguez-Sosa, M. (2014). Helminth parasites alter protection against Plasmodium infection. Biomed Res Int *2014*, 913696.

Salazar-Castañón, V.H., Juárez-Avelar, I., Legorreta-Herrera, M., Govezensky, T., and Rodriguez-Sosa, M. (2018). Co-infection: the outcome of Plasmodium infection differs according to the time of pre-existing helminth infection. Parasitol Res.

Salgame, P., Yap, G.S., and Gause, W.C. (2013). Effect of helminth-induced immunity on infections with microbial pathogens. Nat Immunol *14*, 1118-1126.

Sallusto, F., Lenig, D., Förster, R., Lipp, M., and Lanzavecchia, A. (1999). Two subsets of memory T lymphocytes with distinct homing potentials and effector functions. Nature *401*, 708-712.

Sans-Fons, M.G., Yeramian, A., Pereira-Lopes, S., Santamaría-Babi, L.F., Modolell, M., Lloberas, J., and Celada, A. (2013). Arginine transport is impaired in C57Bl/6 mouse macrophages as a result of a deletion in the promoter of Slc7a2 (CAT2), and susceptibility to Leishmania infection is reduced. J Infect Dis *207*, 1684-1693.

Sartono, E., Kruize, Y.C., Kurniawan, A., van der Meide, P.H., Partono, F., Maizels, R.M., and Yazdanbakhsh, M. (1995). Elevated cellular immune responses and interferon-gamma release after long-term diethylcarbamazine treatment of patients with human lymphatic filariasis. J Infect Dis *171*, 1683-1687.

Sasaki, Y., Yoshimoto, T., Maruyama, H., Tegoshi, T., Ohta, N., Arizono, N., and Nakanishi, K. (2005). IL-18 with IL-2 protects against Strongyloides venezuelensis infection by activating mucosal mast cell-dependent type 2 innate immunity. J Exp Med *202*, 607-616.

Satoh, T., Nakagawa, K., Sugihara, F., Kuwahara, R., Ashihara, M., Yamane, F., Minowa, Y., Fukushima, K., Ebina, I., Yoshioka, Y.*, et al.* (2017). Identification of an atypical monocyte and committed progenitor involved in fibrosis. Nature *541*, 96-101.

Scalfone, L.K., Nel, H.J., Gagliardo, L.F., Cameron, J.L., Al-Shokri, S., Leifer, C.A., Fallon, P.G., and Appleton, J.A. (2013). Participation of MyD88 and interleukin-33 as innate drivers of Th2 immunity to Trichinella spiralis. Infect Immun *81*, 1354-1363.

Scheer, S., Krempl, C., Kallfass, C., Frey, S., Jakob, T., Mouahid, G., Mone, H., Schmitt-Graff, A., Staeheli, P., and Lamers, M.C. (2014). S. mansoni bolsters anti-viral immunity in the murine respiratory tract. PLoS One *9*, e112469.

Schluns, K.S., Kieper, W.C., Jameson, S.C., and Lefrançois, L. (2000). Interleukin-7 mediates the homeostasis of naïve and memory CD8 T cells in vivo. Nat Immunol *1*, 426-432.

Schmitz, J., Owyang, A., Oldham, E., Song, Y., Murphy, E., McClanahan, T.K., Zurawski, G., Moshrefi, M., Qin, J., Li, X.*, et al.* (2005). IL-33, an interleukin-1-like cytokine that signals via the IL-1 receptor-related protein ST2 and induces T helper type 2-associated cytokines. Immunity *23*, 479-490.

Schneider, C., O'Leary, C.E., von Moltke, J., Liang, H.E., Ang, Q.Y., Turnbaugh, P.J., Radhakrishnan, S., Pellizzon, M., Ma, A., and Locksley, R.M. (2018). A Metabolite-Triggered Tuft Cell-ILC2 Circuit Drives Small Intestinal Remodeling. Cell.

Schnoeller, C., Rausch, S., Pillai, S., Avagyan, A., Wittig, B.M., Loddenkemper, C., Hamann, A., Hamelmann, E., Lucius, R., and Hartmann, S. (2008). A helminth immunomodulator reduces allergic and inflammatory responses by induction of IL-10-producing macrophages. J Immunol *180*, 4265-4272.

Schuijs, M.J., Hartmann, S., Selkirk, M.E., Roberts, L.B., Openshaw, P.J., and Schnoeller, C. (2016). The Helminth-Derived Immunomodulator AvCystatin Reduces Virus Enhanced Inflammation by Induction of Regulatory IL-10+ T Cells. PLoS One *11*, e0161885.

Schulz, C., Gomez Perdiguero, E., Chorro, L., Szabo-Rogers, H., Cagnard, N., Kierdorf, K., Prinz, M., Wu, B., Jacobsen, S.E., Pollard, J.W*., et al.* (2012). A lineage of myeloid cells independent of Myb and hematopoietic stem cells. Science *336*, 86-90.

Schüler, T., Hämmerling, G.J., and Arnold, B. (2004). Cutting edge: IL-7-dependent homeostatic proliferation of CD8+ T cells in neonatal mice allows the generation of long-lived natural memory T cells. J Immunol *172*, 15-19.

Scott, C.L., Zheng, F., De Baetselier, P., Martens, L., Saeys, Y., De Prijck, S., Lippens, S., Abels, C., Schoonooghe, S., Raes, G*., et al.* (2016). Bone marrow-derived monocytes give rise to self-renewing and fully differentiated Kupffer cells. Nat Commun *7*, 10321.

Seno, H., Miyoshi, H., Brown, S.L., Geske, M.J., Colonna, M., and Stappenbeck, T.S. (2009). Efficient colonic mucosal wound repair requires Trem2 signaling. Proc Natl Acad Sci U S A *106*, 256-261.

Serradell, M.C., Guasconi, L., Cervi, L., Chiapello, L.S., and Masih, D.T. (2007). Excretory-secretory products from Fasciola hepatica induce eosinophil apoptosis by a caspase-dependent mechanism. Vet Immunol Immunopathol *117*, 197-208.

Sharma, A., Chen, Q., Nguyen, T., Yu, Q., and Sen, J.M. (2012). T cell factor-1 and β-catenin control the development of memory-like CD8 thymocytes. J Immunol *188*, 3859-3868.

Shimokawa, C., Kanaya, T., Hachisuka, M., Ishiwata, K., Hisaeda, H., Kurashima, Y., Kiyono, H., Yoshimoto, T., Kaisho, T., and Ohno, H. (2017). Mast Cells Are Crucial for Induction of Group 2 Innate Lymphoid Cells and Clearance of Helminth Infections. Immunity *46*, 863-874.e864.

Shin, E.H., Osada, Y., Chai, J.Y., Matsumoto, N., Takatsu, K., and Kojima, S. (1997). Protective roles of eosinophils in Nippostrongylus brasiliensis infection. Int Arch Allergy Immunol *114 Suppl 1*, 45-50.

Shook, B., Xiao, E., Kumamoto, Y., Iwasaki, A., and Horsley, V. (2016). CD301b+ Macrophages Are Essential for Effective Skin Wound Healing. J Invest Dermatol *136*, 1885-1891.

Sintes, J., Cuenca, M., Romero, X., Bastos, R., Terhorst, C., Angulo, A., and Engel, P. (2013). Cutting edge: Ly9 (CD229), a SLAM family receptor, negatively regulates the development of thymic innate memory-like CD8+ T and invariant NKT cells. J Immunol *190*, 21-26.

Siracusa, M.C., Saenz, S.A., Hill, D.A., Kim, B.S., Headley, M.B., Doering, T.A., Wherry, E.J., Jessup, H.K., Siegel, L.A., Kambayashi, T*., et al.* (2011). TSLP promotes interleukin-3-independent basophil haematopoiesis and type 2 inflammation. Nature *477*, 229-233.

Smith, K.A., Harcus, Y., Garbi, N., Hämmerling, G.J., MacDonald, A.S., and Maizels, R.M. (2012). Type 2 innate immunity in helminth infection is induced redundantly and acts autonomously following CD11c(+) cell depletion. Infect Immun *80*, 3481-3489.

Smith, K.A., Hochweller, K., Hämmerling, G.J., Boon, L., MacDonald, A.S., and Maizels, R.M. (2011). Chronic helminth infection promotes immune regulation in vivo through dominance of CD11cloCD103- dendritic cells. J Immunol *186*, 7098-7109.

Smith, N.L., Patel, R.K., Reynaldi, A., Grenier, J.K., Wang, J., Watson, N.B., Nzingha, K., Yee Mon, K.J., Peng, S.A., Grimson, A.*, et al.* (2018). Developmental Origin Governs CD8. Cell.

Smith, P., Mangan, N.E., Walsh, C.M., Fallon, R.E., McKenzie, A.N., van Rooijen, N., and Fallon, P.G. (2007). Infection with a helminth parasite prevents experimental colitis via a macrophage-mediated mechanism. J Immunol *178*, 4557-4566.

Smith, P., Walsh, C.M., Mangan, N.E., Fallon, R.E., Sayers, J.R., McKenzie, A.N., and Fallon, P.G. (2004). Schistosoma mansoni worms induce anergy of T cells via selective up-regulation of programmed death ligand 1 on macrophages. J Immunol *173*, 1240-1248.

Smits, H.H., Hammad, H., van Nimwegen, M., Soullie, T., Willart, M.A., Lievers, E., Kadouch, J., Kool, M., Kos-van Oosterhoud, J., Deelder, A.M.*, et al.* (2007). Protective effect of Schistosoma mansoni infection on allergic airway inflammation depends on the intensity and chronicity of infection. J Allergy Clin Immunol *120*, 932-940.

Sokol, C.L., Barton, G.M., Farr, A.G., and Medzhitov, R. (2008). A mechanism for the initiation of allergen-induced T helper type 2 responses. Nat Immunol *9*, 310-318.

Sorel, O., Tuddenham, L., Myster, F., Palmeira, L., Kerkhofs, P., Pfeffer, S., Vanderplasschen, A., and Dewals, B.G. (2015). Small RNA deep sequencing identifies viral microRNAs during malignant catarrhal fever induced by alcelaphine herpesvirus 1. The Journal of general virology *96*, 3360-3372.

Sosinowski, T., White, J.T., Cross, E.W., Haluszczak, C., Marrack, P., Gapin, L., and Kedl, R.M. (2013). CD8α+ dendritic cell trans presentation of IL-15 to naive CD8+ T cells produces antigen-inexperienced T cells in the periphery with memory phenotype and function. J Immunol *190*, 1936-1947.

Soumelis, V., Reche, P.A., Kanzler, H., Yuan, W., Edward, G., Homey, B., Gilliet, M., Ho, S., Antonenko, S., Lauerma, A.*, et al.* (2002). Human epithelial cells trigger dendritic cell mediated allergic inflammation by producing TSLP. Nat Immunol *3*, 673-680.

Spinelli, L., Carpentier, S., Montanana Sanchis, F., Dalod, M., and Vu Manh, T.P. (2015). BubbleGUM: automatic extraction of phenotype molecular signatures and comprehensive visualization of multiple Gene Set Enrichment Analyses. BMC genomics *16*, 814.

Sprent, J., and Surh, C.D. (2011). Normal T cell homeostasis: the conversion of naive cells into memory-phenotype cells. Nat Immunol *12*, 478-484.

Stein, M., Keshav, S., Harris, N., and Gordon, S. (1992). Interleukin 4 potently enhances murine macrophage mannose receptor activity: a marker of alternative immunologic macrophage activation. The Journal of experimental medicine *176*, 287-292.

Steinfelder, S., Andersen, J.F., Cannons, J.L., Feng, C.G., Joshi, M., Dwyer, D., Caspar, P., Schwartzberg, P.L., Sher, A., and Jankovic, D. (2009). The major component in schistosome eggs responsible for conditioning dendritic cells for Th2 polarization is a T2 ribonuclease (omega-1). The Journal of experimental medicine *206*, 1681-1690.

Stelekati, E., and Wherry, E.J. (2012). Chronic bystander infections and immunity to unrelated antigens. Cell Host Microbe *12*, 458-469.

Stemberger, C., Huster, K.M., Koffler, M., Anderl, F., Schiemann, M., Wagner, H., and Busch, D.H. (2007). A single naive CD8+ T cell precursor can develop into diverse effector and memory subsets. Immunity *27*, 985-997.

Stevenson, P.G., Belz, G.T., Altman, J.D., and Doherty, P.C. (1999a). Changing patterns of dominance in the CD8+ T cell response during acute and persistent murine gamma-herpesvirus infection. European journal of immunology *29*, 1059-1067.

Stevenson, P.G., Belz, G.T., Castrucci, M.R., Altman, J.D., and Doherty, P.C. (1999b). A gamma-herpesvirus sneaks through a CD8(+) T cell response primed to a lytic-phase epitope. Proceedings of the National Academy of Sciences of the United States of America *96*, 9281-9286.

Stiemsma, L.T., Reynolds, L.A., Turvey, S.E., and Finlay, B.B. (2015). The hygiene hypothesis: current perspectives and future therapies. Immunotargets Ther *4*, 143-157.

Strachan, D.P. (1989). Hay fever, hygiene, and household size. BMJ *299*, 1259-1260.

Su, Z., Segura, M., and Stevenson, M.M. (2006). Reduced protective efficacy of a blood-stage malaria vaccine by concurrent nematode infection. Infect Immun *74*, 2138-2144.

Sullivan, B.M., Juedes, A., Szabo, S.J., von Herrath, M., and Glimcher, L.H. (2003). Antigen-driven effector CD8 T cell function regulated by T-bet. Proc Natl Acad Sci U S A *100*, 15818-15823.

Summers, R.W., Elliott, D.E., Urban, J.F., Thompson, R., and Weinstock, J.V. (2005a). Trichuris suis therapy in Crohn's disease. Gut *54*, 87-90.

Summers, R.W., Elliott, D.E., Urban, J.F., Thompson, R.A., and Weinstock, J.V. (2005b). Trichuris suis therapy for active ulcerative colitis: a randomized controlled trial. Gastroenterology *128*, 825-832.

Surh, C.D., and Sprent, J. (2000). Homeostatic T cell proliferation: how far can T cells be activated to self-ligands? J Exp Med *192*, F9-F14.

Sutherland, T.E., Logan, N., Rückerl, D., Humbles, A.A., Allan, S.M., Papayannopoulos, V., Stockinger, B., Maizels, R.M., and Allen, J.E. (2014). Chitinase-like proteins promote IL-17-mediated neutrophilia in a tradeoff between nematode killing and host damage. Nat Immunol *15*, 1116-1125.

T'Jonck, W., Guilliams, M., and Bonnardel, J. (2018). Niche signals and transcription factors involved in tissue-resident macrophage development. Cell Immunol *330*, 43-53.

Takemoto, N., Intlekofer, A.M., Northrup, J.T., Wherry, E.J., and Reiner, S.L. (2006). Cutting Edge: IL-12 inversely regulates T-bet and eomesodermin expression during pathogen-induced CD8+ T cell differentiation. J Immunol *177*, 7515-7519.

Tamoutounour, S., Guilliams, M., Montanana Sanchis, F., Liu, H., Terhorst, D., Malosse, C., Pollet, E., Ardouin, L., Luche, H., Sanchez, C*., et al.* (2013). Origins and functional specialization of macrophages and of conventional and monocyte-derived dendritic cells in mouse skin. Immunity *39*, 925-938.

Tan, C.S.E., Lawler, C., and Stevenson, P.G. (2017). CD8+ T cell evasion mandates CD4+ T cell control of chronic gamma-herpesvirus infection. PLoS pathogens *13*, e1006311.

Tanchot, C., Lemonnier, F.A., Pérarnau, B., Freitas, A.A., and Rocha, B. (1997). Differential requirements for survival and proliferation of CD8 naïve or memory T cells. Science *276*, 2057-2062.

Tarique, A.A., Logan, J., Thomas, E., Holt, P.G., Sly, P.D., and Fantino, E. (2015). Phenotypic, functional, and plasticity features of classical and alternatively activated human macrophages. Am J Respir Cell Mol Biol *53*, 676-688.

Taub, D.D., and Cox, G.W. (1995). Murine Th1 and Th2 cell clones differentially regulate macrophage nitric oxide production. J Leukoc Biol *58*, 80-89.

Taylor, B.C., Zaph, C., Troy, A.E., Du, Y., Guild, K.J., Comeau, M.R., and Artis, D. (2009a). TSLP regulates intestinal immunity and inflammation in mouse models of helminth infection and colitis. J Exp Med *206*, 655-667.

Taylor, J.J., Krawczyk, C.M., Mohrs, M., and Pearce, E.J. (2009b). Th2 cell hyporesponsiveness during chronic murine schistosomiasis is cell intrinsic and linked to GRAIL expression. J Clin Invest *119*, 1019-1028.

Taylor, M.D., Harris, A., Nair, M.G., Maizels, R.M., and Allen, J.E. (2006). F4/80+ alternatively activated macrophages control CD4+ T cell hyporesponsiveness at sites peripheral to filarial infection. J Immunol *176*, 6918-6927.

Taylor, M.D., LeGoff, L., Harris, A., Malone, E., Allen, J.E., and Maizels, R.M. (2005). Removal of regulatory T cell activity reverses hyporesponsiveness and leads to filarial parasite clearance in vivo. J Immunol *174*, 4924-4933.

Taylor, M.D., van der Werf, N., Harris, A., Graham, A.L., Bain, O., Allen, J.E., and Maizels, R.M. (2009c). Early recruitment of natural CD4+ Foxp3+ Treg cells by infective larvae determines the outcome of filarial infection. Eur J Immunol *39*, 192-206.

Taylor, M.J., Hoerauf, A., and Bockarie, M. (2010). Lymphatic filariasis and onchocerciasis. Lancet *376*, 1175-1185.

Teng, X., Li, D., Champion, H.C., and Johns, R.A. (2003). FIZZ1/RELMalpha, a novel hypoxia-induced mitogenic factor in lung with vasoconstrictive and angiogenic properties. Circ Res *92*, 1065-1067.

Terrazas, C., de Dios Ruiz-Rosado, J., Amici, S.A., Jablonski, K.A., Martinez-Saucedo, D., Webb, L.M., Cortado, H., Robledo-Avila, F., Oghumu, S., Satoskar, A.R.*, et al.* (2017). Helminth-induced Ly6C. Sci Rep *7*, 40814.

Terrazas, L.I. (2008). The complex role of pro- and anti-inflammatory cytokines in cysticercosis: immunological lessons from experimental and natural hosts. Curr Top Med Chem *8*, 383-392.

Terrazas, L.I., Bojalil, R., Govezensky, T., and Larralde, C. (1998). Shift from an early protective Th1-type immune response to a late permissive Th2-type response in murine cysticercosis (Taenia crassiceps). J Parasitol *84*, 74-81.

Terrazas, L.I., Cruz, M., Rodríguez-Sosa, M., Bojalil, R., García-Tamayo, F., and Larralde, C. (1999). Th1-type cytokines improve resistance to murine cysticercosis caused by Taenia crassiceps. Parasitol Res *85*, 135-141.

Terrazas, L.I., Montero, D., Terrazas, C.A., Reyes, J.L., and Rodríguez-Sosa, M. (2005). Role of the programmed Death-1 pathway in the suppressive activity of alternatively activated macrophages in experimental cysticercosis. Int J Parasitol *35*, 1349-1358.

Thawer, S., Auret, J., Schnoeller, C., Chetty, A., Smith, K., Darby, M., Roberts, L., Mackay, R.M., Whitwell, H.J., Timms, J.F.*, et al.* (2016). Surfactant Protein-D Is Essential for Immunity to Helminth Infection. PLoS pathogens *12*, e1005461.

Thawer, S.G., Horsnell, W.G., Darby, M., Hoving, J.C., Dewals, B., Cutler, A.J., Lang, D., and Brombacher, F. (2014). Lung-resident CD4(+) T cells are sufficient for IL-4Ralpha-dependent recall immunity to Nippostrongylus brasiliensis infection. Mucosal immunology *7*, 239-248.

Thomas, G.D., Rückerl, D., Maskrey, B.H., Whitfield, P.D., Blaxter, M.L., and Allen, J.E. (2012). The biology of nematode- and IL4Rα-dependent murine macrophage polarization in vivo as defined by RNA-Seq and targeted lipidomics. Blood *120*, e93-e104.

Thorley-Lawson, D.A., and Gross, A. (2004). Persistence of the Epstein-Barr virus and the origins of associated lymphomas. The New England journal of medicine *350*, 1328-1337.

Toenjes, S.A., and Kuhn, R.E. (2003). The initial immune response during experimental cysticercosis is of the mixed Th1/Th2 type. Parasitol Res *89*, 407-413.

Toenjes, S.A., Spolski, R.J., Mooney, K.A., and Kuhn, R.E. (1999). The systemic immune response of BALB/c mice infected with larval Taenia crassiceps is a mixed Th1/Th2-type response. Parasitology *118 (Pt 6)*, 623-633.

Togno-Peirce, C., Nava-Castro, K., Terrazas, L.I., and Morales-Montor, J. (2013). Sex-associated expression of co-stimulatory molecules CD80, CD86, and accessory molecules, PDL-1, PDL-2 and MHC-II, in F480+ macrophages during murine cysticercosis. Biomed Res Int *2013*, 570158.

Townsend, M.J., Fallon, P.G., Matthews, D.J., Jolin, H.E., and McKenzie, A.N. (2000). T1/ST2-deficient mice demonstrate the importance of T1/ST2 in developing primary T helper cell type 2 responses. J Exp Med *191*, 1069-1076.

Tripathi, P., Morris, S.C., Perkins, C., Sholl, A., Finkelman, F.D., and Hildeman, D.A. (2016). IL-4 and IL-15 promotion of virtual memory CD8+ T cells is determined by genetic background. European journal of immunology *46*, 2333-2339.

Tsai, C.Y., Hu, Z., Zhang, W., and Usherwood, E.J. (2011). Strain-dependent requirement for IFN-γ for respiratory control and immunotherapy in murine gammaherpesvirus infection. Viral Immunol *24*, 273-280.

Tucker, M.S., Karunaratne, L.B., Lewis, F.A., Freitas, T.C., and Liang, Y.S. (2013). Schistosomiasis. Curr Protoc Immunol *103*, Unit 19.11.

Turner, J.D., Jenkins, G.R., Hogg, K.G., Aynsley, S.A., Paveley, R.A., Cook, P.C., Coles, M.C., and Mountford, A.P. (2011). CD4+CD25+ regulatory cells contribute to the regulation of colonic Th2 granulomatous pathology caused by schistosome infection. PLoS Negl Trop Dis *5*, e1269.

Turner, J.D., Pionnier, N., Furlong-Silva, J., Sjoberg, H., Cross, S., Halliday, A., Guimaraes, A.F., Cook, D.A.N., Steven, A., Van Rooijen, N.*, et al.* (2018). Interleukin-4 activated macrophages mediate immunity to filarial helminth infection by sustaining CCR3-dependent eosinophilia. PLoS pathogens *14*, e1006949.

Urban, J.F., Maliszewski, C.R., Madden, K.B., Katona, I.M., and Finkelman, F.D. (1995). IL-4 treatment can cure established gastrointestinal nematode infections in immunocompetent and immunodeficient mice. J Immunol *154*, 4675-4684.

Urban, J.F., Noben-Trauth, N., Donaldson, D.D., Madden, K.B., Morris, S.C., Collins, M., and Finkelman, F.D. (1998). IL-13, IL-4Ralpha, and Stat6 are required for the expulsion of the gastrointestinal nematode parasite Nippostrongylus brasiliensis. Immunity *8*, 255-264.

Urban, J.F., Noben-Trauth, N., Schopf, L., Madden, K.B., and Finkelman, F.D. (2001). Cutting edge: IL-4 receptor expression by non-bone marrow-derived cells is required to expel gastrointestinal nematode parasites. J Immunol *167*, 6078-6081.

Vallance, B.A., Matthaei, K.I., Sanovic, S., Young, I.G., and Collins, S.M. (2000). Interleukin-5 deficient mice exhibit impaired host defence against challenge Trichinella spiralis infections. Parasite Immunol *22*, 487-492.

van den Biggelaar, A.H., Rodrigues, L.C., van Ree, R., van der Zee, J.S., Hoeksma-Kruize, Y.C., Souverijn, J.H., Missinou, M.A., Borrmann, S., Kremsner, P.G., and Yazdanbakhsh, M. (2004). Long-term treatment of intestinal helminths increases mite skin-test reactivity in Gabonese schoolchildren. J Infect Dis *189*, 892-900.

van der Kleij, D., Latz, E., Brouwers, J.F., Kruize, Y.C., Schmitz, M., Kurt-Jones, E.A., Espevik, T., de Jong, E.C., Kapsenberg, M.L., Golenbock, D.T.*, et al.* (2002). A novel host-parasite lipid cross-talk. Schistosomal lyso-phosphatidylserine activates toll-like receptor 2 and affects immune polarization. J Biol Chem *277*, 48122-48129.

van der Werf, N., Redpath, S.A., Azuma, M., Yagita, H., and Taylor, M.D. (2013). Th2 cell-intrinsic hypo-responsiveness determines susceptibility to helminth infection. PLoS Pathog *9*, e1003215.

van Die, I., and Cummings, R.D. (2017). The Mannose Receptor in Regulation of Helminth-Mediated Host Immunity. Frontiers in immunology *8*, 1677.

van Die, I., van Vliet, S.J., Nyame, A.K., Cummings, R.D., Bank, C.M., Appelmelk, B., Geijtenbeek, T.B., and van Kooyk, Y. (2003). The dendritic cell-specific C-type lectin DC-SIGN is a receptor for Schistosoma mansoni egg antigens and recognizes the glycan antigen Lewis x. Glycobiology *13*, 471-478.

Van Dyken, S.J., and Locksley, R.M. (2013). Interleukin-4- and interleukin-13-mediated alternatively activated macrophages: roles in homeostasis and disease. Annual review of immunology *31*, 317-343.

van Furth, R., Cohn, Z.A., Hirsch, J.G., Humphrey, J.H., Spector, W.G., and Langevoort, H.L. (1972). The mononuclear phagocyte system: a new classification of macrophages, monocytes, and their precursor cells. Bull World Health Organ *46*, 845-852.

van Liempt, E., van Vliet, S.J., Engering, A., García Vallejo, J.J., Bank, C.M., Sanchez-Hernandez, M., van Kooyk, Y., and van Die, I. (2007). Schistosoma mansoni soluble egg antigens are internalized by human dendritic cells through multiple C-type lectins and suppress TLR-induced dendritic cell activation. Mol Immunol *44*, 2605-2615.

van Stipdonk, M.J., Lemmens, E.E., and Schoenberger, S.P. (2001). Naïve CTLs require a single brief period of antigenic stimulation for clonal expansion and differentiation. Nat Immunol *2*, 423-429.

van Vliet, S.J., van Liempt, E., Saeland, E., Aarnoudse, C.A., Appelmelk, B., Irimura, T., Geijtenbeek, T.B., Blixt, O., Alvarez, R., van Die, I., and van Kooyk, Y. (2005). Carbohydrate profiling reveals a distinctive role for the C-type lectin MGL in the recognition of helminth parasites and tumor antigens by dendritic cells. Int Immunol *17*, 661-669.

Vannella, K.M., Barron, L., Borthwick, L.A., Kindrachuk, K.N., Narasimhan, P.B., Hart, K.M., Thompson, R.W., White, S., Cheever, A.W., Ramalingam, T.R., and Wynn, T.A. (2014). Incomplete deletion of IL-4Ralpha by LysM(Cre) reveals distinct subsets of M2 macrophages controlling inflammation and fibrosis in chronic schistosomiasis. PLoS pathogens *10*, e1004372.

Vannella, K.M., Ramalingam, T.R., Borthwick, L.A., Barron, L., Hart, K.M., Thompson, R.W., Kindrachuk, K.N., Cheever, A.W., White, S., Budelsky, A.L*., et al.* (2016). Combinatorial targeting of TSLP, IL-25, and IL-33 in type 2 cytokine-driven inflammation and fibrosis. Sci Transl Med *8*, 337ra365.

Vella, A.T., and Pearce, E.J. (1992). CD4+ Th2 response induced by Schistosoma mansoni eggs develops rapidly, through an early, transient, Th0-like stage. J Immunol *148*, 2283-2290.

Ventre, E., Brinza, L., Schicklin, S., Mafille, J., Coupet, C.A., Marçais, A., Djebali, S., Jubin, V., Walzer, T., and Marvel, J. (2012). Negative regulation of NKG2D expression by IL-4 in memory CD8 T cells. J Immunol *189*, 3480-3489.

Venturiello, S.M., Giambartolomei, G.H., and Costantino, S.N. (1993). Immune killing of newborn Trichinella larvae by human leucocytes. Parasite Immunol *15*, 559-564.

Venturiello, S.M., Giambartolomei, G.H., and Costantino, S.N. (1995). Immune cytotoxic activity of human eosinophils against Trichinella spiralis newborn larvae. Parasite Immunol *17*, 555-559.

Verykokakis, M., Boos, M.D., Bendelac, A., Adams, E.J., Pereira, P., and Kee, B.L. (2010a). Inhibitor of DNA binding 3 limits development of murine slam-associated adaptor protein-dependent "innate" gammadelta T cells. PLoS One *5*, e9303.

Verykokakis, M., Boos, M.D., Bendelac, A., and Kee, B.L. (2010b). SAP protein-dependent natural killer T-like cells regulate the development of CD8(+) T cells with innate lymphocyte characteristics. Immunity *33*, 203-215.

Villarino, A., Laurence, A., Robinson, G.W., Bonelli, M., Dema, B., Afzali, B., Shih, H.Y., Sun, H.W., Brooks, S.R., Hennighausen, L.*, et al.* (2016). Signal transducer and activator of transcription 5 (STAT5) paralog dose governs T cell effector and regulatory functions. eLife *5*.

Voldsgaard, A., Bager, P., Garde, E., Åkeson, P., Leffers, A.M., Madsen, C.G., Kapel, C., Roepstorff, A., Thamsborg, S.M., Melbye, M.*, et al.* (2015). Trichuris suis ova therapy in relapsing multiple sclerosis is safe but without signals of beneficial effect. Mult Scler *21*, 1723-1729.

von Moltke, J., Ji, M., Liang, H.E., and Locksley, R.M. (2016). Tuft-cell-derived IL-25 regulates an intestinal ILC2-epithelial response circuit. Nature *529*, 221-225.

Vázquez-Mendoza, A., Carrero, J.C., and Rodriguez-Sosa, M. (2013). Parasitic infections: a role for C-type lectins receptors. Biomed Res Int *2013*, 456352.

Walker, A.J. (2011). Insights into the functional biology of schistosomes. Parasit Vectors *4*, 203.

Wammes, L.J., Mpairwe, H., Elliott, A.M., and Yazdanbakhsh, M. (2014). Helminth therapy or elimination: epidemiological, immunological, and clinical considerations. Lancet Infect Dis *14*, 1150-1162.

Wang, I.H., Suomalainen, M., Andriasyan, V., Kilcher, S., Mercer, J., Neef, A., Luedtke, N.W., and Greber, U.F. (2013). Tracking viral genomes in host cells at single-molecule resolution. Cell Host Microbe *14*, 468-480.

Wang, S., Yang, T., Zhang, X., Xia, J., Guo, J., Wang, X., Hou, J., Zhang, H., Chen, X., and Wu, X. (2016). Construction of In Vivo Fluorescent Imaging of Echinococcus granulosus in a Mouse Model. Korean J Parasitol *54*, 291-299.

Warming, S., Costantino, N., Court, D.L., Jenkins, N.A., and Copeland, N.G. (2005). Simple and highly efficient BAC recombineering using galK selection. Nucleic acids research *33*, e36.

Weinberg, J.B., Lutzke, M.L., Alfinito, R., and Rochford, R. (2004). Mouse strain differences in the chemokine response to acute lung infection with a murine gammaherpesvirus. Viral Immunol *17*, 69-77.

Weinreich, M.A., Odumade, O.A., Jameson, S.C., and Hogquist, K.A. (2010). T cells expressing the transcription factor PLZF regulate the development of memory-like CD8+ T cells. Nat Immunol *11*, 709-716.

Weinreich, M.A., Takada, K., Skon, C., Reiner, S.L., Jameson, S.C., and Hogquist, K.A. (2009). KLF2 transcription-factor deficiency in T cells results in unrestrained cytokine production and upregulation of bystander chemokine receptors. Immunity *31*, 122-130.

Whelan, M., Harnett, M.M., Houston, K.M., Patel, V., Harnett, W., and Rigley, K.P. (2000). A filarial nematode-secreted product signals dendritic cells to acquire a phenotype that drives development of Th2 cells. J Immunol *164*, 6453-6460.

White, J.T., Cross, E.W., Burchill, M.A., Danhorn, T., McCarter, M.D., Rosen, H.R., O'Connor, B., and Kedl, R.M. (2016). Virtual memory T cells develop and mediate bystander protective immunity in an IL-15-dependent manner. Nat Commun *7*, 11291.

White, J.T., Cross, E.W., and Kedl, R.M. (2017). Antigen-inexperienced memory CD8+ T cells: where they come from and why we need them. Nature reviews. Immunology *17*, 391-400.

White, R.R., and Artavanis-Tsakonas, K. (2012). How helminths use excretory secretory fractions to modulate dendritic cells. Virulence *3*, 668-677.

Wiesel, M., Crouse, J., Bedenikovic, G., Sutherland, A., Joller, N., and Oxenius, A. (2012). Type-I IFN drives the differentiation of short-lived effector CD8+ T cells in vivo. Eur J Immunol *42*, 320-329.

Wilbers, R.H., Westerhof, L.B., van Noort, K., Obieglo, K., Driessen, N.N., Everts, B., Gringhuis, S.I., Schramm, G., Goverse, A., Smant, G.*, et al.* (2017). Production and glyco-engineering of immunomodulatory helminth glycoproteins in plants. Sci Rep *7*, 45910.

Wilen, C.B., Lee, S., Hsieh, L.L., Orchard, R.C., Desai, C., Hykes, B.L., McAllaster, M.R., Balce, D.R., Feehley, T., Brestoff, J.R.*, et al.* (2018). Tropism for tuft cells determines immune promotion of norovirus pathogenesis. Science *360*, 204-208.

Witte, M.B., and Barbul, A. (2003). Arginine physiology and its implication for wound healing. Wound Repair Regen *11*, 419-423.

Wolint, P., Betts, M.R., Koup, R.A., and Oxenius, A. (2004). Immediate cytotoxicity but not degranulation distinguishes effector and memory subsets of CD8+ T cells. J Exp Med *199*, 925-936.

World Health Organization (2014). WHO | Metrics: Disability-Adjusted Life Year (DALY). In WHO (World Health Organization).

World Health Organization (2016). Endemicity Taenia Solium 2015. (WHO).

World Health Organization (2018a). Neglected tropical diseases. In WHO (World Health Organization).

World Health Organization (2018b). Schistosomiasis.

World Health Organization (2018c). Soil-transmitted helminth infections.

Worthington, J.J., Klementowicz, J.E., Rahman, S., Czajkowska, B.I., Smedley, C., Waldmann, H., Sparwasser, T., Grencis, R.K., and Travis, M.A. (2013). Loss of the TGFβ-activating integrin αvβ8 on

dendritic cells protects mice from chronic intestinal parasitic infection via control of type 2 immunity. PLoS Pathog *9*, e1003675.

Wynn, T.A. (2004). Fibrotic disease and the T(H)1/T(H)2 paradigm. Nat Rev Immunol *4*, 583-594.

Wynn, T.A., Morawetz, R., Scharton-Kersten, T., Hieny, S., Morse, H.C., 3rd, Kuhn, R., Muller, W., Cheever, A.W., and Sher, A. (1997). Analysis of granuloma formation in double cytokine-deficient mice reveals a central role for IL-10 in polarizing both T helper cell 1- and T helper cell 2-type cytokine responses in vivo. J Immunol *159*, 5014-5023.

Wynn, T.A., Reynolds, A., James, S., Cheever, A.W., Caspar, P., Hieny, S., Jankovic, D., Strand, M., and Sher, A. (1996). IL-12 enhances vaccine-induced immunity to schistosomes by augmenting both humoral and cell-mediated immune responses against the parasite. J Immunol *157*, 4068-4078.

Xue, J., Schmidt, S.V., Sander, J., Draffehn, A., Krebs, W., Quester, I., De Nardo, D., Gohel, T.D., Emde, M., Schmidleithner, L*., et al.* (2014). Transcriptome-based network analysis reveals a spectrum model of human macrophage activation. Immunity *40*, 274-288.

Yang, J., Zhao, J., Yang, Y., Zhang, L., Yang, X., Zhu, X., Ji, M., Sun, N., and Su, C. (2007). Schistosoma japonicum egg antigens stimulate CD4 CD25 T cells and modulate airway inflammation in a murine model of asthma. Immunology *120*, 8-18.

Yang, Z., Grinchuk, V., Urban, J.F., Bohl, J., Sun, R., Notari, L., Yan, S., Ramalingam, T., Keegan, A.D., Wynn, T.A*., et al.* (2013). Macrophages as IL-25/IL-33-responsive cells play an important role in the induction of type 2 immunity. PLoS One *8*, e59441.

Yona, S., Kim, K.W., Wolf, Y., Mildner, A., Varol, D., Breker, M., Strauss-Ayali, D., Viukov, S., Guilliams, M., Misharin, A*., et al.* (2013). Fate mapping reveals origins and dynamics of monocytes and tissue macrophages under homeostasis. Immunity *38*, 79-91.

Yoshimoto, T., Tsutsui, H., Tominaga, K., Hoshino, K., Okamura, H., Akira, S., Paul, W.E., and Nakanishi, K. (1999). IL-18, although antiallergic when administered with IL-12, stimulates IL-4 and histamine release by basophils. Proc Natl Acad Sci U S A *96*, 13962-13966.

Youngblood, B., Hale, J.S., Kissick, H.T., Ahn, E., Xu, X., Wieland, A., Araki, K., West, E.E., Ghoneim, H.E., Fan, Y*., et al.* (2017). Effector CD8 T cells dedifferentiate into long-lived memory cells. Nature *552*, 404-409.

Yu, Y., Deng, W., and Lei, J. (2015). Interleukin-33 promotes Th2 immune responses in infected mice with Schistosoma japonicum. Parasitol Res *114*, 2911-2918.

Zaiss, D.M., Yang, L., Shah, P.R., Kobie, J.J., Urban, J.F., and Mosmann, T.R. (2006). Amphiregulin, a TH2 cytokine enhancing resistance to nematodes. Science *314*, 1746.

Zaiss, D.M.W., Gause, W.C., Osborne, L.C., and Artis, D. (2015a). Emerging functions of amphiregulin in orchestrating immunity, inflammation, and tissue repair. Immunity *42*, 216-226.

Zaiss, M.M., Maslowski, K.M., Mosconi, I., Guenat, N., Marsland, B.J., and Harris, N.L. (2013). IL-1β suppresses innate IL-25 and IL-33 production and maintains helminth chronicity. PLoS Pathog *9*, e1003531.

Zaiss, M.M., Rapin, A., Lebon, L., Dubey, L.K., Mosconi, I., Sarter, K., Piersigilli, A., Menin, L., Walker, A.W., Rougemont, J.*, et al.* (2015b). The Intestinal Microbiota Contributes to the Ability of Helminths to Modulate Allergic Inflammation. Immunity *43*, 998-1010.

Zeippen, C., Javaux, J., Xiao, X., Ledecq, M., Mast, J., Farnir, F., Vanderplasschen, A., Stevenson, P., and Gillet, L. (2017). The Major Envelope Glycoprotein of Murid Herpesvirus 4 Promotes Sexual Transmission. Journal of virology *91*.

Zeng, R., Spolski, R., Finkelstein, S.E., Oh, S., Kovanen, P.E., Hinrichs, C.S., Pise-Masison, C.A., Radonovich, M.F., Brady, J.N., Restifo, N.P.*, et al.* (2005). Synergy of IL-21 and IL-15 in regulating CD8+ T cell expansion and function. J Exp Med *201*, 139-148.

Zhang, R., Sun, Q., Chen, Y., Sun, X., Gu, Y., Zhao, Z., Cheng, Y., Zhao, L., Huang, J., Zhan, B., and Zhu, X. (2018). Ts-Hsp70 induces protective immunity against Trichinella spiralis infection in mouse by activating dendritic cells through TLR2 and TLR4. PLoS Negl Trop Dis *12*, e0006502.

Zhao, A., McDermott, J., Urban, J.F., Gause, W., Madden, K.B., Yeung, K.A., Morris, S.C., Finkelman, F.D., and Shea-Donohue, T. (2003). Dependence of IL-4, IL-13, and nematode-induced alterations in murine small intestinal smooth muscle contractility on Stat6 and enteric nerves. J Immunol *171*, 948-954.

Zhao, A., Urban, J.F., Anthony, R.M., Sun, R., Stiltz, J., van Rooijen, N., Wynn, T.A., Gause, W.C., and Shea-Donohue, T. (2008). Th2 cytokine-induced alterations in intestinal smooth muscle function depend on alternatively activated macrophages. Gastroenterology *135*, 217-225.e211.

Zhou, B., Comeau, M.R., De Smedt, T., Liggitt, H.D., Dahl, M.E., Lewis, D.B., Gyarmati, D., Aye, T., Campbell, D.J., and Ziegler, S.F. (2005). Thymic stromal lymphopoietin as a key initiator of allergic airway inflammation in mice. Nat Immunol *6*, 1047-1053.

Ziegler, T., Rausch, S., Steinfelder, S., Klotz, C., Hepworth, M.R., Kühl, A.A., Burda, P.C., Lucius, R., and Hartmann, S. (2015). A novel regulatory macrophage induced by a helminth molecule instructs IL-10 in CD4+ T cells and protects against mucosal inflammation. J Immunol *194*, 1555-1564.